

Towards New Therapies for Endovascular Revascularization Procedures

Submitted by

Benjamin Thierry

Department of Biomedical Engineering

McGill University

Montreal, Quebec, Canada

June 2003

A thesis submitted to the Faculty of Graduate Studies and Research in
partial fulfillment of the requirements of the degree of Doctorate in
Biomedical Engineering (Ph.D.)

© Benjamin Thierry, 2003



Library and
Archives Canada

Bibliothèque et
Archives Canada

Published Heritage
Branch

Direction du
Patrimoine de l'édition

395 Wellington Street
Ottawa ON K1A 0N4
Canada

395, rue Wellington
Ottawa ON K1A 0N4
Canada

Your file Votre référence

ISBN: 0-612-98382-X

Our file Notre référence

ISBN: 0-612-98382-X

NOTICE:

The author has granted a non-exclusive license allowing Library and Archives Canada to reproduce, publish, archive, preserve, conserve, communicate to the public by telecommunication or on the Internet, loan, distribute and sell theses worldwide, for commercial or non-commercial purposes, in microform, paper, electronic and/or any other formats.

The author retains copyright ownership and moral rights in this thesis. Neither the thesis nor substantial extracts from it may be printed or otherwise reproduced without the author's permission.

AVIS:

L'auteur a accordé une licence non exclusive permettant à la Bibliothèque et Archives Canada de reproduire, publier, archiver, sauvegarder, conserver, transmettre au public par télécommunication ou par l'Internet, prêter, distribuer et vendre des thèses partout dans le monde, à des fins commerciales ou autres, sur support microforme, papier, électronique et/ou autres formats.

L'auteur conserve la propriété du droit d'auteur et des droits moraux qui protègent cette thèse. Ni la thèse ni des extraits substantiels de celle-ci ne doivent être imprimés ou autrement reproduits sans son autorisation.

In compliance with the Canadian Privacy Act some supporting forms may have been removed from this thesis.

Conformément à la loi canadienne sur la protection de la vie privée, quelques formulaires secondaires ont été enlevés de cette thèse.

While these forms may be included in the document page count, their removal does not represent any loss of content from the thesis.

Bien que ces formulaires aient inclus dans la pagination, il n'y aura aucun contenu manquant.


Canada

ACKNOWLEDGEMENTS

I am deeply grateful to my supervisor, Prof. Maryam Tabrizian (Department of Biomedical Engineering, McGill), for her invaluable support, patience and advice and for introducing me to scientific research throughout all these years of collaboration. Her energy, enthusiasm and scientific integrity have been a constant source of motivation in the completion of my graduate studies. It has been a great pleasure for me to work for such a long time under her supervision.

Je tiens à remercier également chaleureusement mes co-superviseurs pour leur aide, conseil et soutien. Merci donc au Prof. Françoise Winnik (Faculté de Pharmacie et de Chimie, U. de Montréal) pour sa patience envers le « non-chimiste » que je suis. Ses conseils scientifiques pertinents, sa compétence et son enthousiasme communicatif m'auront été précieux tout au long de mes recherches. Merci aussi au Prof. Yahye Merhi (Institut de Cardiologie de Montréal) de m'avoir introduit au « monde de l'hémocompatibilité ». Au delà de ses compétences scientifiques et de sa rigueur intellectuelle, sa disponibilité ainsi que sa gentillesse auront été grandement appréciées. Thank also goes to Dr. Jim Silver for its long distance co-supervision and through him to Nitinol Devices and Components. His advices, questions, comments and corrections have always been pertinent and useful.

I respectfully thank the members of the Jury, Prof. J. Kozinski (Pro-Dean), Prof. R.E. Kearny (Chair), Prof. S. Prakash and Prof. R. Lobow (external member) for their detailed evaluation of this thesis and valuable suggestions and criticism of the manuscript.

Je remercie Suzie Poulin et Marie-France Pépin (Ecole Polytechnique de Montréal) pour leur aide précieuse en matière d'analyse de surface. Mes remerciements vont aussi à Jean-François Théorêt, Nathalie Jacobs et Danielle Libersan (Institut de Cardiologie de Montréal) pour leur aide, conseil et support dans les essais d'hémocompatibilité. Merci également à Louis Villeneuve (Institut de Cardiologie de Montréal) pour les analyses de microscopie confocale, et au Dr. Sébastien Gouin pour son aide dans la synthèse des dérivés de l'acide hyaluronique.

I am very thankful to my co-authors, Prof. Hans J. Griesser for help in plasma polymerization processes and Dr. Bilodeau for advice and corrections in my manuscript. Thanks also to Patricia Cap for manuscripts reviewing.

I would like to express my sincere gratitude to all students from Dr. Tabrizian's, lab as well as students from Dr. Winnik's and Dr Mehri's labs. For their help in administrative matters, I thank Pina Sorrini.

This work could not have been performed without the financial assistance from the Natural Science and Engineering Research Council of Canada and Nitinol Devices and Components.

Lastly, my warmest thanks are due to the people who have patiently supported me through all these years: Maryam and Samira Mubareka, Dr. David Apoil Savery, Dr. Elliot Beaubien, Mehdi El Idrissi El Yacoubi, Dr. Marc Allain, Nathalie Garneau and my family.

TABLE OF CONTENTS

ACKNOWLEDGEMENTS -----	ii
TABLE OF CONTENTS -----	iv
LIST OF FIGURES -----	ix
LIST OF TABLES -----	xiv
LIST OF SYMBOLS -----	xv
PREFACE: CONTRIBUTIONS OF AUTHORS -----	xvii
ABSTRACT -----	xviii
RÉSUMÉ -----	xix
1. INTRODUCTION AND RATIONALE OF RESEARCH -----	1
2. THESIS OBJECTIVES AND OUTLINE -----	4
2.1. THESIS OBJECTIVES -----	4
2.1.1. Objective 1 – Part I: Surface modification of metallic endovascular stent ---	4
2.1.2. Objective 2 – Part II: Development of a biodegradable membrane-covered stent -----	5
2.1.3. Objective 3 – Part III: To develop a strategy toward <i>in vivo</i> repair of blood vessel using self-assembled structures. -----	5
2.2. THESIS OUTLINE -----	6
2.2.1. Literature review -----	6
2.2.2. Experimental parts of the Thesis -----	7
2.2.3. Conclusions and future development -----	7
2.2.4. Succinct description of the papers included -----	7

3. LITERATURE REVIEW – SECTION 1: ENDOVASCULAR DEVICES IN REVASCULARIZATION PROCEDURES -----9

3.1. An Introduction to endovascular devices -----	9
3.1.1. Historical perspectives-----	10
3.1.2. Clinical indications-----	12
3.1.3. Complications-----	12
3.1.4. Metallic Alloys Used in Endovascular Procedures-----	14
3.1.5. Biomechanical considerations-----	15
3.1.6. Inorganic coatings-----	17
3.1.7. Thromboresistant coatings-----	18
3.1.8. Membrane-covered stents-----	19
3.1.9. Radioactive stents -----	20
3.1.10. Biodegradable stents -----	21
3.1.11. Drug-eluting stents -----	22
3.1.12. CONCLUSIONS -----	23
3.1.13. Reference -----	24

4. LITERATURE REVIEW – SECTION 2: BIOSTABILITY AND BIOCOMPATIBILITY OF ENDOVASCULAR DEVICES ----- 29

4.1. Paper 1.-----	29
4.1.1. Abstract-----	29
4.1.2. Introduction to the biocompatibility and biostability of endovascular devices -----	30
4.1.3. Current concepts in endovascular procedures-----	33
4.1.4 Considerations on the biostability of metallic devices-----	39
4.1.5. Are alloys used in endovascular surgery stable? -----	43

4.1.6. Considerations for the Biocompatibility of endovascular devices -----	47
4.1.7. Future perspectives-----	52
4.1.8. Reference-----	54
 PART I. STENTS-----	 68
6. BIOMIMETIC SURFACE-----	70
6.1. PAPER 2-----	70
6.1.1. Abstract-----	70
6.1.2. Introduction -----	71
6.1.3. Experimental-----	74
6.1.4. Results -----	82
6.1.5. Discussion-----	96
6.1.6. Conclusion -----	99
6.1.7. References-----	100
 7. ANTI-PROLIFERATIVE STENTS-----	 103
7.1. PAPER 3-----	103
7.1.1. Abstract-----	103
7.1.2. Introduction -----	104
7.1.3. Experimental-----	106
7.1.4. Results and discussion-----	112
7.1.5. Conclusions -----	125
7.1.6. References-----	127
7.2. PAPER 4-----	133
7.2.1. Abstract. -----	133

7.2.2. Introduction -----	134
7.2.3. Experimental -----	138
7.2.4. Results and discussion -----	143
7.2.5. Conclusion -----	154
7.2.6. Reference -----	156
 PART II. MEMBRANE-COVERED STENTS -----	159
8. BIODEGRADABLE MEMBRANE-COVERED STENT -----	160
8.1. PAPER 5 -----	160
8.1.1. Abstract -----	160
8.1.2. Introduction -----	161
8.1.3. Experimental -----	163
8.1.4. Results -----	170
8.1.5. Discussion -----	177
8.1.6. Conclusion -----	181
8.1.7. Reference -----	182
 PART III. NANOCOATINGS ON ARTERIES -----	187
9. SELF-ASSEMBLED CHITOSAN/HYALURONAN NANOCOATINGS -----	189
9.1. PAPER 6 -----	189
9.1.1. Abstract -----	189
9.1.2. Communication -----	190
9.1.3. References -----	196
9.1.4. Supporting Informations -----	198

9.2. PAPER 7-----	204
9.2.1. Introduction -----	204
9.2.2. Experimental -----	206
9.2.3. Results and discussion -----	207
9.2.4. Conclusion -----	210
9.2.4. REFERENCES -----	211
10. CONCLUSIONS AND FUTURE DEVELOPMENTS -----	213
10.1. SUMMARY OF RESEARCH -----	213
10.2. SUGGESTIONS FOR FUTURE RESEARCH-----	217
10.2.1. Reference -----	222
11. BIBLIOGRAPHY -----	224
APPENDIX -----	252

LIST OF FIGURES

Figure 3.1. Current stent designs and materials allow increased flexibility. Nitinol SMART stent from Nitinol Devices & Components -----	10
Figure 3.2. Deployment of a self-expandable stent -----	15
Figure 3.3. Membrane-covered stent during its deployment. -----	20
Figure 4.1. Scanning Electron Micrographs of retrieved Stentor endograft -----	33
Figure 4.2. Hyperplasia is the response of the artery to the injury created during angioplasty and to the presence of the metallic devices-----	35
Figure 4.3. Reactivity of a passive metal in physiological fluid; I & II: Growth of the oxide layer, III: ions release and IV: binding with macromolecules -----	38
Figure 4.4. AFM analysis of electropolished NiTi stent showing smooth surface with polycrystalline grain oxide -----	39
Figure 4.5. SEM micrographs of a fractured stainless steel Greenfield vena cava filter showing corrosion-fatigue degradation-----	42
Figure 4.6. Nickel release in Hank's physiological solution for mechanically polished (MP) stainless steel (MP ST), NiTi (MP NiTi) and MP35N (MP MP35N), electropolished stainless steel (EP ST) and NiTi (EP NiTi), and acid passivated MP35N (PA MP35N) -----	44
Figure 4.7. Typical cyclic polarization curves in de-aerated Hank's balanced salt solution of electropolished NiTi and stainless steel (316L) -----	45
Figure 6.1. Hyaluronic acid derivative HA-PEG synthetic route.-----	75
Figure 6.2. ¹ H-NMR in D ₂ O at 400 Mhz: (1) native HA, (2) HA-NH ₂ , (3) HA-PEG -	81
Figure 6.3. Resolved XPS spectrum of: PlasmaAA surface on NiTi, C1s (A), and N1s (B); and PolyAA surface on NiTi: C1s (C), and N1s (D)-----	85

Figure 6.4. C1s XPS high resolution simulation of HA-PEG spin coated on a Si wafer	88
Figure 6.5. (A) Resolved XPS C1s spectrum of: (1) PlasmaAA, (2) HA-PEG immobilized on PlasmaAA, and (3) HA-PEG spin coated on a Si wafer; (B) Resolved XPS C1s spectrum of: (1) PolyAA, (2) HA immobilized on PolyAA, (3) HA-PEG immobilized on PolyAA, and (4) HA-PEG spin coated on a Si wafer--	92
Figure 6.6. AFM height images in tapping mode of (I) PolyAA, (II) HA-PEG-polyAA; Images dimension are 1 μm^2 , and Z scales are 15 nm	93
Figure 6.7. Platelet adhesion on NiTi, HA-PEG-polyAA and glass as control	94
Figure 6.8. Neutrophil adhesion on damaged artery (Media), NiTi, and HA-PEG-polyAA	95
Figure 6.9. Confocale microscopy image showing the immobilization of FITC-avidin on the HA-PEG-polyAA surface	96
Figure 7.1.1. Hyaluronan derivatives (HA-NH ₂ and HA-DTPA) synthetic route.	107
Figure 7.1.2. Schematic of the immobilization of HA-DTPA on functionalized surfaces	109
Figure 7.1.3. Resolved XPS spectrum of HA-DTPA spin coated on Si wafer: C1s (a), O1s (b) and N1s (c)	116
Figure 7.1.4. XPS C1s spectrum of: (1) NiTi-PolyAA, (2) HA-DTPA-NiTi, and (3) HA-DTPA spin coated on Si wafer	118
Figure 7.1.5. Positive mode ToF-SIMS spectra recorded for Yttrium-HA-DTPA immobilized NiTi. The insert shows the characteristic peak of yttrium at m/z 88.9	121
Figure 7.1.6. ToF-SIMS molecular imaging of the m/z cations characteristics of polyAA (CH ₄ N), HA-DTPA (C ₂ H ₅ O), titanium (Ti), and yttrium (Y)	122
Figure 7.1.7. Loss of radionuclide from the ¹¹¹ In-HA-DTPA-NiTi (mol. % of the total amount of radionuclide) in PBS at 38°C	124

Figure 7.1.8. Fibrinogen adsorption on Teflon and HA-DTPA-Teflon in the dynamic <i>in vitro</i> assay-----	125
Figure 7.2.1. Schematic diagram of the deposition of CH/HA self-assembled multilayer on NiTi substrates-----	139
Figure 7.2.2. Contact angles with water (Advancing, receding) and hysteresis as a function of the number of layers-----	144
Figure 7.2.3. Amount of In111-HA ($\mu\text{g}/\text{cm}^2$) as a function of the number of layer for the CH/HA and CH-SNP/HA polyelectrolytes self-assembled onto NiTi substrates -----	145
Figure 7.2.4. Positive ion ToF-SIMS spectra (m/z 0-100) for (I) PEI modified NiTi and (II) PEI-HA(CH/HA) ₄ self-assembled coating on NiTi-----	147
Figure 7.2.5. Chemical imaging of a PEI-HA(CH/HA) ₄ self-assembled multilayer showing the distribution of CH_3CO^+ , Ti and Ni ions on the surface ($7.9 \mu\text{m}^2$)---	147
Figure 7.2.6. AFM tapping mode height and amplitude images of (I) the mechanically polished NiTi, (II) PEI-HA(CH/HA) ₂ coated NiTi, PEI-HA(CH/HA) ₅ coated NiTi and PEI-HA(CH/HA) ₁₀ coated NiTi -----	150
Figure 7.2.7. Platelet adhesion on NiTi, NiTi-PEI-HA(CH/HA) ₄ and NiTi-PEI-HA(CH-SNP/HA) ₄ -----	152
Figure 7.2.8. Neutrophil adhesion on damaged artery (Media), NiTi, and NiTi-PEI-HA(CH/HA) ₄ -----	152
Figure 7.2.9. Confocal microscopy images of: (I) PEI-HA(CH/HA) ₄ coated NiTi wires; (II) Cross-section of a damaged artery maintained in contact with the coated wire for 48 h in PBS -----	153
Figure 8.1. Schematic of the preparation of the CH-PEO membrane-covered stent with or without external porous layer -----	165
Figure 8.2. Macroscopic observation of the CH-PEO membrane covered stent showing the ability of the membrane to sustain the mechanical deformation of the metallic stent -----	171

Figure 8.3. Scanning electron microscopic images of the membrane covered stent --	172
Figure 8.4. Swelling behavior in PBS (pH 7.4) of (A) CH-PEO membrane and (B) CH-PEO porous membrane; The inset shows the swelling behavior of CH-PEO membrane in comparison to (C) CH membrane-----	173
Figure 8.5. Platelet adhesion ($n \geq 5$) in an ex vivo porcine model on CH-PEO, damaged (Media) and intact arteries (Endo)-----	175
Figure 8.6. Leukocyte adhesion ($n \geq 5$) in an ex vivo porcine model on CH-PEO, damaged (Media) and intact arteries (Endo)-----	175
Figure 8.7. Platelet adhesion ($n \geq 4$) after 90 min incubation in PRP on chitosan (CH), CH-PEO and heparin complexed-CH-PEO (CH-PEO-Hep) membranes. Damaged arteries (Media) were used as control-----	176
Figure 8.8. Arginine release behavior in PBS of the CH-PEO membrane-----	177
Figure 9.1.1. Chemical structure of chitosan (CH) and hyaluronan (HA) -----	191
Figure 9.1.2. Amount of ^{111}In -HA Vs. layers; Solid lines: CH/HA (moderate and high ionic strength) and CH/HA-L-Arg on collagen coated glass; Dashed lines: CH/HA on damaged or healthy endothelium -----	192
Figure 9.1.3. Confocal microscopy imaging of a section of a (CH/HA-FITC) ₅ coated damaged artery showing the transmural disposition of the fluorescently labeled polymer after 1) 0 h and 2) 24 h perfusion with PBS-----	194
Figure 9.1.4. Platelet adhesion ($n \geq 4$) on damaged endothelium (damaged endo), (CH/HA) ₅ and (CH/HA-L-Arg) ₅ coated damaged endothelium ((CH/HA) ₅ and (CH/HA-L-Arg) ₅) -----	195
Figure 9.1.S1. Thickness of the CH/HA multilayer self-assemblies prepared using non labeled HA or Gd-labeled HA (Gd-HA) (from QCM-D measurements)-----	200
Figure 9.1.S2. Fractional release of L-Arginine loaded multilayer in PBS. The inset shows the initial release-----	202
Figure 9.2.1. Polysaccharides used in the self-assembly process -----	205

Figure 9.2.2. QCM frequency shift ($\Delta f/v$) during the buildup of the CH/HA multilayer -----208

Figure 9.2.3. QCM frequency shift ($\Delta f/v$) during the buildup of the DNA-containing multilayer. The multilayer deposition was initiated with a PEI/HA/CH assembly followed by DNA/CH bilayers as indicated. The completed self-assembly was exposed to a fibrinogen solution (Fib) -----208

Figure 9.2.4. ^{51}Cr -Platelet adhesion after 30 min perfusion in vitro on damaged arteries (Media), and (CH/HA)₅ coated damaged arteries (M*) -----210

LIST OF TABLES

Table 3.1 Selected randomized clinical trials -----	11
Table 3.2 Characteristic of the ideal stent -----	16
Table 4.1 Most of the available stents, stent-grafts and membrane-covered stents in 2001 -----	34
Table 4.2 Metals and alloys used in vascular devices and selected properties (E: elastic modulus, YS: yield strength, UTS: ultimate tensile strength, ρ density) -----	37
Table 6.1. XPS measured atomic ratio (%) for modified surfaces; values with a 70° take-off angle given in parentheses -----	88
Table 6.2. Simulation of XPS C1s peak recorded on plasma polymerized allylamine modified surfaces -----	89
Table 6.3. Simulation of XPS C1s peak recorded on poly-allyl amine grafted surfaces	89
Table 6.4. Contact angle measured on NiTi modified surfaces-----	91
Table 7.1.1 XPS measured atomic ratio for NiTi modified surfaces (at 0° take-off angle); values with a 75° take-off angle given in parentheses. (Salts and contamination not shown) -----	115
Table 7.1.2 Simulation of XPS C1s, O1s and N1s peaks recorded on NiTi modified surfaces -----	115
Table 7.1.3 Contact angle measured on modified surfaces-----	120
Table 7.2.1 Molecules used for the self-assembled coating-----	137
Table 7.2.2 ToF-SIMS normalized intensities of the CH_3CO^+ peak (M/z 43.0174) as a function of the number of layer -----	146

LIST OF SYMBOLS

316L	Stainless steel
AFM	Atomic force microscopy
CH	Chitosan
CPD	Critical point drying
CPM	Counts per minute
DNA	Deoxyribonucleic acid
ECM	Extracellular matrix
HA	Hyaluronan (hyaluronic acid)
L-b-L	Layer-by-Layer
L-Arg	L-Arginine
Ni	Nickel
NiTi	NiTi alloy
Nitinol	NiTi alloy
NO	Nitric oxide
ODN	Oligonucleotide
PBS	Phosphate buffer solution
PDGF	Platelet derived growth factor
PEG	polyethylene glycol
PEI	Polyethylene imine
PLT	Platelet
PMN	Polymorphonuclear neutrophils

QCM	Quartz crystal microbalance
SEM	Scanning electron microscopy
SMC	Smooth muscle cell
SNP	Sodium nitroprusside
Ti	Titanium
ToF-SIMS	Time of flight – Secondary ions mass spectrometry
VEGF	Vascular endothelial growth factor
XPS	X-ray photoelectron spectroscopy

PREFACE: CONTRIBUTIONS OF AUTHORS

This thesis is presented as a collection of manuscripts written by the candidate in collaboration with co-authors. All the manuscripts are based on experimental data collected and analyzed by the candidate and as such, his name appears first in the authorship list of all manuscripts. The next authors appear as a function of their relative contributions to the scientific work of the manuscript. The supervisor of this work, Dr. M. Tabrizian, has been fully involved in all the work reported in these manuscripts and accordingly appears as the last author in all the manuscripts. Dr. Y. Mehri (all manuscripts) and Dr. J. Silver (manuscripts 2, 3, 4, and 5) were involved both scientifically and financially (Through the NSERC grant as a co-author for Dr. Merhi and through Nitinol Devices and Components as industrial partner for Dr. Silver). Dr. F. Winnik was involved scientifically in manuscripts 2, 3, 4, 6 and 7. Dr L. Bilodeau has been involved in the chapter introducing endovascular devices and was involved financially in the work as a co-author of the NSERC grant. Dr. H.J. Griesser has been involved in the plasma polymerization of NiTi alloy described in the manuscript 2 of this thesis.

ABSTRACT

Surgical revascularization by either natural or synthetic grafts, as well as less invasive percutaneous transluminal angioplasty (PTA), with or without stent implantation, is currently used in the treatment of vascular diseases. Despite its less invasive nature, stent implantation remains limited by in-stent restenosis within the stent struts. Although systemic administration of therapeutic drugs has shown disappointing results, the local delivery or presentation of therapeutic molecules/drugs/genetic material is a promising area for development.

The work that forms the basis of this thesis attempts to develop new devices or new strategies to achieve more efficient delivery of therapeutic biomacromolecules to the vascular walls during revascularization procedures. The work can be divided into three 3 Parts: (I) Modification of endovascular stents by hybrid coatings: two strategies involved the surface modification of the devices by plasma polymerization, followed by covalent immobilization of hyaluronan conjugated or able to be conjugated with a bioactive component (peptides/proteins or radionuclides). The last section of the Part I described the development of bioactive coating based on the Layer-by-Layer self-assembly of polysaccharide multilayers. (II) Development of a biodegradable membrane-covered stent: A chitosan-PEG blend has been used to engineer a biodegradable membrane-covered device for endovascular procedures. This membrane-covered device was able to sustain physiologic pressure, showed very small water permeability, displayed an appropriate haemocompatibility and could be used for drug delivery. (III) Development of nanocoatings to be self-assembled *in situ* onto the vascular wall: self-assembled multilayers have been investigated to protect damaged arteries and to control the healing processes by efficiently delivering therapeutic biomolecules to the vascular wall. These nanometric coatings have been deposited onto blood vessel by the Layer-by-Layer technique and have shown great potential for drug delivery of various macromolecules such as NO-donor or plasmid DNA.

RÉSUMÉ

Les procédures chirurgicales de revascularization ainsi que les procédures minimallement invasives d'angioplastie avec ou sans implantation d'endoprothèses coronaires (stents) sont communément utilisées dans le traitement des maladies vasculaires. En depit de sa nature moins invasive, l'implantation de stent reste limitée par l'occurrence de restenose intra-stent, i.e. la réocclusion du vaisseau traité. L'administration systémique de médicament s'est révélée peu efficace pour prévenir la restenose. Cependant, la libération locale de médicament offre de nouvelles modalités de traitement.

Le travail décrit dans cette thèse vise à développer de nouveaux dispositifs et de nouvelles procédures dans le domaine des la revascularisation endoluminale. Cette étude se compose de trois parties : (I) modification d'endoprothèses par des recouvrements hydrides, c'est-à-dire des recouvrements augmentant la biocompatibilité du dispositif tout en incluant une composante bioactive sont proposées. Les composantes bioactives peuvent subséquemment être libérée ou présentée au niveau de la paroi vasculaire. Deux approches utilisent une fonctionnalisation par plasma de la prothèse pour immobiliser de manière covalente un dérivé de l'acide hyaluronique. La troisième approche étudiée repose sur l'auto-assemblage du chitosan et de l'acide hyaluronique par la technique dite de « couche par couche ». (II) développement d'une endoprothèse recouverte d'une membrane biodégradable ; Cette membrane biodégradable est constituée d'un mélange de chitosan et de polyéthylène glycol. Les propriétés mécaniques excellentes de ce mélange permettent à la membrane de suivre les déformations de la prothèse lors de son déploiement. La membrane est caractérisée de plus par une très bonne perméabilité à l'eau ainsi que par une résistance à la pression suffisante pour autoriser son utilisation endovasculaire. Des tests d'adhésion plaquettaires ont montré que l'hécomcompatibilité de la membrane – complexée ou non avec de l'héparine – étaient appropriée. La possibilité d'incorporer un principe actif

dans la membrane a été également prouvée. (III) développement d'une procédure visant à auto-assembler des multicouches nanométriques sur la paroi vasculaire. Celle-ci repose sur l'auto-assemblage *in situ* de multicouche de chitosan et d'acide hyaluronique. Ces multicouches nanométriques sont stables dans les conditions physiologiques et diffusent dans la paroi vasculaire. Les artères endommagées protégées par ces structures sont significativement moins thrombogènes. Ces nano-structures sont également utilisées pour exposer la paroi vasculaire à des molécules biologiquement actives, telles que des peptides ou de l'ADN. Ces nano-structures offrent des perspectives très intéressantes, notamment pour la libération de molécules actives et la prévention de la restenose.

1. INTRODUCTION AND HYPOTHESIS OF RESEARCH

By the mid-1990s, disease of the vasculature had become the leading cause of death within western society, with over 500,000 casualties a year in the United States alone. Surgical revascularization by either natural (i.e. saphenous vein or internal mammary artery grafts) or synthetic grafts, as well as less invasive percutaneous transluminal coronary angioplasty (PTCA), with or without stent implantation, is currently used in the treatment of such diseases. Implantation of endovascular metallic stents has become the procedure of choice in endovascular revascularization procedures. Over 1,000,000 stent procedures are forecasted worldwide for 2005, representing an annual growth rate of 5%. Despite its less invasive nature, stent implantation remains limited by in-stent restenosis within the stent struts (10 to 40% depending on conditions). In-stent restenosis is due mainly to neointimal thickening, characterized by smooth muscle cell hyper-proliferation and migration towards the intima, and excessive extra-cellular matrix synthesis in the intima.

Although systemic administration of therapeutic drugs has shown disappointing results, the local delivery or presentation of therapeutic molecules/drugs/genetic material is a promising area for development. In particular, the recent successes obtained with drug-eluting stents, i.e., stents that release in a predictable fashion anti-proliferative drugs, have underscored the potential for local delivery of bioactive components. Important issues such as the cost of these new devices, the long-term safety of the drugs, and the biocompatibility of the polymeric matrix, however, remain to be addressed. The effect of the permanent presence of metallic implants within the blood vessel should also be questioned. Others methods to create intelligent bioactive interfaces need to be investigated as they may provide relief from the many side effects of stent implantation.

The work described in this thesis is aimed at developing such new strategies in the field of endovascular revascularization. These strategies relied on the use of a metallic stent (Parts I&II) used as a template to create a biologically hybrid surface (Part I) or a membrane-covered device (Part II). Part III of this work describes a new process to protect an angioplasty-damaged artery combined with an efficient way to target a drug/gene to the vascular wall.

Part I. Recent clinical reports have proved the potential of strategies using the device as a template to locally deliver therapeutic molecules. In the first three approaches described in this thesis, metallic stents were thus modified with hybrid coatings, i.e., biocompatible coatings incorporating bioactive components to be either presented or delivered locally. The combination of the improved biocompatibility of the devices with the biologic activity of the bioactive components, antiproliferative drugs or radionuclides is expected to be beneficial in the setting of stent implantation.

Part II. Membrane-covered stents are now widely investigated in diseases of the vasculature such as aneurysm and vein graft disease. A biodegradable membrane-covered stent with drug delivery ability is proposed to circumvent the limitations of current devices made with synthetic materials.

Part III. Revascularization procedures create mechanical injuries to the vascular wall, which in turn activate blood components and initiate restenosis. Conversely, drug delivery to the vascular wall remains limited by the wash out of the therapeutic macromolecules by blood flow or lack of solubility of hydrophobic drugs. In this work, the layer-by-layer technique has been used to self-assemble a polysaccharide multilayer, tens of nanometers thick, onto damaged vascular wall. This has led to the new concept of a self-assembled nanocoating used to protect a damaged artery from thrombogenesis and to control its healing through the incorporation of drugs/genes, described in this section of the thesis.

All the strategies proposed in this thesis are original and aimed at offering innovative, efficient and cost-effective devices or procedures in the field of diseases of the vasculature.

1.1. THESIS HYPOTHESIS

Hypothesis 1: Control of the interfacial properties of biomaterials (e.g. stents) and pathological tissues (e.g. damaged arteries) can reduce the outcomes associated to revascularization procedures since these interfacial properties mediate the biological interactions (living/living and living/synthetic materials).

Hypothesis 2: Molecular level surface structures can be used to achieve bioactive materials. These structures can be engineered through various techniques such as plasma polymerization and layer-by-layer self-assembly of polyelectrolytes.

Hypothesis 3: By combining molecular level surface structures with local delivery of bioactive components, more efficient therapeutic strategies can be developed in the field of endoluminal revascularization.

2. THESIS OBJECTIVES AND OUTLINE

2.1. THESIS OBJECTIVES

The main objective of this thesis is to propose new strategies for minimally invasive revascularization procedures. To address the wide range of conditions requiring revascularization, three different approaches – surface coatings of metallic stents, biodegradable membrane covered stent and self-assembled nanocoating on damaged blood vessels - were investigated and are presented here in three distinct parts.

2.1.1. Objective 1 – Part I: Surface modification of metallic endovascular stent

The widespread use of stents in revascularization procedures and the recent success achieved with drug-eluting stents encouraged us to modify commercially-available stents to modulate their bioactivity once implanted. These modifications were aimed at creating biomimetic surfaces that could enhance endothelialization and/or hybrid surfaces with improved biocompatibility and anti-proliferative properties. These coatings are explained in Part I of this thesis. Specific objectives of the work include:

- a) To engineer biomimetic surfaces by immobilizing hyaluronan (HA) onto metallic implants and to subsequently immobilize bioactive molecules on the HA coated layer;
- b) To develop and characterize a biocompatible hybrid coating based on the immobilization of a radionuclide-HA conjugate;

- c) To develop self-assembled bioactive biocompatible coatings that could be used for local delivery of molecules with anti-proliferative properties.

2.1.2. Objective 2 – Part II: Development of a biodegradable membrane-covered stent

The development of a biodegradable-membrane-covered stent is described in Part II of this thesis. Specific objectives of the work include:

- a) To propose a method suitable for covering a metallic stent with a biodegradable membrane made of the biocompatible natural polymer chitosan;
- b) To investigate the properties of the membrane-covered stent in view of its utilization in endovascular procedures. This includes its haemocompatibility and mechanical properties such as water permeation and burst pressure resistance;
- c) To investigate its ability for local delivery/presentation of bioactive macromolecules to the vascular wall.

2.1.3. Objective 3 – Part III: To develop a strategy toward *in vivo* repair of blood vessel using self-assembled structures.

An innovative procedure to protect an angioplasty-damaged blood vessel and to enhance its healing using a self-assembled nanocoating is described in Part III of this thesis. Specific objectives of this work include:

- a) To investigate and characterize the self-assembly by the Layer-by-Layer technique of chitosan and hyaluronan;

- b) To determine whether this self-assembling processes could be used to achieve *ex vivo* a protective nanocoating of a damaged vascular wall;
- c) To load bioactive macromolecules within the nanocoatings to modulate their biological activity;

2.2. THESIS OUTLINE

The present thesis is presented as a collection of manuscripts accepted, submitted or to be submitted for publication in peer-reviewed journals. A review of the literature is first presented. Each objective described in the previous chapter is then specifically addressed in three different parts. A reference list is presented for each manuscript and each chapter and a bibliography including all the references used in this work has been included.

2.2.1. Literature review

The literature review is divided into two sections. The first section introduces endovascular revascularization procedures and provides a description of current endovascular devices – stents and membrane-covered stents. This section is adapted from a book chapter (“Stents” by B. Thierry, L. Bilodeau, and M. Tabrizian) to be published in the Encyclopedia of Biomaterials and Biomedical Engineering (Marcel Dekker, Inc.). The second section reviews the biocompatibility and biostability of the endovascular implants currently used in the clinical practice and describes the recent developments in the field. This manuscript will be published in the Journal of Endovascular Surgery (manuscript 1).

2.2.2. Experimental parts of the Thesis

The experimental work of this thesis is described in three different parts regrouping six manuscripts. Manuscripts 2, 3 and 4 address the surface coating of metallic endovascular stents (Part I). Manuscript 5 describes the development of the biodegradable-membrane covered stent (Part II). Manuscripts 6 and 7 provide the proof of principle and characterization of the self-assembled nanocoating deposited on damaged blood vessels (Part III).

2.2.3. Conclusions and future development

The specific objectives are discussed in view of the main goal of the work, i.e. developing new devices and new strategies for endovascular revascularization procedures. The conclusion is dedicated to address the clinical potential of the strategies described in this thesis, and suggestions towards further development are made.

2.2.4. Succinct description of the papers included

Manuscript 1, to be published in the *Journal of Endovascular Therapy*, reviews the biocompatibility and biostability of metallic devices used in revascularization procedures. This manuscript also describes the recent developments in the field such as drug eluting stents.

Manuscript 2, to be submitted to the *Journal of Biomedical Materials Research*, presents the development of biomimetic surfaces based on the immobilization of hyaluronan and bioactive molecules. This fulfills objective 1a of the thesis.

Manuscript 3, accepted for publication in *Biomaterials*, reports on the surface modification of endovascular stents with a thromboresistant coating incorporating radionuclides. This manuscript fulfills objective 1b of the thesis.

Manuscript 4, accepted for publication in *Biomacromolecules*, proposes a hybrid bioactive coating based on the self-assembly of the natural polysaccharide chitosan and hyaluronan. An anti-proliferative component has been loaded in this self-assembled coating. This manuscript fulfills objective 1c of the thesis.

Manuscript 5, to be submitted to *Biomaterials*, describes a biodegradable membrane covered stent based on a chitosan-polyethylene glycol network. This manuscript fulfills objective 2 of the thesis.

Manuscript 6, published in the *Journal of the American Chemical Society*, describes the development of the self-assembled nanocoating on damaged blood vessels.

Manuscript 7, to be submitted, further characterizes the self-assembled nanocoating and extends its use to the local delivery of bioactive molecules such as DNA.

3. LITERATURE REVIEW – SECTION 1: ENDOVASCULAR DEVICES IN REVASCULARIZATION PROCEDURES

3.1. An Introduction to endovascular devices

Stents are metallic implantable tubular devices (Fig. 1) used as mechanical scaffolds to the vascular wall during revascularization procedures of coronary or peripheral arteries or lumen enlargement of hollow structure such as the tracheo-bronchial tree biliary duct and urinary tract. 316L stainless steel, nitinol – or NiTi alloy, tantalum and cobalt-chromium-based alloys are the materials most commonly used in the design of endovascular devices. The beneficial effect of coronary stenting over conventional balloon angioplasty has been demonstrated in the BELgian-NEtherlands STENT (BENESTENT-I) and Stent REStenosis Study (STRESS) studies in the early 90's^{1,2}. In these landmark studies, restenosis, defined as the renarrowing of the vessel (definition angiographic: >50% diameter stenosis at 6 months follow-up), was significantly reduced. Since then, intensive research in the field of adjunctive pharmacological therapies, implantation techniques and stent design have further reduced the clinical outcomes associated with stent implantation, namely sub-acute thrombosis and need for target vessel revascularization (restenosis). Stenting is now a well-established technique in endovascular interventions, representing as much as 70-85 % of all percutaneous coronary interventions, with about 1,000,000 stents being placed each year worldwide. Currently, more than fifty types of stents, and, more recently, stent-grafts with various designs (mesh structure, coil, slotted tube, ring, etc) and compositions, have received FDA approval or CE marking. The worldwide market is estimated to be US\$5 billion in 2002 for both coronary and peripheral interventions, with an annual growth rate of 5%. The recent availability of drug-eluting stents with perspectives of even greater

restenosis reduction potential is likely to change the features of interventional cardiology.

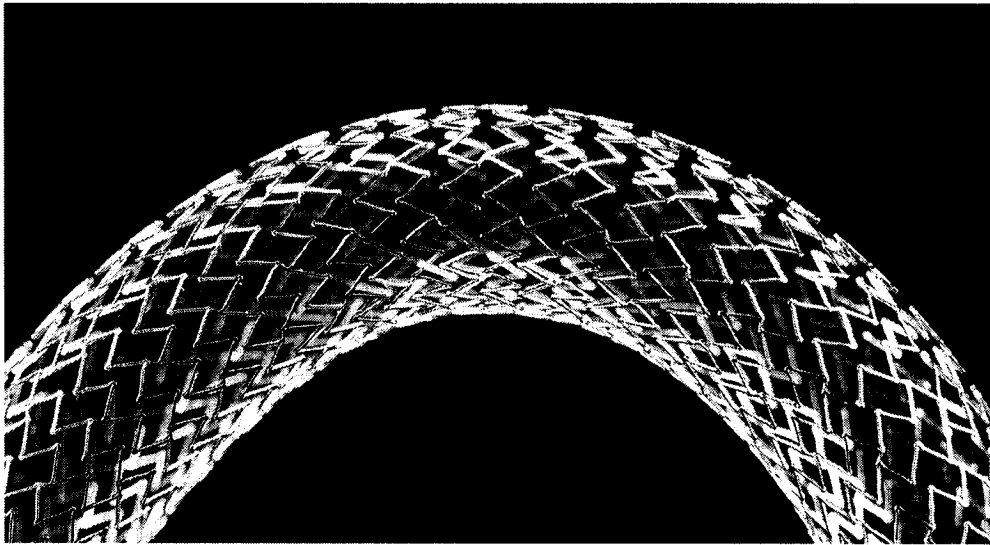


Figure 3.1. Current stent designs and materials allow increased flexibility. Nitinol SMART stent from Nitinol Devices & Components.

3.1.1. Historical perspectives

Charles Dotter introduced the idea of endovascular stents in 1964, and demonstrated in 1983 its feasibility in the revascularization of diseased arteries. Stents were initially investigated to prevent recoil and constrictive remodeling of balloon revascularized arteries. In 1986, Jacques Puel performed the first human coronary stent implantation in Toulouse (France) using an ancestor of the self-expandable Wallstent. Since then, the BENESTENT and STRESS studies have shown the beneficial effects of elective coronary stenting following balloon angioplasty, versus angioplasty alone, in coronary revascularization (Table I) ^{1; 2}. The beneficial effect of stent over balloon angioplasty has been attributed to larger acute lumen dimensions and to the prevention of constrictive remodeling. The Palmaz-Schatz stent was the first FDA approved device in 1994. Two major breakthroughs have clearly expanded the use of stents in percutaneous

revascularization procedures and significantly improved the initial outcomes of the procedures: Intravascular ultrasound (IVUS) and anti-platelet therapy. IVUS studies have demonstrated the importance of *optimal* stent deployment (Symmetry, struts apposition, minimal area) and the need for high-pressure balloon post-inflation to achieve proper stent expansion within the vessel ³. The optimal stent deployment concept suppressed the need for anti-vitamin K therapy (Warfarin) and in turn reduced the risk of bleeding. The benefit of antiplatelet therapy over traditional therapy, based on heparin and coumadin, along with aspirin and dipyridamole, namely significant reduction in sub-acute thrombosis and bleeding was demonstrated in the randomized ISAR and STARS trials (Table I). Current revascularization procedures with stents are characterized by thrombotic occlusion rates lower than 2% and very high procedural success rates (> 95%).

Table 3.1 Selected randomized clinical trials

Trial		Composite events	Restenosis
BENESTENT	Balloon	AC=2.7 %	32 %
	Stent	AC=3.5 %	22 %
STRESS	Balloon	AC=1.5 %	42 %
	Stent	AC=3.4 %	31 %
ISAR	ASA+Triclo	D, MI, Rev= 1.6 %	-
	ASA only	-	-
	ASA+Coumarin	D, MI, Rev= 6.2 %	-
STARS	ASA+Triclo	D, MI, Rev= 0.6 %	-
	ASA only	D, MI, Rev= 3.6 %	-
	ASA+Coumarin	D, MI, Rev= 2.4 %	-
SISA	Balloon	AC= 7.1 %	33 %
	Stent	AC= 3 %	28 %
SIRIUS	Stent	-	35 %
	Sirolimus-coated stent	-	3 %
TAXUS	Stent	AC= 0 %	11 %
	Taxol-coated stent	AC= 0 %	0 %

BELgian NETHERlands STENT (BENESTENT), Stent REStenosis Study (STRESS), Intracoronary Stenting and Antithrombotic Regimens (ISAR), STent Anticoagulation Regimen Study (STARS), Stenting In Small Arteries (SISA), SIRolImUS (SIRIUS); ASA: Aspirin, Triclo: Triclopidine; AC: Acute Closure, D: Death, Rev: Revascularization.

3.1.2. Clinical indications

Stents reduce the risk of acute vessel closure and its consequence, the need for emergency coronary artery bypass graft surgery, and have been demonstrated to improve clinical outcomes in specific conditions. From randomized trials, those conditions are the treatment of abrupt or threatened vessel closure during angioplasty, primary reduction in restenosis in *de novo* focal lesions in vessels > 3 mm in diameter, focal lesions in saphenous vein grafts, and chronic total occlusions ⁴. Stents are also successfully used in many other conditions such as restenotic lesions, acute coronary syndromes (unstable angina and acute myocardial infarction), multivessel diseases, and the treatment of iliac and renal artery stenosis. However, their benefit in bifurcating lesions, in small vessel diameters (<3mm), in diabetic patients, and in diseases of the femoral, popliteal and carotid arteries is still being debated. The use of stents is likely to increase due to the recent availability of devices designed to treat these specific conditions, such as small artery or vein graft disease, as well as broadening of the available stent properties.

3.1.3. Complications

In spite of major technical advances in the past two decades, endovascular revascularization procedures remain limited by the cascade of events subsequent to device implantation.

Subacute thrombosis

Early stent implantations were plagued by a high rate of thrombotic occlusions (8-10%) of the revascularized vessel, mainly due to suboptimal deployment of the devices and its inherent thrombogenicity. As previously mentioned, high pressure deployment techniques combined with enhanced antiplatelet therapy have drastically reduced the risk of vessel thrombotic occlusion of the vessel (1.7%). The thrombogenicity of the metallic alloys may still contribute to platelet activation, and in turn initiate neointimal hyperplasia.

In-Stent Restenosis

Despite reduced restenosis rates in short lesions such as demonstrated in randomized trials, stenting is still associated with late in-stent restenosis. Based on clinical studies, restenosis rate can range from 8 to 50% depending on lesion complexity, reference vessel diameter plaque burden and systemic conditions such as diabetes ^{5; 6}. In-stent restenosis is a multi-factorial phenomenon that involves thrombus formation, inflammation, cellular proliferation and extra-cellular matrix synthesis within the treated vessel ⁷. The cascade of events is initiated by arterial injury following angioplasty and is usually limited to the first 6 months following the procedure. Thrombus growth resulting from exposure of the extra cellular matrix in the endothelium-denudated vessel wall and from the presence of the metallic device lead to the release of biological factors, including PDGF- β , TGF- β , bFGF, thrombin, etc, which in turn can initiate medial smooth muscle cell migration (SMC) and proliferation. Medial injury with disruption of the internal elastic laminae also directly stimulates SMCs migration and proliferation. This cell growth is associated with extracellular matrix secretion that further participates in the neointimal thickening. The presence of

inflammatory cells has been reported in addition to SMCs in the surrounding tissues⁸. A strong correlation between the extent of medial damage, inflammation and restenosis has been reported from human pathological studies⁷. There is growing evidence that neointimal hyperplasia following stent implantation is strongly related to a prolonged inflammatory state of the stented artery.

Issues such as stent embolization, side branch occlusion, coronary perforation or infection of the stented vessels are infrequent complications but could have potentially catastrophic effects.

3.1.4. Metallic Alloys Used in Endovascular Procedures

While many efforts have focused on the development of devices with improved design, biofunctionality and surface properties, only a few alloys are routinely employed for stent manufacturing. They are generally made from one of three alloy classes: 316L stainless steel, nitinol (or NiTi alloy), and, to a lesser extent, cobalt-chromium alloy such as Elgiloy®.

The differences in the mechanical properties of these materials strongly influence the properties of the devices and thus possibilities in terms of design. Stainless steel-based stents are balloon-expandable devices that require a plastic deformation to be deployed in the treated artery. Nitinol is gaining popularity in the design of multiple permanent vascular implants, such as coronary and peripheral stents, atrial septal defect occlusion systems, and vena cava filters, due to its unique mechanical properties. These devices can be designed as self-expandable due to the superelasticity of nitinol (Figure 3.2). Tantalum was also used in the manufacture of coronary stents such as the Wiktor-GX but was nearly abandoned due to its exaggerated radiopacity. Cobalt chromium alloy

stents are currently under investigation (Multi-link Vision, Guidant and S8, Medtronic AVE). These alloys enable thinner strut thickness compared with stainless steel-based devices without reducing radial strength and radiopacity. They may also be less prone to biocorrosion than stainless steel devices.

New materials are being investigated to improve mechanical properties, radiopacity, MRI compatibility and haemocompatibility^{9; 10}. Differences in RX radiopacity and magnetic resonance compatibility inherent in the materials themselves translate clinically into differences in the visibility of the devices. Radiopaque markers, mainly gold and platinum, may be used to improve the visibility of these devices (e.g. beStent with proximal and distal gold markers).

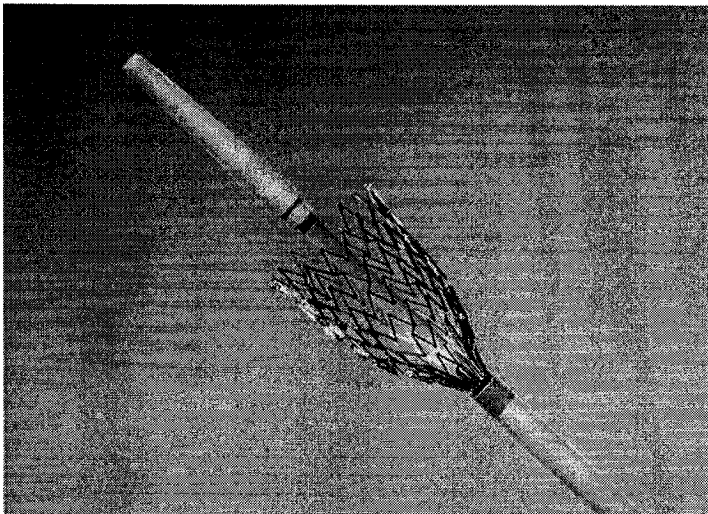


Figure 3.2. Deployment of a self-expandable stent

3.1.5. Biomechanical considerations

“The greater lumen the better” concept that has prevailed based on minimal lumen diameter as the strongest predictive factor for restenosis, has led to the idea that all stents were equals in terms of clinical outcomes. As a consequence, stents were

evaluated on their potential to achieve maximal lumen gain. There is now evidence that stent design also strongly influences the outcome of the revascularization procedure. Recent studies have indeed pointed out the dependency of thrombus formation and neointimal proliferation on the type and design of the stent ¹¹⁻¹³. Follow-up angiography in a cohort of 3,370 patients has shown that stent design was the second strongest risk factor, after artery size, with restenosis ranging from 20.0% to 50.3%, depending on the stent type ¹³. It seems that reduced strut thickness represents the crucial factor for restenosis prevention. Much work remains, however, to determine precisely which features of the stent are detrimental to implantation.

The “ideal” stent, should have a low profile, good trackability, and flexibility with a high- and well-distributed radial strength for optimal scaffolding (Table 3.2). The delivery system should be highly reliable and allow precise placement of the device. The improvements in both delivery system and device properties have drastically increased the conditions wherein stents could be used, e.g., the availability of a stent designed specifically for small arteries. The beStent (4-crown from Medtronic AVE) was compared in randomized studies to balloon angioplasty and proved to be superior in the treatment of <3 mm vessels. In addressing a wide variety of vessels and indications, the concept of an ideal stent has been evolving toward the idea that a different stent would best suit each indication. Nonetheless, it is likely that the choice of the best device will continue to rely on the clinician’s expertise on a case-to-case basis.

Table 3.2 Characteristic of the ideal stent

Low profile	Thromboresistance
Reliable delivery system	Biocompatibility
Trackability	Corrosion resistance
Elasticity	Radiopacity
Flexibility	
Conformity	
Uniform radial strength	
Availability for various lesions	

It is obvious that the intrinsic properties of the material itself influence the overall biomechanical properties of the device and should be taken into consideration in their design. While stainless steel stents are mainly used in intracoronary procedures, NiTi alloy is becoming the material of choice for peripheral applications. Nitinol stents differ in many aspects from stainless steel or tantalum stents. Indeed, the properties of balloon stents are mainly related to their design. There are currently four designs widely used, i.e., slotted tube stents, ring stents and, to a much lesser extent, mesh stents and coil stents. Slotted tube stents are the most widely used devices (beStent 2, Multilink Tetra, BiodivYsio, etc) and are characterized by good radial strength but less conformability, compared with ring stents (AVE S670-S7, NIR, etc), which are made of repeating cells and usually display good flexibility, more suitable for the treatment of lesions requiring good conformability. New slotted tube design devices with thinner stent struts, such as the PURA AS, the Sorin Carbostent or the 0.08-mm Tenax, could also perform well in such applications.

3.1.6. Inorganic coatings

Inorganic coatings have been investigated on endovascular stents, such as diamond-like carbon, hydrogen-rich amorphous silicon carbide (a-SiC:H) and amorphous titanium oxide¹⁴⁻¹⁶. Such inorganic coatings improve the overall biocompatibility of the stent with the advantage of low thrombogenicity in comparison with uncoated devices. In addition, titanium-nitric-oxide-coated stainless steel stents significantly reduced neointimal hyperplasia in an experimental model¹⁷. Along with increased biocompatibility, these inorganic coatings may also improve significantly the corrosion properties and in turn reduce the release of ions in the surrounding vessel wall. Five inorganic-coated stents are available: Tenax (Biotronik, Germany), Sirius Carbostent (Sorin Biomedica Cardio, Italy), Diamond Flex (Phystis, Germany), BioDiamond

(Plasma Chem, Germany) and the MAC carbon stent (AMG, Germany). To date, the long-term beneficial effects of inorganic coatings have not been demonstrated by randomized trials. Gold coatings have also been used with the expectation that the inertness of gold would increase the overall biocompatibility while increasing the radiopacity of the device. Clinical studies have, however, reported an increased likelihood for restenosis that may be related to coating defect rather than gold itself¹⁸. This strongly suggests that, along with biomechanical considerations, the processing itself could influence the outcome of the procedure.

3.1.7. Thromboresistant coatings

Many approaches have been investigated to reduce thrombogenicity of metallic endovascular stents, using heparin, phosphorylcholine or r-hirudin coatings, for instance. While these coatings have been proven to reduce thrombus formation on the device and as a consequence lower the subacute thrombosis rate in animal model, the beneficial long-term clinical impact of these devices remains uncertain. Heparin-coated stents are commercially available and have been investigated in many experimental and clinical studies. For example, the heparin-coated BX Velocity stent, wherein heparin is immobilized on the surface and remains free to inhibit thrombi formation, has recently been accepted by the FDA. These devices are well tolerated but failed to prevent neointimal hyperplasia^{5; 6}. Along with its anti-coagulant properties, heparin has been shown, *in vitro*, to have an anti-proliferative action on SMCs. However, local delivery of heparin from either delivery catheters or stents did not prove to be beneficial. The lack of activity of heparin-coated devices is likely to be related to suboptimal tissue concentration of the drug. Phosphorylcholine-coated Biodiv Ysio stents also hold promise in revascularization of small arteries, which remains a very challenging issue. Phosphorylcholine coating has been demonstrated *in vitro* to prevent strongly platelet adhesion to the metallic surface. The phosphorylcholine-based coating is also being investigated as a drug delivery platform through hydrophobic interactions^{19; 20}.

3.1.8. Membrane-covered stents

As initially described by Parodi, stent-grafts or membrane-covered stents are subclasses of stents developed for the endovascular treatment of abdominal aortic aneurysms (AAA)²¹. Stent-grafts are made of a conventional segment of bypass graft supported at the ends by expandable metallic stents. Membrane-covered stents are endovascular stents covered with or covering a synthetic membrane (Fig. 3). The membrane is usually made of a conventional surgical material such as Dacron, ePTFE or polyurethane. These devices are currently being used or are in clinical trials for aneurysmal or AV-fistula repair, arterial rupture sealing, coronary and peripheral occlusive diseases and for the treatment of aortocoronary vein graft disease²²⁻²⁵. In the particular setting of saphenous vein graft disease, membrane covered stents, either PTFE sandwiched between 2 stainless steel layers (JOGRAFT, JOMED) or stainless steel sandwiched between 2 PTFE layers (SYMBIOT, Boston Scientific), are being investigated with the goal of reducing the risk of distal embolization of the friable plaque and reducing restenosis.

Chronic inflammatory reactions and delayed endothelialization of the membrane have been reported following implantation²⁶. The impaired endothelialization of the synthetic membranes could translate into higher risk of sub-acute thrombosis rates. One-year implantation studies, however, by Virmani *et al.* have demonstrated good results with ePTFE-nitinol grafts, with complete endothelialization observed within 6 months²⁷. Issues such as graft migration, graft fretting against the vascular wall, extravasation of blood into the aneurysm sac after stent-graft deployment so-called endoleak, and structural failure of the graft, such as those reported by Guidoin *et al.*, however, give rise to some concerns about the long-term efficacy of these devices²⁸.

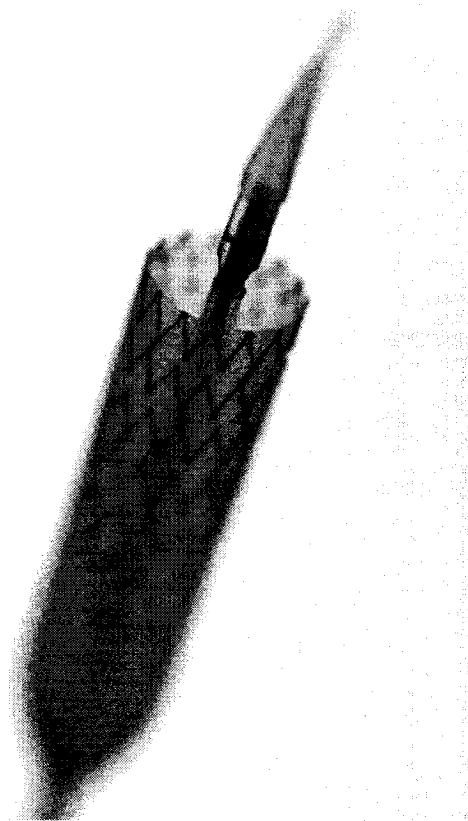


Figure 3.3. Membrane-covered stent during its deployment.

3.1.9. Radioactive stents

Brachytherapy, i.e. the use of radiotherapy to inhibit neointimal proliferation, represent the treatment of choice if in-stent restenosis occurs. Radiation treatments inhibit the ability of cells to clonogenically divide, thus preventing acute cellular proliferation and migration, usually triggered by vascular wall injury. It is delivered in situ via catheter based removable radioactive source (Ribbon or beads). Stents have also been investigated as a radiation delivery platform with the idea that prolonged exposure of the arterial wall to low radiation doses may be beneficial ²⁹. Most of the experiments have been performed using 32-phosphorus implanted stents. Dose-dependant inhibition has been reported with the β -emitting ³²P stents ³⁰. Edge-restenosis caused by intense radiation decay at stent outer limits and high rate of subacute thrombosis have limited

their development³¹. The hot-ends approach has been proposed to circumvent the edge-effect by reducing the dose's fall-off at the stent margins. Conversely, the investigation of radionuclides with more appropriate physical properties (γ radiation, shorter half-life, etc) could renew interest in the field. The emergence of efficient anti-restenosis drug-eluting stents will likely restrict use of radiation therapy as a mode of treatment of restenosis.

3.1.10. Biodegradable stents

While the scaffolding effect of the stent is beneficial in the short term, the presence of metallic devices may mediate chronic inflammatory reactions and in turn stimulate restenosis. To circumvent the latter, the concept of a biodegradable stent has been proposed. This stent should display the same mechanical properties, e.g., radial strength, of a metallic implant but then slowly disappear (biodegradation) once the artery is stabilized. Tamai and coworkers have recently reported the first clinical application of biodegradable stents made of poly-L-lactic acid (PLLA) monofilament. Follow-up at 6 months indicated an acceptable rate of restenosis (10.6 %) ³². The potential of local delivery of biologically-active components from such biodegradable stents may favor their development.

It is noteworthy that the intriguing concept of a metallic biodegradable stent based on corrosion biodegradation of magnesium or iron (Fe >99.8%) has been recently introduced, respectively, by Heublein et al. and Peuster et al. ^{33; 34}.

3.1.11. Drug-eluting stents

The development of drug-eluting stents, that could efficiently deliver biologically-active drugs to the vascular wall, has been the object of much investigation in recent years. Early work using various drugs and coatings were often disappointing due to poor drug efficacy, uncertain drug dosage or require duration of delivery and most commonly unstable and pro-inflammatory polymeric coating. The excellent results recently reported using anti-proliferative drugs, such as sirolimus and paclitaxel, have, however, generated hope that restenosis will no longer compromise endovascular revascularization³⁵⁻³⁸. These cytotoxic hydrophobic drugs derived from cancer chemotherapy or kidney allograft rejection treatment can be retained in the vascular wall when eluted from the stent and can selectively target proliferating cells within the artery. The mechanical scaffold offered by the metallic stent conjugated with the anti-proliferative properties of these drugs translate, at least in initial clinical studies, into very low restenosis rates. The CE Mark approval of the sirolimus-coated Cypher™ stent (Cordis) and the enthusiastic results of the US SIRIUS trial with this device have further motivated ever-increasing activity in the field of drug-eluting stents. Sirolimus is a natural macrocyclic lactone with potent anti-proliferative and anti-inflammatory properties. Sirolimus eluted from the stent platform binds to SMCs cytosolic receptor proteins and inhibits cyclin-dependent kinase complexes, thus mediating cell arrest in the late G1 phase. Paclitaxel prevents microtubule organization and as a consequence inhibits several steps in SMC migration and proliferation. Along with sirolimus and paclitaxel, many drugs are currently under investigation for stent-based delivery. This includes everolimus, tacrolimus, estradiol, dexamethasone, angiopeptin, batimastat and c-myc antisense oligonucleotide.

Regardless of the type of drug, proper coating and drug delivery platform remain the key issue in optimizing the anti-restenotic effect of these devices. Two different approaches are currently being used to achieve delivery of the drugs, i.e., polymer-coated devices (Cordis/sirolimus Cypher stent and Boston Scientific/paclitaxel stent) and direct elution from dip-coated stents (Cook/paclitaxel stent). The potential long-

term degradation and inflammatory effect of the polymer coatings versus control of the release rate are the key elements in the debate between these two approaches. The disappointing results obtained in the Guidant's DELIVER trial, using Cook Inc's ACHIEVE™ stent that did not employ a polymer coating to elute the drug, suggest that sustained release is highly desirable to optimize the beneficial action of the drug. However, much work remains to be done to assess the long-term safety of these new devices and determine their clinical potential. Along with possible damaging effects to the artery of the anti-proliferative components, the biocompatibility of the coated surfaces requires further investigation and potentially optimization. In particular, delayed reendothelialization and late thrombosis seems to be a potential outcome of these anti-proliferative strategies ³⁹. The very low restenosis rates observed so far (< 5%) in clinical trials using drug-eluting stents may just represent a delayed healing, and long-term studies in humans are required to show whether the benefit is maintained.

3.1.12. CONCLUSIONS

Over the past decade, stenting has become the procedure of choice in many intra arterial revascularization procedures. Advances in stent technology are likely to further increase their use in an always growing number of conditions. In particular, new devices with excellent mechanical properties based on improved design or new materials offer exciting possibilities to treat challenging pathologies. The availability of devices designed to specific situations like small vessels diseases or bifurcation lesions is also noteworthy. Drug eluting stents that locally deliver therapeutic amounts of anti-proliferative drugs may solve the issue of restenosis that have continuously plagued stent implantation. Despite the increase in cost associated with the used of these devices, the elimination of restenosis will translate in a further increase use of stent toward balloon angioplasty and surgery. The success of the pharmaceutical strategies combined with stents has however increased the hope that pharmaceutical strategies alone will be able to cure endovascular diseases. Systemic therapies with new drugs, nanoparticle-

based local drug delivery, and gene therapy are for example promising research areas that could in the future reduce the need for the mechanical scaffold to the vascular wall offered by the stents.

3.1.13. Reference

1. Serruys PW, de Jaegere P, Kiemeneij F, Macaya C, Rutsch W, Heyndrickx G, Emanuelsson H, Marco J, Legrand V, Materne P, et al: A comparison of balloon-expandable-stent implantation with balloon angioplasty in patients with coronary artery disease. Benestent Study Group. *N Engl J Med* 1994;331:489-95
2. Fischman DL, Leon MB, Baim DS, Schatz RA, Savage MP, Penn I, Detre K, Veltri L, Ricci D, Nobuyoshi M: A randomized comparison of coronary-stent placement and balloon angioplasty in the treatment of coronary artery disease. Stent Restenosis Study Investigators. *N Engl J Med* 1994;331:496-501
3. Moussa I, Di Mario C, Di Francesco L, Reimers B, Blengino S, Colombo A: Subacute stent thrombosis and the anticoagulation controversy: changes in drug therapy, operator technique, and the impact of intravascular ultrasound. *Am J Cardiol* 1996;78:13-7
4. Gershlick AH: Role of stenting in coronary revascularisation. *Heart* 2001;86:104-12
5. Babapulle MN, Eisenberg MJ: Coated stents for the prevention of restenosis: Part II. *Circulation* 2002;106:2859-66
6. Babapulle MN, Eisenberg MJ: Coated stents for the prevention of restenosis: Part I. *Circulation* 2002;106:2734-40

7. Welt FG, Rogers C: Inflammation and restenosis in the stent era. *Arterioscler Thromb Vasc Biol* 2002;22:1769-76
8. Grewe PH, Deneke T, Machraoui A, Barmeyer J, Muller KM: Acute and chronic tissue response to coronary stent implantation: pathologic findings in human specimen. *J Am Coll Cardiol* 2000;35:157-63
9. Bhargava B, De Scheerder I, Ping QB, Yanming H, Chan R, Soo Kim H, Kollum M, Cottin Y, Leon MB: A novel platinum-iridium, potentially gamma radioactive stent: evaluation in a porcine model. *Catheter Cardiovasc Interv* 2000;51:364-8
10. van Dijk LC, van Holten J, van Dijk BP, Matheijssen NA, Pattynama PM: A precious metal alloy for construction of MR imaging-compatible balloon-expandable vascular stents. *Radiology* 2001;219:284-7
11. Colombo A, Stankovic G, Moses JW: Selection of coronary stents. *J Am Coll Cardiol* 2002;40:1021-33
12. Kandzari DE, Tchong JE, Zidar JP: Coronary artery stents: evaluating new designs for contemporary percutaneous intervention. *Catheter Cardiovasc Interv* 2002;56:562-76
13. Kastrati A, Mehilli J, Dirschinger J, Pache J, Ulm K, Schuhlen H, Seyfarth M, Schmitt C, Blasini R, Neumann FJ, Schomig A: Restenosis after coronary placement of various stent types. *Am J Cardiol* 2001;87:34-9
14. Nan H, Ping Y, Xuan C, Yongxang L, Xiaolan Z, Guangjun C, Zihong Z, Feng Z, Yuanru C, Xianghuai L, Tingfei X: Blood compatibility of amorphous titanium oxide films synthesized by ion beam enhanced deposition. *Biomaterials* 1998;19:771-6
15. Gutensohn K, Beythien C, Bau J, Fenner T, Grewe P, Koester R, Padmanaban K, Kuehn P: In vitro analyses of diamond-like carbon coated stents. Reduction Of metal ion release, platelet activation, and thrombogenicity. *Thromb Res* 2000;99:577-85
16. Heublein B, Ozbek C, Pethig K: Silicon carbide-coated stents: clinical experience in coronary lesions with increased thrombotic risk. *J Endovasc Surg* 1998;5:32-6

17. Windecker S, Mayer I, De Pasquale G, Maier W, Dirsch O, De Groot P, Wu YP, Noll G, Leskosek B, Meier B, Hess OM: Stent coating with titanium-nitride-oxide for reduction of neointimal hyperplasia. *Circulation* 2001;104:928-33
18. Kastrati A, Schomig A, Dirschinger J, Mehilli J, von Welser N, Pache J, Schuhlen H, Schilling T, Schmitt C, Neumann FJ: Increased risk of restenosis after placement of gold-coated stents: results of a randomized trial comparing gold-coated with uncoated steel stents in patients with coronary artery disease. *Circulation* 2000;101:2478-83
19. New G, Moses JW, Roubin GS, Leon MB, Colombo A, Iyer SS, Tio FO, Mehran R, Kipshidze N: Estrogen-eluting, phosphorylcholine-coated stent implantation is associated with reduced neointimal formation but no delay in vascular repair in a porcine coronary model. *Catheter Cardiovasc Interv* 2002;57:266-71
20. Lewis AL, Tolhurst LA, Stratford PW: Analysis of a phosphorylcholine-based polymer coating on a coronary stent pre- and post-implantation. *Biomaterials* 2002;23:1697-706
21. Parodi JC, Ferreira M: Historical prologue: why endovascular abdominal aortic aneurysm repair? *Semin Interv Cardiol* 2000;5:3-6
22. Kribs S: Endovascular stent grafting: a review. *Can Assoc Radiol J* 2001;52:145-52
23. Baldus S, Koster R, Reimers J, Kahler J, Meinertz T, Hamm CW: Membrane-covered stents: a new treatment strategy for saphenous vein graft lesions. *Catheter Cardiovasc Interv* 2001;53:1-4
24. Stockx L: Stent-grafts in the superficial femoral artery. *Eur J Radiol* 1998;28:182-8
25. Kessel DO, Wijesinghe LD, Robertson I, Scott DJ, Raat H, Stockx L, Nevelsteen A: Endovascular stent-grafts for superficial femoral artery disease: results of 1-year follow-up. *J Vasc Interv Radiol* 1999;10:289-96
26. Dolmatch BL, Dong YH, Trerotola SO, Hunter DW, Brennecke LH, LaBounty R: Tissue response to covered Wallstents. *J Vasc Interv Radiol* 1998;9:471-8

27. Virmani R, Kolodgie FD, Dake MD, Silver JH, Jones RM, Jenkins M, Gillespie DL: Histopathologic evaluation of an expanded polytetrafluoroethylene- nitinol stent endoprosthesis in canine iliofemoral arteries. *J Vasc Interv Radiol* 1999;10:445-56
28. Guidoin R, Marois Y, Douville Y, King MW, Castonguay M, Traore A, Formichi M, Staxrud LE, Norgren L, Bergeron P, Becquemin JP, Egana JM, Harris PL: First-generation aortic endografts: analysis of explanted Stentor devices from the EUROSTAR Registry. *J Endovasc Ther* 2000;7:105-22
29. Chorny M, Fishbein I, Golomb G: Drug delivery systems for the treatment of restenosis. *Crit Rev Ther Drug Carrier Syst* 2000;17:249-84
30. Drachman DE, Simon DI: Restenosis: Intracoronary Brachytherapy. *Curr Treat Options Cardiovasc Med.* 2002;4:109-118
31. Serruys PW, Kay IP: I like the candy, I hate the wrapper: the (32)P radioactive stent. *Circulation* 2000;101:3-7
32. Tamai H, Igaki K, Kyo E, Kosuga K, Kawashima A, Matsui S, Komori H, Tsuji T, Motohara S, Uehata H: Initial and 6-month results of biodegradable poly-l-lactic acid coronary stents in humans. *Circulation* 2000;102:399-404
33. Heublein B, Rhode R, Huasdorf G, Hartung W, Haverich R: Biocorrosion, a new principle for temporary cardiovascular implants ? *Eur. Heart J.* 2000;21:286
34. Peuster M, Wohlsein P, Brugmann M, Ehlerding M, Seidler K, Fink C, Brauer H, Fischer A, Hausdorf G: A novel approach to temporary stenting: degradable cardiovascular stents produced from corrodible metal-results 6-18 months after implantation into New Zealand white rabbits. *Heart* 2001;86:563-9
35. Rensing BJ, Vos J, Smits PC, Foley DP, van den Brand MJ, van der Giessen WJ, de Feijter PJ, Serruys PW: Coronary restenosis elimination with a sirolimus eluting stent: first European human experience with 6-month angiographic and intravascular ultrasonic follow-up. *Eur Heart J* 2001;22:2125-30
36. Heldman AW, Cheng L, Jenkins GM, Heller PF, Kim DW, Ware M Jr, Nater C, Hruban RH, Rezai B, Abella BS, Bunge KE, Kinsella JL, Sollott SJ, Lakatta EG, Brinker JA, Hunter WL, Froehlich JP: Paclitaxel stent coating inhibits neointimal

hyperplasia at 4 weeks in a porcine model of coronary restenosis. *Circulation* 2001;103:2289-95

37. Fox R: American Heart Association 2001 scientific sessions: late-breaking science-drug-eluting stents. *Circulation* 2001;104:E9052

38. Sousa JE, Costa MA, Abizaid AC, Rensing BJ, Abizaid AS, Tanajura LF, Kozuma K, Van Langenhove G, Sousa AG, Falotico R, Jaeger J, Popma JJ, Serruys PW: Sustained suppression of neointimal proliferation by sirolimus-eluting stents: one-year angiographic and intravascular ultrasound follow-up. *Circulation* 2001;104:2007-11

39. Liistro F, Colombo A: Late acute thrombosis after paclitaxel eluting stent implantation. *Heart* 2001;86:262-4

4. LITERATURE REVIEW – SECTION 2: BIOSTABILITY AND BIOCOMPATIBILITY OF ENDOVASCULAR DEVICES

4.1. Paper 1.

Biocompatibility and biostability of metallic endovascular implants – states of the art and perspectives

Benjamin Thierry; Maryam Tabrizian

Copyright © 2003 J Endovasc Ther. 2003 Aug;10(4):807-24.

Reprinted by permission of the International Society of Endovascular Specialist

4.1.1. Abstract

More than one million metallic endovascular devices are implanted each year, but the quest for the perfect material continues. In this article, the relative properties of metallic materials commonly used in these endovascular applications are reviewed. The importance of interfacial properties in the overall biocompatibility of metals and alloys

has been recognized for a long time and will be addressed. Particularly, in blood contacting devices setting, these properties modulate their hemocompatibility and in turn, strongly influence implantation outcomes. Particular emphasis is given in this paper to the potential corrosion of metallic endovascular materials. Recent retrieval analysis of stent-grafts in the Eurostar registry have indeed shown worrying evidence of degradation of the metallic frame over time, which is not surprising as any implanted metallic device is prone to corrosion. The corrosion behavior of metallic endovascular materials will be discussed along with the specific surface treatments used in the production processes. Issues relative to corrosion assays will be also reviewed in terms of their relevance to *in vivo* applications. The biocompatibility of metallic implants is indeed strongly related to the amount and toxicity of degradation material released in the surrounding tissues. In particular, nickel, chromium and cobalt have been shown to elicit cytotoxic, allergic and carcinogenic reactions, and the potential adverse effects of degradation products with respect to endovascular applications will be described. Finally, this review addresses future perspectives of metallic devices in endovascular procedures in view of the recent promises of anti-proliferative strategies that are likely to profoundly modify current procedures.

Key words: Review, corrosion, stents, restenosis, ions

4.1.2. Introduction to the biocompatibility and biostability of endovascular devices

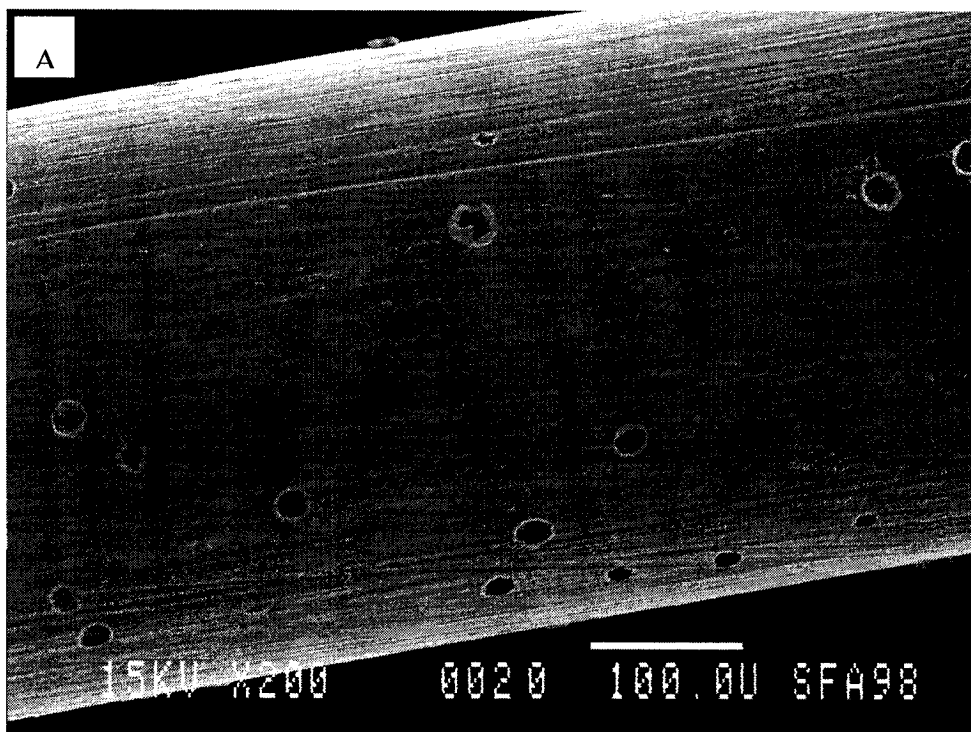
The use of metallic implants in surgery dates back to the 16th century, possibly earlier, with the use of gold in dentistry, still extensively employed in modern clinical practice. Endovascular implants such as stents and stent-grafts take advantage of the mechanical properties of metallic alloys. Stenting is now a well-established technique in

endovascular interventions, representing as much as 70-85 % of all percutaneous coronary interventions, with over 1,000,000 stents being placed each year worldwide. Surprisingly, there is little data on the relative acute and long-term biocompatibility of the metallic alloys used in the manufacture of these devices. 316L stainless steel, Elgiloy[®] and nitinol alloys and, to a much lesser extent, tantalum, MP35N, platinum, etc, are materials commonly used for coronary and peripheral stents, stent-grafts, IVC filters and other endovascular devices. We have previously demonstrated that electropolished nitinol stents were significantly less thrombogenic in an *ex vivo* model than electropolished stainless steel Palmaz stents¹. While the clinical relevance of this difference remains unknown, this study underlies the need for better knowledge of the interfacial reactions between metallic endovascular devices and the biological environment of the artery.

Conversely, as stated by the FDA, the long-term biodegradation of metallic devices remains a serious issue in the biomaterials field². Retrieval analyses of stainless steel plates and screws, implanted for as long as 55 years, have reported no traces of corrosion³. However the question of *in vivo* metallic alloy stability has been raised by the retrieval analysis of stent-grafts showing traces of pitting corrosion and fractures of nitinol wires (Fig. 4.1)^{4; 5}. Moreover, the woven polyester sleeve of explanted Stentor endografts showed holes and openings in the fabric. The extensive changes and damage to these devices after 5 to 53 months of implantation are worrying in view of their long-term patency. In addition to the risk of mechanical loss of integrity, degradation products such as metal ions are a real concern because of their potential adverse biological responses, namely allergy, cytotoxicity, and carcinogenicity. Degradation products are well known for their proinflammatory effects and may be subtle contributors to the inflammatory reactions commonly associated with restenotic arteries. A intriguing relation between nickel and molybdenum contact allergies and occurrence of restenosis following stainless steel stent implantation was also recently suggested by Koster *et al*⁶. Conversely, the disappointing clinical results obtained with the gold-coated stainless steel Inflow stent stressed the importance of appropriate material choice and processing^{7; 8}. These clinical reports underlie the fact that biomaterials used in

cardiovascular applications cannot be considered as stable in the aggressive milieu of the living body. Despite advances in materials sciences, interactions between metallic alloy devices and tissues and physiological fluids/tissues will likely continue to occur. When dealing with this issue, one must address the following questions: to what extent do these interactions damage the implantation and under what time line does this damage occur?⁹

This review aims to present the metals and alloys used in the manufacture of FDA and CE approved endovascular implants and to discuss their relative biocompatibility and biostability. In particular, we address their stability vis a vis corrosive phenomena and discuss the potential adverse biological effects of degradation products with respect to endovascular applications.



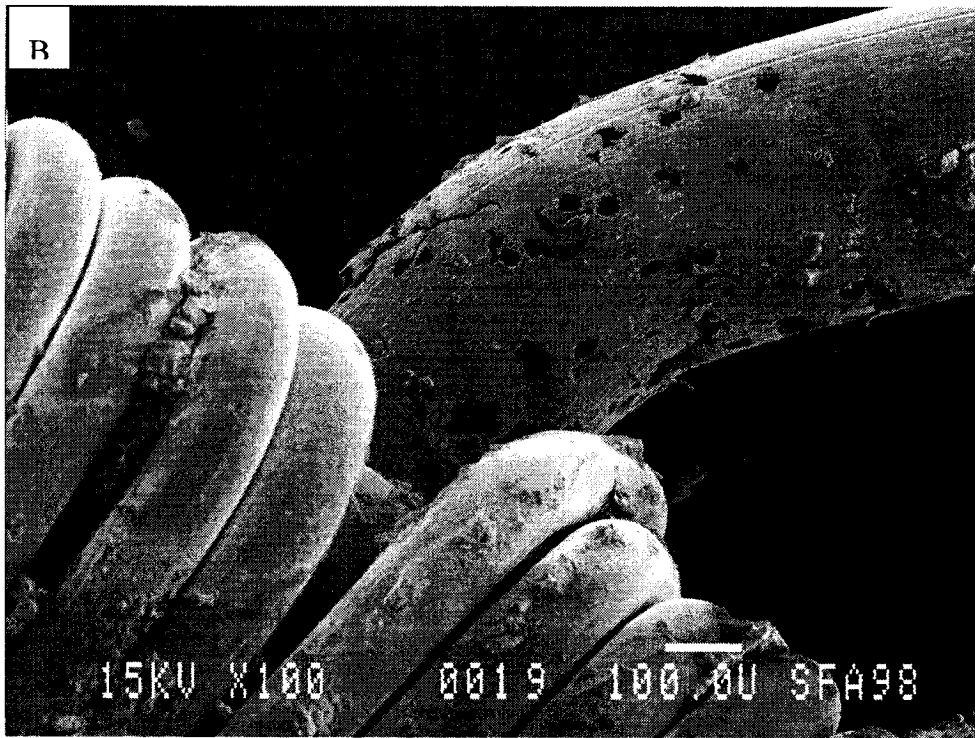


Figure 4.1. Scanning Electron Micrographs of retrieved Stentor endograft showing (A) Severe corroded area close to the platinum marker (x100) and (B) pitting corrosion on the nitinol wire from the endograft metallic frame (x200). Reproduced with authorization of Guidoin et al.

4.1.3. Current concepts in endovascular procedures

Currently, more than fifty types of stents, and more recently stent-grafts, with various designs and compositions have received the FDA approval or CE marking (Table 4.I). The worldwide market is estimated to be US\$2.5 billion for both coronary and peripheral interventions, with an annual growth rate of 5%. In spite of major technical advances in the past two decades, endovascular revascularization procedures remain limited by the subsequent cascade of events following device implantation. Based on clinical studies, the restenosis rate can be expected to be significantly higher than the 8-10 % observed for ideal lesions, and up to 30-50% for complex conditions or specific

associated pathologies such as diabetics^{10; 11}. As schematized in Fig. 2, in-stent restenosis is a multi-factorial phenomenon that involves thrombus formation, inflammation, cellular proliferation and extra-cellular matrix synthesis within the treated vessel.

Table 4.1 Most of the available stents, stent-grafts and membrane-covered stents in 2001

	Stents	Stent- grafts and membrane-covered stents
Stainless steel	Freedom, Freedom Force, Crossflex, GR II, GR I, V-Flex, V-Flex plus, DivYsio, BeStent, IRIS II, Spiral Force, TENAX (a-SiC:H coated), Palmaz-Schatz, JOSTENT Plus, Flex, BX, PURA-A, -VARIO, R-Stent, In Flow, In Flow gold (gold coated), Parallel, Multi-link, SOLO, S-Flex, JoStent, Perflex, Intrastent, AVE Micro II, gfx, BARD xt Navius (Full hard Stainless steel), NIR	Jomed (PTFE) Zenith (polyester)
NiTi	Cardiocoil, Radius, Paragon, SMART, Expender, Memotherm, Symphony	Cragg-Endopro (woven polyester) Passenger (polyester sleeve) Vanguard (dacron) Hemobahn (ePTFE) Talent (dacron) AneuRx (dacron) Quantum LP (polyurethane foam) Excluder (PTFE) Anaconda (dacron) aSpire (PTFE)
Tantalum	Wiktor-GX, -i, TENSUM (a-SiC:H coated), Strecker	
Elgiloy and others	Wallstent	Wallgraft (dacron) Ancure (dacron) LifePath (woven polyester) Endologix (Algiloy, PTFE)

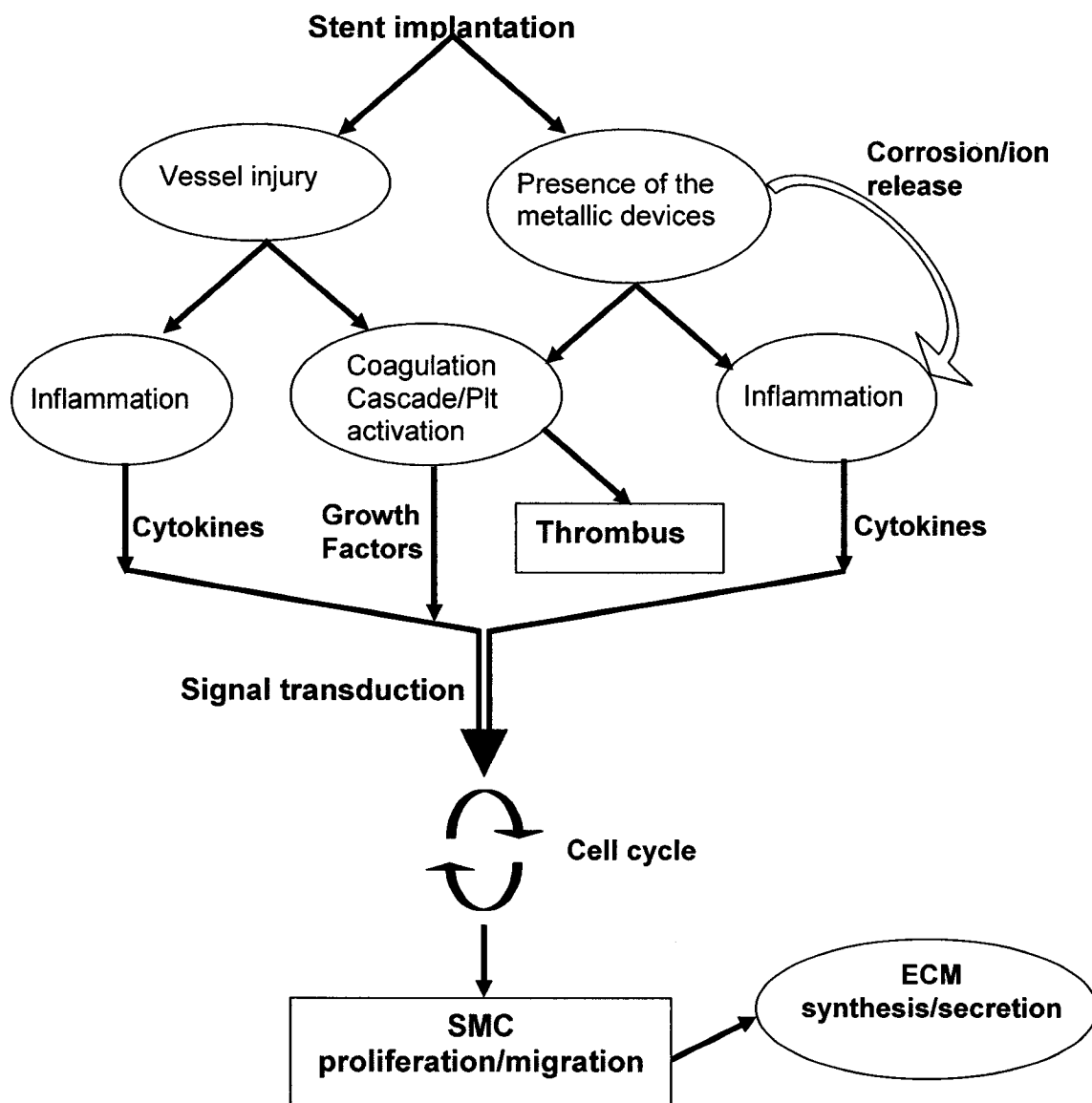


Figure 4.2. Hyperplasia is the response of the artery to the injury created during angioplasty and to the presence of the metallic devices. The end stage of the processes is the proliferation/migration of smooth muscles cells (SMC) and extra-cellular matrix (ECM) synthesis/secretion.

4.1.3.1. Metallic alloys used in endovascular procedures

While many efforts have focused on the development of devices with improved design, biofunctionality and surface properties, only a few alloys are routinely employed in the manufacture of stents and stent-grafts. They are generally made from one of three alloy classes: stainless steel, nitinol (or NiTi alloy), and, to a lesser extent, Elgiloy® (Table 4.2). Medical grade stainless steels (ISO 5832-1 and ASTM F138 and F139) such as the 316 L are austenitic steels with high chromium content (17-19 wt. %) wherein nickel (13-15 wt. %) is used as the primary microstructure stabilizer. Stainless steel-based stents are balloon expandable devices that require a plastic deformation to be deployed in the treated artery. In turn, their properties are mainly related to their design. Nitinol, a nearly equiatomic nickel and titanium intermetallic alloy, is gaining popularity in the design of minimally invasive devices, such as coronary and peripheral stents, atrial septal defect occlusion systems, and vena cava filters, due to its unique mechanical properties. Nitinol-based devices rely on the mechanical properties of the alloy, i.e. superelasticity and shape memory effect, to be self-expanded within the vessel and comprehension of the material's characteristics is necessary in order to understand the device's properties. (For interested readers, more detailed discussions on NiTi alloy properties can be found in the literature^{12;13}). The cobalt-chromium-nickel-molybdenum-iron alloy Elgiloy® described in the ASTM standard F1058-91 is used in the design of the self expandable Wallstent and Wallgraft (Schneider). Tantalum is also used in the manufacture of devices such as Wiktor-GX. New materials are being investigated to improved mechanical properties, radiopacity, MRI compatibility and hemocompatibility^{14; 15}. Differences in RX radiopacity and magnetic resonance compatibility inherent in the materials themselves translate in the clinical practice into differences in the visibility of the devices^{16; 17}. Radiopaque markers, mainly platinum, may be used to improve the visibility of these devices. It is noteworthy that the intriguing concept of a metallic biodegradable stent based on corrosion biodegradation

of magnesium or iron (Fe >99.8%) has been recently introduced, respectively, by Heublein et al. and Peuster et al.^{18; 19}.

Table 4.2 Metals and alloys used in vascular devices and selected properties (E: elastic modulus, YS: yield strength, UTS: ultimate tensile strength, ρ density)

		Composition (wt. %)	Selected properties	Advantages	Disadvantages
316L steel (ASTM F138)	Stainless	C: 0.03 (max.) Mn: 2.0 (max.) P: 0.025 S: 0.01 Si: 0.75 Cr: 17.00-19.00 Ni: 13.00-15.00 Mo: 2.00-3.00 Fe: Balance	E: ~200 Gpa YS: 190-690 UTS: 490-1600 ρ : 7.9 g/cm ³	Cost Availability Processing	Corrosion Incompatibility MRI
NiTi		Ni: 55.5 Co: 0.0275 Cu: 0.010 Fe: 0.022 C: 0.012 Al: 0.05 Nb: 0.01 Si: 0.01 W: 0.0265 Ti: Balance	E: 20 to 83 Gpa YS: 195-690 GPa UTS: 900-1900 ρ : 6.5 g/cm ³	Mechanical properties (Superelasticity and shape memory) Compatibility MRI Thromboresistance	Corrosion Processing Fatigue
Elgiloy (ASTM F1058)		Co : 40% Cr : 20 Ni : 15.5 Mb : 7 Mang : 2 C : 0.15 Fe : balance	E: 200 Gpa YS: 1650-2450 GPa UTS: 2000-2700 Gpa ρ : 8.5 g/cm ³	Compatibility MRI Mechanical properties	Corrosion
Tantalum (ASTM F560)	Ta		E: 180 Gpa YS: 140-345 GPa UTS: 200-500 Gpa ρ : 16.6 g/cm ³	Corrosion Compatibility MRI	Machining Mechanical properties

4.1.3.2. Surface treatments

As stated in the FDA's cardiology guidance documents, particular attention should be paid to the surface treatment of endovascular devices². Most metallic materials used in the manufacture of these devices are indeed passive alloys or metals and in the presence of oxygen, oxides spontaneously grow on the alloy surface (Reaction I&II, Fig. 4.3);

these materials impart their corrosion resistance and surface properties from these uniform oxide layers, e.g. Cr_2O_3 for stainless steel and Elgiloy[®], TiO_2 for nitinol or Ta_2O_5 and TaOH for tantalum. Therefore, the biostability of metal implants often relies on appropriate processing and a surface finish that reinforce the native oxide layer. Treatments such as acid passivation or electropolishing, which is used extensively in the final manufacturing process for endoluminal stents, as prescribed in the ASTM F86 standard²⁰, have been reported to significantly improve the stability of materials such as nitinol and stainless steel, and in turn lower the risks associated with implantation²¹. Electropolishing removes the native oxide to form a more homogeneous layer, resulting in a smoother surface, with roughness in the range of nanometers, suitable for blood contacting devices (Fig. 4.4)^{1; 22}.

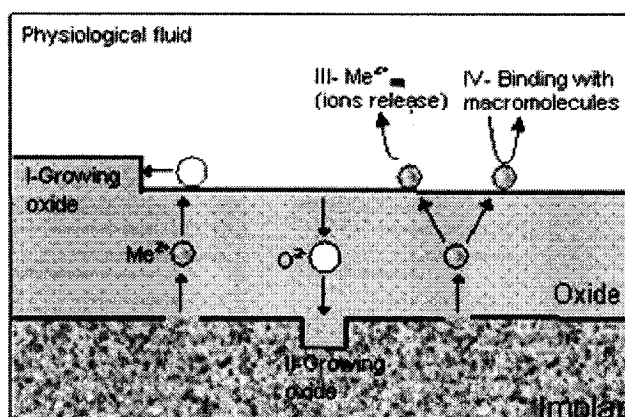


Figure 4.3. Reactivity of a passive metal in physiological fluid; I & II: Growth of the oxide layer, III: ions release and IV: binding with macromolecules

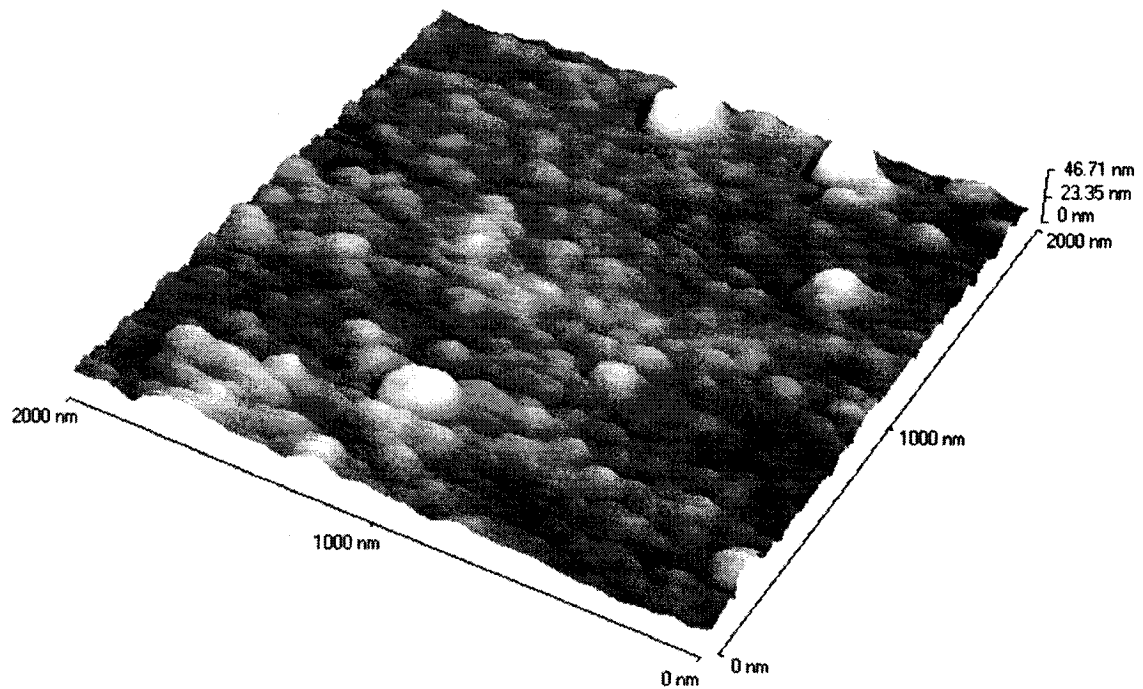


Figure 4.4. AFM analysis of electropolished NiTi stent showing smooth surface with polycrystalline grain oxide (surface roughness $R_a = 3.3$ nm, Topometrix TMX 2010 AFM in contact mode)

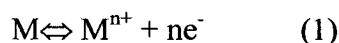
4.1.4 Considerations on the biostability of metallic devices

4.1.4.1 Corrosion in the physiological environment

Physiological fluids contain dissolved oxygen and also chloride, hydroxide, phosphate, bicarbonate, sodium, potassium, calcium and magnesium ions that constitute a very corrosive electrolyte. Particularly, chloride ions found at a concentration of approximately 0.1 N in physiological fluids are well known for their effect on enhancing localized corrosion. The presence of inorganic and organic macromolecules,

such as proteins, greatly influences corrosion of passive materials^{23; 24}. In a recent paper, Wataha and coworkers have used saline, saline with 3% bovine serum albumin (BSA), or complete cell- culture medium with 3% serum as test solution and reported significant influence on ion release of dental materials²⁵. Milosev and Strehblow have suggested that the enhanced stainless steel dissolution in the protein containing media is related to the formation of organometallic complexes at the passive layer-solution interface²⁶. Cells, and in particular macrophage responses to degradation products, may enhance corrosion through release of intracellular components, production of reactive metabolic species, and associated proinflammatory action^{27; 28}. The acidic pH values (as low as 4) associated with tissue inflammation may also greatly increase corrosion phenomena.

Corrosion is a multifactorial process and some basic facts should be kept in mind when considering the stability of metallic devices. Corrosion can be described as the oxidation of the material, i.e. the increase of its valence state, according to the equation 1.



These processes are driven by thermodynamic forces and the free energy of the reaction should be positive to allow oxidation. This is unfortunately the case for most alloys used in medical applications, such as titanium or chromium. Metals can be classified in the electrochemical series as noble and stable metals, such as gold and platinum, or as more reactive and unstable ones, such as titanium. Oxidation is controlled by kinetics factors associated with the oxide layer on the surface of passive metals and alloys. While gold is unlikely to corrode due to its thermodynamic stability, titanium owns its excellent corrosion resistance to its TiO₂ protective oxide layer. The passive layer acts as a physical barrier preventing the migration of ionic species and electron towards the metal (reaction III and IV, Fig. 4.3). As a consequence, the more efficient this barrier is on the surface, the more resistant it is to corrosion. To fulfill this protective role, the oxide layer should be free of defects on both an atomic and macroscopic level. The

small amount of ionic defects in TiO_2 , due to its almost stoichiometric 2:1 ratio, explains the excellent corrosion behavior of titanium.

4.1.4.2. Biocorrosion modes

The metallic ions M^{n+} formed during the corrosion process can contribute to the formation (or growth) of the oxide layer or can be released. Degradation products include nanoscale-sized particles, colloidal organometallic complexes, metallic ions, and inorganic metallic salts and oxides^{29; 30}. When a passive alloy is placed in a physiological environment (either *in vitro* in a physiological solution or *in vivo*), three situations may generally occur: The protective oxide layer could uniformly break down, leading to high corrosion rates (unlikely to occur *in vivo*); the alloy may remain in the passive state (no changes are observed except a possible increase in oxide layer thickness or small amount of passive ion release); finally, as illustrated in Figure 4.1, small areas of the surface can corrode (defined as pitting or localized corrosion). The latter is related to the presence of defects in the protective oxide layer, such as grain boundaries or chemical heterogeneity, initiating local breakdown of the oxide layer. In particular, 316L stainless steel and nitinol are susceptible to pitting corrosion *in vivo*. Ryan and colleagues have recently nicely described the relation between stainless steel pitting process and the chemical changes around manganese sulphide inclusions³¹.

The fracture and stress cracks in the metallic frame of the endografts, described by Riepe and coworkers, are not surprising since corrosive environments can significantly accelerate fatigue crack growth such as those arising from blood pulsatile oscillation³². As shown in the Figure 4.5, fatigue corrosion was also reported to cause the fracture of a stainless steel Greenfield vena cava filter³³. Fatigue cracks may be initiated by localized corrosion or by defects from machining. The effects of cyclic loads have been investigated on endovascular-constituting materials, with nitinol having the lowest

“fatigue-crack growth” resistance³⁴. This latter concept should be considered in the design of small devices, characterized by stent-struts diameter as small as 150 μm . The excessive corrosion on nitinol wire in the area close to platinum markers (Fig. 4.1) also suggests the occurrence of galvanic corrosion. This phenomenon is defined as the formation of a galvanic couple associated with anodic degradation of the active metal (in this case NiTi) and the cathodic protection of the noble metal (i.e. platinum)³⁵. However, from mixed-potential theory, galvanic corrosion alone may not be able to breakdown the passivity of electropolished nitinol⁹.

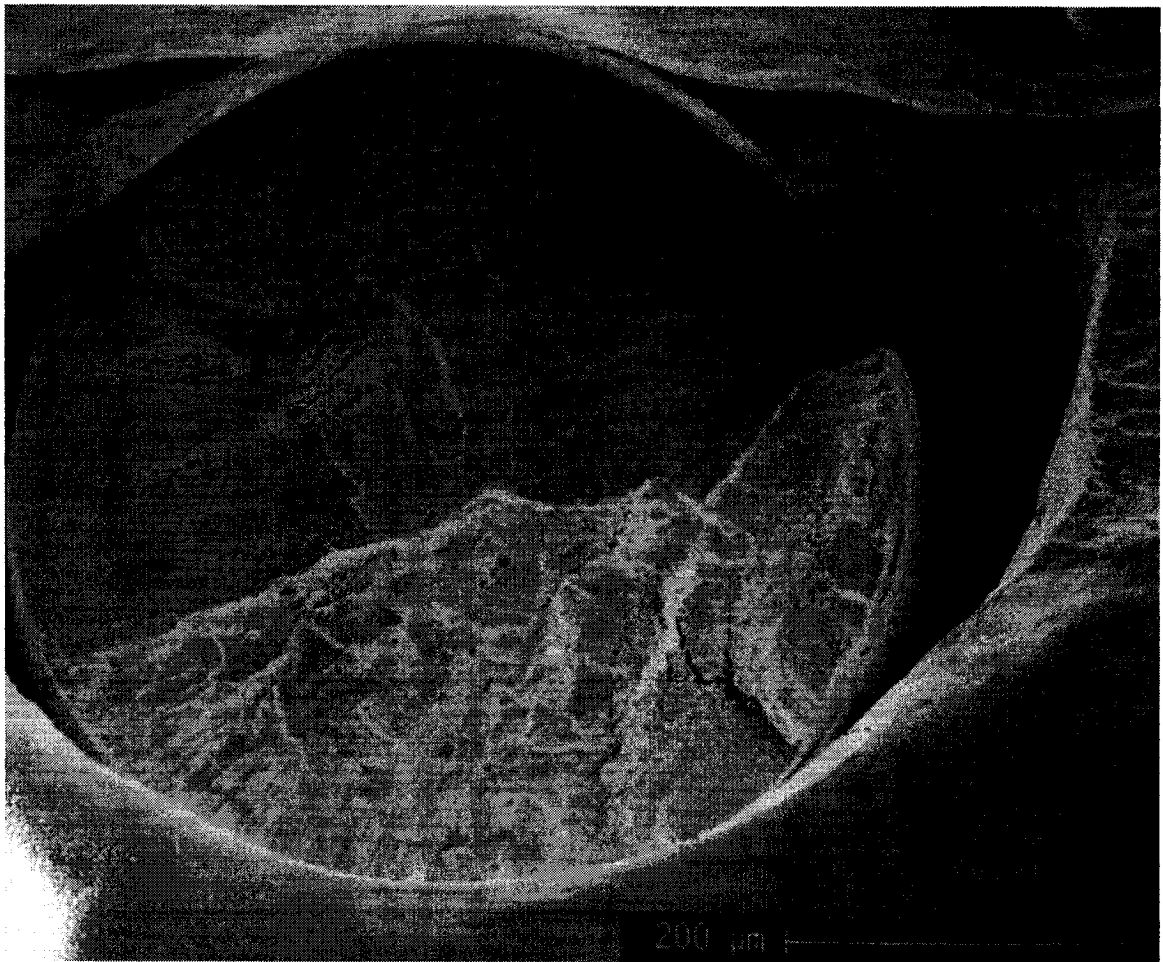


Figure 4.5. SEM micrographs of a fractured stainless steel Greenfield vena cava filter showing corrosion-fatigue degradation. Reproduced with authorization of Gatti et al.

4.1.4.3. *In vitro* evaluation of corrosion behavior

The corrosion resistance of metal alloys has been widely studied *in vitro* using mainly potentiostatic and potentiodynamic assays, scratch tests, impedance measurements, and immersion assays combined with atomic absorption spectroscopy. Despite the existence of ASTM standards on the corrosion testing of metallic materials³⁶⁻³⁸, differences in the experimental settings such as the electrolyte, scan rates, and electrode holders can explain the conflicting results in the literature. In addition, it is not possible to conclude on the corrosion resistance of metallic biomaterials, since it is strongly related to the design of the device and the processing, especially the surface finish. As recommended by the FDA, testing of the devices should hence be conducted in their final condition and in assays that are representative of the clinical use². Cyclic polarization has been widely used to accelerate and investigate mechanisms of corrosion³⁶. While physiological solutions such as Ringer's or Hank's have been widely used for corrosion assays, others electrolytes can also be employed for a more relevant simulation of physiological fluids, e.g., those containing serum proteins. These issues raise the general question of the clinical relevance of such assays since the *in vitro* environment may not be representative of *in vivo* conditions.

4.1.5. Are alloys used in endovascular surgery stable?

While numerous studies have reported on the *in vitro* corrosion behavior of metallic endovascular materials, data on devices in final form and condition of use are sparse. The case of nitinol is very instructive since this alloy can be processed to present good resistance to corrosion, while the raw alloy is prone to pitting phenomena. It is thus not surprising that a scattered range of corrosion resistance has been reported for nitinol in the literature. Trépanier and Venugopalan have investigated the dependence of nitinol,

316L stainless steel and cobalt-chrome MP35N alloys toward passivation treatment in passive dissolution assays in Hank's solution (Fig. 4.6)³⁹. Both nitinol and MP35N were very responsive to passivation with an ion release reduction of 75% and 90%, respectively, at 1 h compared with the mechanically-polished alloys. All alloys presented relatively low dissolution rates, and the ion release decreased under the apparatus sensitivity within a few hours for both materials. As stated by Heintz et al., it is likely that the reported instability of the nitinol endografts resulted from inefficient processing of the alloy, and that newer generation devices may be expected to be more resistant⁵. A recent investigation of human orthopedic NiTi implants showed that the alloy was not significantly damaged after as many as 12 months following implantation⁴⁰.

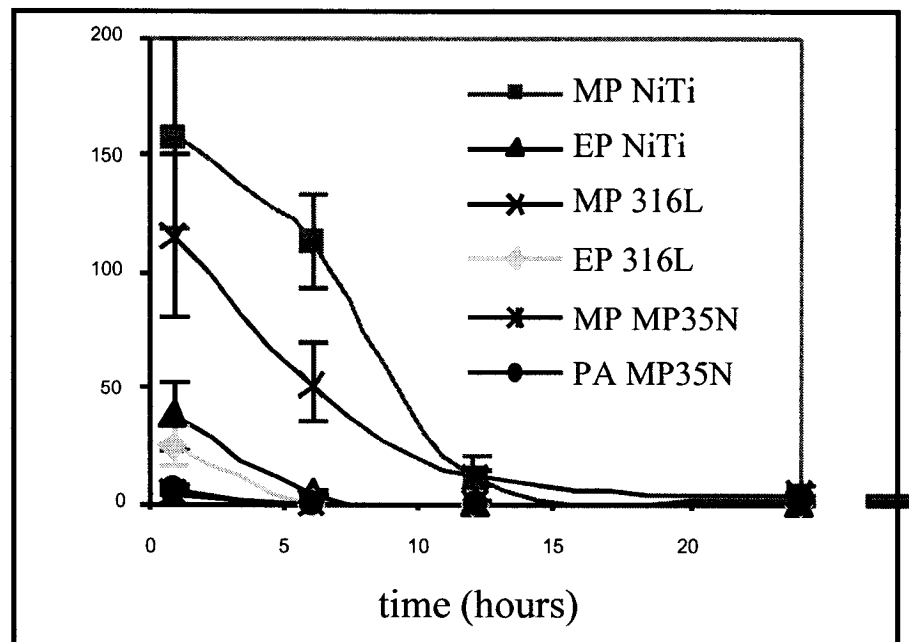


Figure 4.6. Nickel release in Hank's physiological solution for mechanically polished (MP) stainless steel (MP ST), NiTi (MP NiTi) and MP35N (MP MP35N), electropolished stainless steel (EP ST) and NiTi (EP NiTi), and acid passivated MP35N (PA MP35N). Reproduced with authorization of Trépanier et al.

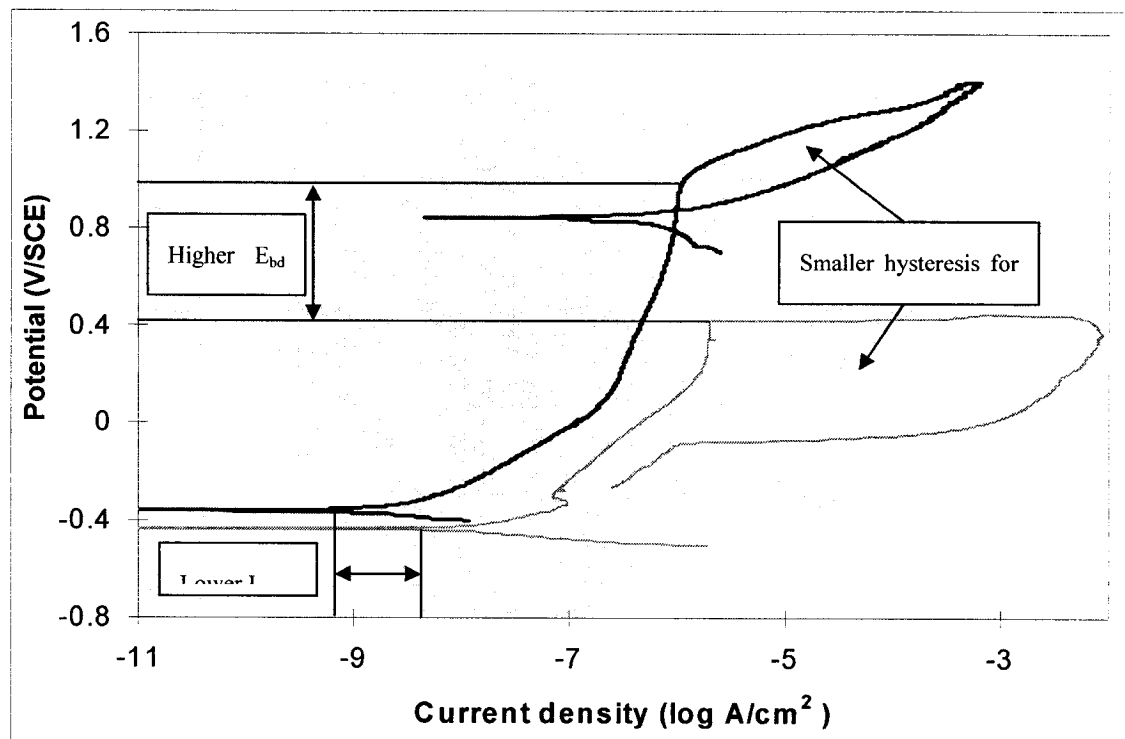


Figure 4.7. Typical cyclic polarization curves in de-aerated Hank's balanced salt solution of electropolished NiTi and stainless steel (316L). NiTi alloy shows higher breakdown potential (E_{bd}), lower I_{corr} and smaller hysteresis than stainless steel.

Figure 4.7 shows representative cyclic polarization curves in de-aerated Hank's solution of electropolished nitinol and 316L discs previously reported by our groups⁴¹. Not surprisingly, both materials exhibit relatively high breakdown potential values (E_{bd}), nitinol presenting, however, almost two-time greater E_{bd} than 316L, agreeing with previously published data⁴²⁻⁴⁴. The relatively high breakdown potential values reported in these studies seem to assess the resistance of these alloys to local breakdown of the passive film. The aggressiveness of the biological environment and implant-related factors may however lead to unexpected pitting corrosion *in vivo*. For instance, local residual strain created during deployment of balloon expandable stents may initiate this

phenomenon. It is noteworthy that, once initiated, pitting corrosion is likely to propagate for both materials at much lower potential than the breakdown potential. Using commercially-available stents and home-made stent-holding fixtures, Venugopalan has calculated corrosion rates (CR) (based on ASTM G102 standard³⁷) of 6 to 189×10^{-6} mm/years for nitinol and 225 to 334×10^{-6} mm/years for stainless steel⁴⁵. The latter gives an indication of the potential passive dissolution *in vivo* agreeing with the results from direct release assays^{39; 41; 43}.

The cobalt-chromium-nickel-molybdenum-iron alloy Elgiloy[®] described in the ASTM standard F1058-91 is used in the design of the self expandable Wallstent and Wallgraft (Schneider). The chromium oxide layer confers to this alloy a resistance to corrosion similar to or greater than 316L stainless steel⁴⁶. Tantalum is well known for its excellent corrosion resistance provided by its oxide/hydroxide surface. It presents a wide passivation range and is unlikely to corrode in usual endovascular applications⁴⁷. It is rather difficult to conclude on the relative stability of endovascular implants made of these materials since it depends mostly on appropriate design and processing. However from *in vitro* analyses, nitinol and cobalt alloys may be considered as more resistant to corrosion than 316L stainless steel when passivated according to ASTM F86.

At this point we would like to stress the fact that these considerations can be applied only to the bare alloys. The questionable use of multiple stents in close contact or sub-optimal coatings are examples of specific conditions that may significantly modify the stability of the metallic materials. The disappointing results reported by Katrati *et al.* with gold-coated stainless steel stents may be attributed to an increase in the biodegradation due to corrosion⁷. Despite experimental evidence of the beneficial effects of gold coating, clinical implantation of the gold coated inflow stent was indeed associated with a significantly increased restenosis rate. Edelman and coworkers have shown that the increase in neointimal proliferation following gold-coated stent implantation could be abolished by thermal treatment of the coatings⁸. This strongly

suggests the potential catastrophic results of inappropriate material selection and processing in endovascular applications.

4.1.6. Considerations for the Biocompatibility of endovascular devices

4.1.6.1. Biomechanical considerations

Recent studies have pointed out the dependency of thrombus formation and neointimal proliferation on the type and design of the stent⁴⁸⁻⁵². Follow-up angiography in a cohort of 3,370 patients has shown that stent design was the second strongest risk factor, after artery size, with restenosis ranging from 20.0% to 50.3%, depending on the stent type⁵². The newer-generation stents, such as the ACS Multinlink stent have been shown to reduce in-stent hyperplasia. Many authors have attempted to define the “ideal” stent: low profile, trackability, elasticity, flexibility, radio-opacity, and high- and well-distributed radial strength^{53; 54}. It is obvious that the intrinsic properties of the material itself influence the overall biomechanical properties of the device; thus, nitinol stents differ in many aspects from stainless steel or tantalum stents. Self-expansion minimizes the need for balloon post-dilatation and allows more uniform radial expansion along with less longitudinal shortening in comparison to balloon-expandable devices^{55; 56} which has been reported to reduce endothelium damage⁵⁷. The effects of the continual expansion of oversized nitinol stents (10-15%) have been demonstrated to accommodate neointimal formation, but this remains controversial^{56; 58-60}. Conversely, the over-expansion required to compensate for the acute recoil of balloon stents can be expected to increase injury to the vessel. As defined by D. Stoeckel, the crush-recoverability and the biased stiffness (or stress hysteresis) of NiTi alloys are particularly well-adapted to the design of peripheral endovascular devices¹². Despite higher radial strength, stainless steel devices can be permanently deformed if outside forces exceed their buckling resistance. On the contrary, nitinol devices will return to

their deployed shape even if completely crushed, which may be extremely important in superficial vessels such as the carotid artery. Mukherjee et al. have reported, however, similar neurological outcomes following nitinol or stainless steel carotid stent implantation⁶¹. When dealing with these biomechanical considerations, rather than addressing the confusing notion of the “ideal stent”, it would be more relevant to consider the best stent-pathology combination for optimal results. It is likely that the choice of the best device will continue to rely on the clinician’s expertise on a case-to-case basis.

4.1.6.2. Considerations on metals/biological components interfacial interactions

The interfacial properties of synthetic materials mediate their interaction with any biological fluids and tissues. In particular, biomaterials in contact with blood have motivated a wide array of research, but the issue of blood compatibility remains unresolved⁶². While it is beyond the aim of this paper to review the cascade of events associated with exposure to blood of synthetic biomaterials, patterns relevant to metallic biomaterials will be discussed. The interested reader is referred to specific reviews on the subject for complementary information⁶²⁻⁶⁶. Free energy, electrostatic charge, topography and chemical composition are known to be the relevant surface properties when dealing with blood-contacting devices. When a biomaterial comes in contact with blood, a buildup of a hydration layer occurs within a few seconds, followed by the rapid adsorption/desorption of a layer of plasma proteins,⁶⁷. The nature and conformation of this adsorbed layer strongly depends on the interfacial properties of the biomaterials. As reported by Simon and coworkers, the processes mediating protein adsorption/desorption/conformational changes remain unclear⁶⁸. Subsequent biological events such as cellular invasion, immune or inflammatory responses at the interface are thus mediated by this proteinaceous layer. Much effort has been devoted to the design of fouling-resistant surfaces, i.e., surfaces that resist the adsorption of any biological components, mainly using polyethylene oxide (PEO) or polysaccharides. However, bare

metallic surfaces are inherently thrombogenic and device implantations are always conjugated with anti-platelet/coagulant therapies. Surface topography has long been recognized as an important factor in thrombogenic reactions; many studies have demonstrated the correlation between roughness and thrombogenicity, and smooth electropolished surfaces have been demonstrated to reduce thrombus formation^{22; 69}. Independent of physical parameters such as roughness, the nature of the material itself has been shown to modulate the thrombogenicity of stainless steel and nitinol stents. Using an *ex vivo* pig model, we have recently reported that nitinol induced less platelet and fibrinogen deposition than stainless steel¹. Despite the low thrombogenic risk associated with modern stent implantation, the latter may be of clinical relevance since activated platelets trapped in a thrombus release chemicals that can in turn modulate neointimal hyperplasia (Fig. 4.2). Conversely, as well demonstrated by Sprague et al. using atomic force microscopy, electrostatic forces from electropolished nitinol and stainless steel surfaces were significantly different both in terms of intensities and lengths of action⁷⁰.

4.1.6.3. Biologic responses to degradation products

Retrieval analyses of the first-generation of endografts have shown that these devices may be prone *in vivo* to degradation associated with mechanical or corrosive factors. The fractures of the metallic wires reported in the retrieval analyses of the Stentor devices were presumably initiated by corrosion and stress-corrosion⁵. In turn, they may have contributed to the failure of the graft, for instance by allowing endoleaks. The biological reactions to degradation products can also be detrimental to the success of the implantation. The biocompatibility of metallic materials has been related to “the electrochemical interaction that results in the release of metallic ions into the tissue, and the toxicology of these released substances”⁷¹. The toxic, carcinogenic and inflammatory potentials of metallic components have been investigated by numerous authors both *in vitro* and *in vivo* for orthopedic, orthodontic and dental metallic devices.

Nitinol, 316L stainless steel, Elgiloy and tantalum implanted in soft tissue presented rare or minimal local adverse reactions^{46; 72-75}. The threshold for local and systemic adverse responses of the host remain unknown, however, and clinical data is sparse in the field of endovascular devices. The questions relevant to the *in vivo* biocompatibility of these implants are: What is the timing of the degradation process? What is the concentration of released degradation products? What is their fate? At this time, there are only a few answers⁷⁶.

4.1.6.3.1. Local adverse response.

As discussed in this paper, it is likely that metallic devices release degradation products to some extent in surrounding tissues. The systemic increase in ionic serum concentration occasionally associated with either successful or failed orthopedic implants, such as total joint replacements³⁰, is unlikely to occur in the case of stents with which much smaller amounts of metal are expected to be released. Hence, the potential carcinogenicity of metallic ions such as nickel or cobalt⁷⁷ may not be a concern in their case. Still, local accumulation of degradation products in the surrounding blood vessel may potentiate adverse reactions. Released metal ions such as nickel or chromium may participate in the chronic inflammatory reaction observed in restenotic arteries, for example. Shih and coworkers have shown the ability of 316L stainless steel and nitinol degradation products to induce *in vitro* rat aortic smooth muscle cell toxicity^{78; 79}. A nickel concentration above 11.7 ppm was enough to elicit such reactions, which is in agreement with other *in vivo* studies^{80; 81}. Using a laser ablation technique coupled with mass spectroscopy, Wataha *et al.* have correlated the release of nickel from nickel-containing wires implanted subcutaneously in rats to the inflammatory reaction. The main conclusion of this study was that concentrations lower than 5 µg/g seems to be well accepted but higher concentrations promote the inflammatory reaction. Nickel was reported to extend up to 3-4 mm from the wire after 7 days. The effects of metal ions in general, and nickel in particular, have been investigated widely but the dose/timing response remains unclear. Even low sub-toxic

doses may have a proinflammatory effect⁸². Nickel ions particularly have been reported *in vitro* to induce soft tissue inflammation at sub-toxic concentrations through direct activation of monocytes and cytokine-indirect stimulation of endothelial cells^{83; 84}. These inflammatory conditions may accelerate the corrosion of the devices, which further increases the release of these proinflammatory substances.

4.1.6.3.2. Metal hypersensitivity in the setting of endovascular interventions.

Small amounts of metallic ions such as nickel, chromium, molybdenum cobalt, and, to a lesser extent, tantalum and titanium, can be recognized as antigens when bound with native proteins to form hapten complexes. These complexes can then activate the immune system and generate a metal hypersensitivity, mostly through a Type-IV delayed cell-mediated response⁸⁵. The mechanism of T-cell activation by metal ions is not yet fully understood⁸⁶. The cell-mediated response can be very harmful and can generate excessive inflammation. As reviewed by Hallab *et al.*, degradation products of orthopedic implants have often been related to metal hypersensitivity⁸⁷, although the relationship remains unclear. The study of Koster and coworkers, along with the case-report of Gimenez-Arnau *et al.*, gives rise to the question of metal hypersensitivity in endovascular techniques^{6; 88}. A generalized eczematous dermatitis was elicited by the endograft treatment of an AAA in a 79-year old woman; it was found positive to nickel sulfate and cobalt chloride in epicutaneous patch tests. Such an excessive hypersensitivity response is, however, likely to be an extremely rare complication. Nevertheless, metal hypersensitivity may participate in the foreign body reactions associated with stent implantation. Patients with a history of metal allergy may be more susceptible to developing reactions to an endovascular metallic device. As stated by Koster and colleagues, the need for routine allergic testing prior to implantation is questionable. From what we have learned through orthopedic clinical experience, further investigations seem required to assess the potential risks associated with such immune reactions toward metallic endovascular devices.

4.1.7. Future perspectives

The growing stent market has motivated intensive research aimed at developing more efficient endovascular devices through new designs, materials or coatings for existing materials. To date, most of the efforts focus on the improvement in design and development of biologically-active or inert coatings. The excellent results recently reported using anti-proliferative drugs, such as Sirolimus and Paclitaxel, have generated unprecedented enthusiasm⁸⁹⁻⁹². These drugs selectively target proliferating cells within the artery and have been shown to inhibit restenosis. Two different approaches are being investigated to achieve delivery of the drugs, i.e., polymer-coated devices (Cordis/sirolimus stent and Boston Scientific./paclitaxel stent) and direct elution from dip-coated stents (Cook/paclitaxel stent). The potential long-term degradation and inflammatory effect of the polymer coatings versus control of the release rate are the key elements in the debate between these two approaches. Brachytherapy, i.e. the use of radiotherapy to inhibit neointimal proliferation, has also shown promising results in both clinical and experimental studies. Dose-dependant inhibition has been reported with the β -emitting ^{32}P stents^{56; 93}. As demonstrated by the recent INHIBIT study, radiotherapy has been found to be particularly efficient in the treatment of in-stent restenosis⁹⁴. It remains limited at this point, however, by subacute thrombogenicity of irradiated arteries and renarrowing at the edge of the stent - the so-called “candy-wrapper effect”.⁹⁵⁻⁹⁷. Both drug-eluting and, to a much lesser extent, radioactive stents hold promises in view of the prevention of what has been the nightmare of all interventional cardiologists for the past 10 years: in-stent restenosis. However, much work remains to be done to assess the long-term safety of these new devices and determine their clinical potential. Along with possible damaging effects to the artery of the anti-proliferative components, i.e. drug or radiation, the biocompatibility of the coated surfaces requires further investigation and potentially optimization. In particular, late thrombosis seems to be a common outcome of these anti-proliferative strategies⁹⁸;

⁹⁹. The long-term results following anti-proliferative strategies associated with stenting have been questioned in clinical trials and may only just delay hyperplasia^{100; 101}. Thromboresistant phosphorylcholine-based coating has been used as a drug delivery platform through hydrophobic interactions^{102; 103}. Such a thromboresistant coating on the *Biodiv Ysio* stents also holds promise in revascularization of small arteries, which remains a very challenging issue¹⁰⁴. Many approaches have been previously investigated to reduce thrombogenicity of metallic endovascular devices, using heparin or r-hirudin coatings for instance¹⁰⁵⁻¹⁰⁹.

Inorganic coatings have also been investigated, such as diamond-like carbon, hydrogen-rich amorphous silicon carbide (a-SiC:H) and amorphous titanium oxide¹¹⁰⁻¹¹². Such inorganic coatings improve the overall biocompatibility of the stent and presented low thrombogenicity in comparison with uncoated devices. Titanium-nitric-oxide-coated stainless steel stents significantly reduced neointimal hyperplasia in an experimental study¹¹³. Along with increased biocompatibility, these inorganic coatings may also improve significantly the corrosion properties and in turn reduce the release of ions in the surrounding vessel wall. At present, the long-term beneficial effects of inorganic coatings have not been demonstrated by randomized trials.

While exciting results have recently been achieved using the above-described modified stents, the presence of metallic devices within the delicate environment of an artery still hampers the success of revascularization procedures. It is the authors' belief that within few years new technologies will reduce the need for such metallic devices in angioplasty. The recent study by Yasuda and coworkers yields promise in view of decreasing the almost systematic use of stents in angioplasty procedures^{114; 115}. Catheter-based local delivery of a novel anti-mitotic agent was shown to prevent restenosis in an iliac artery rabbit model. Other pharmaceutical approaches may be found useful, as demonstrated by the study using local delivery of L-arginine¹¹⁶. All together these results confirm the tremendous potential of pharmaceutical strategies in the setting of revascularization procedures.

Acknowledgements

This work was partly supported by NSERC. The authors are grateful to Dr. Y. Marois, Dr A.M. Gatti and C. Trépanier for providing authorization to reproduce Figure 1, Figure 4 and Figure 6. We also wish to thank Dr. E. Beaubien and Mrs P. Cap for their help in reviewing the manuscript.

4.1.8. References

1. Thierry B, Merhy Y, Bilodeau L, Trépanier C, Tabrizian M: Nitinol versus stainless steel stents: acute thrombogenicity study in an ex vivo porcine model. *Biomaterials* 2002;23:2997-3005
2. Chwirut, D. J., Oktay, H. S., and Ryan, T. Nitinol Interventional Cardiology Devices - FDA's Perspective. Pelton, A., Hodgson, D., Russell, S., and Duerig, T. Shape Memory and Superelastic Technologies. March 1997. Santa Clara, SMST.
3. Disegi, J. and Zardiackas, L. Retrieval Analysis of Stainless Steel Plate/Screws Implanted for 55 Years [Abstract]. The Proceeding of the 27th Meeting of the Society For Biomaterials. Minneapolis, USA , Society For Biomaterials 2000
4. Guidoin R, Marois Y, Douville Y, King MW, Castonguay M, Traore A, Formichi M, Staxrud LE, Norgren L, Bergeron P, Becquemin JP, Egana JM, Harris PL: First-generation aortic endografts: analysis of explanted Stentor devices from the EUROSTAR Registry. *J Endovasc Ther* 2000;7:105-22
5. Heintz C, Riepe G, Birken L, Kaiser E, Chakfe N, Morlock M, Delling G, Imig H: Corroded nitinol wires in explanted aortic endografts: an important mechanism of

failure? *J Endovasc Ther* 2001;8:248-53

6. Koster R, Vieluf D, Kiehn M, Sommerauer M, Kahler J, Baldus S, Meinertz T, Hamm CW: Nickel and molybdenum contact allergies in patients with coronary in- stent restenosis. *Lancet* 2000;356:1895-7
7. Kastrati A, Schomig A, Dirschinger J, Mehilli J, von Welser N, Pache J, Schuhlen H, Schilling T, Schmitt C, Neumann FJ: Increased risk of restenosis after placement of gold-coated stents: results of a randomized trial comparing gold-coated with uncoated steel stents in patients with coronary artery disease. *Circulation* 2000;101:2478-83
8. Edelman ER, Seifert P, Groothuis A, Morss A, Bornstein D, Rogers C: Gold-coated NIR stents in porcine coronary arteries. *Circulation* 2001;103:429-34
9. Venugopalan R, Trépanier C: Assessing the corrosion behaviour of Nitinol for minimally-invasive device design. *Min Invas Ther & Allied Technol* 2000;9:67-74
10. Gershlick AH: Role of stenting in coronary revascularisation. *Heart* 2001;86:104-12
11. Narins CR, Ellis SG: Prevention of in-stent restenosis. *Semin Interv Cardiol* 1998;3:91-103
12. Stoeckel D: Nitinol medical devices and implants. *Min Invas Ther & Allied Technol* 2000;9:81-88
13. Pelton AR, DiCello J, Miyazaki S: Optimisation of processing and properties of medical grade Nitinol wire. *Nitinol medical devices and implants* 2000;9:107-118
14. Bhargava B, De Scheerder I, Ping QB, Yanming H, Chan R, Soo Kim H, Kollum M, Cottin Y, Leon MB: A novel platinum-iridium, potentially gamma radioactive stent: evaluation in a porcine model. *Catheter Cardiovasc Interv* 2000;51:364-8

15. van Dijk LC, van Holten J, van Dijk BP, Matheijssen NA, Pattynama PM: A precious metal alloy for construction of MR imaging-compatible balloon-expandable vascular stents. *Radiology* 2001;219:284-7
16. Manke C, Nitz WR, Lenhart M, Volk M, Geissler A, Feuerbach S, Link J: Magnetic resonance monitoring of stent deployment: in vitro evaluation of different stent designs and stent delivery systems. *Invest Radiol* 2000;35:343-51
17. Maintz D, Fischbach R, Juergens KU, Allkemper T, Wessling J, Heindel W: Multislice CT angiography of the iliac arteries in the presence of various stents: in vitro evaluation of artifacts and lumen visibility. *Invest Radiol* 2001;36:699-704
18. Heublein B, Rhode R, Huasdorf G, Hartung W, Haverich R: Biocorrosion, a new principle for temporary cardiovascular implants ? *Eur. Heart J.* 2000;21:286
19. Peuster M, Wohlsein P, Brugmann M, Ehlerding M, Seidler K, Fink C, Brauer H, Fischer A, Hausdorf G: A novel approach to temporary stenting: degradable cardiovascular stents produced from corrodible metal-results 6-18 months after implantation into New Zealand white rabbits. *Heart* 2001;86:563-9
20. ASTM F86, Standard Practice for Surface Preparation and Marking of Metallic Surgical Implants , in *Annual Book of ASTM standards: Medical Devices and Services*. American Society for Testing and Materials, 1995, pp 6-8
21. Trepanier C, Tabrizian M, Yahia LH, Bilodeau L, Piron DL: Effect of modification of oxide layer on NiTi stent corrosion resistance. *J Biomed Mater Res* 1998;43:433-40
22. De Scheerder I, Verbeken E, Van Humbeeck J: Metallic surface modification. *Semin Interv Cardiol* 1998;3:139-44
23. Clark GC, Williams DF: The effects of proteins on metallic corrosion. *J Biomed Mater Res* 1982;16:125-34
24. Khan MA, Williams RL, Williams DF: The corrosion behaviour of Ti-6Al-4V, Ti-

- 6Al-7Nb and Ti-13Nb-13Zr in protein solutions. *Biomaterials* 1999;20:631-7
25. Wataha JC, Nelson SK, Lockwood PE: Elemental release from dental casting alloys into biological media with and without protein. *Dent Mater* 2001;17:409-14
 26. Milosev I, Strehblow HH: The behavior of stainless steels in physiological solution containing complexing agent studied by X-ray photoelectron spectroscopy. *J Biomed Mater Res* 2000;52:404-12
 27. Mu Y, Kobayashi T, Sumita M, Yamamoto A, Hanawa T: Metal ion release from titanium with active oxygen species generated by rat macrophages in vitro. *J Biomed Mater Res* 2000;49:238-43
 28. Hutchinson, B. S. and Bumgardner, J. D. Evaluation of the Effect of Cells on the Corrosion Behavior of an Implants Alloys. The Proceeding of the World Biomaterials Congress. Minneapolis, USA , Society for Biomaterials. 2000
 29. Woodman JL, Black J, Jiminez SA: Isolation of serum protein organometallic corrosion products from 316LSS and HS-21 in vitro and in vivo. *J Biomed Mater Res* 1984;18:99-114
 30. Jacobs JJ, Skipor AK, Patterson LM, Hallab NJ, Paprosky WG, Black J, Galante JO: Metal release in patients who have had a primary total hip arthroplasty. A prospective, controlled, longitudinal study. *J Bone Joint Surg Am* 1998;80:1447-58
 31. Ryan MP, Williams DE, Chater RJ, Hutton BM, McPhail DS: Why stainless steel corrodes. *Nature* 2002;415:770-4
 32. Wang YZ: Corrosion Fatigue, in Uhlig's (ed): *Corrosion Handbook, Second Edition*. 2000, pp 221-232
 33. Emanuelli G, Gatti AM, Cigada A, Brunella MF: Physico-chemical observations on a failed Greenfield vena cava filter. *J Cardiovasc Surg (Torino)* 1995;36:121-5

34. McKelvey AL, Ritchie RO: Fatigue-crack propagation in Nitinol, a shape-memory and superelastic endovascular stent material. *J Biomed Mater Res* 1999;47:301-8
35. Reclaru L, Lerf R, Eschler P-Y, Blatter A, Meyer J-M: Pitting, crevice and galvanic corrosion of REX stainless-steel/CoCr orthopedic implant material. *Biomaterials* in Press
36. ASTM G 5, Standard reference test method for making potentiostatic and potentiodynamic anodic polarization measurements , in *Annual Book of ASTM standards: Metals, test methods and analytical procedures*. Am Soc Test Mater, 1995, pp 48-58
37. ASTM G102, Standard practice for calculation of corrosion rates and related information from electrochemical measurements, in *Annual Book of ASTM standards: Metals, test methods and analytical procedures*. Am Soc Test Mater, pp 401-407
38. ASTM F746, Standard test method for pitting or crevice corrosion of metallic surgical implant materials, in *Annual Book of ASTM standards: Medical devices and services*. Am Soc Test Mater, pp 192-7
39. Trepanier, C., Venugopalan, R., Messer, R., Zimmerman, J., and Pelton, A. R. Effect of Passivation Treatments on Nickel Release from Nitinol. The Proceeding of the World Biomaterials Congress. Hawaii, USA , Society for Biomaterials 2000
40. Fili P, Lausmaa J, Musialek J, Mazanec K: Structure and surface of TiNi human implants. *Biomaterials* 2001;22:2131-8
41. Thierry B, Tabrizian M, Trepanier C, Savadogo O, Yahia L: Effect of surface treatment and sterilization processes on the corrosion behavior of NiTi shape memory alloy. *J Biomed Mater Res* 2000;51:685-93
42. Ryhanen J, Niemi E, Serlo W, Niemela E, Sandvik P, Pernu H, Salo T: Biocompatibility of nickel-titanium shape memory metal and its corrosion

- behavior in human cell cultures. *J Biomed Mater Res* 1997;35:451-7
43. Wever DJ, Veldhuizen AG, de Vries J, Busscher HJ, Uges DR, van Horn JR: Electrochemical and surface characterization of a nickel-titanium alloy. *Biomaterials* 1998;19:761-9
 44. Rondelli G: Corrosion resistance tests on NiTi shape memory alloy. *Biomaterials* 1996;17:2003-8
 45. Venugopalan R: Corrosion testing of stents: a novel fixture to hold entire device in deployed form and finish. *J Biomed Mater Res* 1999;48:829-32
 46. Clerc CO, Jedwab MR, Mayer DW, Thompson PJ, Stinson JS: Assessment of wrought ASTM F1058 cobalt alloy properties for permanent surgical implants. *J Biomed Mater Res* 1997;38:229-34
 47. Gotman I: Characteristics of metals used in implants. *J Endourol* 1997;11:383-9
 48. Garasic JM, Edelman ER, Squire JC, Seifert P, Williams MS, Rogers C: Stent and artery geometry determine intimal thickening independent of arterial injury. *Circulation* 2000;101:812-8
 49. Kastrati A, Mehilli J, Dirschinger J, Dotzer F, Schuhlen H, Neumann FJ, Fleckenstein M, Pfafferott C, Seyfarth M, Schomig A: Intracoronary stenting and angiographic results: strut thickness effect on restenosis outcome (ISAR-STereo) trial. *Circulation* 2001;103:2816-21
 50. Hoffmann R, Jansen C, Konig A, Haager PK, Kerckhoff G, Vom Dahl J, Klauss V, Hanrath P, Mudra H: Stent design related neointimal tissue proliferation in human coronary arteries; an intravascular ultrasound study. *Eur Heart J* 2001;22:2007-14
 51. Yoshitomi Y, Kojima S, Yano M, Sugi T, Matsumoto Y, Saotome M, Tanaka K, Endo M, Kuramochi M: Does stent design affect probability of restenosis? A randomized trial comparing Multilink stents with GFX stents. *Am Heart J*

2001;142:445-51

52. Kastrati A, Mehilli J, Dirschinger J, Pache J, Ulm K, Schuhlen H, Seyfarth M, Schmitt C, Blasini R, Neumann FJ, Schomig A: Restenosis after coronary placement of various stent types. *Am J Cardiol* 2001;87:34-9
53. Gunn J, Cumberland D: Does stent design influence restenosis? *Eur Heart J* 1999;20:1009-13
54. Dyet JF, Watts WG, Ettles DF, Nicholson AA: Mechanical properties of metallic stents: how do these properties influence the choice of stent for specific lesions? *Cardiovasc Intervent Radiol* 2000;23:47-54
55. Sheth S, Litvack F, Dev V, Fishbein MC, Forrester JS, Eigler N: Subacute thrombosis and vascular injury resulting from slotted-tube nitinol and stainless steel stents in a rabbit carotid artery model. *Circulation* 1996;94:1733-40
56. Carter AJ, Scott D, Laird JR, Bailey L, Kovach JA, Hoopes TG, Pierce K, Heath K, Hess K, Farb A, Virmani R: Progressive vascular remodeling and reduced neointimal formation after placement of a thermoelastic self-expanding nitinol stent in an experimental model. *Cathet Cardiovasc Diagn* 1998;44:193-201
57. Harnek J, Zoucas E, Carlemalm E, Cwikiel W: Differences in endothelial injury after balloon angioplasty, insertion of balloon-expanded stents or release of self-expanding stents: An electron microscopic experimental study. *Cardiovasc Intervent Radiol* 1999;22:56-61
58. Yu ZX, Tamai H, Kyo E, Kosuga K, Hata T, Okada M, Nakamura T, Komori H, Tsuji T, Takeda S, Motohara S, Uehata H: Comparison of the self-expanding Radius stent and the balloon-expandable Multilink stent for elective treatment of coronary stenoses: A serial analysis by intravascular ultrasound. *Catheter Cardiovasc Interv* 2002;56:40-45
59. Roguin A, Grenadier E, Linn S, Markiewicz W, Beyar R: Continued expansion of the nitinol self-expanding coronary stent: angiographic analysis and 1-year clinical

follow-up. *Am Heart J* 1999;138:326-33

60. Taylor AJ, Gorman PD, Kenwood B, Hudak C, Tashko G, Virmani R: A comparison of four stent designs on arterial injury, cellular proliferation, neointima formation, and arterial dimensions in an experimental porcine model. *Catheter Cardiovasc Interv* 2001;53:420-5
61. Mukherjee D, Kalahasti V, Roffi M, Bhatt DL, Kapadia SR, Bajzer C, Reginelli J, Ziada KM, Hughes K, Yadav JS: Self-expanding stents for carotid interventions: comparison of nitinol versus stainless-steel stents. *J Invasive Cardiol* 2001;13:732-5
62. Brash JL: Exploiting the current paradigm of blood-material interactions for the rational design of blood-compatible materials. *J Biomater Sci Polym Ed* 2000;11:1135-46
63. Ratner BD: Blood compatibility--a perspective. *J Biomater Sci Polym Ed* 2000;11:1107-19
64. Eto K, Goto S, Shimazaki T, Sakakibara M, Yoshida M, Isshiki T, Handa S: Two distinct mechanisms are involved in stent thrombosis under flow conditions. *Platelets* 2001;12:228-35
65. Janatova J: Activation and control of complement, inflammation, and infection associated with the use of biomedical polymers. *ASAIO J* 2000;46:S53-62
66. Basmadjian D, Sefton MV, Baldwin SA: Coagulation on biomaterials in flowing blood: some theoretical considerations. *Biomaterials* 1997;18:1511-22
67. Vogler EA: Water and the acute biological response to surfaces. *J Biomater Sci Polym Ed* 1999;10:1015-45
68. Simon C, Palmaz JC, Sprague EA: Protein interactions with endovascular prosthetic surfaces. *J Long Term Eff Med Implants* 2000;10:127-41

69. Park JY, Gemmell CH, Davies JE: Platelet interactions with titanium: modulation of platelet activity by surface topography. *Biomaterials* 2001;22:2671-82
70. Sprague EA, Palmaz JC, Simon C, Watson A: Electrostatic forces on the surface of metals as measured by atomic force microscopy. *J Long Term Eff Med Implants* 2000;10:111-25
71. Williams D. F.: Biomaterials and Biocompatibility: An Introduction, in *Fundamental Aspects of Biocompatibility*. Boca Raton, FL, 1981, pp 2-3
72. Ryhanen J, Kallioinen M, Tuukkanen J, Junila J, Niemela E, Sandvik P, Serlo W: In vivo biocompatibility evaluation of nickel-titanium shape memory metal alloy: muscle and perineural tissue responses and capsule membrane thickness. *J Biomed Mater Res* 1998;41:481-8
73. Matsuno H, Yokoyama A, Watari F, Uo M, Kawasaki T: Biocompatibility and osteogenesis of refractory metal implants, titanium, hafnium, niobium, tantalum and rhenium. *Biomaterials* 2001;22:1253-62
74. Trepanier C, Leung TK, Tabrizian M, Yahia LH, Bienvenu JG, Tanguay JF, Piron DL, Bilodeau L: Preliminary investigation of the effects of surface treatments on biological response to shape memory NiTi stents. *J Biomed Mater Res* 1999;48:165-71
75. Formichi M, Marois Y, Roby P, Marinov G, Stroman P, King MW, Douville Y, Guidoin R: Endovascular repair of thoracic aortic aneurysm in dogs: evaluation of a nitinol-polyester self-expanding stent-graft. *J Endovasc Ther* 2000;7:47-67
76. Geary RL, Nikkari ST, Wagner WD, Williams JK, Adams MR, Dean RH: Wound healing: a paradigm for lumen narrowing after arterial reconstruction. *J Vasc Surg* 1998;27:96-106; discussion 106-8
77. Vahey JW, Simonian PT, Conrad EU 3rd: Carcinogenicity and metallic implants. *Am J Orthop* 1995;24:319-24

78. Shih CC, Shih CM, Chen YL, Su YY, Shih JS, Kwok CF, Lin SJ: Growth inhibition of cultured smooth muscle cells by corrosion products of 316 L stainless steel wire. *J Biomed Mater Res* 2001;57:200-7
79. Shih CC, Lin SJ, Chen YL, Su YY, Lai ST, Wu GJ, Kwok CF, Chung KH: The cytotoxicity of corrosion products of nitinol stent wire on cultured smooth muscle cells. *J Biomed Mater Res* 2000;52:395-403
80. Wataha JC, O'Dell NL, Singh BB, Ghazi M, Whitford GM, Lockwood PE: Relating nickel-induced tissue inflammation to nickel release in vivo. *J Biomed Mater Res* 2001;58:537-44
81. Uo M, Watari F, Yokoyama A, Matsuno H, Kawasaki T: Dissolution of nickel and tissue response observed by X-ray scanning analytical microscopy. *Biomaterials* 1999;20:747-55
82. Schmalz G, Schuster U, Schweikl H: Influence of metals on IL-6 release in vitro. *Biomaterials* 1998;19:1689-94
83. Wataha JC, Lockwood PE, Marek M, Ghazi M: Ability of Ni-containing biomedical alloys to activate monocytes and endothelial cells in vitro. *J Biomed Mater Res* 1999;45:251-7
84. Wataha JC, Ratanasathien S, Hanks CT, Sun Z: In vitro IL-1 beta and TNF-alpha release from THP-1 monocytes in response to metal ions. *Dent Mater* 1996;12:322-7
85. Budinger L, Hertl M: Immunologic mechanisms in hypersensitivity reactions to metal ions: an overview. *Allergy* 2000;55:108-15
86. Thomssen H, Hoffmann B, Schank M, Hohler T, Thabe H, Meyer zum Buschenfelde KH, Marker-Hermann E: Cobalt-specific T lymphocytes in synovial tissue after an allergic reaction to a cobalt alloy joint prosthesis. *J Rheumatol* 2001;28:1121-8

87. Hallab N, Merritt K, Jacobs JJ: Metal sensitivity in patients with orthopaedic implants. *J Bone Joint Surg Am* 2001;83-A:428-36
88. Gimenez-Arnau A, Riambau V, Serra-Baldrich E, Camarasa JG: Metal-induced generalized pruriginous dermatitis and endovascular surgery. *Contact Dermatitis* 2000;43:35-40
89. Rensing BJ, Vos J, Smits PC, Foley DP, van den Brand MJ, van der Giessen WJ, de Feijter PJ, Serruys PW: Coronary restenosis elimination with a sirolimus eluting stent: first European human experience with 6-month angiographic and intravascular ultrasonic follow-up. *Eur Heart J* 2001;22:2125-30
90. Heldman AW, Cheng L, Jenkins GM, Heller PF, Kim DW, Ware M Jr, Nater C, Hruban RH, Rezai B, Abella BS, Bunge KE, Kinsella JL, Sollott SJ, Lakatta EG, Brinker JA, Hunter WL, Froehlich JP: Paclitaxel stent coating inhibits neointimal hyperplasia at 4 weeks in a porcine model of coronary restenosis. *Circulation* 2001;103:2289-95
91. Fox R: American Heart Association 2001 scientific sessions: late-breaking science-drug-eluting stents. *Circulation* 2001;104:E9052
92. Sousa JE, Costa MA, Abizaid AC, Rensing BJ, Abizaid AS, Tanajura LF, Kozuma K, Van Langenhove G, Sousa AG, Falotico R, Jaeger J, Popma JJ, Serruys PW: Sustained suppression of neointimal proliferation by sirolimus-eluting stents: one-year angiographic and intravascular ultrasound follow-up. *Circulation* 2001;104:2007-11
93. Drachman DE, Simon DI: Restenosis: Intracoronary Brachytherapy. 2002;4:109-118
94. Waksman R, Raizner AE, Yeung AC, Lansky AJ, Vandertie L: Use of localised intracoronary beta radiation in treatment of in-stent restenosis: the INHIBIT randomised controlled trial. *Lancet* 2002;359:551-7
95. Lowe HC, Oesterle SN, Khachigian LM: Coronary in-stent restenosis: current

- status and future strategies. *J Am Coll Cardiol* 2002;39:183-93
96. Serruys PW, Kay IP: I like the candy, I hate the wrapper: the (32)P radioactive stent. *Circulation* 2000;101:3-7
 97. Albiero R, Colombo A: European high-activity (32)P radioactive stent experience. *J Invasive Cardiol* 2000;12:416-21
 98. Liistro F, Gimelli G, Di Mario C, Nishida T, Montorfano M, Carlino M, Colombo A: Late acute thrombosis after coronary brachytherapy: when is the risk over? *Catheter Cardiovasc Interv* 2001;54:216-8
 99. Liistro F, Colombo A: Late acute thrombosis after paclitaxel eluting stent implantation. *Heart* 2001;86:262-4
 100. Brenner DJ, Miller RC: Long-term efficacy of intracoronary irradiation in inhibiting in-stent restenosis. *Circulation* 2001;103:1330-2
 101. Liistro F, Stankovic G, Di Mario C, Takegi T, Chieffo A, Moshiri S, Montorfano M, Carlino M, Briguori C, Pagnotta P, Albiero R, Corvaja N, Colombo A: First Clinical Experience With a Paclitaxel Derivate-Eluting Polymer Stent System Implantation for In-Stent stenosis Immediate and Long-Term Clinical and Angiographic Outcome. *Circulation* 2002;105:1183-1886
 102. Lewis AL, Cumming ZL, Goreish HH, Kirkwood LC, Tolhurst LA, Stratford PW: Crosslinkable coatings from phosphorylcholine-based polymers. *Biomaterials* 2001;22:99-111
 103. Lewis AL, Tolhurst LA, Stratford PW: Analysis of a phosphorylcholine-based polymer coating on a coronary stent pre- and post-implantation. *Biomaterials* 2002;23:1697-706
 104. Grenadier E, Roguin A, Hertz I, Peled B, Boulos M, Nikolsky E, Amikam S, Kerner A, Cohen S, Beyar R: Stenting very small coronary narrowings (< 2 mm) using the biocompatible phosphorylcholine-coated coronary stent. *Catheter*

105. Nelson SR, deSouza NM, Allison DJ: Endovascular stents and stent-grafts: is heparin coating desirable? *Cardiovasc Interv Radiol* 2000;23:252-5
106. Vrolix MC, Legrand VM, Reiber JH, Grollier G, Schali J, Brunel P, Martinez-Elbal L, Gomez-Recio M, Bar FW, Bertrand ME, Colombo A, Brachman J: Heparin-coated Wiktor stents in human coronary arteries (MENTOR trial). MENTOR Trial Investigators. *Am J Cardiol* 2000;86:385-9
107. van der Giessen WJ, van Beusekom HM, Eijgelshoven MH, Morel MA, Serruys PW: Heparin-coating of coronary stents. *Semin Interv Cardiol* 1998;3:173-6
108. Kocsis JF, Llanos G, Holmer E: Heparin-coated stents. *J Long Term Eff Med Implants* 2000;10:19-45
109. Lahann J, Klee D, Pluester W, Hoecker H: Bioactive immobilization of r-hirudin on CVD-coated metallic implant devices. *Biomaterials* 2001;22:817-26
110. Nan H, Ping Y, Xuan C, Yongxang L, Xiaolan Z, Guangjun C, Zihong Z, Feng Z, Yuanru C, Xianghuai L, Tingfei X: Blood compatibility of amorphous titanium oxide films synthesized by ion beam enhanced deposition. *Biomaterials* 1998;19:771-6
111. Gutensohn K, Beythien C, Bau J, Fenner T, Grewe P, Koester R, Padmanaban K, Kuehnl P: In vitro analyses of diamond-like carbon coated stents. Reduction Of metal ion release, platelet activation, and thrombogenicity. *Thromb Res* 2000;99:577-85
112. Heublein B, Ozbek C, Pethig K: Silicon carbide-coated stents: clinical experience in coronary lesions with increased thrombotic risk. *J Endovasc Surg* 1998;5:32-6
113. Windecker S, Mayer I, De Pasquale G, Maier W, Dirsch O, De Groot P, Wu YP, Noll G, Leskosek B, Meier B, Hess OM: Stent coating with titanium-nitride-oxide for reduction of neointimal hyperplasia. *Circulation* 2001;104:928-33

114. Sturek M, Reddy HK: New tools for prevention of restenosis could decrease the "oculo- stento" reflex. *Cardiovasc Res* 2002;53:292-3
115. Yasuda S, Noguchi T, Gohda M, Arai T, Tsutsui N, Nakayama Y, Matsuda T, Nonogi H: Local delivery of low-dose docetaxel, a novel microtubule polymerizing agent, reduces neointimal hyperplasia in a balloon-injured rabbit iliac artery model. *Cardiovasc Res* 2002;53:481-6
116. Suzuki T, Hayase M, Hibi K, Hosokawa H, Yokoya K, Fitzgerald PJ, Yock PG, Cooke JP, Suzuki T, Yeung AC: Effect of local delivery of L-arginine on in-stent restenosis in humans. *Am J Cardiol* 2002;89:363-7

PART I. STENTS

Endovascular stent implantation has become the procedure of choice in revascularization procedures. As defined in the section 2 of the literature review, the biocompatibility of these metallic devices relies on their biostability, biomechanical compatibility with the vascular environment and interfacial properties. Current trend in endovascular devices focus on 2 fields of investigation, the use of more biocompatible materials and the development of bioactive devices that can interact with the vascular wall. The more promising results toward improving the biocompatibility of metallic endovascular devices have been achieved using coatings with biocompatible materials such as phosphorylcholine. These coatings are expected in turn to reduce the thrombogenic and chronic inflammatory reactions associated to stent implantation. On the other hand, bioactive devices generally require the incorporation of therapeutic biomolecules to be delivered or presented to the vascular wall. Excellent results in this field have been reported recently with drug-eluting stents.

The main objective of the 3 manuscripts (2, 3, and 4) presented in the part I of this thesis was to combine these two approaches to further reduce complications associated with stent implantation. Surface modification methods of metallic substrates have been developed to fulfill the objectives defined in Chapter 2. The experimental work has been done onto NiTi alloy used as a model for metallic substrate. One of the goals was to develop surface modification methods readily applicable to commercially available devices made with various metallic alloys such as NiTi or stainless steel.

The first specific objective was to develop a biomimetic coating based on the immobilization of hyaluronan. Hyaluronan is a natural biopolymer present in the extracellular matrix. Modification of 3-D hyaluronan scaffold with adhesive peptides has been previously described in the field of tissue engineering. As a first step toward the development of biomimetic hyaluronan-adhesive molecules surfaces, HA has been

covalently immobilized onto metallic surfaces and further modified with a protein used as a model for adhesive molecules. This work (Manuscript 2) will be submitted to the *Journal of Biomedical Materials Research*.

The second specific objective was to develop radioactive devices for endovascular revascularization. Clinical use of stent-based vascular brachytherapy (i.e. the use of radioactive stents) is limited by the main associated side-effect, high rate of restenosis at the margins of the devices. The clinical experience is however limited to the 32-P stent. Many radionuclides could be more advantageous but their incorporation into a metallic stent requires extensive – and expensive - work. The approach investigated in this work relied on the immobilization of a conjugate of hyaluronan with a strong chelating agent, diethylenetriaminopentaacetic acid (DTPA). Once immobilized onto the surface, the DTPA moieties could be used to chelate various radionuclides with very different physical properties. This system could thus be a very useful tool to investigate the effect of these radionuclides in the vascular brachytherapy procedures. The combination of the biocompatibility of HA conjugated with the antiproliferative activity of appropriate radionuclides is also expected to offer new insights on the clinical use of radioactive devices in the field of revascularization. This work (Manuscript 3) has been accepted for publication in *Biomaterials*.

The third specific objective pursues the specific objective 2, i.e. creating hybrid coatings incorporating a bioactive component while enhancing the biocompatibility of the device. The approach used relied on the so-called layer-by-layer technique. This technique allows the sequential self-assembly of charged polyelectrolytes onto substrates. The two natural polysaccharides hyaluronan and chitosan have been selected for their biological activities and used to modify the surface of NiTi alloy. The manuscript presented here (Manuscript 4) submitted to *Biomacromolecules* describes the characterization of the self-assembly processes on the metallic NiTi alloy and the investigation of its potential toward the creation of biocompatible hybrid coatings.

6. BIOMIMETIC SURFACE

6.1. PAPER 2

Effective Immobilization of Hyaluronan on Metal Surfaces: Towards Bio-Mimetic Haemocompatible Coatings

Benjamin Thierry, Françoise M. Winnik, Yahye Merhi, Hans J. Griesser, Jim Silver,
Maryam Tabrizian

6.1.1. Abstract

Biomimetic surfaces offer exciting options to modulate the biocompatibility of biomaterials such as endovascular devices. The challenge is to create surfaces that undergo specific surface/cell interactions but do not suffer from non-specific fouling. Presented here is a new approach towards biomimetic surfaces, involving first the covalent immobilization, of a carboxylate terminated PEGylated hyaluronan (HAPEG)

onto plasma functionalized metallic surfaces (NiTi alloy) and, second, the modification of immobilized HAPEG. The metal substrates were aminated via two different plasma functionalization processes. Hyaluronan, a natural glycosaminoglycan and the major constituent of the extracellular matrix, was grafted to substrates by reaction of surface amines with the carboxylic acid terminated PEG spacer using carbodiimide chemistry. The surface modification was monitored at each step by X-ray photoelectron spectroscopy (XPS). HA-immobilized surfaces displayed increased hydrophilicity and reduced fouling, compared to bare surfaces, when exposed to human platelet (PLT) in an *in vitro* assay with radiolabeled platelets ($204.1 \pm 123.8 \times 10^3$ PLT/cm² vs. $538.5 \pm 100.5 \times 10^3$ PLT/cm² for bare metal, $p < 0.05$). A fluorescently labeled avidin was linked to HAPEG surfaces in order to demonstrate, by confocal fluorescence microscopy, the ability of the surfaces to be linked to bioactive proteins. The creation of surfaces that display the biocompatibility and fouling resistance of hyaluronan together with the bioactivity of conjugates, such as RGD containing peptides, is expected to promote specific surface/cell interactions and, in turn, to enhance the long term biocompatibility of biomaterials.

Keywords: Hyaluronan, Biomimetic, plasma functionalization, haemocompatibility, RGD peptides.

6.1.2. Introduction

It has been long recognized the interactions of biomaterials with biological components are regulated to a large extent by their interfacial properties. Most biological materials interact with moieties via ligand/receptor binding pathways, but resist non-specific

adhesion. On the contrary, synthetic materials are generally thrombogenic and do not offer a favourable environment for the growth of endothelial cells. The design of biomimetic coatings able to control cellular invasion has thus emerged as a promising tool for crafting truly biocompatible implants. Surface immobilization of adhesive peptides and, to a lesser extent growth factors, has been successfully used for this purpose¹⁻⁴. Non-specific fouling of these surfaces may, however, compromise their activity. A truly biomimetic surface should be able to resist non-specific adsorption and to enhance cell adhesion and proliferation by incorporating bioactive molecules.

The quest for ‘non-fouling’ surfaces, i.e. surfaces that resist unspecific interactions with biological components, has been the object of much investigation over the past years⁵⁻⁹. Significant advances have been made in understanding the molecular mechanisms involved in the interactions of surfaces with biological components, in particular comprehension of the role of hydration forces^{6; 10; 11}. In the case of blood-contacting materials, fouling of surfaces results from the adsorption of plasma proteins which initiates the blood coagulation cascade or bacterial adhesion. Previous studies have shown that poly(ethyleneglycol) (PEG) modified surfaces are the best candidates for non-fouling coatings. A number of natural polysaccharides, such as hyaluronan (HA), also possess unique non-fouling properties. HA is a linear anionic glycosaminoglycan composed of repeating disaccharide units of D-glucuronic acid and N-acetylglucosamine. HA is a major constituent of the extracellular matrix and is involved in biological events, such as cell differentiation and migration. Immobilization of HA onto synthetic materials has been reported as an effective way to bioengineer anti-fouling surfaces^{8; 12; 13}. Moreover, an RGD grafted-HA 3-D matrix has been used successfully as scaffold for tissue engineering¹⁴. Thus, it should be possible to develop biomimetic coatings by covalent immobilization of HA on a functionalized metallic surface and subsequent reaction of immobilized HA with bioactive molecules.

The immobilization of native HA on surfaces presents several challenges. First, it is necessary to activate a chemically-inert substrate in order to promote covalent or

physical linkage of HA to the surface. Plasma-based functionalization of synthetic biomaterials is widely employed to immobilize molecules on polymeric or metallic surfaces. It is a convenient method to tailor the surface chemistry of a biomaterial, while keeping its bulk properties unmodified. Direct immobilization of HA onto plasma-modified surfaces has been carried out previously, but the grafting yields were low¹⁵.

In this study, we have explored various routes to immobilize HA on functionalized surfaces. Primary amine groups were introduced onto metallic surfaces by two different methods, which we have compared in their effectiveness to react with HA and its derivatives. One process involves direct plasma polymerization of allylamine onto NiTi surfaces, the other is a two-step procedure based on reductive grafting of poly(allylamine) on an acetaldehyde plasma polymerized surface. Since the covalent linkage of native HA to surfaces has been reported to proceed sluggishly, we introduced a hydrophilic PEG spacer between the surface-reactive groups and the HA backbone (HA-PEG), using a procedure employed previously to attach radionuclide-HA conjugates on endovascular stents and catheters for radiation-based therapy against restenosis¹⁶. The polymer immobilization was achieved successfully via either a one-step or a two-step functionalization procedure, as determined by X-ray photoelectron spectroscopy. Because of the rapid loss in reactivity of the surface-introduced amines and lack of reproducibility of the one-step method, the two-step functionalization procedure was selected to create biomimetic HA-surfaces. The HA-PEG-immobilized surfaces were characterized by atomic force microscopy and haemocompatibility assays. Their use in the creation of hybrid surfaces was demonstrated by immobilization of fluorescently-labeled avidin. This work set up the basis for the formation of hybrid surfaces conjugating the biocompatibility and biological activity of HA with the specific activity of bioactive molecules grafted on the HA-PEG surface. In particular, immobilization of a growth factor, such as the vascular endothelial growth factor, may be achieved via the route described here to address the unsolved issue of non-fouling blood contacting materials.

6.1.3. Experimental

6.1.3.1. Materials

NiTi Discs (Ni: 55.8 wt%), provided by Nitinol Devices & Components (NDC, USA), were used as substrates. The discs (diameter: 12 mm, Ni: 55.8 wt%) were mechanically polished to a mirror-like finish using a 1- μ m diamond paste and further electropolished by NDC according to ASTM standards for metallic biomaterials¹⁷. Sodium hyaluronate (HA, MW ~ 600,000) was supplied by Hyal Pharmaceutical Corp (Canada). Allyl amine, acetaldehyde, poly(allylamine), 1-ethyl-3-(3-dimethylaminopropyl) carbodiimide (EDC), dicyclohexylcarbodiimide (DCC) and N-hydroxysulfosuccinimide (NHS) were purchased from Aldrich Chemical Corp. and used as received. Ethylenediamine (EDA) was purchased from Fluka and purified by distillation prior to use. Poly(ethyleneglycol) bis (carboxymethyl) ether (MW = 600) and fluorescein labeled avidin were obtained from Sigma Chemicals. All other reagents were of chemical grade. Ultrapure water (Milli-Q) with a resistivity ~18.2 M Ω .cm was used in all experiments.

6.1.3.2. Synthesis of the hyaluronan derivatives

A two-step procedure (Fig 6.1) was used to prepare hyaluronan derivatives. First, ethylenediamine was reacted with the carboxylic acid groups of HA to introduce primary amine groups along the HA backbone, then carboxylic acid-terminated PEG chains were linked to HA by amidation. Both reactions were carried out under conditions designed to prevent crosslinking of the hyaluronan derivatives. EDA:2HCl (10 eq.) and 1-ethyl-3-(3-dimethylaminopropyl) carbodiimide (EDC, 1.3 eq.) were

added sequentially to a solution of HA in a 2-(N-morpholino)ethanesulfonic acid (MES) buffer (0.1 M, pH 5.0). The reaction was allowed to proceed overnight. The polymer (HA-NH₂) was purified by exhaustive dialysis against deionized water and recovered by freeze-drying.

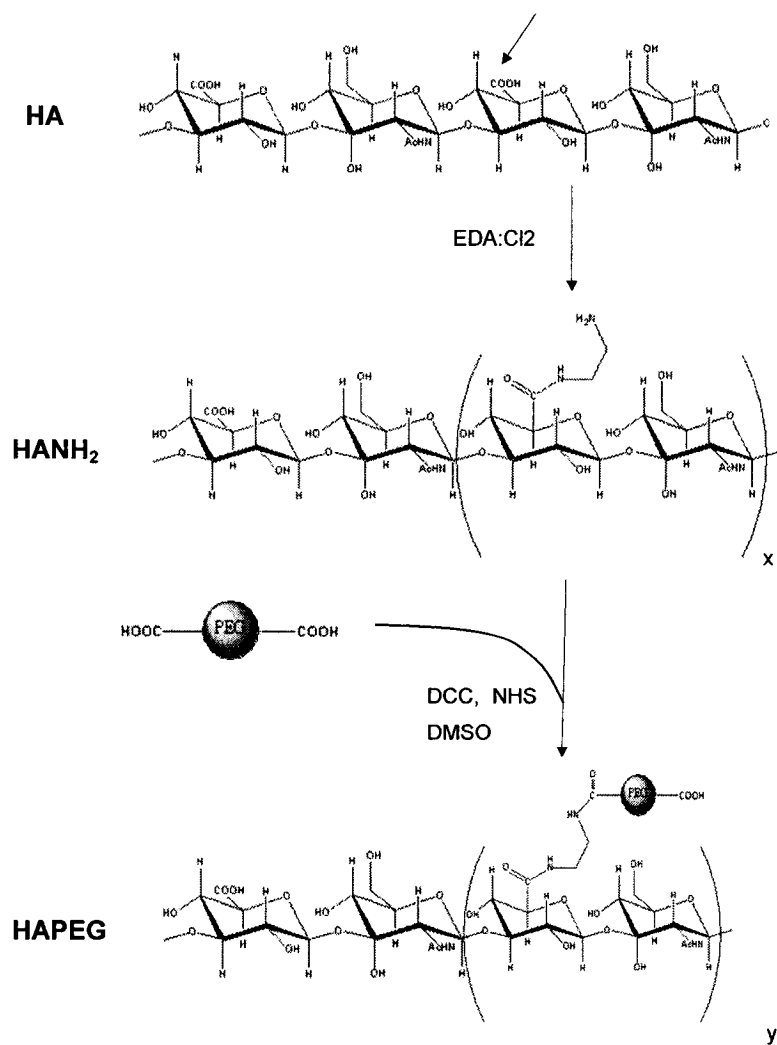


Figure 6.1. Hyaluronic acid derivative HA-PEG synthetic route.

PEG spacers were then grafted using the amino functionalities introduced in the first step. Poly(ethyleneglycol)bis(carboxymethyl) ether (600 g/mol) was dissolved in dry dimethylsulfoxide (DMSO) in the presence of Et₃N under N₂ flow. N-hydroxysulfosuccinimide (NHS, 1.1 eq.) and dicyclohexylcarbodiimide (DCC, 1.1 eq.) were added to the mixture and the reaction was maintained for 15 h at pH=10 at room temperature. The solution was filtered to remove isourea (by-product of the DCC-promoted ester activation reaction). It was then added slowly over 60 min to a HA-NH₂ solution of pH=10. The reaction was continued for 24 h. The reaction mixture was purified by dialysis against water for 7 days. The polymer HA-PEG was isolated by lyophilization.

6.1.3.3. Polymer characterization

HA derivatives were characterized using nuclear magnetic resonance (NMR) and gel permeation chromatography (GPC). ¹H-NMR spectra were recorded with a 400 MHz AMX-400 Bruker NMR spectrometer with solutions in deuterated water (purchased from Cambridge Isotope Inc), using water as an internal standard. The polymer concentration was 1% w/w. Gel permeation chromatography (GPC) measurements were performed with a Waters 510 programmable HPLC system equipped with a Waters 410 differential refractometer. The analysis was performed using Ultrahydrogel 500 and Ultrahydrogel 250 columns eluted with aqueous sodium nitrite (0.1 M) (flow rate: 0.7 mL/min, 30 °C) and calibrated with pullulan standards.

6.1.3.4. Surface functionalization

Two plasma-based functionalization schemes were employed to introduce amine groups on the surface of NiTi substrates. The first scheme involved direct polymerization of allyl amine on the surface (PlasmaAA). The second scheme consisted of two steps: plasma polymerization of acetaldehyde on a NiTi surface and subsequent grafting of poly(allylamine) via reductive amination (PolyAA).

6.1.3.4.1. One-step process. A radio frequency (13.56 MHz) glow discharge system was employed to deposit a thin film of plasma polymerized allyl amine on NiTi substrates. The Radio frequency (RF) plasma generator (Tegal Corp., Richmond Ca) was capacitatively coupled to the reactor using copper electrode. NiTi discs were introduced in the Pyrex glass reactor and a stable argon pressure was achieved (250 mTorr) at a power of 30 W. The polymerization was initiated by introduction of allyl amine in the discharge region through a needle valve. The polymerization was achieved via a 10-min exposure to plasma with the total pressure stabilized at 400 mTorr. The level of amine group grafting on the surface was estimated by derivatization of the amine with pentafluorobenzaldehyde (PFB) and XPS analysis, as described by Fally and coworkers¹⁸.

6.1.3.4.2. Two-step process. Plasma polymerization of acetaldehyde (99% purity) vapor was carried on NiTi substrates in a high frequency plasma generator at CISRO Molecular Sciences (Clayton South MDC, Australia), as previously described^{5; 19}. The surfaces were then reacted with an aqueous solution of poly(allylamine) hydrochloride (MW 70 KDa, Aldrich, 3 mg/mL, pH 6.8-7) in the presence of sodium cyanoborohydride (NaCNBH₃, 3mg/mL) as the reducing agent of the intermediate Schiff base.

6.1.3.5. Covalent immobilization of HA and HA derivative on functionalized surfaces

Either HA or HA-PEG were attached to plasma-modified surfaces via carbodiimide activated amide formation. First, activation of the carboxylic acids of HA-PEG (or native HA) was done by adding 1-ethyl-3-(3-dimethylaminopropyl) carbodiimide (EDC) and N-hydroxysuccinimide (NHS) in excess to a solution of HA-PEG (or HA) (0.1% w/w) in a MES buffer (0.1 M, pH 4.7) at room temperature for 20 min. Then functionalized metallic substrates (PlasmaAA or PolyAA) were then immersed in the activated HA-PEG (HA) solutions. The coupling reaction was allowed to proceed for 7h under gentle agitation at room temperature. The metallic substrates were washed thoroughly with ultrapure Milli-Q water for 48 h to remove non-covalently attached HA-PEG and unreacted reagents. They were dried under a nitrogen flow before surface analysis.

6.1.3.6. Surface characterization

The control surface for XPS analysis was prepared by spin-coating an aqueous HA-PEG solution (0.1% w/w) on a clean Si wafer using a commercial system (Laurell Technologies corporation, North Wales, PA).

X-ray Photoelectron Spectroscopy analyses were performed in a Vacuum Generators ESCALAB 3 MK II instrument, using non-monochromatized MgK α radiation (1253.6 eV) with an experimentally determined spectral resolution of 0.7 eV and a standard error less than 0.1 eV. Sample charge-up was not observed. Collection and analysis of the data were done using the Sursoft program. Spectra were recorded at two take-off angles (10 and 75° with respect to the surface) to modulate the depth of probe of the surface. Atomic concentration data were calculated using sensitivity factors determined on pure materials. In high resolution analysis, the spectra were referenced to C-H/C-C

at 285 eV in the C1S spectrum except for HA-spin coated Si where the spectra were referenced to C-O at 286.7 eV. High resolution spectra were accumulated at 0.05-eV intervals and, after a Shirley-type background substraction, the components peaks were separated using a nonlinear least mean squares program.

Contact Angle studies were performed with a Video Contact Angle System (VCA 2500, Ast, Billerica, Ma) using a 1- μ L droplet of Milli-Q water (18.2 M Ω) on the sample surfaces. The contact angles were determined semi-manually from the droplet image with a precision of $\pm 2^\circ$.

A DI AFM instrument (Nanoscope III, Digital Instruments, Santa Barbara, Ca) was operated in tapping mode on several area (5 μm^2) of the surface. The measurements were conducted in air with a scan rate of 0.5 Hz.

6.1.3.7. Haemocompatibility of the HA-immobilized surfaces

Platelet adhesion assay was done as described elsewhere²⁰. Briefly, a platelet rich plasma (PRP) was prepared by centrifugation (1800 rpm for 15 min) of blood drawn from healthy volunteers. The PRP was then centrifuged at 2200 rpm for 10 min and the platelet poor plasma (PPP) was recovered as the supernatant. Platelets were carefully resuspended in buffer and then incubated with 250 μCi of $^{111}\text{InCl}_3$ for 15 min. The platelets were then recovered by centrifugation and resuspended in the PPP to 2.5×10^6 platelets/mL. The samples (n=4) were placed into polystyrene dishes (Corning Inc.). A freshly prepared ^{111}In -platelet solution (3 mL) was then added to each well and the platelet adhesion was allowed to proceed for 60 min with gentle shaking. After incubation, the samples were recovered and washed 4 times with saline. The samples were then fixed in a 2 % glutaraldehyde solution and the amount of platelet was

determined using a gamma counter (1470 WizardTM, Wallac, Finland) after correction for background and decay.

Adhesion of ¹¹¹In polymorphonuclear neutrophils (PMNs) was determined as previously described^{20; 21}. Briefly, an extracorporeal procedure using *ex vivo* perfusion chambers and radiolabeling was used in four pigs. The shunt consisted in a two parallel silicon tubing channel circuit connecting the femoral artery to the perfusion chambers and returning to the femoral vein. Injured arterial segments from normal porcine aortas were prepared as described previously and were used as thrombogenic control²¹. The blood was allowed to circulate into the extracorporeal circuit for 15 min at a physiological wall shear rate of 424 sec⁻¹ before being flushed with saline for 30 sec. The total amount of PMNs adsorbed on the samples (n=5) was calculated by measuring the radioactivity retained on the samples and knowing the activity of blood samples used as reference and using hematology achieved prior to each experiment. All procedures were approved by the Montreal Heart Institute ethics committee.

6.1.3.8. Protein immobilization on HA surfaces

Avidin was used as a model protein to investigate the reactivity of surface immobilized HA-PEG towards further grafting of bioactive molecules such as a peptide or growth factors. HA-modified substrates were immersed in a MES buffer (0.1 M, pH 6.5). Subsequently, NHS and EDC were added in sequence (EDC:NHS 1:2 mol:mol). The resulting solution was stirred for 10 min. A stock solution of fluorescently labeled avidin in PBS (1 mg/mL) was added to achieve a final concentration of 80 µg/mL. The reaction was allowed to proceed overnight. The treated surfaces were thoroughly rinsed with water for 3 days to remove weakly bound proteins. All manipulations were performed in the dark to prevent photobleaching. Samples (n=2) were observed with an Axiovert inverted microscope equipped with an LSM 510 confocal system (Zeiss).

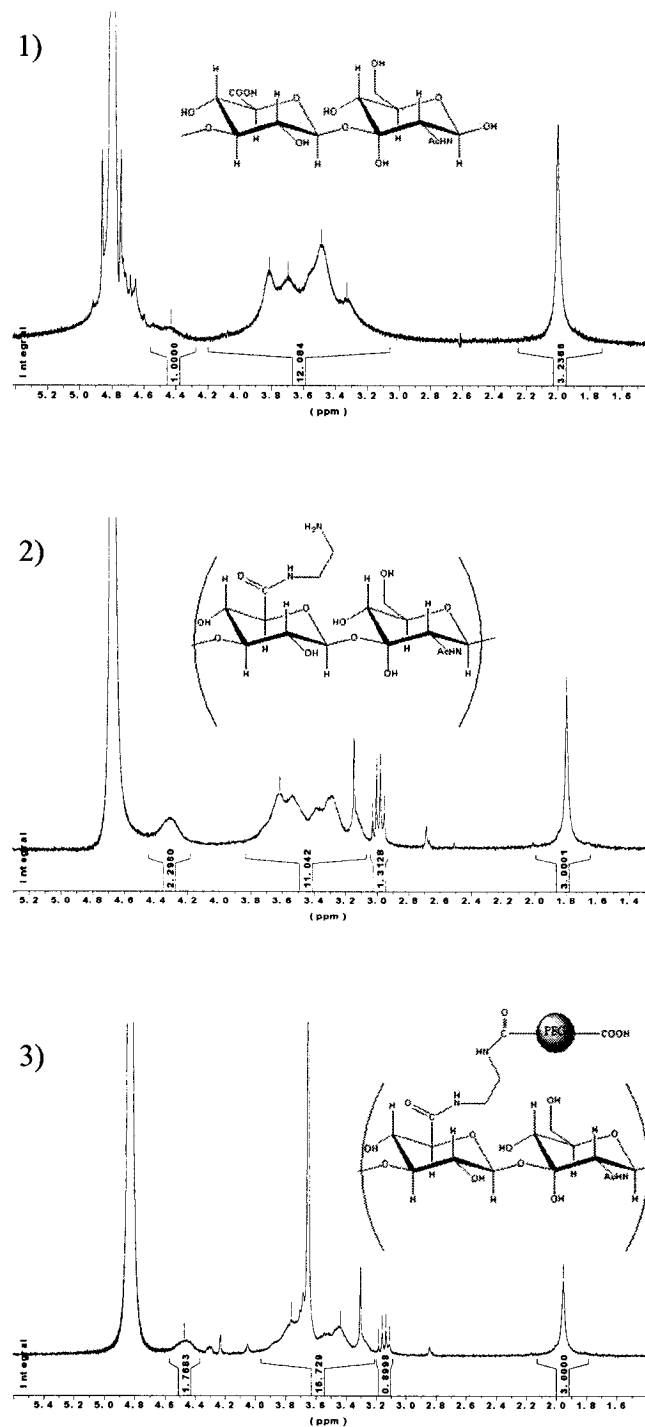


Figure 6.2. ^1H -NMR in D_2O at 400 Mhz: (1) native HA, (2) HA- NH_2 , (3) HA-PEG

6.1.4. Results

6.1.4.1. Preparation and chemical characterization of HA-modified surfaces

The surfaces investigated in this study were obtained by covalent attachment onto aminated surfaces of hyaluronan grafted with carboxylic-acid-terminated polyethyleneglycol chains, which play the role of spacers as well as linking moieties. In this section, the preparation of the modified HA is reported first. Then, we describe how HA-modified surfaces were obtained and present evidence of the successful outcome of the HA-surface linkage.

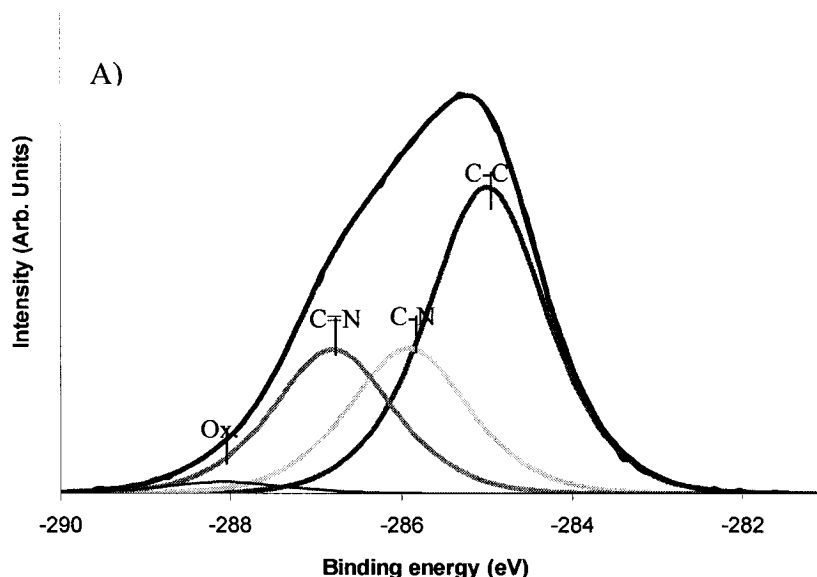
6.1.4.1.1. Preparation and characterization of HA-PEG

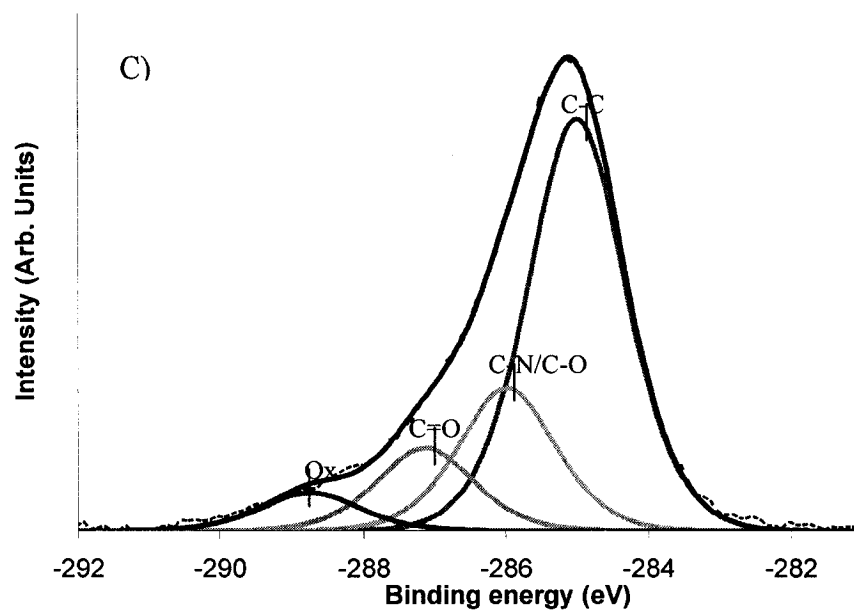
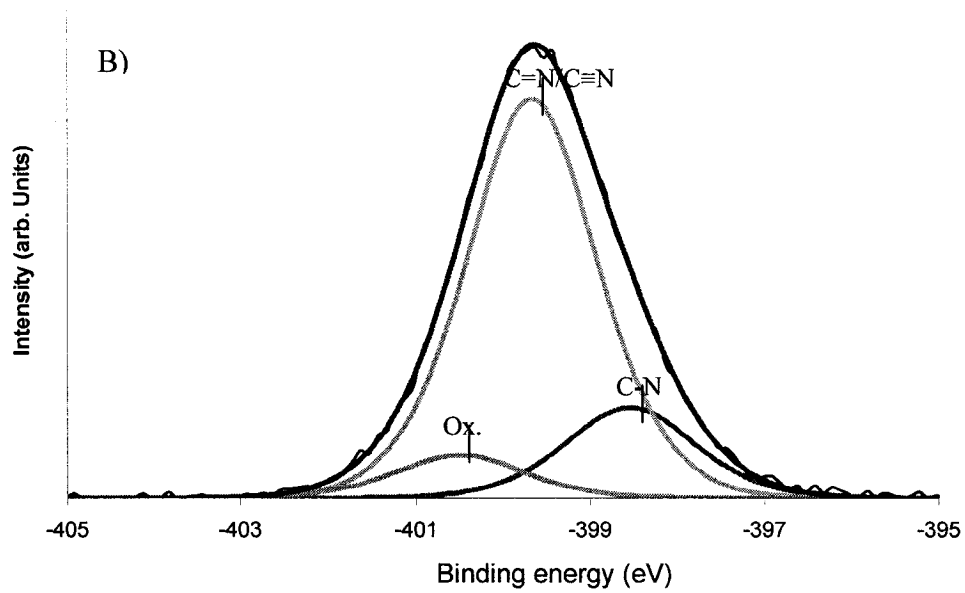
The HA-PEG sample was obtained by a two-step procedure, involving first the preparation of aminated-HA (HA-NH₂) by reaction of a fraction of the carboxylic acid functions of the glucuronic acid units with ethylenediamine in the presence of a carbodiimide, and, second, reaction of a carboxylic acid terminated poly(ethyleneglycol) derivative with the primary amine groups of HA-NH₂ (Figure 6.1). The presence of the ethylenediamine groups on the polymer was ascertained from the ¹H NMR spectrum of HA-NH₂, which presents a signal at δ 3.05 ppm, attributed to the ethylene protons of the ethylenediamine moieties. This signal, together with the singlet at δ 1.89 ppm attributed to the acetamide methyl protons resonance, was used to estimate the degree of functionalization of HA-NH₂, \sim 0.25 mol-NH₂/glucuronic acid residue (Fig. 6.2). The successful grafting of poly(ethyleneglycol) chains into HA-NH₂ was confirmed by the presence of a signal of δ 3.7 ppm, characteristic of the methylene groups of PEG, in the ¹H-NMR spectrum of HA-PEG, (Fig. 6.2). The level of PEG incorporation, estimated from the ¹H-NMR spectrum of HA-PEG, was \sim 0.20 mol PEG/mol glucuronic acid. The molecular weight of HA-PEG (\sim 3000 000 dalton), determined by GPC, was lower than that of the starting HA. This observation may

indicate that HA underwent some degree of depolymerization during the chemical transformations, or else, it may reflect the fact that the conformation of HA is altered upon substitution with PEG. It confirms however that no crosslinking took place during the preparation of HA-PEG. Analysis by GPC also confirmed the absence of unreacted dicarboxylated-PEG.

6.1.4.1.2. Preparation and chemical characterization of modified surfaces

The modified polymer HA-PEG was attached to NiTi surfaces by reaction of the terminal carboxylic acid groups of the PEG substituents with primary amines linked to the metallic surfaces. Two different methods were used to aminate NiTi surfaces: (a) plasma polymerization of allylamine onto bare NiTi surfaces, yielding PlasmaAA surfaces; and (b) plasma polymerization of acetaldehyde onto bare NiTi, followed by covalent attachment of polyallylamine to the aldehyde groups on the surface via reductive amination, yielding PAA surfaces.





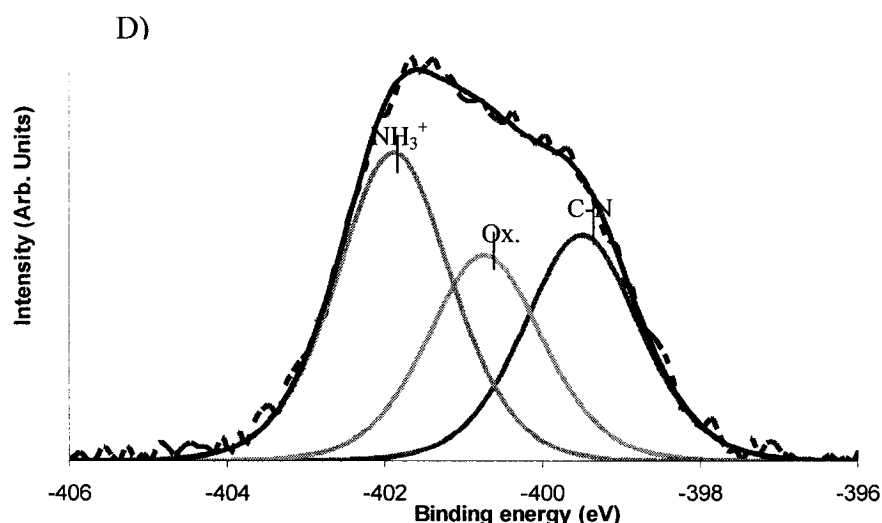


Figure 6.3. Resolved XPS spectrum of: PlasmaAA surface on NiTi, C1s (A), and N1s (B); and PolyAA surface on NiTi: C1s (C), and N1s (D)

(a) *Aminated surfaces obtained by plasma polymerization of allylamine (PlasmaAA).* The XPS survey spectrum of a functionalized NiTi surface presents a nitrogen peak (binding energy: ~ 399 eV, 19.1%) but no signal due to either Ni or Ti, confirming the successful outcome of the allylamine polymerization. The XPS elemental composition of PlasmaAA on a NiTi surface is reported in Table 6.1. The high resolution XPS spectrum of the C 1s and N 1s peaks of PlasmaAA surfaces was interpreted using data reported in previous studies^{18;22}. Four components were necessary to simulate the C 1s peak (Fig. 6.3-A and Table 6.2). The first component, at 285.0 eV, was attributed to unfunctionalized hydrocarbon (50 %). The second and third components can be attributed to carbon singly bonded to nitrogen (285.9 eV, 24 %), and to carbons of imine or nitrile groups (286.8 eV, 23 %), respectively. The high percentage of the third component (imine-nitrile), together with the presence in simulations of the N 1s peak of a component at 399.6 eV (75 %), indicate that fragmentation of the monomer occurred

during polymerization, resulting in the formation of imine and nitrile functions on the PlasmaAA surfaces (see Fig. 6.3-B and Table 6.2). The presence of a fourth component at 288.1 eV (2 %) in the simulated spectrum of the C 1s signal, together with the presence of O in the elemental XPS spectrum (3 %), point to some adventitious oxidation of the plasma polymerized surface upon exposure to air. This side reaction has been observed previously^{22; 23}.

(b) Aminated surfaces obtained by reaction of poly(allyl amine) with NiTi surfaces subjected to acetaldehyde plasma polymerization (PAA)

Successful introduction of poly(allylamine) on acetaldehyde-modified NiTi surfaces was confirmed by their survey XPS spectrum, which presents a nitrogen peak (402 eV, 7.2 %) and intense peaks at 285 eV and 532 eV, corresponding to C 1s and O 1s, respectively. No signal due to the metallic substrate could be detected by XPS elemental analysis. The C1s high resolution XPS spectrum of PAA surfaces (Fig. 6.3-C) is dominated by a hydrocarbon component (60.9 %), but presents also peaks attributed to C-N, C-O and C=O carbon atoms. Two types of nitrogen peaks are present in the N 1s high resolution spectrum (Fig. 6.3-D and Table 6.3): (i) a peak due to oxidized species (amide) indicating ambient oxidation of the PAA; and (ii) a peak characteristic of quaternary amines, with a signal of 401.9 eV (41.7 % of the total N signal). Note that the PAA XPS spectrum also displays a Cl signal (ratio N/Cl = 0.4), consistent with the presence of ammonium chloride functions on the surface. The XPS spectrum also presents an oxygen signal and the intensity of the signal depends on the take-off angle selected for analysis (13.4 % to 11.4% at 10° and 70° take-off angle, Table 1). Varying the take-off angle yields the depth profile of the surface elemental composition. The dependence of the oxygen peak intensity on the depth of analysis can be taken as an indication that, depending on the take-off angle, the XPS spectrum of PAA surfaces may also present peaks contributed by oxygen functionalities present in the acetaldehyde plasma polymerized underlayer. Therefore, it is not possible to attribute precisely the nitrogen C-N and oxygen C-O peaks, which may originate either from the acetaldehyde polymerized layer or from the poly(allyl amine) immobilized layer

(c) HA-derivative immobilized surfaces.

Successful grafting of HA-PEG on the aminated surfaces (PlasmaAA and PolyAA) is validated by a significant increase in the surface's oxygen concentration detected in the survey XPS spectra of HA-immobilized surfaces (Table 6.1), compared to that of aminated functionalized surfaces (28.5 % vs. 3% for plasmaAA and 26.8 % Vs. 13.4 % for PolyAA). Concurrently, their nitrogen content decreased (12 % Vs. 19.1 % for plasmaAA and 4.6 %Vs. 7.2 % for PolyAA).

Simulation and interpretation of the high resolution C1s XPS spectrum of HA-PEG modified surfaces were difficult, due to overlap of components from the plasma polymerized films (prior to reaction with HA-PEG) with the signals due to immobilized HA-PEG. To facilitate spectral assignments, we analyzed by XPS surfaces obtained by direct spin-coating of HA-PEG on a Si wafer and used the spectral data obtained to assign signals due to HA-PEG on the functionalized surfaces. The XPS survey spectrum of spin-coated films presents the following peaks attributable to HA-PEG: 285 eV (C 1s, 61.1%), 532 eV (O 1s, 34%) and 401 eV (N 1s, 4.9%) (Table 6.1). The high-resolution C 1s spectrum was analyzed in terms of four distinct components (Fig. 6.4): a 285 eV component corresponding to unfunctionalized hydrocarbon (C-C environment) used as reference, a component originating from carbon singly bound to oxygen or nitrogen (at 286.5 eV), and contributions due to carbonyl carbons (at 287.9 eV) and the carbons of the amide or carboxylate functions (at 289.5 eV). The unexpectedly high concentration of C in the elemental XPS analysis, which correlates well with the unusually strong hydrocarbon peak (285 eV) in the C1s high resolution (Tables 6.2 & 6.3), may be attributed to some level of contamination. The O 1s signal (not shown) has a major component at 531.5 eV, attributed to the ether oxygen functions of the PEG grafted to the HA backbone. The high resolution N 1s spectrum (not shown) presents a signal due to amide nitrogen (400 eV), providing further evidence that the PEG groups of HA-PEG are bound covalently to the HA backbone. Note that the nitrogen signal also has a component characteristic of quaternary amines, an indication that not all the amine

groups of HA-NH₂ are linked to PEG moieties, in agreement with the conclusions drawn from the analysis of the ¹H NMR spectra of HA-NH₂ and HA-PEG (*vide supra*).

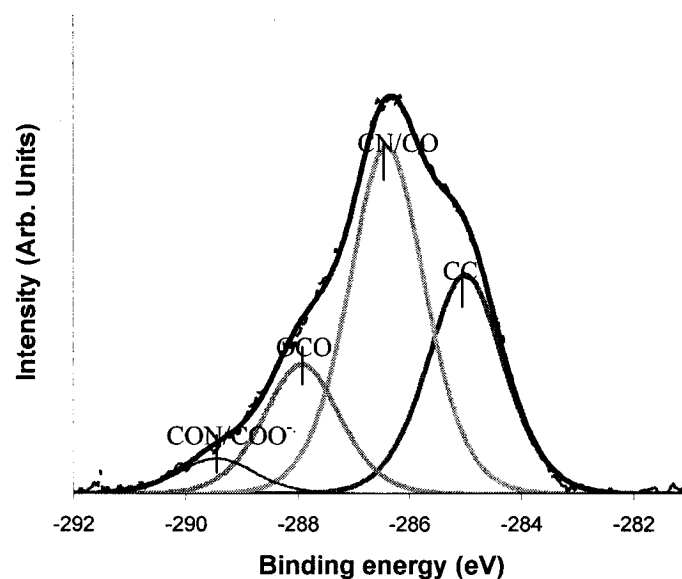


Figure 6.4. C1s XPS high resolution simulation of HA-PEG spin coated on a Si wafer

Table 6.1. XPS measured atomic ratio (%) for modified surfaces; values with a 70° take-off angle given in parentheses

sample	description	C	O	N
HAPEG SP	Spin-coated on silicium wafers	61.1	34	4.9
PolyAA	Poly(allylamine) grafted on surface	75.3	13.4 (11.4)	7.2
HA-PEG-PolyAA	HA-DTPA immobilized on PolyAA	68.6	26.8	4.6
HA-PolyAA	Unmodified HA immobilized on PolyAA	70.1	25.5	4.4
PlasmaAA	Plasma polymerized allyl amine on NiTi	79.9	3	19.1
HAPEG-PlasmaAA	HAPEG immobilized on plasmaAA	59.5	28.5	12
Cont. plasmaAA	PlasmaAA in buffer	73.8	16.7	9.5

Table 6.2. Simulation of XPS C1s peak recorded on plasma polymerized allylamine modified surfaces

Sample	% Contribution in the simulation C1s Core Level			
	CC	CN/CO	OCO	CON/COO ⁻
HAPEG_SP	30	47.6	17.6	4.8
PlasmaAA	50.2	24	23.8	2
HAPEG- PlasmaAA	44.6	35.1	12.8	7.4
Cont. plasmaAA	48.9	23.3	17.3	10.5

Table 6.3. Simulation of XPS C1s peak recorded on poly-allyl amine grafted surfaces

Sample	% Contribution in the simulation C1s Core Level			
	CC	CN/CO	OCO	CON/CO O ⁻
HAPEG_SP	30	47.6	17.6	4.8
PolyAA	60.9	21.2	12.3	5.7
HA-PEG- PolyAA	42.6	34.5	16	6.9
HA-PolyAA	45.7	23.7	20.2	10.4

With the help of the data gathered from the analysis of the HA-PEG spin-coated surfaces, we were able to attribute all the signals observed in the high resolution XPS spectra of the polyAA-HA-PEG and PlasmaAA-HA-PEG surfaces, but the presence, in these surfaces, of signals due to the underlying plasma polymerized layer made it difficult to determine quantitatively the amount of polysaccharide bound to the surface. The broadening of the C1s peak, together with the increase of the C-O surface content, provide further support to the successful outcome of the immobilization process (Fig. 6.5 and Tables 6.2 & 6.3). The C1s spectra of both surfaces present a strong component at 285 eV attributed to hydrocarbon carbons, 44.6 % and 42.6 % for PlasmaAA-HA-PEG and PolyAA-HA-PEG, respectively. Since, this component contributes to 30% of the total C 1s signal in the reference XPS spectrum of spin-coated HA-PEG surfaces, it can be concluded that the thickness of the HA-PEG layer on plasma polymerized

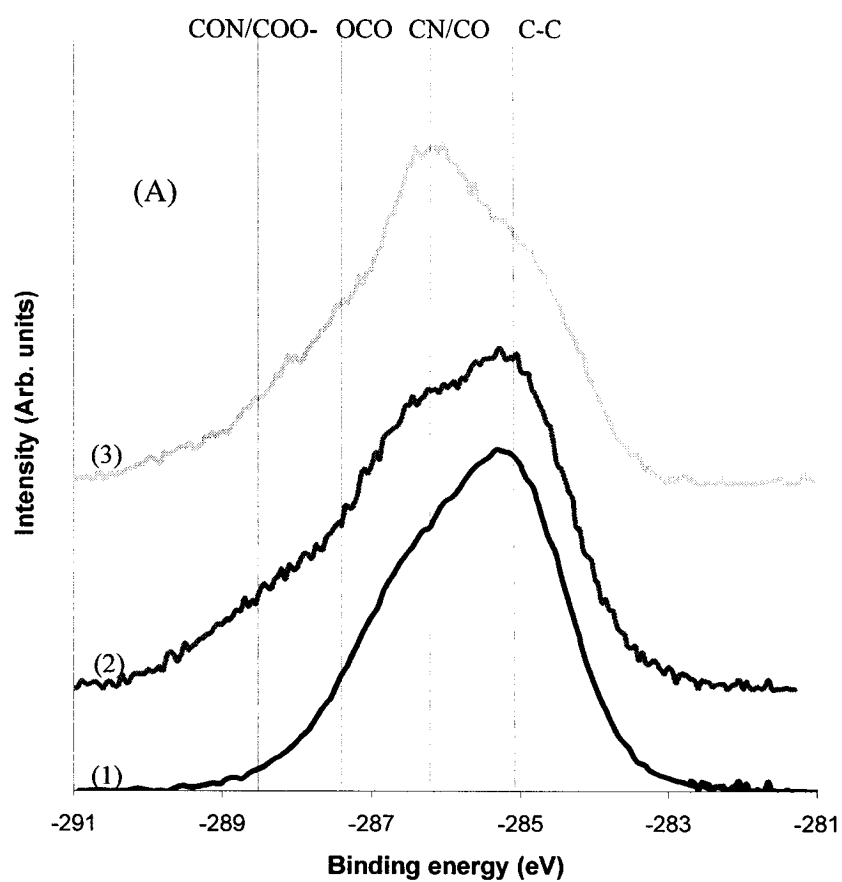
surfaces is less than the XPS probed depth (estimated about 10 nm) for both plasma treatments.

Water contact angle measurements, using the sessile drop technique (Table 6.4), indicate that both the HA-PEG-plasmaAA and the HA-PEG-polyAA specimens are significantly more hydrophilic than plasma modified surfaces. The hydrophilic nature of these surfaces, attributed to the presence of highly hydrated HA, further confirms the successful immobilization of HA-PEG onto both PolyAA and Plasma-AA surfaces.

As noted in the experimental section, functionalized NiTi surfaces (PolyAA) were treated also with native HA in order to assess the effect of the PEG-linkers on the outcome of surface modification. The elemental surface composition of HA-modified surfaces, obtained from XPS survey spectra, presents a significant contribution from carbon. The C1s peak can be simulated using contributions from CN/CO carbons, C-C carbons, and various oxidized carbon species (Table 6.3 and Figure 6.5). Note that in HA-PolyAA surfaces, the CN/CO component of the C1s peak is much weaker than in surfaces obtained by immobilization of HA-PEG (23.7 % Vs. 34.5 %), implying that the immobilization of native HA on PolyAA resulted in poorer grafting yields, compared to those of HA-PEG (Fig. 6.5 and Table 6.3). The surface oxygen concentration of HA-PolyAA surfaces, however, was higher than PolyAA surfaces (25.5 %, Table 6.1). Careful analysis of the high resolution XPS spectrum of HA immobilized on PolyAA indicates that the broadening of the C1s peak, compared to native HA, is caused, at least in part, by the presence of high energy components which must be attributed to functionalities formed by inadvertent oxidation of the PolyAA film, rather than to immobilized HA. The observed increase in oxygen surface concentration, therefore, may be another indication of the oxidation of PlasmaAA surfaces.

Table 6.4. Contact angle measured on NiTi modified surfaces

sample	θ°
plasmaAA	53 ± 3
polyAA	70 ± 6
HAPEG-plasmaAA	37 ± 4
HAPEG-polyAA	35 ± 5



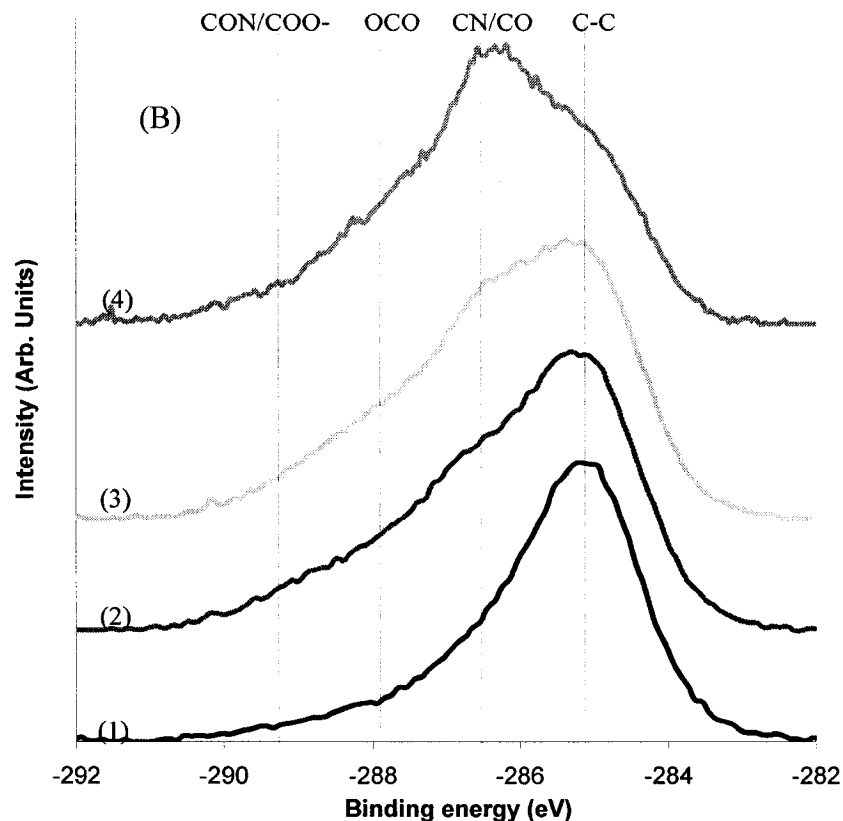


Figure 6.5. (A) Resolved XPS C1s spectrum of: (1) PlasmaAA, (2) HA-PEG immobilized on PlasmaAA, and (3) HA-PEG spin coated on a Si wafer; (B) Resolved XPS C1s spectrum of: (1) PolyAA, (2) HA immobilized on PolyAA, (3) HA-PEG immobilized on PolyAA, and (4) HA-PEG spin coated on a Si wafer

6.1.4.2. Investigation of the HA-PEG-polyAA surfaces in blood contacting applications

Morphology.

The morphology of the HA-PEG immobilized surfaces was probed by tapping mode AFM. Images of PolyAA (I) and HAPEG-polyAA (II) surfaces exposed to air are presented in Fig. 6.6. It is possible to detect some pinholes in the coating (~ 50 nm),

presumably related to defects created during the plasma polymerization treatment, but overall the surfaces are smooth. HA-PEG-PolyAA surfaces presented a meshed-network with small features about 10 nm that may correspond to HA chains.

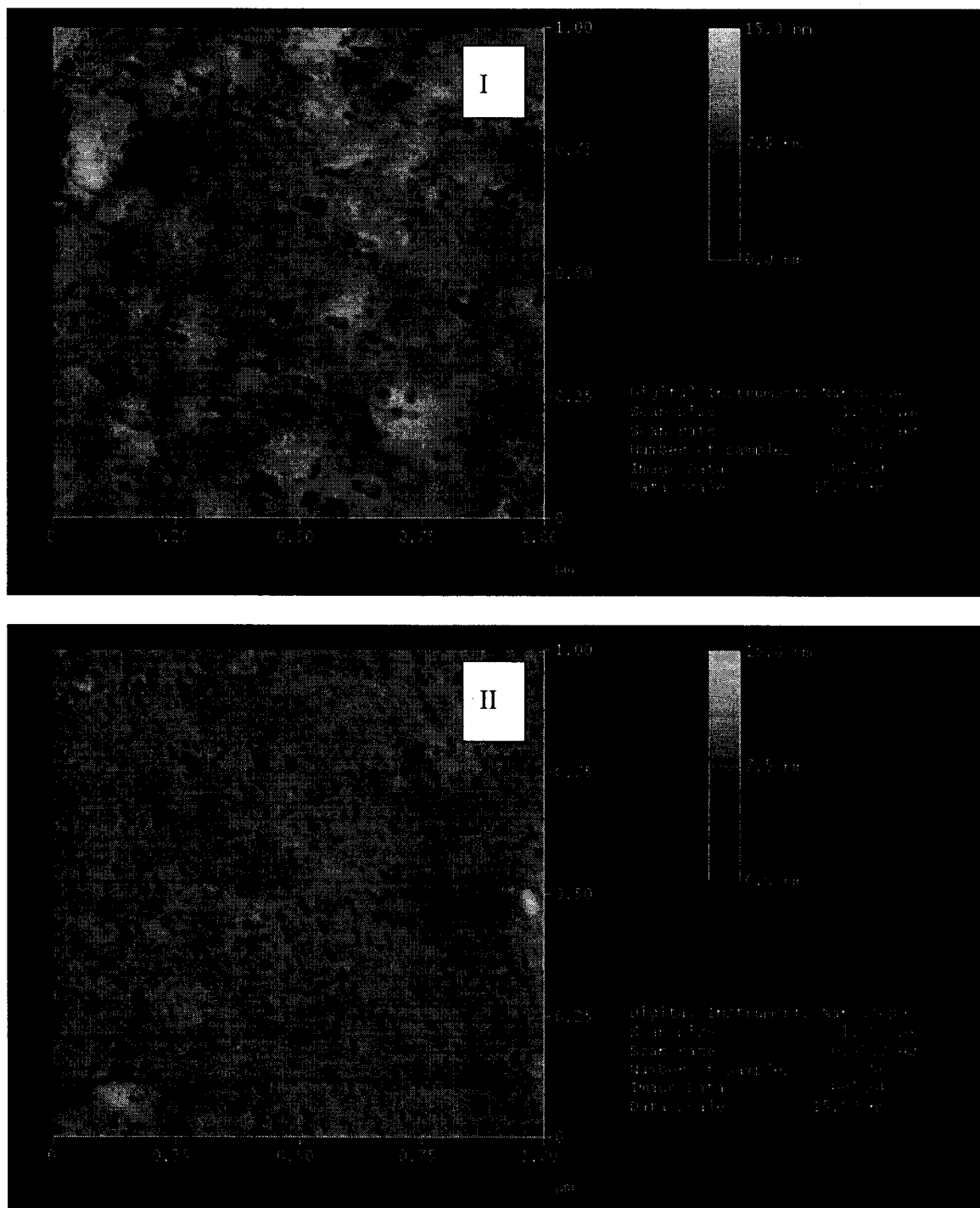


Figure 6.6. AFM height images in tapping mode of (I) PolyAA, (II) HA-PEG-polyAA; Images dimension are 1 μm^2 , and Z scales are 15 nm.

Haemocompatibility

The adhesion of ^{111}In -marked platelets on bare metallic surfaces and HA-modified surfaces was measured after a 60-min exposure. In this *in vitro* adsorption assay, platelet adhesion on HA-PEG modified surfaces ($204.1 \pm 123.8 \times 10^3 \text{ PLQ/cm}^2$) was significantly lower than on bare NiTi, which averaged $538.5 \pm 100.5 \times 10^3 \text{ PLQ/cm}^2$ at 60 min in the PRP (62 % reduction, $P < 0.05$ by Student-t-test) (Fig. 6.7). Glass used as a control presented platelet adhesion in the same range as NiTi ($471.7 \pm 238 \times 10^3 \text{ PLQ/cm}^2$).

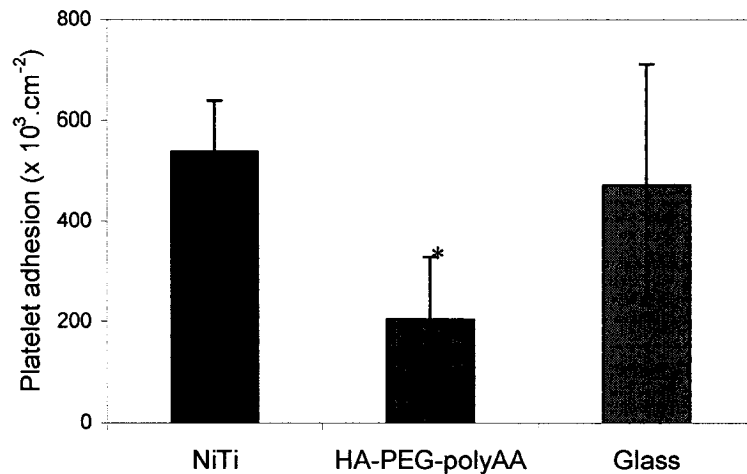


Figure 6.7. Platelet adhesion on NiTi, HA-PEG-polyAA and glass as control; * $p < 0.05$ Vs NiTi

Neutrophil adhesion on HA-PEG-polyAA surfaces was investigated next in an *ex vivo* porcine model and compared to that obtained on bare NiTi and damaged arteries (Media) used as control thrombogenic surfaces. As anticipated, the adhesion of

neutrophils on damaged arteries was high. It was much lower on bare metal surfaces as well as on HA-PEG-modified surfaces samples ($P < 0.05$, Fig. 6.8). Neutrophils adhered to a larger extent to the HA-PEG-polyAA surfaces than to bare metallic surfaces ($9 \pm 2.7 \times 10^3$ PMN/cm² Vs. $3.9 \pm 3.8 \times 10^3$ PMN/cm², $P > 0.05$).

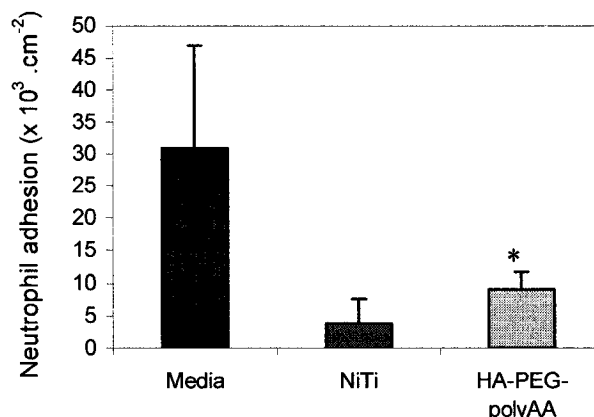


Figure 6.8. Neutrophil adhesion on damaged artery (Media), NiTi, and HA-PEG-polyAA; Mean \pm SEM; * $p < 0.05$ vs. Media (Student-t-test)

Protein immobilization

In order to test the suitability of HA-PEG modified surfaces as substrates for the immobilization of bioactive molecules, we conjugated to the surfaces a fluorescently-labeled protein and characterized the modified surfaces by confocal fluorescence microscopy. The protein, FITC-avidin, was linked to HA-PEG-polyAA surfaces in the presence of NHS and EDC. Parts of the surface were scratched prior to incubation with the protein, in order to remove sections of the HA-PEG layer, allowing a direct comparison of bare metal surfaces and HA-PEG treated surfaces. A strong fluorescence signal was detected in all areas exposed to the labeled proteins, except in the scratched

area (Figure 6.9), confirming for covalent linkage of the protein to the surface. These preliminary results open up the possibility of attaching various bioactive compounds to HA-PEG modified surfaces.



Figure 6.9. Confocal microscopy image showing the immobilization of FITC-avidin on the HA-PEG-polyAA surface. Arrow corresponds to the scratch denuding the HA-PEG layer and exposing the metallic surface.

6.1.5. Discussion

The bioactive surfaces described here present unique features, which result from the synergy between the intrinsic biological properties of hyaluronan and the chemical composition and morphology of the polymer layer immobilized on a metal surface.

A key element of our approach lies in the fact that, rather than attempting to bind HA directly to aminated surfaces, via the glucuronic acid carboxylates, a carboxylate terminated PEGylated HA was employed to favor reaction of surface amines with polymer-linked carboxylic acid groups. Mason et al showed previously that immobilization of native HA on functionalized surfaces usually proceeds rather sluggishly¹⁵. The same study reported much higher grafting yields using succinic anhydride spacers grafted onto HA. We chose to add a short hydrophilic PEG spacer between the HA backbone and the reactive carboxylic acid since PEG chains are biocompatible and their flexibility enhances the mobility of terminal carboxylic groups, compared with that of the glucuronic acid carboxylates which are bound to the polymer backbone itself. The modification of HA was best achieved by first coupling ethylenediamine to HA using water-soluble EDC as coupling agent. Control of the delicate balance between the rates of decomposition of this coupling agent, the formation of the active intermediate, and the formation of the amide bond was achieved by appropriate selection of the reaction medium pH.²⁴ Due to its low pKa value, EDA exists mostly in the unprotonated form at the pH selected and reacts readily with the active intermediate, allowing one to control the extent of HA amination.

Two different amination methods were employed to introduce amine groups on NiTi surfaces. Through a combination of XPS analysis and contact angle measurements, we were able to demonstrate that surface amine groups introduced on the metallic surface by either method react with HA-PEG. The difference in the chemistry of the aminated 'primer' layer and the complexity of the XPS simulation prevented quantitative comparison of the HA-PEG surfaces obtained with the two different aminated surfaces. This two-step functionalization, similar to the strategy previously used to immobilize carboxymethyl-dextran on polymeric surfaces by McLean et al⁵ allowed us to prepare reproducible surfaces with good HA-PEG coverage. In contrast, and in agreement with previous reports¹⁸, plasma polymerization of allyl amine onto NiTi proceeded by a complex mechanism, creating surfaces presenting imine and nitrile groups in addition to

the expected primary amine groups detected by derivatization with pentafluoro benzaldehyde (data not shown). The poor reproducibility of the direct plasma polymerization of allylamine process, together with rapid loss of reactivity of the PlasmaAA surface upon exposure to ambient conditions^{22; 23} led us to favor the more reliable two-step process. Based on the work of Hartley and coworkers with dextran, the expected higher potential for reorganization in solution of the HA immobilized layer upon hydration of the poly(allylamine) interlayer/HA was also expected to translate into higher biological activity¹⁹.

HA-PEG immobilized onto PolyAA functionalized surfaces was further characterized by AFM and blood compatibility assays. The HA-PEG modified surfaces present a mesh-like structure (Fig. 6.5) resulting from intermolecular association of HA chains on the surface. HA has been shown to self-associate in double-helical arrangements²⁵. As shown by the AFM analyses, HA-PEG-polyAA surfaces were smooth and uniform, at least within the subcellular scale. HA-PEG coated surfaces presented significantly reduced platelet adhesion (62 %) in an *in vitro* assay compared to bare metal surfaces. This result is in agreement with other reports on applications of HA as a fouling resistant material^{8; 13; 15; 26}. However, HA-PEG immobilized surfaces failed to prevent PMN adhesion in *ex vivo* assays and, in fact, even tended to increase adhesion. We and others have already observed the enhanced adhesion of monocyte and PMN on HA immobilized surfaces^{27; 28}. It may be related to non-specific adsorption or ligand/receptor binding on HA. The increase in PMN adhesion on HA-surfaces is modest though, compared to the adhesion of PMN on damaged arteries.

Fluorescently-labeled avidin was reacted with HA-PEG surfaces via carbodiimide mediated amide linkage between protein amine groups and HA-PEG carboxylic acid groups. This experiment was performed to test the suitability of HA-PEG surfaces to act as substrates for the immobilization of adhesive molecules or growth factors. It has been demonstrated by others that RGD synthetic peptides or growth factors immobilized on

synthetic surfaces can retain their activity¹⁻⁴. Further experiments are required to investigate the bioactivity of such immobilized molecules on the HA-PEG surfaces.

6.1.6. Conclusion

The present study indicates that covalent linkage of a modified hyaluronan onto plasma functionalized surfaces generates substrates which hold great promise as a means to tailor the specific activity of biomaterials. They are thromboresistant and readily amenable to functionalization with proteins, peptides, or other active agents. A key feature of the work lies in the strategy selected to link HA to the surface, namely to separate the reactive group from the HA backbone via a short PEG moiety. This methodology not only enhances the reactivity of HA but it also leads to smoothly meshed and highly hydrated surfaces, known to act as excellent non-fouling biomaterials. By combining the bioactivity of the grafted molecules with the biocompatibility and fouling resistance of the HA surface, this approach may enhance the long-term biocompatibility of metallic implants.

Acknowledgments.

This work was supported by an NSERC - strategic grant. We thank Nitinol Devices & Components for their technical and financial support. The authors wish to thank especially S. Poulin for her precious technical assistance and useful discussions about XPS analysis. Thanks also go to S. Gouin for the synthesis of HAPEG conjugate and Prof. Sipeha for help the direct plasma polymerization process.

6.1.7. References

1. Tiwari A, Salacinski HJ, Punshon G, Hamilton G, Seifalian AM: Development of a hybrid cardiovascular graft using a tissue engineering approach. *FASEB J* 2002;16:791-6
2. Shakesheff K, Cannizzaro S, Langer R: Creating biomimetic micro-environments with synthetic polymer-peptide hybrid molecules. *J Biomater Sci Polym Ed* 1998;9:507-18
3. Puleo DA, Kissling RA, Sheu MS: A technique to immobilize bioactive proteins, including bone morphogenetic protein-4 (BMP-4), on titanium alloy. *Biomaterials* 2002;23:2079-87
4. Kuhl PR, Griffith-Cima LG: Tethered epidermal growth factor as a paradigm for growth factor- induced stimulation from the solid phase. *Nat Med* 1996;2:1022-7
5. McLean KM, Johnson G, Chatelier RC, Beumer GJ, Steele JG, Griesser HJ: Method of immobilization of carboxymethyl-dextran affects resistance to tissue and cell colonization. *Colloids Surf B Biointerfaces* 2000;18:221-234
6. Morra M: On the molecular basis of fouling resistance. *J Biomater Sci Polym Ed* 2000;11:547-69
7. Shen M, Pan YV, Wagner MS, Hauch KD, Castner DG, Ratner BD, Horbett TA: Inhibition of monocyte adhesion and fibrinogen adsorption on glow discharge plasma deposited tetraethylene glycol dimethyl ether. *J Biomater Sci Polym Ed* 2001;12:961-78
8. Morra M, Cassineli C: Non-fouling properties of polysaccharide-coated surfaces. *J Biomater Sci Polym Ed* 1999;10:1107-24
9. Ruiz L, Hilborn JG, Leonard D, Mathieu HJ: Synthesis, structure and surface dynamics of phosphorycholine functional biomimicking polymers. *Biomaterials* 1998;19:987-98

10. Vogler EA: Water and the acute biological response to surfaces. *J Biomater Sci Polym Ed* 1999;10:1015-45
11. Rowe AJ: Probing hydration and the stability of protein solutions - a colloid science approach. *Biophys Chem* 2001;93:93-101
12. Cassinelli C, Morra M, Pavesio A, Renier D: Evaluation of interfacial properties of hyaluronan coated poly(methylmethacrylate) intraocular lenses. *J Biomater Sci Polym Ed* 2000;11:961-77
13. Verheye S, Markou CP, Salame MY, Wan B, King SB 3rd, Robinson KA, Chronos NA, Hanson SR: Reduced thrombus formation by hyaluronic acid coating of endovascular devices. *Arterioscler Thromb Vasc Biol* 2000;20:1168-72
14. Glass JR, Dickerson KT, Stecker K, Polarek JW: Characterization of a hyaluronic acid-Arg-Gly-Asp peptide cell attachment matrix. *Biomaterials* 1996;17:1101-8
15. Mason M, Vercruysse KP, Kirker KR, Frisch R, Marecak DM, Prestwich GD, Pitt WG: Attachment of hyaluronic acid to polypropylene, polystyrene, and polytetrafluoroethylene. *Biomaterials* 2000;21:31-6
16. Thierry B, Winnik FM, Mehri Y, Silver J, Tabrizian M: Radionuclides-hyaluronic acid-conjugate thromboresistant coatings to prevent in-stent restenosis. *Biomaterials (In press)*
17. ASTM F86, Standard Practice for Surface Preparation and Marking of Metallic Surgical Implants, in *Annual Book of ASTM standards: Medical Devices and Services*. American Society for Testing and Materials, 1995, pp 6-8
18. Fally, F., Doneux, C., Riga, J., and Verbist, J. J. Quantification of the functional groups present at the surface of plasma polymers deposited from propylamine, allylamine, and propargylamine. *J Appl Polym Sci* 1995 v56(n5):597-614.
19. Hartley PG, McArthur SL, McLean KM, Griesser HJ: Physicochemical Properties of Polysaccharide Coatings Based on Grafted Multilayer Assemblies. *Langmuir* 2002;18:2483-2494

20. Thierry B, Merhi Y, Bilodeau L, Trépanier C, Tabrizian M: Nitinol versus stainless steel stents: acute thrombogenicity study in an ex vivo porcine model. *Biomaterials* 2002;23:2997-3005
21. Merhi Y, King M, Guidoin R: Acute thrombogenicity of intact and injured natural blood conduits versus synthetic conduits: neutrophil, platelet, and fibrin(ogen) adsorption under various shear-rate conditions. *J Biomed Mater Res* 1997;34:477-85
22. Calderon JG, Harsch A, Gross GW, Timmons RB: Stability of plasma-polymerized allylamine films with sterilization by autoclaving. *J Biomed Mater Res* 1998;42:597-603
23. Gengenbach, T. R., Vasic, Z. R., Li, S., Chatelier, R. L., and Griesser, H. J. Contributions of restructuring and oxidation to the aging of the surface of plasma polymers containing heteroatoms. *Plasmas Polym v 2(n 2)*, p 91-114. 97.
24. Nakajima N, Ikada Y: Mechanism of amide formation by carbodiimide for bioconjugation in aqueous media. *Bioconjug Chem* 1995;6:123-30
25. Cowman MK, Min L, Balazs EA: Tapping mode atomic force microscopy of hyaluronan: extended and intramolecularly interacting chains. *Biophys. J.* 1998;75:2030-2037
26. Barbucci R, Magnani A, Rappuoli R, Lamponi S, Consumi M: Immobilisation of sulphated hyaluronan for improved biocompatibility. *J Inorg Biochem* 2000;79:119-25
27. DeFife KM, Shive MS, Hagen KM, Clapper DL, Anderson JM: Effects of photochemically immobilized polymer coatings on protein adsorption, cell adhesion, and the foreign body reaction to silicone rubber. *J Biomed Mater Res* 1999;44:298-307
28. Thierry B, Winnik FM, Mehri Y, Silver J, Tabrizian M: Self-Assembled Bioactive Coatings of Endovascular Stents. *Submitted*

7. ANTI-PROLIFERATIVE STENTS

7.1. PAPER 3

Radionuclides-hyaluronan-conjugate thromboresistant coatings to prevent in-stent restenosis

Benjamin Thierry, Françoise M. Winnik, Yahye Merhi, Jim Silver, Maryam Tabrizian

7.1.1. Abstract

Catheter-based brachytherapy is one of the most effective modalities to inhibit hyperplasia following revascularization procedures. Radioactive stents have failed, however, to prevent clinical hyperplasia due to excessive late lumen loss on the edge of the devices. Numerous strategies have been proposed to circumvent the drawbacks of irradiation therapies, such as the use of more appropriate radionuclides or the “hot end” stents approach. This paper describes versatile radioactive devices obtained by coating plasma functionalized surfaces – stents or catheters - with a hyaluronan (HA) – diethylenetriamine pentaacetic acid (DTPA) conjugate (HA-DTPA) complexed with a γ or β radionuclide. Yttrium and indium were used as radionuclide models, due to their suitability for endovascular radiotherapy. XPS and ToF-SIMS analyses confirmed the successful immobilization of the HA-DTPA conjugate on both metallic (NiTi) and polymeric (Teflon) plasma functionalized surfaces. HA-DTPA coated surfaces were significantly more hydrophilic than bare surfaces (39.5° Vs 67° on NiTi substrate and 29° Vs 128° on Teflon substrate). Therapeutic doses of yttrium and indium were easily

loaded onto the surfaces and remained stable over 2 weeks with a radionuclide loss of about 6%. The HA-DTPA-coated Teflon surfaces presented significantly less fibrinogen adsorption than uncoated materials in an *in vitro* flow model. This approach, which combines the haemocompatibility of HA coated surfaces and the anti-proliferative effects of an appropriate radiotherapy, constitutes a promising methodology to alleviate the restenosis induced by existing devices.

Copyright © 2003 Elsevier Science Ltd.

Reprinted by permission of Elsevier

Keywords: Stent, catheter, restenosis, hyaluronan, haemocompatibility, surface modification.

7.1.2. Introduction

Thrombosis and neointimal thickening remain the major limitations associated with percutaneous transluminal angioplasty (PTA). The injury created to the endothelium, and to the medial and adventitial layers during revascularization procedures is thought to initiate these adverse reactions. Randomized trials have established stenting as the procedure of choice in PTA. However, despite the beneficial effect of vessel scaffolding, neointimal hyperplasia within the stented artery results in in-stent restenosis rates of 10% for ideal lesions and up to 50% for complex conditions or in the case of associated pathologies, such as diabetics^{1; 2}. Procedures targeting cellular hyperproliferation through intracoronary radiation or local release of antiproliferative drugs have shown promising results in both experimental and clinical models³⁻¹⁰. Radiation treatments inhibit the ability of cells to clonogenically divide, thus preventing acute cellular proliferation and migration usually triggered by vascular wall injury. To date, the FDA

has approved three radiation delivery catheter systems¹¹. Current brachytherapy methods use radioactive wire or seed sources and liquid-filled balloons. Intracoronary radiation therapies remain, however, limited by long term side-effects such as late lumen loss at the extremities of the irradiated areas, the so called 'edge-effect', and late thrombosis^{10; 12}. Extending the radiation margins to 14.5 mm at each end of the stented vessel has, however, been shown to minimize the edge effect¹³. Stents have also been investigated as a radiation delivery platform with the idea that prolonged exposure of the arterial wall to low radiation doses may be beneficial¹⁴. Unfortunately, clinical studies have revealed an increased occurrence of late thrombosis and edge-effect^{7; 15}. While the excellent results seen so far in clinical trials with drug eluting stents seems to preclude further investigation of radioactive stents, they may just be a result of delayed healing and long-term studies (24-30 months) in humans are needed to show whether the benefit is maintained¹⁶. Until very long-term results on drug-coated stents are in, it will be important to keep looking into alternative solutions such as radioactive stents.

Most clinical studies in the field of radioactive stents have been carried out with ³²P stainless steel devices¹⁷⁻¹⁹. There is a real need to develop and assess new devices for intracoronary radiation using different types of radionuclides, varying parameters such as the type of emission produced (γ -or β -emitters), the emission half-life, and the radiation energy, which affects the depth of dose distribution. Such fundamental properties need to be assessed, together with more practical issues, such as the nature of the sources, the minimal shielding requirements, and the ease and cost of manufacturing. The effects of such fundamental parameters on the *in-vivo* fate of radioactive stents could be assessed readily by the direct application of radioactive coatings onto commercially available stents or catheters. The feasibility of this approach was explored in the study described here. We have designed a stent coating which not only can carry numerous radionuclides but also creates a haemocompatible and lubricant surface. Briefly, the general procedure involves two steps: (1) functionalization of the bare device with amine groups and (2) covalent immobilization of a hyaluronan (HA) diethylenetriaminepentaacetic acid (DTPA) conjugate (HA-DTPA) on the device surface using the amine functionalities as anchoring groups. HA is a naturally-occurring linear polysaccharide consisting of alternating N-acetyl- β -D-glucosamine and β -D-

glucuronic acid residues linked (1→3) and (1→4), respectively. It is present in the extracellular matrix of mammalian connective tissues and plays an important structural and mechanical role in various tissues, participates in the control of tissue hydration and water transport, and affects numerous biological processes, such as inflammation, tumor metastasis and development²⁰. It has been used to bioengineer anti-fouling surfaces and HA-based coating appears as a promising way to improve the haemocompatibility of blood-contacting devices^{21; 22}. DTPA has long been recognized for its superior metal-binding properties. Its complex with gadolinium is used clinically as a contrast agent in magnetic resonance imaging. The complex of DTPA with radionuclide has been investigated recently in the prophylactic treatment of restenosis using a balloon^{23; 24}. The radionuclide Yttrium-90 (⁹⁰Y) has been found to be particularly suitable in endovascular radiotherapy since it is a pure β -emitter ($E_{b,max} = 2.28$ MeV, $E_{b,ave} = 0.94$ MeV) and it has a half-life of 64.1 hours. In this study the polysaccharide conjugate HA-DTPA bound to device surfaces was charged with either ⁸⁹Y (non-radioactive) or indium-111 (¹¹¹In, gamma emitter, half-life 67.44 h). We present here the preparation and physicochemical characterization of the modified devices as well as an assessment of their non-fouling properties using an *in-vitro* flow model.

7.1.3. Experimental

7.1.3.1. Hyaluronic acid diethylenetriaminepentaacetic acid conjugation

Sodium hyaluronate (HA, MW ~ 500,000) was obtained from Hyal Inc. (Mississauga, ON, Canada). HA-DTPA was prepared following the sequence of reactions shown in Fig. 7.1.1 and described previously²⁵. Briefly, ethylene diamine hydrochloride (EDA:2HCl, 10 eq.) was added to a solution of 1-ethyl-3-(3-dimethylaminopropyl) carbodiimide (EDC, 1.3 eq.) and HA in MES buffer (g-morpholine ethane sulfonic acid, 0.1 M, pH 5.0). The reaction mixture was kept overnight at room temperature to yield

(HA-NH₂), which was purified by dialysis against water and recovered by freeze-drying. Diethylenetriaminepentaacetic acid (DTPA) was activated by reaction with N-hydroxysulfosuccinimide (NHS, 1.1 eq.) and dicyclohexylcarbodiimide (DCC, 1.1 eq.) in dry dimethylsulfoxide (DMSO) in the presence of triethylamine and under N₂. The reaction mixture was kept for 15 h at pH10 at room temperature. It was then added by drops over 60 min to a solution of HA-NH₂ (pH 10). The resulting reaction mixture was kept at room temperature for 24 h. It was then dialyzed against deionized water for 7 days using membranes with a MW cut-off of 3,500 daltons. The polymer HA-DTPA was recovered by lyophilization.

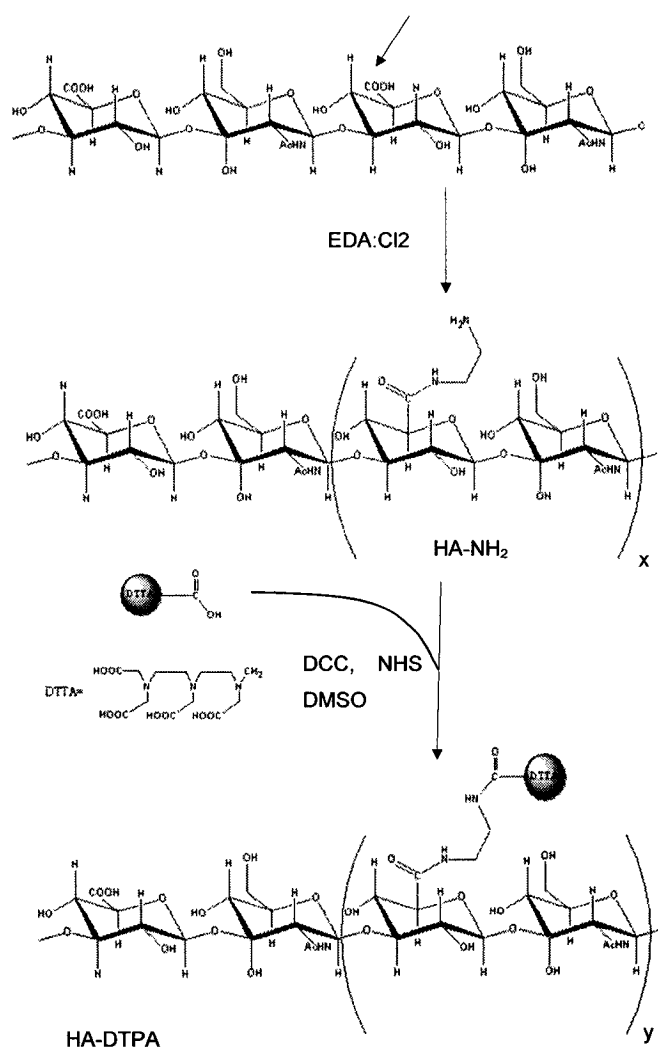


Figure 7.1.1. Hyaluronan derivatives (HA-NH₂ and HA-DTPA) synthetic route.

The absence of unreacted low-molecular weight compounds was established by gel permeation chromatography. The conjugation of DTPA was confirmed by ^1H -NMR analysis of a solution of the polymer in D_2O : (δ , ppm): 1.2 (q, CH_2 from DTPA), 1.99 (singlet, N-CO-CH_3), 3.0-3.2 (broad, CH_2 from DTPA), 4.55 broad (1-CH). The level of DTPA incorporation (0.16 mol DTPA/disaccharide unit or 0.32 mol DTPA/ g polymer) was determined by a colorimetric assay described in detail elsewhere²⁵.

7.1.3.2. Surface functionalization

NiTi discs (Ni: 55.8 wt%) provided by Cordis Corporation - Nitinol Devices & Components (Fremont, CA) were polished mechanically to a mirror-like finish using a 1- μm diamond paste. They were subsequently electropolished according to ASTM standards²⁶. Teflon samples were used as polymeric substrates. The surfaces were modified first by plasma polymerization of acetaldehyde (99% purity, Aldrich) vapor in a high-frequency plasma generator under controlled conditions. The surfaces were then reacted with a poly(allylamine) hydrochloride (MW 70 KDa, Aldrich) solution (3 mg/mL) in deionized water at pH 6.8-7 using sodium cyanoborohydride (NaCNBH_3 , 3 mg/mL) as the reducing agent for the intermediate Schiff base linkage. This procedure allows the covalent linkage of a polyamine spacer onto substrates, as described by McLean et al²⁷.

7.1.3.3. Covalent immobilization of HA-DTPA on functionalized surfaces (Fig. 7.1.2)

HA-DTPA was dissolved overnight in a 0.1 M MES buffer of pH 4.7 (1 % (w/w)). The solution was placed in glass vials. Activation of the HA-DTPA carboxylic acids

was achieved by a 20-min treatment with an excess of EDC and N-hydroxysulfosuccinimide (NHS). The amine-functionalized substrates obtained following procedure 2.2 were immersed into solutions of activated HA-DTPA. The coupling reaction was allowed to proceed for 7 h. The modified surfaces, HA-DTPA-NiTi and HA-DTPA-Teflon, were thoroughly washed with deionized water to remove all unbound materials.

Control surfaces for ToF-SIMS and XPS analyses were prepared by spin-coating HA-DTPA from an aqueous solution onto silicon wafers using a commercial spin coating system (Laurell Technologies Corporation, North Wales, PA). Prior to coating, the silicon wafers were treated for 10 min with isopropanol and DCC in an ultrasonic bath. They were dried under a nitrogen flow. The level of hydrocarbon contamination (< 9 %) was determined by XPS analysis.

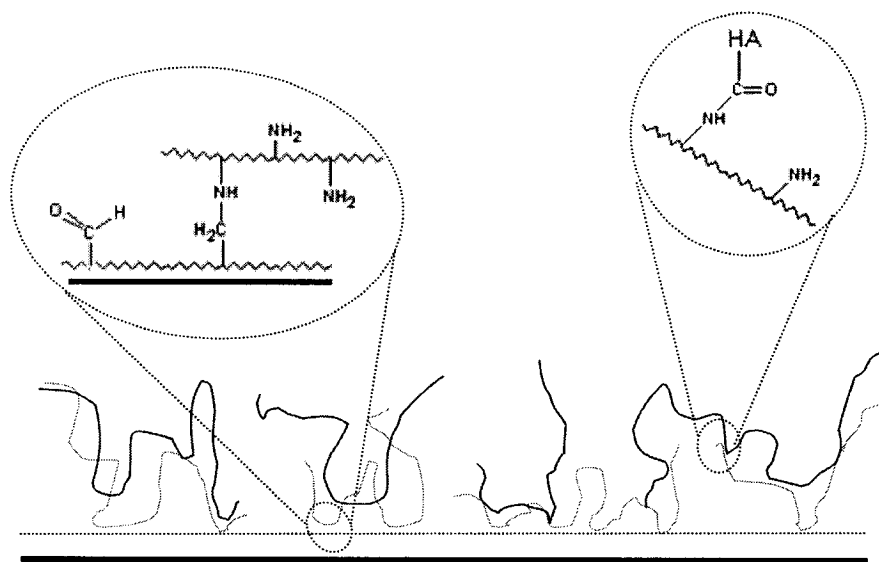


Figure 7.1.2. Schematic of the immobilization of HA-DTPA on functionalized surfaces

7.1.3.4. Radiolabelling of HA-DTPA immobilized surface

Complexation of HA-DTPA modified substrates was carried out first with non-radioactive yttrium (^{89}Y) to establish and fine-tune the experimental procedures which were then carried out with radioactive indium (^{111}In). HA-DTPA-grafted surfaces were immersed in an aqueous solution of the radionuclides (0.2 mM YCl_3 or 100 $\mu\text{Ci/mL}$ for InCl_3) at room temperature for 1 h. The samples were recovered, rinsed with deionized water for 1 h, dried under a nitrogen stream and stored for further analysis. The stability of the HA-DTPA- ^{111}In complex linked to the surfaces was assessed by incubation of the HA-DTPA- ^{111}In modified surfaces in 40 mL of phosphate buffered saline (PBS: 137 mM NaCl, 2.7 mM KCl, 4.3 mM Na_2HPO_4 , 1.4 mM KH_2PO_4 in pure water at pH 7.4) at 37 °C. At various time intervals, a solution aliquot (1 mL) was collected and the amount of radioactivity released in solution was determined using a Gamma counter (1470 WizardTM, Wallac, Finland). Data were corrected to account for the natural decay of ^{111}In .

7.1.3.5. Surface characterization

Contact angle measurements, X-ray photoelectron microscopy (XPS) and time-of-flight secondary ions mass spectrometry (ToF-SIMS) were used to characterize the properties of the functionalized surfaces, HA-DTPA immobilized surfaces and HA-DTPA-radionuclide loaded surfaces. NiTi was used as substrate for the characterization of these surfaces.

Contact angles of various substrates were measured with a Video Contact Angle System (VCA 2500, Ast, Billerica, Ma) applying a 1- μ L droplet of deionized water (18.2 M Ω) on the samples' surfaces. The contact angles were determined semi-manually from the droplet image within a precision of $\pm 2^\circ$. To investigate the potential reorientation of the HA chains upon hydration, contact angles were measured on HA-DTPA modified substrates that had been immersed in water for 2 hr. Advancing and receding contact angles were obtained from dynamic contact angle measurements of deionized water droplets. XPS analyses were performed in a Vacuum Generators ESCALAB 3 MK II instrument, using aluminium-filtered MgK α radiation (1253.6 eV) with an experimentally determined spectral resolution of 0.7 eV and a standard error lower than 0.1 eV. Sample charge-up was not observed. The vacuum in the analysis chamber was below 10^{-9} Pa. Collection and analysis of the data were done using the Sursoft program. Spectra were recorded at two take-off angles (10 and 75° with respect to the surface) to modulate the depth of probe of the surface. Atomic concentrations were calculated using sensitivity factors determined on pure materials. Deconvolutions of the C1s, N1s and O1s peaks were performed to gain information on the chemical environment of the carbon, nitrogen and oxygen atoms in the probed surface (about 4 to 10 nm depending of the take-off angle) High resolution spectra were accumulated at 0.05-eV intervals and, after a Shirley-type background subtraction, the components' peaks were separated using a nonlinear least-mean-squares program. All spectra were referenced to C-H/C-C at 285 eV in the C1s spectrum except in the case of the substrates obtained by spin coating HA-DTPA on NiTi surfaces where the spectra were referenced to C-O at 286.5 eV.

Time-of-flight secondary ions mass spectrometry analyses were recorded using an ION TOF IV spectrometer from ION-TOF (Germany) equipped with a primary ion Ga $^+$ beam operated at 15 keV. Areas of 500 μm^2 were analyzed well-under the so-called "static" condition with an ion dose about 10^9 ions/cm 2 . Calibration of the mass spectra was based on hydrocarbon peaks such as CH $_3^+$, C $_2$ H $_5^+$ and C $_3$ H $_7^+$.

7.1.3.6. Protein adsorption in an *in-vitro* dynamic flow model

The adsorption of fibrinogen on the HA-DTPA modified Teflon samples was achieved using a dynamic flow chamber specially designed to expose 0.16 cm² of the surfaces under a one-dimensional laminar parallel flow. A small amount of ¹²⁵I-Fibrinogen (250 µCi, Amersham International) was added under gentle stirring to a solution of fibrinogen (Sigma, 1 mg/mL) in PBS buffer kept at 37 °C. Prior to the experiment, each surface was hydrated in a saline solution for 1 h. The hydrated surface was then placed inside the perfusion chamber. The entire perfusion circuit was washed for 1 min with PBS. The fibrinogen solution was then allowed to circulate for 1 h at 37 °C at a physiological wall shear rate of 454 sec⁻¹. At the end of the experiment, saline solution was circulated in the circuit for 1 min to rinse the samples without exposure to air to avoid a Langmuir-Blodgett-like transfer of protein at the air-water interface. The amount of ¹²⁵I-fibrinogen adsorbed was determined using a Gamma counter (1470 WizardTM, Wallac, Finland). Data were corrected to account for the natural decay and the background²⁸.

7.1.4. Results and discussion

7.1.4.1. Preparation of HA-DTPA coated substrates

Several factors guided our selection of the chemical modification scheme employed in this study. First, it was imperative to create strong linkage between the metal surface of the stent and the polymer substrate; second, the surface exposed to the blood stream had to possess non-thrombogenic characteristics, and, third, it had to be readily

amenable to radiolabeling. These considerations led us to select HA-DTPA as an excellent candidate in our quest for non-fouling radiolabeled devices and to opt for a three-step surface modification sequence, involving plasma modification with acetaldehydes, grafting of poly(allylamine), and finally covalent linkage of HA-DTPA. In the following sections we describe each step of the surface engineering.

7.1.4.1.1. Conjugation of DTPA onto sodium hyaluronan

The synthesis of HA-DTPA was performed in two steps starting with a high molecular weight hyaluronan, following a procedure reported earlier^{25; 29}. In the first step, the carboxylic acid groups of the glucuronic acid residues were allowed to react with ethylenediamine by means of a carbodiimide coupling agent yielding HA-NH₂ (Fig. 7.1.1). In the second step, NHS-activated DTPA was grafted on HA-NH₂ to form an amide linkage with the primary amine groups introduced in the first step. The reaction conditions were optimized, and high levels of DTPA were achieved. The HA-DTPA sample employed in this study has a level of DTPA substitution of about 16 % mol DTPA/mol d-glucuronic acid.

With the HA-DTPA samples we developed an analytical protocol that will permit us, ultimately, to determine the amount of HA-DTPA grafted on stents or similar substrates. A HA-DTPA film thick enough to prevent detection of any signal from the Si substrate by XPS or ToF-SIMS was deposited onto a silicon wafer by spin coating. XPS elemental analysis of this HA-DTPA film indicated an atomic % of C: 59%, O: 32.7%, N: 8.3% (see Table 7.1.1). The deconvolution pattern of the C1s, N1s and O1s peaks was complex, but consistent with the structure of the HA derivative (Fig. 3 and Table II). Simulation of the C1s peak required 4 contributions, assigned to unfunctionalized hydrocarbon carbons (CH_x environment, 17 %, used as reference at 285 eV), carbons singly bound to oxygen and nitrogen (at 286.2 eV, 38.5 %), carbons doubly bound to oxygen (at 287.3 eV, 25.5 %), and carbons in an amide or carboxylate environment (at 288 eV, 19 %). Consistent with the structure of HA-DTPA, the simulation of the N1s

peak required two components, one assigned to the amide nitrogen (83 %) and one attributed to the protonated amine nitrogen (17 %). These values will be used later as controls to ascertain the presence of HA-DTPA on the various modified substrates and to determine the level of chemical modification.

7.1.4.1.2. Functionalization of metallic substrates

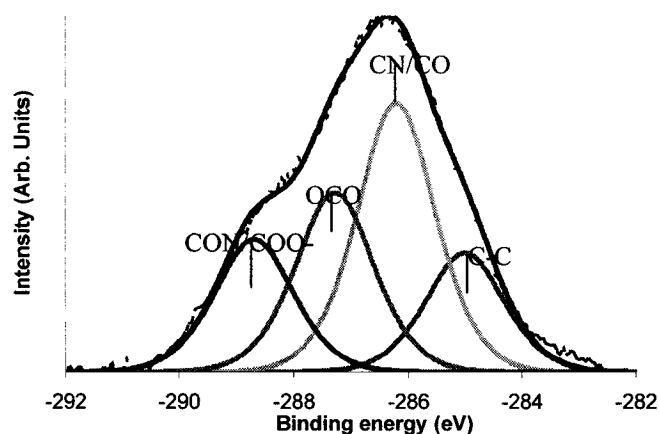
Plasma functionalization was used to introduce reactive chemical functionalities, namely aldehyde groups, onto the chemically inert metallic and polymeric surfaces used as models, NiTi alloy and Teflon, respectively. Thus, acetaldehyde was subjected to plasma polymerization on the substrates and the grafted aldehyde groups served as anchoring points for poly(allylamine) (PolyAA) via sodium cyanoborohydride catalyzed reductive amination. That functionalization of the surfaces took place was confirmed by the appearance of a nitrogen peak at 402 eV in the XPS spectrum of plasma modified NiTi attributed to nitrogen and by the absence of any titanium signal from the metallic substrate. Intense photoelectron peaks were also observed at 285 eV and 532 eV, ascribed to C1s and O1s, respectively. The XPS elemental composition of NiTi-Poly(allylamine) surfaces is reported in Table I. High resolution analysis showed the presence of an N1s peak at 401.88 eV (42 % of the total N signal) (Fig. 7.1.3), indicating the presence of protonated amines, presumably as a hydrochloride since a peak characteristic of Cl (ratio N/Cl = 1.75) was detected as well. The presence of oxygen in the XPS-probed depth and its dependency towards the depth of analysis (13.4 % to 11.4 % at 10° and 70° take-off angle) indicate that in the ultra high vacuum condition of analysis, the thickness of the PolyAA layers is a few nanometers. It is expected that, upon hydration, reorientation of the polymer chains will take place together with a swelling of the surface layer.

Table 7.1.1. XPS measured atomic ratio for NiTi modified surfaces (at 0° take-off angle); values with a 75° take-off angle given in parentheses. (Salts and contamination not shown)

sample	description	C	O	N
HAgDTPA_SP	HAgDTPA spin-coated on silicon wafers	59	32.7	8.3
NiTi-PolyAA	Poly(allylamine) grafted on NiTi surface	75.3	13.4	7.2
HAgDTPA-NiTi	HAgDTPA immobilized on NiTi-PolyAA	65.5(67.7)	27.1(24.7)	7.4(7.6)
HA-NiTi	HA immobilized on NiTi-PolyAA	70.1(69.8)	25.6(24.9)	4.4(5.4)

Table 7.1.2. Simulation of XPS C1s, O1s and N1s peaks recorded on NiTi modified surfaces

Sample	% Contribution in the simulation						
	C1s				N1s		
	CHx	CN/CO	OCO	CON/COO ⁻	CN	CON	NH ₃ ⁺
HAgDTPA_SP	17	38.5	25.5	19	-	83	17
NiTi-PolyAA	61	21	12	5.5	30.5	27	42
HAgDTPA-NiTi	38	31.5	17	13.5	-	75.5	24.5
HA-NiTi	45.5	24	20	10.5	-	63.5	36.5



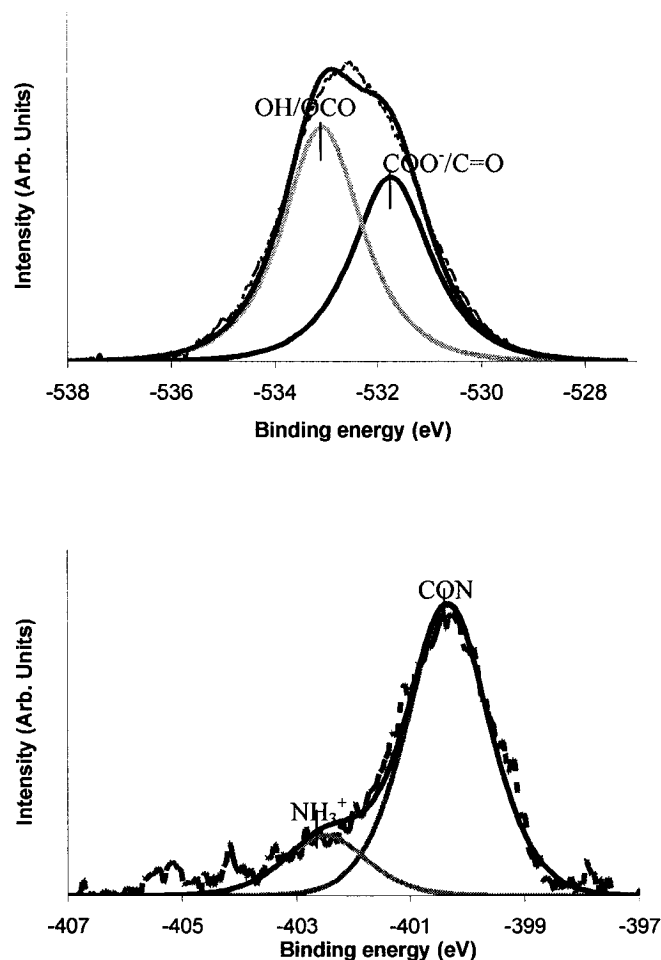


Figure 7.1.3. Resolved XPS spectrum of HA-DTPA spin coated on Si wafer: C1s (a), O1s (b) and N1s (c)

7.1.4.1.3. Immobilization of HA-DTPA onto the amine modified substrates

The poly(allylamine) amino groups introduced on the substrate by the method described in the preceding section were used as reactive handles for the immobilization of HA-DTPA. First, the carboxylic acid groups of HA-DTPA were converted into NHS-activated esters known to react rapidly with amines on the surfaces to form stable amide linkages³⁰. The resulting HA-DTPA-modified NiTi surfaces were subjected to XPS analysis, which revealed an increase in oxygen content (from 13.4 % to 27.1 %)

together with a decrease of the peak at 285 eV (75.3 % to 65.5 %) associated with carbon, compared to the XPS spectrum of the poly(allylamine) modified substrates. The values recorded for the HA-DTPA modified surfaces are close to those measured for HA-DTPA spin-coated on silicon wafer. Deconvolutions of the high resolution spectrum of HA-DTPA immobilized on the surface of poly(allylamine) proved to be difficult to perform, since the spectra include not only signals due to HA-DTPA, but also signals due to the underlying poly(allylamine) and acetaldehyde polymerized surfaces layers. Nonetheless, the broadening of the XPS high resolution spectrum of C1s (Fig. 7.1.4) is consistent with a significant increase of the 286.7 eV component (31.5 %) associated with C-O and, therefore, confirmed the presence of HA-DTPA on the surface.

In some XPS survey spectra we detected a small signal at 458 eV, an energy characteristic of titanium. The signal was barely above the instrument's limit of detection, but its presence may be diagnostic of incomplete coverage of the metal substrate. To assess the origin of the titanium signal, a ToF-SIMS analysis was performed on several samples, since this technique of extremely high sensitivity and surface resolution has proved to be a powerful means to detect the presence of defects in organic coating³¹. The presence of titanium on HA-DTPA-NiTi surfaces was confirmed by their positive ToF-SIMS spectrum (Fig 7.1.5), which presented a peak at m/z 47.95, an energy characteristic of titanium. Mapping of surfaces for titanium ions was performed by ToF-SIMS analysis. As shown in Fig. 7.1.6, which presents a titanium ion map of a HA-DTPA-NiTi substrate, titanium is located mainly in defects such as scratches. These defects may be the result of inappropriate handling of the samples or else may be symptomatic of an inherently poor efficiency of the coating procedures. The latter is a cause for concern since defects are expected to initiate bioadhesion and to promote fouling of surfaces.

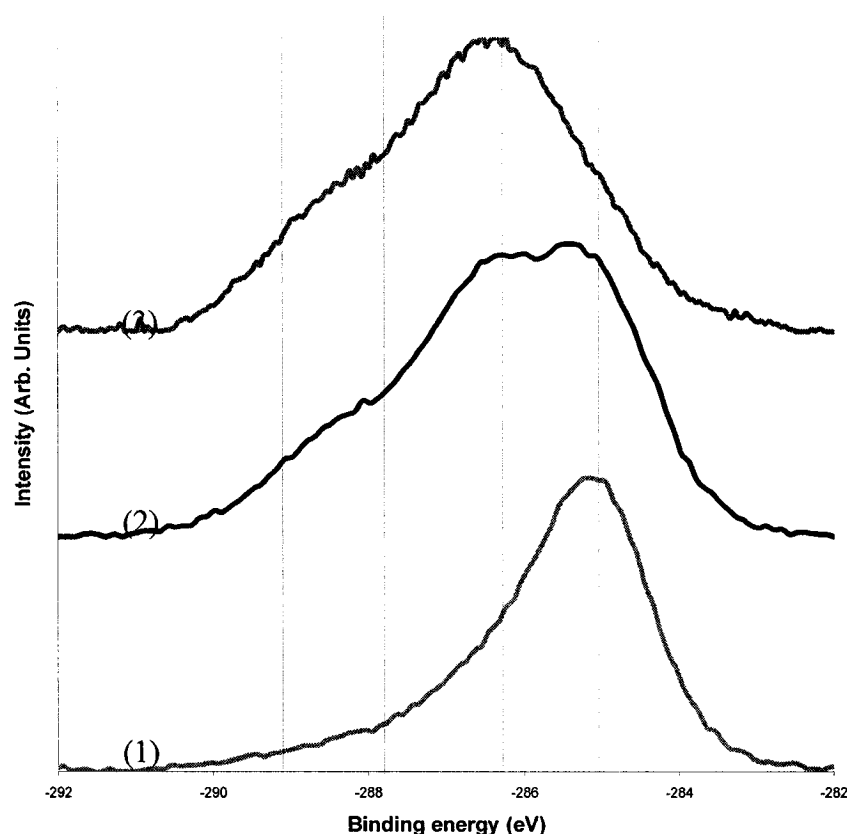


Figure 7.1.4. XPS C1s spectrum of: (1) NiTi-PolyAA, (2) HA-DTPA-NiTi, and (3) HA-DTPA spin coated on Si wafer.

One often uses a combination of peaks, the “fingerprint” of a molecule or polymer, can be used as a means to identify unambiguously this compound on a surface. In the case of the samples probed here, however, the similarity of the surfaces, namely poly(allylamine) grafted on acetaldehyde polymerized NiTi and HA-DTPA-NiTi, significantly complicated the interpretation of the ToF-SIMS spectra. The spectra of HA-DTPA-NiTi obtained by positive sputtering (Fig. 7.1.6) were dominated by hydrocarbon ions (C_2H_3 , C_2H_5 , C_3H_5 , etc), but nitrogen-containing peaks were also detected (CH_3N , CH_4N , CH_4N_2). The latter may be associated with the underlying poly(allylamine). Only a few peaks could be ascribed unambiguously to the HA-DTPA

ions, such as C_2H_3O at $m/z = 43.01$, C_2H_5O at $m/z 45.034$, $COOH$ at $m/z 44.997$). Similar features were revealed by the ToF-SIMS analysis of HA-DTPA-Teflon samples.

While quantitative conclusions from ToF-SIMS spectra are obviously not easy to draw, these results suggest that under the ultrahigh vacuum conditions of the analysis, the outermost surface contained a significant amount of polyallylamine spacers rather than the HA-DTPA derivative. The matrix effects could, however, have affected the sputtering probability of typical HA-DTPA secondary ions. Angle-resolved XPS analysis gave a further indication of the presence of polyAA on the surface, as shown in table 1, with the decrease in the oxygen % in the outermost surface of HA-DTPA-NiTi detected at 75° take-off angle. Similar situations have been reported previously in the case of surfaces modified with polymers of high chain mobility³². As a consequence, the HA-DTPA layer is not stratified over the poly(allylamine) layer, but rather the two polymers form an interpenetrated network. Reorganization of the surface to minimize interfacial energy is expected to occur upon hydration. Hyaluronan is very hydrophilic; thus, it may be expected to migrate towards the substrate/water interface, which would thus become enriched in HA, compared to the dried surfaces. To test this hypothesis we measured the contact angles of water droplets deposited onto various substrates. Contact angle values (Table 7.1.3) indicate that HA-DTPA-NiTi and HA-DTPA-Teflon surfaces are significantly more hydrophilic than unfunctionalized surfaces ($39.5^\circ \pm 2.4$ Vs. $72.5^\circ \pm 1.3$, $p < 0.0001$ for NiTi surfaces, 28 ± 4 Vs. 128 ± 1 , $p < 0.0001$ for Teflon surfaces). One has however to keep in mind that contact angle measurements on bare metals are limited by surface contamination. Contact angle was found to decrease with increasing immersion time (from $39.5^\circ \pm 2.4$ (time 0) to $30.8^\circ \pm 5.6$ on HA-DTPA-NiTi after 2 h immersion in pure water, $p = 0.005$). This observation corroborates our assumption that the HA-DTPA chains undergo a reorganization upon hydration to minimize interfacial energy. The decrease in the contact angle upon hydration could also be the results of water adsorption of the HA-rich hydrophilic surfaces. The presence of hyaluronan chains at the water/solid interface is expected to help in preventing fouling of the surfaces when exposed to blood.

Table 7.1.3. Contact angle measured on modified surfaces

sample	Hydration	θ°
NiTi	-	67 ± 4
NiTi-PolyAA	-	72.5 ± 1.3
HA _g DTPA-NiTi	0	39.5 ± 2.4
	2 h	30.8 ± 5.6
Teflon	-	128 ± 1
HA _g DTPA-Teflon	-	28 ± 4

7.1.4.2. Adsorption of radionuclides on HA-DTPA immobilized NiTi

The chelation of gadolinium(III) by HA-DTPA has been studied in detail previously and appropriate chelation methodology has been reported enabling high efficiency of chelation with no trace of unbound metal²⁵. The same approach was followed here using yttrium and indium as model radionuclides, in view of their high affinity to DTPA and the fact that their properties are appropriate for endovascular radiotherapy. Indeed, chelation of HA-DTPA with either yttrium or indium was achieved easily by treating a solution of HA-DTPA at room temperature with aqueous solutions of 0.02 μM YCl_3 or 100 $\mu\text{Ci/mL}$ InCl_3 , respectively. Other radionuclides such as Sr, Tc, Sm, Re could be similarly used. The outcome of the chelation of yttrium was investigated using XPS and ToF-SIMS analysis. The appearance of a very small peak at 158 eV in XPS survey spectra suggested the incorporation of the ions in the surface (not shown). A positive ToF-SIMS spectrum of the surface presented a peak at m/z 88.91, characteristic of yttrium (Fig. 7.1.5), confirming that chelation of yttrium had indeed occurred. Molecular imaging of drug distribution within a polymeric matrix has been studied

using ToF-SIMS³³. Using the ToF-SIMS imaging mode, the molecular distribution of yttrium in the HA-DTPA modified substrates was shown to be homogeneous over the entire surface (Fig 7.1.6).

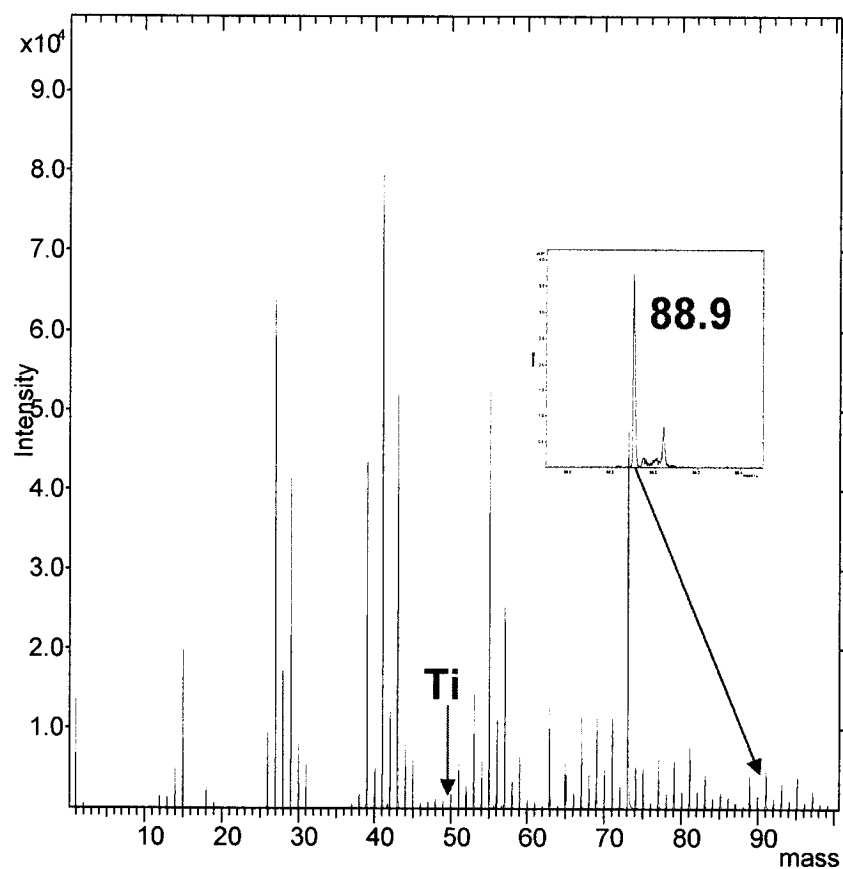


Figure 7.1.5. Positive mode ToF-SIMS spectra recorded for Yttrium-HA-DTPA immobilized NiTi. The insert shows the characteristic peak of yttrium at m/z 88.9.

Field of view: 500.0 × 500.0 μm^2

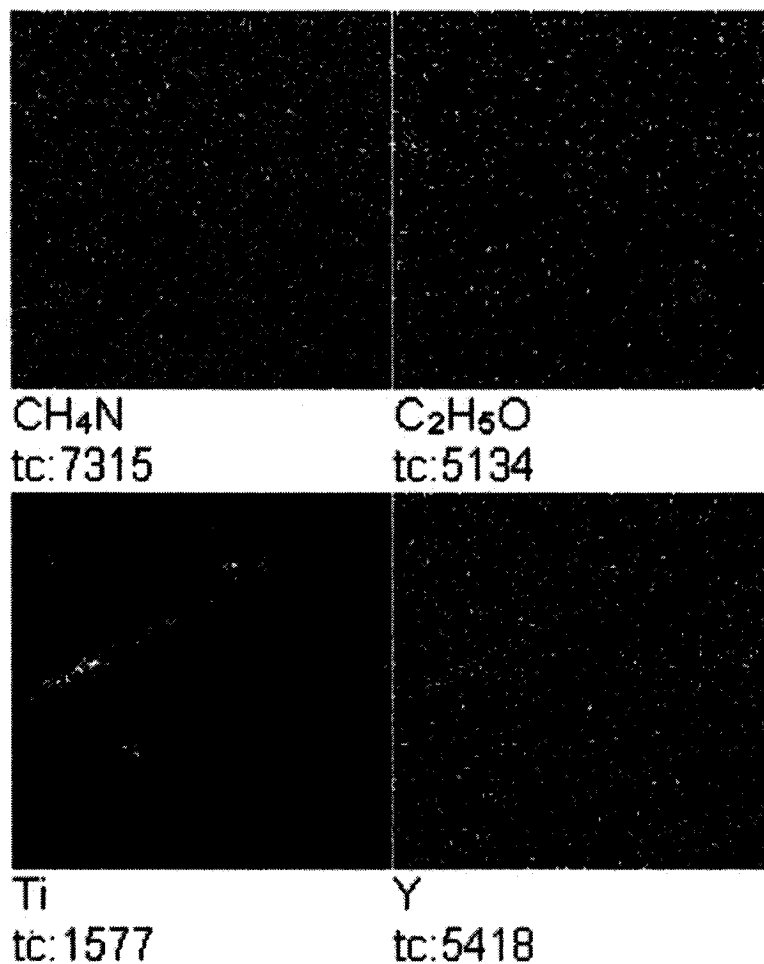


Figure 7.1.6. ToF-SIMS molecular imaging of the m/z cations characteristics of polyAA (CH₄N), HA-DTPA (C₂H₅O), titanium (Ti), and yttrium (Y). Despite the presence of few defects showing metallic rich area, the radionuclide is homogeneously distributed over the surface.

Indium was incorporated in the HA-DTPA modified substrates following the same chelation procedure as described in the case of yttrium. The ¹¹¹In chelation efficiency was monitored with a gamma-counter. The total amount of radionuclide loaded on the surface was about 33 MBq/cm², a value within the therapeutic range estimated to vary from 0.1 MBq/cm² for stent-based delivery devices to tens of MBq/cm² for angioplasty

balloon devices³⁴⁻³⁸. The activity introduced onto the surface could be readily controlled by using a mixture of radioactive/non radioactive compounds.

Next, we assessed the stability of the radionuclide-DTPA-conjugates linked to the surfaces, since in therapeutic application the release of free radioisotope from devices has to be prevented or at least kept to extremely low levels in order to avoid exposure to radiation of non-targeted tissues. The thermodynamic and kinetic stability of the radionuclide-DTPA-conjugates chelates has been widely investigated over the past in view of its application in anti-tumors radiotherapy³⁹. The release of ¹¹¹In from HA-DTPA(¹¹¹In)-coated surfaces upon incubation in PBS was monitored as a function of time by gamma counting of small aliquots. (Fig. 7.1.7) Approximately 6 mol % of the total surface-loaded ¹¹¹In was released in the aqueous medium after 16 days. The loss of radioactivity occurred gradually over time with no indication of an initial “radioactivity burst”, which would be expected if the surfaces were to contain unbound indium. Nonetheless, even though the loss of radioactivity detected was low, it remains of concern if one envisages therapeutic applications, such as permanently-implanted metallic stents. The free radionuclides may be bound to plasma proteins and can then be deposited in organs which display affinity for the radionuclides (or for the proteins bound to the radionuclides). However, one should expect that the very low dose of radiation that could be potentially accumulated in non-targeted organs is far under the toxic dose. In a recent study, a genetically engineered human/murine chimeric IgG with high affinity to carcinoembryonic antigen conjugated with DTPA was developed. ⁹⁰Y labeled DTPA-cT84.66 was tested in twenty-two patients with doses up to 1000 times higher (5 to 22 mCi/m²) than the ones required for therapeutic activity in endovascular radiotherapy, and promising results were reported⁴⁰. One can envisage several routes to prevent or minimize undesirable leaking of radionuclides from coated surfaces implanted *in-vivo*. An attractive approach would be to link it to HA chelating agents, such as the macrocyclic ligand 1,4,7,10-tetraazacyclododecane tetra-acetic acid (DOTA), with affinities towards indium or yttrium higher than DTPA^{41; 42}. The approach successfully investigated in this paper could be used with HA-DOTA conjugates, thus reducing the risk of radiation accumulation into non-targeted organs.

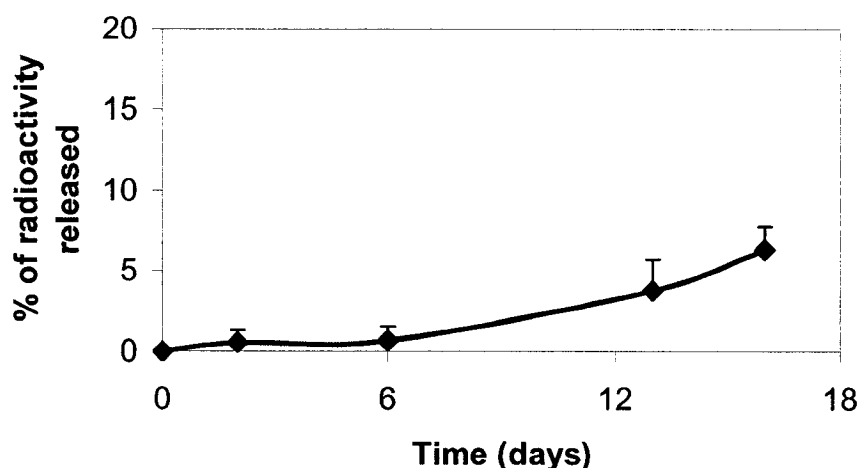


Figure 7.1.7. Loss of radionuclide from the ^{111}In -HA-DTPA-NiTi (mol. % of the total amount of radionuclide) in PBS at 38°C.

7.1.4.3. Adsorption of proteins onto HA-DTPA substrates

HA-DTPA-Teflon substrates were exposed to a solution of human fibrinogen in PBS under physiological flow conditions for 60 min. Fibrinogen, a rather large plasma protein (340 kD) that binds strongly to hydrophobic surfaces, has been widely used as model for “sticky” serum proteins. The adsorption of plasma proteins, such as fibrinogen, fibronectin, vitronectin and von Willebrand factor, triggers blood cells and platelet adhesion to materials. The non-fouling properties of surfaces coated with hyaluronan have been reported in other studies²². While the mechanism underlying this phenomenon remains poorly understood, it may be related to the level of surface hydration and to the conformation of the polymer chains at the water/substrate interface^{27; 43}. It was important to investigate whether the non-fouling properties of HA were conserved in the HA-DTPA devices. The adsorption of fibrinogen on HA-DTPA-Teflon surfaces was significantly lower than on uncoated Teflon (59 % reduction, $p=$

0.014, paired Student-t-test, Fig 7.1.8). While this result is promising, one could have expected a more drastic reduction in the amount of adsorbed proteins on a HA immobilized surface. The presence of the DTPA-radionuclide moieties in the HA backbone could have influenced its interfacial properties when immobilized on a surface. Further tests are needed to assess in detail the interactions of the device surface and biological fluids.

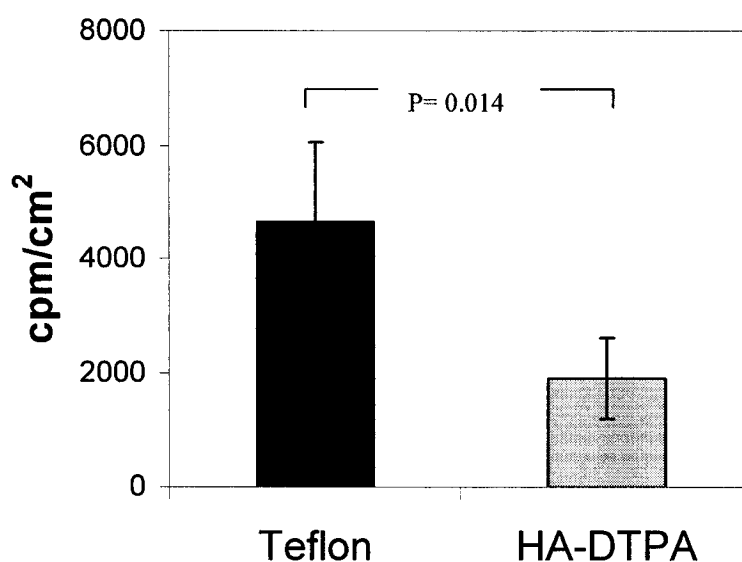


Figure 7.1.8. Fibrinogen adsorption on Teflon and HA-DTPA-Teflon in the dynamic *in vitro* assay.

7.1.5. Conclusions

Catheter-based therapies are used routinely in current clinical practice. Intracoronary radiotherapy has generated enthusiasm over the last few years as an effective means to prevent restenosis and in-stent restenosis, but the use of radioactive stents has been tempered by the disappointing results reported by many investigators. The approach

described here provides a very versatile way to incorporate radioisotopes on the surface of endovascular devices such as stents or catheters. HA-DTPA conjugates have been successfully immobilized on plasma functionalized NiTi and Teflon substrates, leading to very hydrophilic surfaces onto which the adsorption of fibrinogen was greatly reduced, compared with unmodified Teflon surfaces. Radionuclides, such as yttrium and indium, have been loaded onto the surface with excellent incorporation efficiency and good stability. The coated surfaces developed in the present study combine two unique features, the haemocompatibility of the HA-based coatings, and the flexibility in the choice of radionuclides and, consequently, they offer the opportunity to investigate new radionuclides with a broad range of physical properties.

The thromboresistance associated with the HA-based coatings could reduce the need for systemic antithrombotic therapies. Moreover, the extreme lubricity of HA coatings and the radiopacity of radionuclide, may be useful to improve the performance of catheters used in endovascular procedures – with or without the use of therapeutic radiation.

We can point to several features of HA-DTPA coated stents that may need to be studied in more detail and possibly improved. One issue of concern relates to the appropriate dosimetry for endovascular therapy. Most studies, using ^{32}P BX isostents, have shown that radioactive stents inhibit almost completely neointimal hyperplasia, in a dose response manner^{7; 35; 44}. The major limitations associated with stent-based radiation delivery, known as “Candy-Wrapper” or “Edge-effects”, relate, however, to re-narrowing at the stent edges. To reduce the effects, researchers have evaluated the so-called “hot-ends stents”, in which the edges of the stents are made more radioactive in an attempt to increase the exposure dose at the injured proximal and distal edges^{18; 19}. The HA-DTPA coated stent methodology is readily amenable to this therapeutic alternative.

Acknowledgments

This work was partly supported by NSERC grants to MT and FMW. We thank Cordis Corporation - Nitinol Devices & Components (Fremont, CA) for their technical and financial support. The authors wish to thank especially S. Poulin for her precious technical assistance and useful discussions with ToF-SIMS analysis and Dr. S. Gouin for chemical synthesis. Thanks also go to Prof. H.J. Griesser from the Ian Walk Research Institute, Au and TePla America, Inc., for plasma polymerization.

7.1.6. References

- [1] Gershlick AH. Role of stenting in coronary revascularisation. *Heart* 2001;86:104-12.
- [2] Narins CR, Ellis SG. Prevention of in-stent restenosis. *Semin Interv Cardiol* 1998;3:91-103.
- [3] Rensing BJ, Vos J, Smits PC, Foley DP, van den Brand MJ, van der Giessen WJ *et al.* Coronary restenosis elimination with a sirolimus eluting stent: first European human experience with 6-month angiographic and intravascular ultrasonic follow-up. *Eur Heart J* 2001;22:2125-30.
- [4] Heldman AW, Cheng L, Jenkins GM, Heller PF, Kim DW, Ware M Jr *et al.* Paclitaxel stent coating inhibits neointimal hyperplasia at 4 weeks in a porcine model of coronary restenosis. *Circulation* 2001;103:2289-95.
- [5] Fox R. American Heart Association 2001 scientific sessions: late-breaking science-drug-eluting stents. *Circulation* 2001;104:E9052.
- [6] Sousa JE, Costa MA, Abizaid AC, Rensing BJ, Abizaid AS, Tanajura LF *et al.* Sustained suppression of neointimal proliferation by sirolimus-eluting stents: one-

- year angiographic and intravascular ultrasound follow-up. *Circulation* 2001;104:2007-11.
- [7] Drachman DE, Simon DI. Restenosis: Intracoronary Brachytherapy. *Curr Treat Options Cardiovasc Med.* 2002;4:109-18.
 - [8] Elbert DL, Herbert CB, Hubbell JA. Thin Polymer Layers Formed by Polyelectrolyte Multilayer Techniques on Biological Surfaces. *Langmuir* 1999;15:5355-62.
 - [9] Waksman R, Raizner AE, Yeung AC, Lansky AJ, Vandertie L. Use of localised intracoronary beta radiation in treatment of in-stent restenosis: the INHIBIT randomised controlled trial. *Lancet* 2002;359:551-7.
 - [10] Bhargava B, Tripuraneni P. Role of intracoronary brachytherapy for in-stent restenosis? *Lancet* 2002;359:543-4.
 - [11] Sapirstein W, Zuckerman B, Dillard J. FDA approval of coronary-artery brachytherapy. *N Engl J Med* 2001;344:297-9.
 - [12] Liistro F, Gimelli G, Di Mario C, Nishida T, Montorfano M, Carlino M *et al.* Late acute thrombosis after coronary brachytherapy: when is the risk over? *Catheter Cardiovasc Interv* 2001;54:216-8.
 - [13] Cheneau E, Waksman R, Yazdi H, Chan R, Fourdnadjiev J, Berzingi C *et al.* How to fix the edge effect of catheter-based radiation therapy in stented arteries. *Circulation* 2002;106:2271-7.
 - [14] Shih CC, Lin SJ, Chen YL, Su YY, Lai ST, Wu GJ *et al.* The cytotoxicity of corrosion products of nitinol stent wire on cultured smooth muscle cells. *J Biomed Mater Res* 2000;52 :395-403.
 - [15] Lowe HC, Oesterle SN, Khachigian LM. Coronary in-stent restenosis: current status and future strategies. *J Am Coll Cardiol* 2002;39:183-93.

- [16] Virmani R, Farb A, Kolodgie FD . Histopathologic alterations after endovascular radiation and antiproliferative stents: similarities and differences. *Herz* 2002;27:1-6.
- [17] Petelenz B, Rajchel B, Bilski P, Misiak R, Bartyzel M, Wilczek K *et al.* Physical and chemical limitations to preparation of beta radioactive stents by direct neutron activation. *Biomaterials* 2003;24:427-33.
- [18] Serruys PW, Kay IP. I like the candy, I hate the wrapper: the (32)P radioactive stent. *Circulation* 2000;101:3-7.
- [19] Albiero R, Colombo A. European high-activity (32)P radioactive stent experience. *J Invasive Cardiol* 2000;12:416-21.
- [20] Abatangelo, G. and Weigel, P. H. Redefining Hyaluronan. 2000. Amsterdam, Elsevier.
- [21] Verheye S, Markou CP, Salame MY, Wan B, King SB 3rd, Robinson KA *et al.* Reduced thrombus formation by hyaluronic acid coating of endovascular devices. *Arterioscler Thromb Vasc Biol* 2000;20:1168-72.
- [22] Morra M, Cassineli C. Non-fouling properties of polysaccharide-coated surfaces. *J Biomater Sci Polym Ed* 1999;10 :1107-24.
- [23] Das T, Banerjee S, Samuel G, Sarma HD, Ramamoorthy N, Pillai MR. 188Re-ethylene dicysteine: a novel agent for possible use in endovascular radiation therapy. *Nucl Med Commun* 2000;21:939-45.
- [24] Hsieh BT, Hsieh JF, Tsai SC, Lin WY, Huang HT, Ting G *et al.* Rhenium-188-Labeled DTPA: a new radiopharmaceutical for intravascular radiation therapy. *Nucl Med Biol* 1999;26:967-72.
- [25] Gouin S, Winnik FM. Quantitative assays of the amount of diethylenetriaminepentaacetic acid conjugated to water-soluble polymers using

isothermal titration calorimetry and colorimetry. *Bioconjug Chem* 2001;12:372-7.

- [26] ASTM F86, Standard Practice for Surface Preparation and Marking of Metallic Surgical Implants , Annual Book of ASTM standards: Medical Devices and Services, vol. 13.01.American Society for Testing and Materials; 1995. p. 6-8.
- [27] McLean KM, Johnson G, Chatelier RC, Beumer GJ, Steele JG, Griesser HJ. Method of immobilization of carboxymethyl-dextran affects resistance to tissue and cell colonization. *Colloids Surf B Biointerfaces* 2000;18:221-34.
- [28] Thierry B, Merhi Y, Bilodeau L, Trépanier C, Tabrizian M. Nitinol versus stainless steel stents: acute thrombogenicity study in an ex vivo porcine model. *Biomaterials* 2002;23: 2997-3005.
- [29] Gouin S, Valencia Grayeb MV, Winnik FM. Gadolinium Diethylenetriamine Pentaacetic Acid/Hyaluronan Conjugates: Preparation, Properties and Applications , In: Guiseppi-Elie A, Levon K, editors. *Macromolecule-Metal Complexes, Macromolecular Symposia 186*, Wiley-VCH ed. Weinheim, Germany: 2002. p. 105-10.
- [30] Nakajima N, Ikada Y. Mechanism of amide formation by carbodiimide for bioconjugation in aqueous media. *Bioconjug Chem* 1995;6:123-30.
- [31] Brenda M, Döring R, Schernau U. Investigation of organic coatings and coating defects with the help of time-of-flight-secondary ion mass spectrometry (TOF-SIMS). *Prog. Org. Coatings* 1999;35:183-89.
- [32] Ruiz L, Hilborn JG, Leonard D, Mathieu HJ. Synthesis, structure and surface dynamics of phosphorycholine functional biomimicking polymers. *Biomaterials* 1998;19:987-98.
- [33] Belu AM, Davies MC, Newton JM, Patel N. TOF-SIMS characterization and imaging of controlled-release drug delivery systems. *Anal Chem* 2000;72:5625-38.
- [34] Verin V, Popowski Y, de Bruyne B, Baumgart D, Sauerwein W, Lins M *et al.*

- Endoluminal beta-radiation therapy for the prevention of coronary restenosis after balloon angioplasty. The Dose-Finding Study Group. *N Engl J Med* 2001;344:243-9.
- [35] Wardeh AJ, Kay IP, Sabate M, Coen VL, Gijzel AL, Ligthart JM *et al.* beta-Particle-emitting radioactive stent implantation. A safety and feasibility study. *Circulation* 1999;100:1684-9.
- [36] Tepe G, Dinkelborg LM, Brehme U, Muschick P, Noll B, Dietrich T *et al.* Prophylaxis of restenosis with (186)re-labeled stents in a rabbit model. *Circulation* 2001;104:480-5.
- [37] Schulz C, Niederer C, Andres C, Herrmann RA, Lin X, Henkelmann R *et al.* Endovascular irradiation from beta-particle-emitting gold stents results in increased neointima formation in a porcine restenosis model. *Circulation* 2000;101:1970-5.
- [38] Fox RA, Henson PW. The dosimetry for a coronary artery stent coated with radioactive 188Re and 32P. *Phys Med Biol* 2000;45:3643-55.
- [39] McMurry TJ, Pippin CG, Wu C, Deal KA, Brechbiel MW, Mirzadeh S *et al.* Physical parameters and biological stability of yttrium(III) diethylenetriaminepentaacetic acid derivative conjugates. *J Med Chem* 1998;41:3546-9.
- [40] Wong JYC, Chu DZ, Yamauchi DM, Williams LE, Liu A, Wilczynski S *et al.* A phase I radioimmunotherapy trial evaluating 90yttrium-labeled anti-carcinoembryonic antigen (CEA) chimeric T84.66 in patients with metastatic CEA-producing malignancies. *Clin Cancer Res* 2000;6:3855-63.
- [41] Cremonesi M, Ferrari M, Chinol M, Bartolomei M, Stabin MG, Sacco E *et al.* Dosimetry in radionuclide therapies with 90Y-conjugates: the IEO experience. *Q J Nucl Med* 2000;44:325-32.
- [42] Camera L, Kinuya S, Garmestani K, Wu C, Brechbiel MW, Pai LH *et al.*

Evaluation of the serum stability and in vivo biodistribution of CHX- DTPA and other ligands for yttrium labeling of monoclonal antibodies. J Nucl Med 1994;35:882-9.

[43] Morra M. On the molecular basis of fouling resistance. J Biomater Sci Polym Ed 2000;11:547-69.

[44] Albiero R, Adamian M, Kobayashi N, Amato A, Vagheti M, Di Mario C *et al.* Short- and intermediate-term results of (32)P radioactive beta-emitting stent implantation in patients with coronary artery disease: The Milan Dose-Response Study. Circulation 2000;101:18-26.

7.2. PAPER 4

Bioactive Coatings of Endovascular Stents based on Polyelectrolyte Multilayers

Benjamin Thierry, Françoise M. Winnik, Yahye Merhi, Jim Silver, Maryam Tabrizian

Copyright © 2003 ACS. *Biomacromolecules*. 2003 Nov-Dec;4(6):1564-71.

Reprinted by permission of the American Chemical Society

7.2.1. Abstract.

Layer-by-layer self-assembly of two polysaccharides, hyaluronan (HA) and chitosan (CH) was employed to engineer bioactive coatings for endovascular stents. A polyethyleneimine primer layer was adsorbed on the metallic surface to initiate the sequential adsorption of the weak polyelectrolytes. The multilayer growth was monitored using a radiolabeled HA and shown to be linear as a function of the number of layers. The chemical structure, interfacial properties, and morphology of the self-assembled multilayer were investigated by ToF SIMS, dynamic contact angle measurements, and atomic force microscopy (AFM), respectively. The multilayer-coated stents presented enhanced antifouling properties, compared to unmodified stents, as demonstrated by a decrease of platelet adhesion in an *in vitro* assay (38% reduction; $p = 0.036$). An *ex vivo* assay in a porcine model indicated that the coating did not prevent fouling by neutrophils. To assess whether the multilayers may be exploited as in-situ drug delivery systems, the NO-donor sodium nitroprusside (SNP) was

incorporated within the multilayer. SNP-doped multilayers were shown to further reduce platelet adhesion, compared to standard multilayers (40 % reduction). When stents coated with a multilayer containing a fluorescently-labeled HA were placed in intimate contact with the vascular wall, the polysaccharide translocated on the porcine aortic samples as shown by confocal microscopy observation of a treated artery. The enhanced thromboresistance of the self assembled multilayer together with the anti-inflammatory and wound healing properties of hyaluronic acid and chitosan are expected to reduce the neointimal hyperplasia associated with stent implantation.

7.2.2. Introduction

Percutaneous transluminal coronary angioplasty (PTCA) is widely used for the treatment of occlusive blood vessel diseases. Stent implantation, representing as much as 1,000,000 procedures each year, has improved the safety of the procedures and has been shown to reduce restenosis, i.e. the re-obstruction of the targeted artery. The reduction of restenosis is attributed to the scaffolding effect of the stent which prevents elastic recoil and constrictive remodeling of the artery¹. However stent implantation is also associated with an excessive proliferation of vascular smooth muscle cells (SMCs), extracellular matrix synthesis, and a chronic inflammatory reaction which are believed to be initiated by the deep vascular injury and the endothelial cell denudation created during angioplasty and further enhanced by the presence of a foreign metallic device^{1;2}. This complication, known clinically as in-stent restenosis, occurs in about 15 to 30 % of the procedures.

Two new developments in stent technology show promise in alleviating thrombosis and in-stent restenosis. One approach consists attempting to improve the biocompatibility of stents by modifying their surfaces with less thrombogenic and inflammatory materials. These coatings include inorganic materials such as carbon, or silicon carbide, or biomimetic materials such as phosphorylcholine-modified surfaces^{1; 3}. Another approach, which has been shown to be particularly effective in lowering SMCs proliferation and significantly delaying in-stent restenosis, is to coat stents with a layer

loaded with therapeutic agents, such as Rapamycin[®] or Taxol[®], which are released gradually at the implantation site^{1;3}. These drugs are usually embedded into a polymeric matrix. However, early work with stents coated with biodegradable polymers, such as polyglycolic acid/polylactic acid copolymers, polycaprolactone polyhydroxy(butyrate valerate), and polyethyleneoxide/polybutylene terephthalate [PEO/PBTP]) as well as non biodegradable polymers, such as polyurethane [PUR], silicone [SIL], and polyethylene terephthalate [PETP]) were disappointing, and indicated that the polymers triggered long term inflammation⁴. The disappointing clinical results recently obtained with the hexanoyltaxol (QP2)-eluting polymer stents (QuaDS) may also be related to such polymer-induced chronic inflammation at the site of stent implantation⁵. This setback underscores the importance of the biocompatibility of the polymer used as drug carrier material. Other methods to create intelligent biocompatible polymeric interfaces need to be investigated as they may provide relief from the many side effects of stent implantation.

We report here novel coatings for stent created by the formation of insoluble interpolymeric complexes generated by depositing oppositely charged polyelectrolytes. The layer-by-layer self-assembly (L-b-L) of polycations and polyanions into multilayers has emerged as an efficient, versatile, yet simple, technique to create biologically active surfaces. The method relies on the sequential charge inversion of a polymeric surface upon successive immersions of this surface in solutions of oppositely charged polyelectrolytes⁶. The L-b-L technique has been used on various substrates with bioactive molecules, such as drugs, enzymes, DNA or proteins⁷⁻¹³. Bioactive molecules may be incorporated in the multilayer during the polyelectrolyte deposition process, yielding drug-releasing interfaces on various substrates via a process readily applicable to various substrates. We reported recently the deposition of polyelectrolyte multilayers onto angioplasty damaged arteries, resulting in a drastic reduction of thrombogenicity¹⁴.

We describe the preparation and properties of a new bioactive nanocoating of endovascular devices based on the layer-by-layer self-assembly of two natural polysaccharides, chitosan (CH) and hyaluronan (HA) (Table 7.2.1). Chitosan is a linear

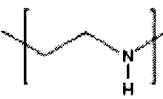
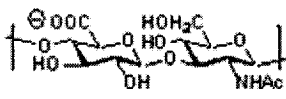
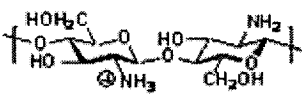
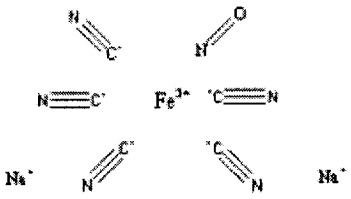
polysaccharide containing two β -1,4-linked sugar residues, *N*-acetyl-D-glucosamine and D-glucosamine, distributed randomly along the polymer chain. It is obtained commercially by partial de-N-acetylation of chitin. The chitosan used in this study contained approximately 15 mol % *N*-acetyl-D-glucosamine residues. It is only soluble in aqueous solutions of low pH, since its pKa value is ~ 6.3 . Hyaluronic acid (HA) is a naturally occurring linear high molecular weight anionic polymer (pKa = 2.9) consisting of alternating *N*-acetyl- β -D-glucosamine and β -D-glucuronic acid residues linked (1 \rightarrow 3) and (1 \rightarrow 4), respectively (Table 7.2.1). It plays an important structural and mechanical role in various tissues, participates in the control of tissue hydration and water transport, and affects numerous biological processes, such as inflammation, tumor metastasis and development¹⁵. The exact role of HA in the fibroproliferative response of vascular vessel towards angioplasty however, remains unclear and contradictory results have been reported¹⁶⁻²¹. The inhibitive effects of HA with respect to hyperplasia observed after either systemic or local delivery suggest that the antiproliferative effects of HA may be associated with its anti-inflammatory properties¹⁶. Both CH and HA have found a variety of applications in biomedical engineering and in cardiovascular applications^{22, 23}. Their use as components of multilayers has been reported in conjunction with oppositely-charged polyelectrolytes such as poly(lysine) in the case of HA^{24, 25}, and dextran sulfate in the case of CH²⁶.

We describe the deposition of CH/HA self-assembled multilayers on metallic substrates and their characterization by time of flight-secondary ions mass spectrometry (ToF-SIMS), atomic force microscopy (AFM), confocal microscopy and dynamic contact angle measurements. Their antifouling properties are evaluated both in vitro and ex vivo in order to assess whether they may enhance the haemocompatibility of metallic endovascular devices.

To determine if HA/CH multilayers can serve as an in-situ drug delivery vehicle, we prepared HA/CH multilayers with sodium nitroprusside (SNP, Table 7.2.1), following methodologies previously used to introduce various ionic dyes and proteins within polyelectrolyte multilayers^{27, 28}. Sodium nitroprusside, a nitrous oxide (NO) donor which spontaneously decomposes in biological environments²⁹ is widely used clinically

to reduce blood pressure and has emerged as a promising modality in the treatment of restenosis³⁰. The success of the NO-based therapies seems to rely on the efficiency of the delivery of therapeutic amounts of NO to the vascular wall. We monitored the effect of SNP incorporation on the physico-chemical properties of the multilayers, to ensure that SNP incorporation did not affect the creation of a multilayer, and we assessed the level of platelet adhesion onto CH/HA-coated surfaces in order to gain insight into the possible beneficial clinical effects against in-stent restenosis of a strategy combining the complexation of natural polysaccharides and the in-situ release of a drug incorporated within the polysaccharide multilayers.

Table 7.2.1. Molecules used for the self-assembled coating

PEI	
HA	
CH	
SNP	

7.2.3. Experimental

Substrate preparation

NiTi discs and wires (Ni: 55.8 wt %) provided by Nitinol Devices & Components (Fremont, CA) were used as substrates. The specimens were polished mechanically to a mirror-like finish using a 0.3- μm alumina paste (discs) or sand-blasted (wires). They were passivated as recommended by ASTM standard³¹. They were subsequently thoroughly cleaned using isopropanol and pure water. Hydrophobic high density polyethylene - HDPE – (medical grade) was used as substrate for the dynamic contact angle measurements.

Preparation of the self-assembled coatings

Solutions of sodium hyaluronate (HA, molecular weight 600,000 dalton, supplied by Hyal, Canada) (1 mg/mL in 0.14 M aqueous NaCl), chitosan (CH, high molecular weight, deacetylation degree > 85 %, obtained from Sigma Chemicals) (1.5 mg/mL in 0.1 M acetic acid (pH 4) containing 0.14 M NaCl) and polyethyleneimine (PEI, molecular weight 70 000 dalton, supplied by Aldrich) (5 mg/mL in 0.14 M aqueous NaCl) were prepared separately. Ultrapure water (18.2 M Ω .cm²) was used in all experiments (Milli Q system, Millipore). A PEI layer was adsorbed first for 20 min onto substrates and used as a precursor layer to initiate the layer-by-layer self-assembly. The multilayer build-up was accomplished by sequential adsorption onto the substrate of the oppositely charged polysaccharide for a period of 5 min (Fig. 7.2.1). Between each step excess polyelectrolyte was removed by washes with 0.14 M NaCl.

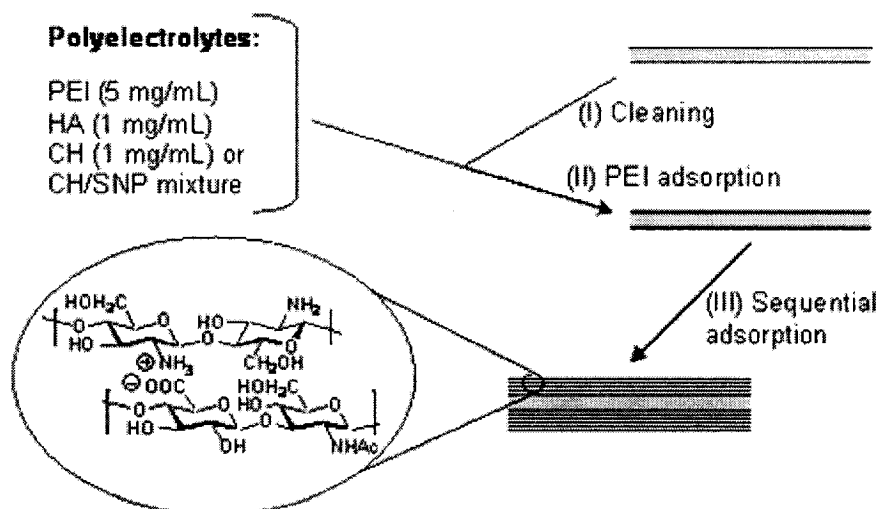


Figure 7.2.1. Schematic diagram of the deposition of CH/HA self-assembled multilayer on NiTi substrates; (I) Cleaning of the metallic substrate; (II) Adsorption of a PEI layer (5 mg/mL, 20 min) and rinsing with pure water; (III) Sequential adsorption of the CH (or CH/SNP mixture, NH_2/SNP molar ratio: 5:1) and HA polyelectrolytes (1 mg/mL, 5 min)

HA derivatives used for characterization

HA derivatives - ^{111}In -HA and HA-fluorescein dichlorotriazine (HA-FITC) - were synthesized to characterize the self-assembled CH/HA multilayers. These derivatives (1 mg/mL in 0.14 M NaCl) were used as described above for the build up of the multilayer.

Diethylenetriaminopentaacetic acid (DTPA), a chelator able to form stable complexes with radionuclides, was linked to HA as previously described to prepare HA-DTPA with a degree of substitution of ~ 0.15 DTPA/ disaccharide unit³². Radiolabeled ^{111}In -HA was prepared as follows: HA-DTPA (29 mg) was dissolved in water (20 mL) for 24 hr in a glass vial. Then $^{111}\text{InCl}_3$ (100 μCi) was introduced in the vial. The resulting solution was stirred at RT for 2 hr to ensure complete complexation. The ^{111}In -HA complex was purified by extensive dialysis against water. The final volume was adjusted to obtain a ^{111}In -HA concentration of 1 mg/mL (0.8×10^6 cpm/mg HA).

The fluorescein-derivative of HA (HA-FITC) was used to monitor the fate of the polymer deposited on the stent when placed in contact with an artery. It was prepared as follows. A solution of FITC from Sigma (4 mg, COOH/Fluorescein molar ratio: 25:1) was added to a solution of HA (80 mg) in aqueous borate buffer (pH 9.4). The reaction mixture was stirred at RT for 3 hr under N₂ in the dark. HA-FITC was purified by dialysis against borate buffer for 12 h and against water for 3 days. It was recovered by lyophilization.

Sodium nitroprusside loading

An aliquot of a stock solution of SNP in water (10 mg/mL) was added to the chitosan coating solution 10 min before beginning the coating procedure to achieve a concentration of 0.2 mol SNP/mol NH₂. The multilayered self-assemblies were built up as described above using the chitosan-SNP solution, instead of a CH solution. All manipulations were done in the dark to prevent decomposition of the SNP.

Characterization

Advancing and receding contact angles were obtained from dynamic contact angle measurements of deionized water droplets. Contact angles of a hydrophobic HD-polyethylene surface coated with various numbers of CH/HA layers³³ were measured with a Video Contact Angle System (VCA 2500, AST, Billerica, Ma) applying a 1- μ L droplet of deionized water (18.2 M Ω) on the samples' surfaces. The contact angles were determined semi-manually from the droplet image with a precision of $\pm 2^\circ$.

Time-of-flight secondary ions mass spectrometry analyses were recorded using an ION TOF IV spectrometer (ION-TOF, Germany) equipped with a primary ion Ga⁺ beam

operated at 15 keV. Areas of about $100\ \mu\text{m}^2$ and $8\ \mu\text{m}^2$ were analyzed under the so-called “static” condition with ion doses of about 10^9 ions/cm². The calibration of the mass spectra in the positive mode was based on hydrocarbon peaks such as CH_3^+ , C_2H_2^+ and C_3H_5^+ and peaks from the metallic substrates when possible. Relative normalized intensities ($I_{\text{coatings}}/(I_{\text{Ti}} + I_{\text{Ni}})$) were determined by dividing the integral of the coating characteristic peaks by the integral of the titanium and nickel peaks originating from the substrate.

Atomic force microscopy analyses were used to further investigate the growth of the coating on mechanically polished NiTi discs. AFM (Nanoscope III, Digital Instruments, Santa Barbara, CA) was performed in the tapping mode to avoid damaging the surface. Areas of about $5\ \mu\text{m}^2$ were scanned with a scan rate of 0.5 Hz.

Translocation of the coating from the metal surface to the vascular wall

The fluorescence of HA-FITC was used to visualize the presence of the polysaccharide coating onto the metallic substrate and to determine its fate when placed in contact with vascular tissues. The specimens were kept in the dark during all the experiments to prevent photobleaching. $\text{HA}(\text{CH}/\text{HA})_4$ multilayers were deposited onto NiTi wires and kept in PBS for various periods of time before being observed with an Axiovert inverted microscope equipped with an LSM 510 confocal system (Zeiss) or kept for translocation studies. Applying a gentle pressure, multilayer coated wires were placed in contact with the luminal surface of fresh aortic porcine arteries placed in a polycarbonate chamber. Wire-contacting arteries were incubated in PBS for 3 days at 4 °C in the dark. Prior to observation by confocal microscopy, the specimens were snap-frozen in 2-methyl-butane using liquid nitrogen and kept at -80°C, to prevent drug diffusion during handling and storage. Tissues were microtomed into 10 μm thick sections with a cryostat and mounted onto a glass slide prior to fixation with 4% paraformaldehyde. The sections were imaged. Corrections for the artery

autofluorescence were performed using a section of porcine artery not exposed to the fluorescent NiTi wires.

Haemocompatibility

Platelet adhesion was investigated as previously described^{14; 34}. Briefly, fresh blood (120 mL) was drawn from healthy, medication-free volunteers. The blood was collected in syringes preloaded with acide citrate dextrose (ACD). Platelet rich plasma (PRP) was prepared by centrifugation of the blood at 1800 rpm for 15 min. The PRP was then centrifuged at 2200 rpm for 10 min and the platelet poor plasma (PPP) was recovered as the supernatant. Platelets were carefully resuspended in citrate buffer and incubated with 250 μ Ci of $^{111}\text{InCl}_3$ for 15 min. The platelets were recovered by centrifugation, resuspended in PPP to a concentration of 2.5×10^6 platelets/mL. A freshly prepared ^{111}In -platelet solution (3 mL) was added to polystyrene dishes (Corning Inc.) containing the test materials. Platelet adhesion was allowed to proceed for 60 min with gentle shaking. After incubation, the samples were recovered, washed 4 times with saline and fixed in a 2 % glutaraldehyde solution. The amount of platelets was determined using a gamma counter (1470 WizardTM, Wallac, Finland) after correction for background signal and radioactivity decay.

The adhesion of ^{111}In polymorphonuclear neutrophils (PMNs) was investigated using an extracorporeal procedure in *ex-vivo* perfusion chambers. The radiolabeling, animal surgery, and extracorporeal procedures were performed as previously described^{34; 35}. Four pigs weighing 28 ± 3 kg were used in the experiments. All procedures followed the American Heart Association guideline for animal research and were approved by the local ethics committee. The extracorporeal shunt consisted of two parallel silicon tubing channel circuits connecting the femoral artery to the perfusion chambers and returning to the femoral vein. Radiolabeled PMNs were re-injected into the animals one hour

before the beginning of the experiments. A home-built parallel plate flow chamber was used. Injured arterial segments from normal porcine aortas were prepared as described previously and were used as control³⁵. The perfusion procedure was initiated by a 1-min wash with saline. The blood was allowed to circulate into the extracorporeal circuit for 15 min at a physiological wall shear rate of 424 sec^{-1} . The circuit was flushed with saline for 30 sec and the samples recovered and fixed in 1.5% glutaraldehyde in gamma-counter vials. The total amount of PMNs adsorbed on the surface was calculated knowing the specific activity of blood samples used as reference and using haematology performed prior to each experiment.

7.2.4. Results and discussion

Preparation and characterization of the self-assembled coating on surfaces

The multilayer coating procedure was initiated by the adsorption of a PEI layer onto a substrate, yielding a positively charged surface subsequently placed in contact, in turn, with a solution of the polyanion HA and then a solution of the polycation CH. The multilayer construction is expected to modify greatly the wettability of the substrate, whether it is a metal or a highly hydrophobic polymer surface. This effect was monitored by measuring the contact angle of a water droplet deposited on the surface (Figure 7.2.2). The advancing and receding contact angles for the bare polyethylene surface (HDPE) were high, with an advancing contact angle of about 100° . Deposition of a layer of PEI and subsequent treatment with a solution of HA resulted in a sharp decrease of the receding angle, but the advancing angle remained high. The large hysteresis of the contact angles suggests that wetting of the HA surface layer triggers significant changes in the conformation of the polymer in the initial stages of multilayer formation or incomplete covering of the polyethylene surface by the multilayer. Both receding and advancing contact angles decreased with increasing layer number,

reaching an advancing angle of about 30° upon deposition of 7 single layers. The contact angles remained constant upon further polyelectrolyte layer deposition. The stabilization of the advancing contact angle obtained after deposition of 4 bilayers led us to conclude that at least 4 bilayers were necessary to mask the substrate with respect to the properties of the multilayer/water interface. As a consequence, HA(CH/HA)₄ self-assembled coatings build on PEI-NiTi were considered as representative of the 3-dimensional polysaccharide multilayer coating and used in the biological assays described below.

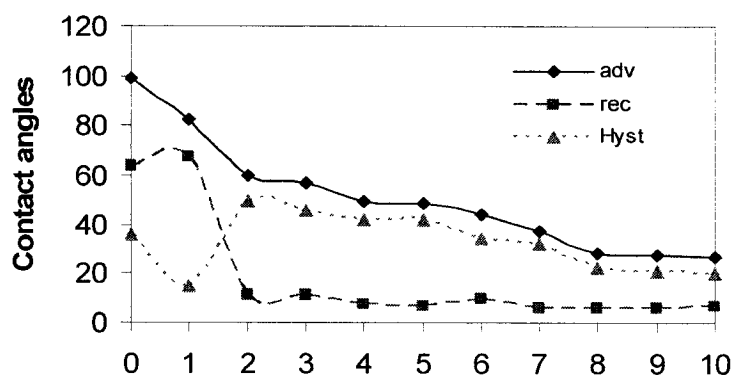


Figure 7.2.2. Contact angles with water (Advancing, receding) and hysteresis as a function of the number of layers. 0: HDPE; 1: PEI layer on HDPE, 2: HDPE-PEI-HA; 3 HDPE-PEI-HA/CH; 4 HDPE-PEI-HA(HA/CH)₁ and so on.

The multilayer build-up procedure was monitored next by measuring the radioactivity of multilayers obtained using ¹¹¹In-HA instead of HA. This highly sensitive method allowed us to quantitate the amount of HA deposited in each step and thus to ascertain that the multilayer build-up procedure follows the general l-b-l mechanism. It should be noted that this analytical method gives us information on the construction of ¹¹¹In-HA/CH multilayers, and not on HA/CH assemblies. Data presented elsewhere indicate that the use of the labeled HA slightly overestimates the amount of HA incorporated in the multilayer under the conditions employed in this work¹⁴. The amount of HA in the

coating increased linearly with the number of layers (Figure 7.2.3, slope: 3.8 μg HA/bilayer, $r^2 = 0.99$ to figure caption), indicating that the two polyelectrolytes follow a typical linear multilayer construction mechanism.

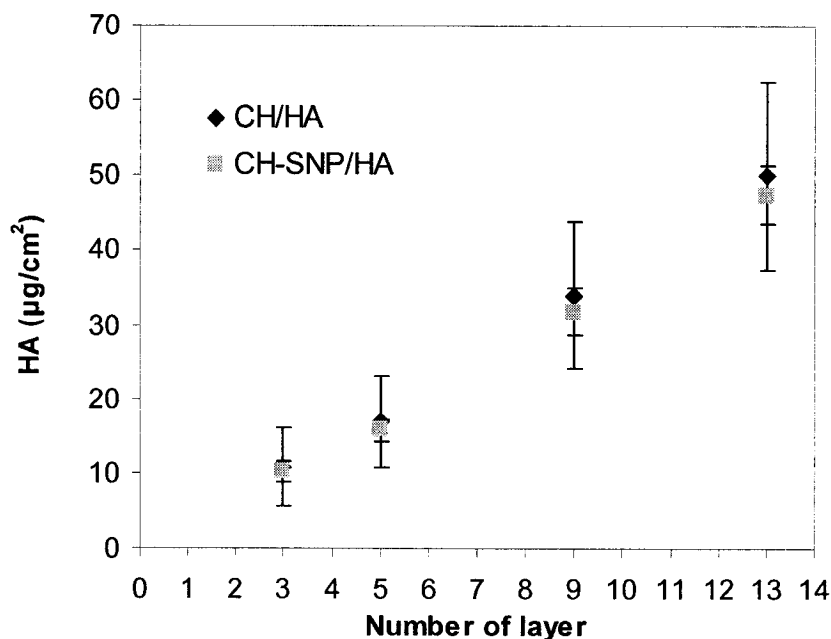


Figure 7.2.3. Amount of In111-HA ($\mu\text{g}/\text{cm}^2$) as a function of the number of layer for the CH/HA and CH-SNP/HA polyelectrolytes self-assembled onto NiTi substrates; 3 NiTi-PEI-HA(CH/HA)₁, 5 NiTi-PEI-HA(CH/HA)₂ and so on.

A more detailed analysis of the nanocoating was obtained by a ToF-SIMS examination of metal surfaces recovered after each coating step. A spectrum of a PEI coated surface presented several nitrogen containing peaks attributed to PEI, e.g. CH_2N^+ (m/z 28.018) $\text{C}_2\text{H}_3\text{N}^+$ (m/z 41.025), $\text{C}_3\text{H}_8\text{N}^+$ (m/z 58.064) (Fig. 7.2.2) and also several peaks characteristic of NiTi (^{46}Ti , m/z 45.954), (^{47}Ti , m/z 46.954), (^{48}Ti , m/z 47.954), (^{48}TiH , m/z 48.956), (^{50}Ti , m/z 45.947), (^{48}TiO , m/z 63.949), (^{58}Ni , m/z 57.936), (^{58}NiH , m/z 58.942), (^{60}Ni , m/z 59.931), suggesting that the metal surface has not been fully coated with PEI. Next, we recorded ToF-SIMS spectra of a HA(CH/HA)₄ self-assembled

coating (Figure 7.2.4). A spectrum of a Si wafer spin-coated with HA was also recorded to attribute the peaks characteristic of HA. In agreement with a previously reported ToF-SIMS analysis of HA, the spectrum of the HA-coated Si wafer presented an intense peak at m/z 43.017 attributed to the CH_3CO^+ ion from the HA N-acetyl³⁶. The normalized intensity of the CH_3CO^+ peak increases as a function of the number of layers (Table 7.2.2). This peak was used to correlate the quantitative information obtained using the ^{111}In -HA and the ToF-SIMS analyses. In addition to a peak at m/z 43.0174, the ToF-SIMS spectrum of the $\text{HA}(\text{CH}/\text{HA})_4$ coated PEI-NiTi (Figure 7.2.4) presents hydrocarbon peaks, such as C_2H_3^+ (m/z 27.022), C_3H_3^+ (m/z 39.022), C_3H_5^+ (m/z 41.0375), C_4H_7^+ (m/z 55.053) as well as oxygen and nitrogen containing peaks, such as CH_4N^+ ($m/z=$ 30.033), $\text{C}_2\text{H}_3\text{N}^+$ ($m/z=$ 41.025), $\text{C}_2\text{H}_2\text{O}^+$ ($m/z=$ 42.099), $\text{C}_2\text{H}_3\text{O}^+$ ($m/z=$ 43.017), $\text{C}_2\text{H}_4\text{NO}^+$ ($m/z=$ 58.027). Peaks due to the metal substrate were still detectable, but their intensity, compared to that of the carbonaceous species, is much weaker than in the spectrum of the PEI-NiTi sample. No ions originating from the metallic substrate were detected on the spectrum of a $\text{HA}(\text{CH}/\text{HA})_{10}$ multilayer coated NiTi sample.

Table 7.2.2. ToF-SIMS normalized intensities of the CH_3CO^+ peak (M/z 43.0174) as a function of the number of layer

Self-assembled coating	CH_3CO^+ normalized intensity
PEI-HA(CH/HA)	32
PEI-HA(CH/HA) ₂	60.9
PEI-HA(CH/HA) ₄	88.7
PEI-HA(CH/HA) ₆	296.8
PEI-HA(CH/HA) ₁₀	No metallic signal detected

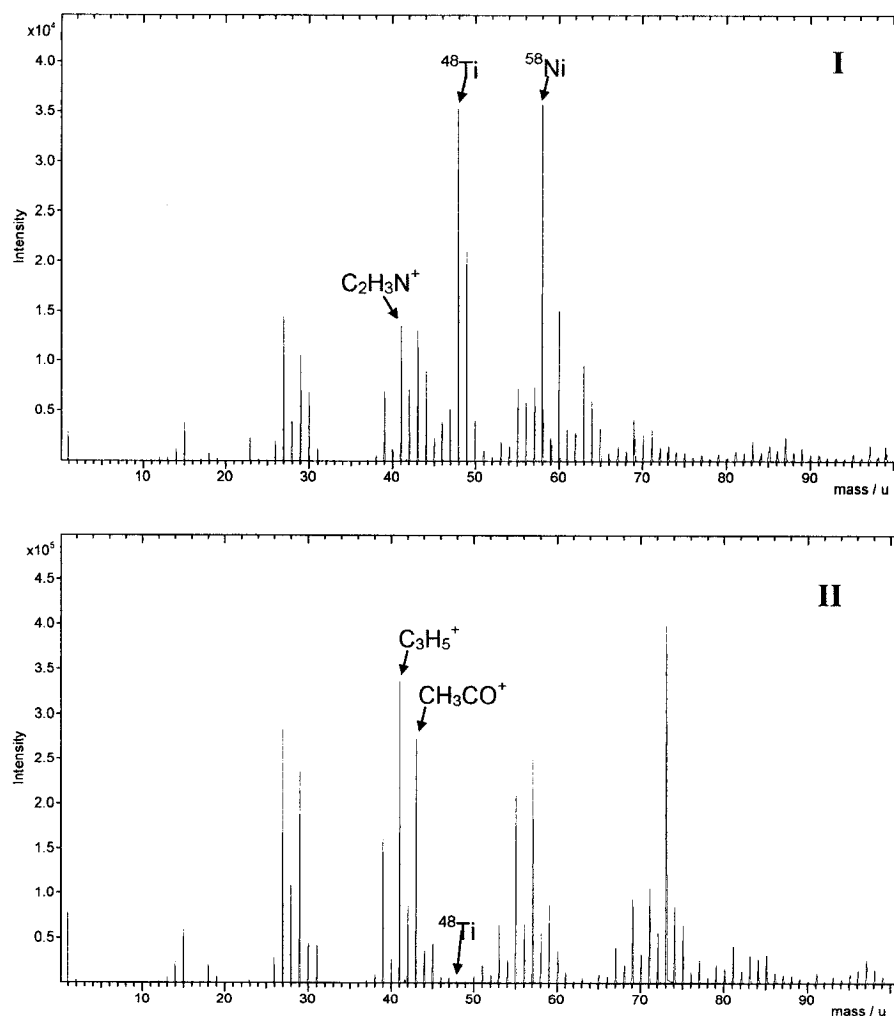


Figure 7.2.4. Positive ion ToF-SIMS spectra (m/z 0-100) for (I) PEI modified NiTi and (II) PEI-HA(CH/HA)₄ self-assembled coating on NiTi.

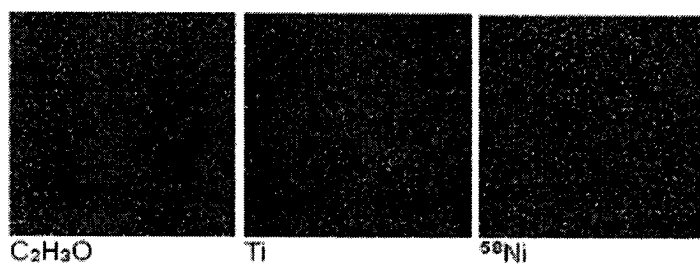
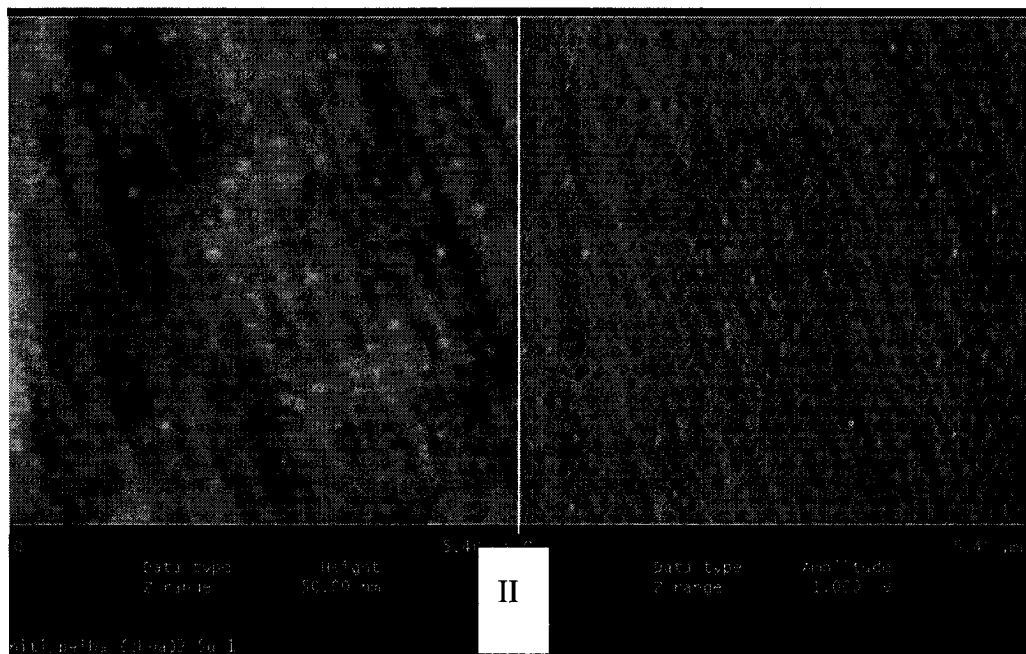
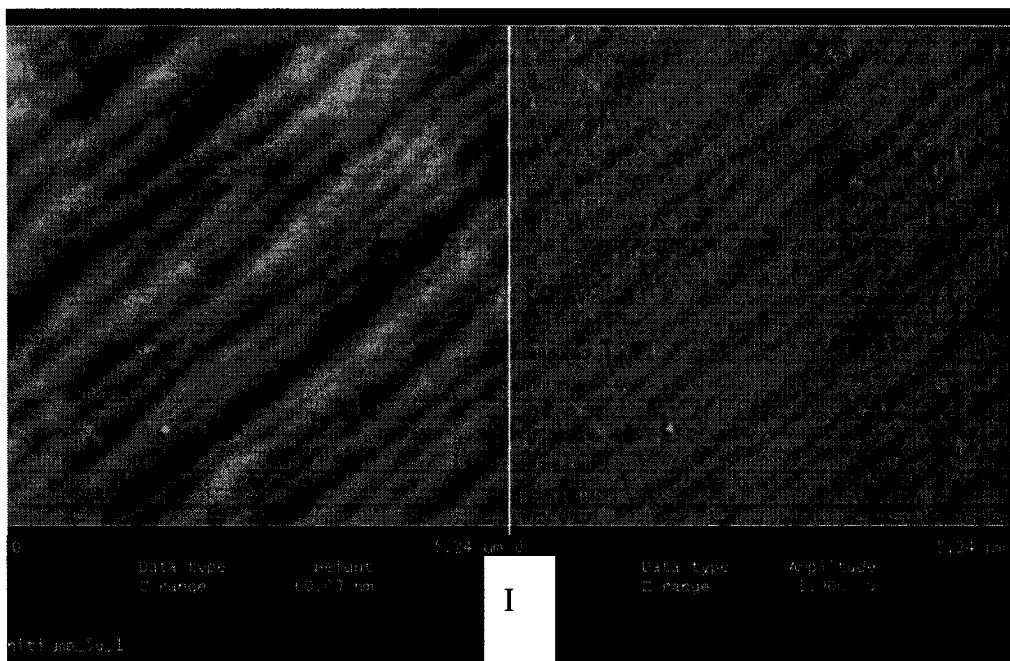


Figure 7.2.5. Chemical imaging of a PEI-HA(CH/HA)₄ self-assembled multilayer showing the distribution of CH_3CO^+ , Ti and Ni ions on the surface (7.9 μm^2)

ToF SIMS imaging allowed us to investigate the uniformity of the self-assembled coating on the scale of a cell (a few μm). $\text{HA}(\text{CH}/\text{HA})_4$ -coatings were imaged using the CH_3CO^+ peak. Homogeneous chemical images were obtained over an $8\ \mu\text{m}^2$ area (Fig.7.2.5). This result confirms the conclusion, drawn from contact angle measurements, that a $\text{HA}(\text{CH}/\text{HA})_4$ multilayer effectively insulates the metal surface from its environment. Chemical mapping of metallic peaks attributed to the substrate was performed as well, yielding homogeneous images of much lower intensity (Figure 7.2.5). This may be attributed to the porosity of the multilayer coating, possibly resulting from exposure of the multilayers to the ultrahigh vacuum imposed by the SIMS analysis. ToF-SIMS investigation of self-assembled multilayer on Si wafers has also shown that atomic or small molecular ions are less surface sensitive than large molecular ions³⁷.

Atomic force microscopy was used to characterize the evolution of surface topography during the multilayer construction. Figure 7.2.6 summarizes our observations for the sequential deposition onto polished NiTi (I) of PEI- $\text{HA}(\text{CH}/\text{HA})_2$ (II), PEI- $\text{HA}(\text{CH}/\text{HA})_5$ (III) and PEI- $\text{HA}(\text{CH}/\text{HA})_{10}$ (IV). The original polished metal surface displayed a slightly striated topography, the striations are believed to be caused by the use of a polishing paste consisting of alumina particles $\sim 0.3\ \mu\text{m}$ in diameter. These surface features were gradually masked in the coated surfaces and replaced by nanosized clusters. These structures increase in size with the number of layers, reaching a height of a few tens of nanometer and an average diameter of 250 nm. The original pattern featured in the images of the mechanically polished metal is completely masked by a multilayer coating consisting of 13 layers. The appearance and growth of small globular features in the hundred of nanometers range may be the indication of the formation of complex coacervates, as reported previously in the case of the layer-by-layer self-assembly of Poly(L-lysine) and HA²⁵.



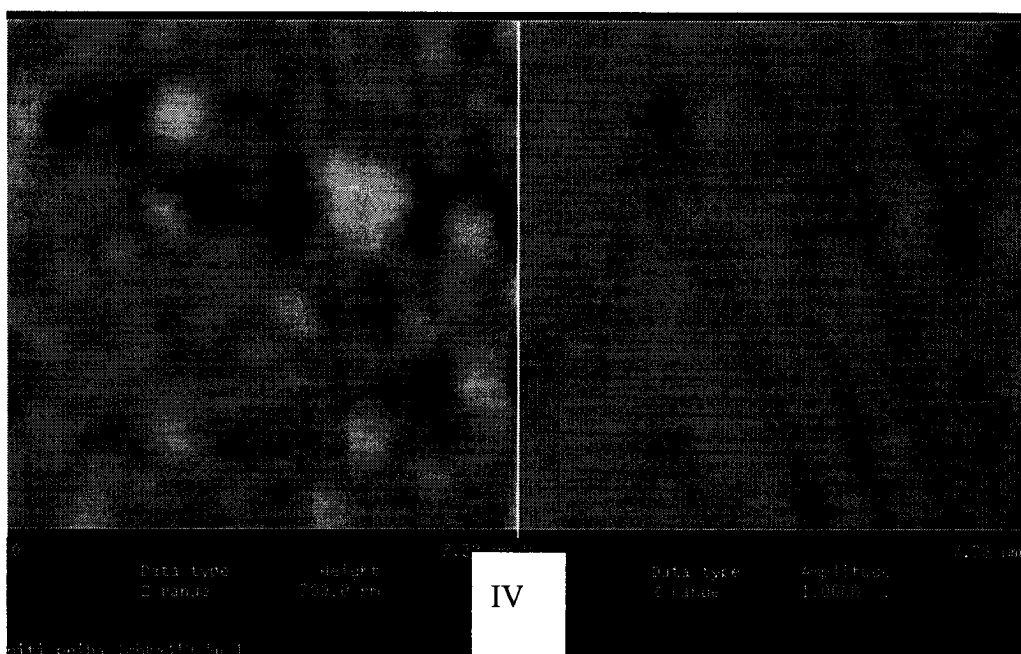
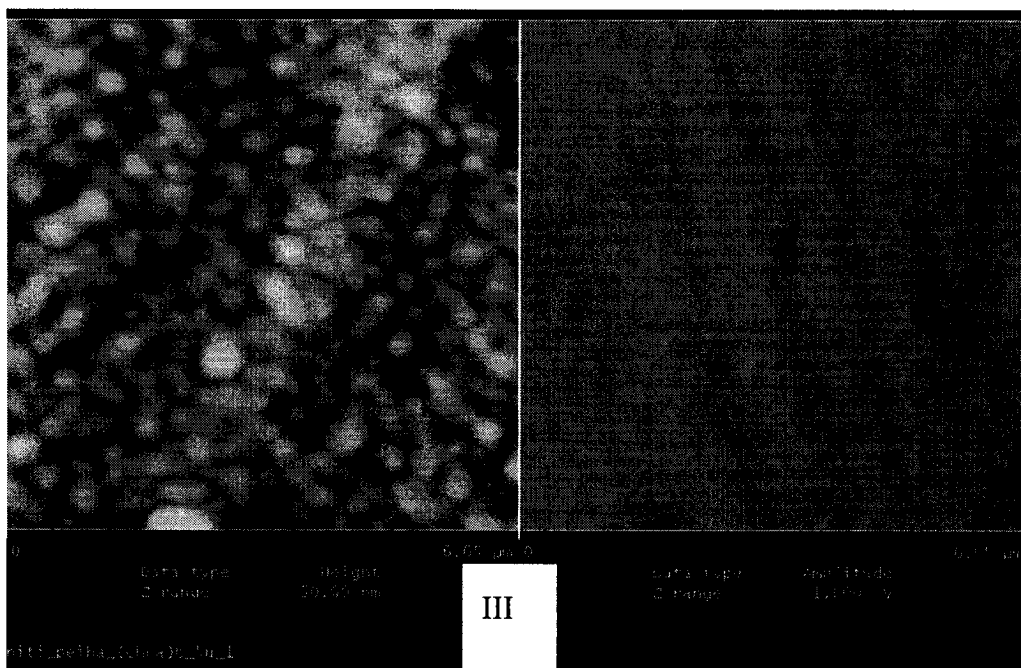


Figure 7.2.6. AFM tapping mode height and amplitude images of (I) the mechanically polished NiTi, (II) PEI-HA(CH/HA)₂ coated NiTi, PEI-HA(CH/HA)₅ coated NiTi and PEI-HA(CH/HA)₁₀ coated NiTi

One of the objectives of this study was to determine if a L-b-L assembled stent coating can act as drug reservoir for in-situ drug release following stent implantation. To test this hypothesis, an anionic drug, sodium nitroprusside (SNP), was incorporated in the multilayer. It was introduced within the coating in the chitosan deposition step, as the cationic polysaccharide is able to form a complex with SNP by electrostatic interactions. That SNP was incorporated into the coating by this method and that the construction mechanism was not disrupted by the presence of small amounts of SNP was established, by the radiolabeling method described above. No difference was observed in the amount of radiolabeled HA deposited as a function of the number of layers whether the multilayers were constructed with chitosan-SNP or chitosan alone (Figure 7.2.3). The ToF SIMS spectrum of an SNP-containing 9-layer assembly exhibited a peak at 55.84 m/z, a value characteristic of Fe which is present in the structure of SNP, but not in any other component of the coating. Taken together the ToF SIMS data and the radiolabeling experiment confirm that premixing chitosan and SNP does not interfere significantly with the L-b-L construction, vouching for the flexibility of the technique in creating functional surfaces.

Haemocompatibility of CH/HA coated NiTi surfaces

The thromboresistance of an HA(CH/HA)₄ coated metallic substrate was investigated using an platelet adhesion assay. As depicted in Figure 7.2.7, platelet adhesion was significantly reduced by 38 % onto NiTi-PEI-HA(CH/HA)₄ after 60 min of exposure to platelet rich plasma ($619.7 \pm 258.0 \times 10^3$ Platelets/cm² versus $1005.9 \pm 97.7 \times 10^3$ Platelets/cm² for bare NiTi; p=0.036). The incorporation of sodium nitroprusside within the multilayered coating further decreased platelet adhesion by 40 % ($371.5 \pm 74.5 \times 10^3$ Platelets/cm² for SNP containing HA(CH/HA)₄ coated NiTi versus $619.7 \pm 258.0 \times 10^3$ Platelets/cm² for HA(CH/HA)₄ NiTi; P=0.09). On the contrary, the CH/HA multilayer did not inhibit polymorphonuclear neutrophils (PMNs) adhesion after a 15-min perfusion in a porcine *ex vivo* assay (Fig. 7.2.8). In fact, PMN adhesion *increased*

slightly onto the coated surface, compared to bare metal ($6.1 \pm 2.2 \times 10^3 / \text{cm}^2$ vs. $3.9 \pm 3.8 \times 10^3 / \text{cm}^2$). PMN adhesion on both bare metal and polysaccharide coated metal surfaces was significantly lower than PMN adhesion on the damaged porcine aortic segment used as control ($30.9 \pm 16.1 \times 10^3 / \text{cm}^2$).

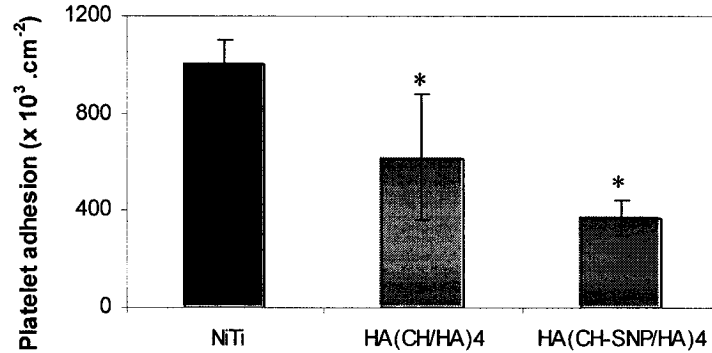


Figure 7.2.7. Platelet adhesion on NiTi, NiTi-PEI-HA(CH/HA)4 and NiTi-PEI-HA(CH-SNP/HA)4; * $p < 0.05$ Vs NiTi.

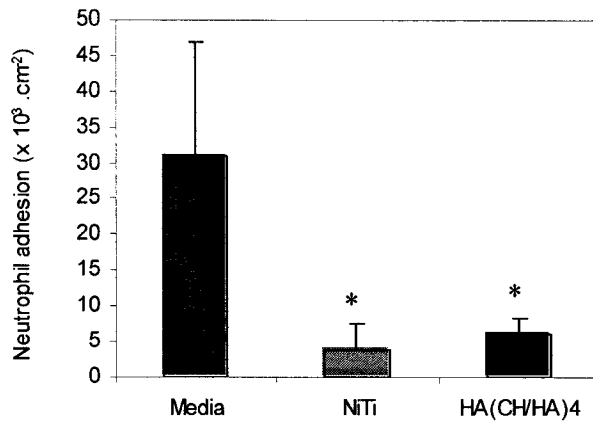


Figure 7.2.8. Neutrophil adhesion on damaged artery (Media), NiTi, and NiTi-PEI-HA(CH/HA)4; Mean \pm SEM; * $P < 0.05$ Vs. Media (Student-t-test)

Platelet adhesion is known to be initiated by adsorption of plasma proteins, such as fibrinogen. The antifouling properties of HA immobilized onto surfaces are well documented. It is believed that they are attributable to the hydration layer surrounding HA molecules on the surface³⁸. Interestingly, the multilayer did not prevent neutrophil adhesion in the *ex-vivo* assays and even slightly increased their adhesion in comparison to bare metal. This is in agreement with previous reports showing adhesion of monocyte and PMN to antifouling hydrophilic surfaces³⁹. The neutrophil adhesion could result from non-specific interactions or from specific adhesion through ligand-receptor mediated interactions such as CD 44 that are expressed on leukocytes. The modest neutrophil adhesion onto polysaccharide multilayer remained however far under the level measured onto damaged arteries.

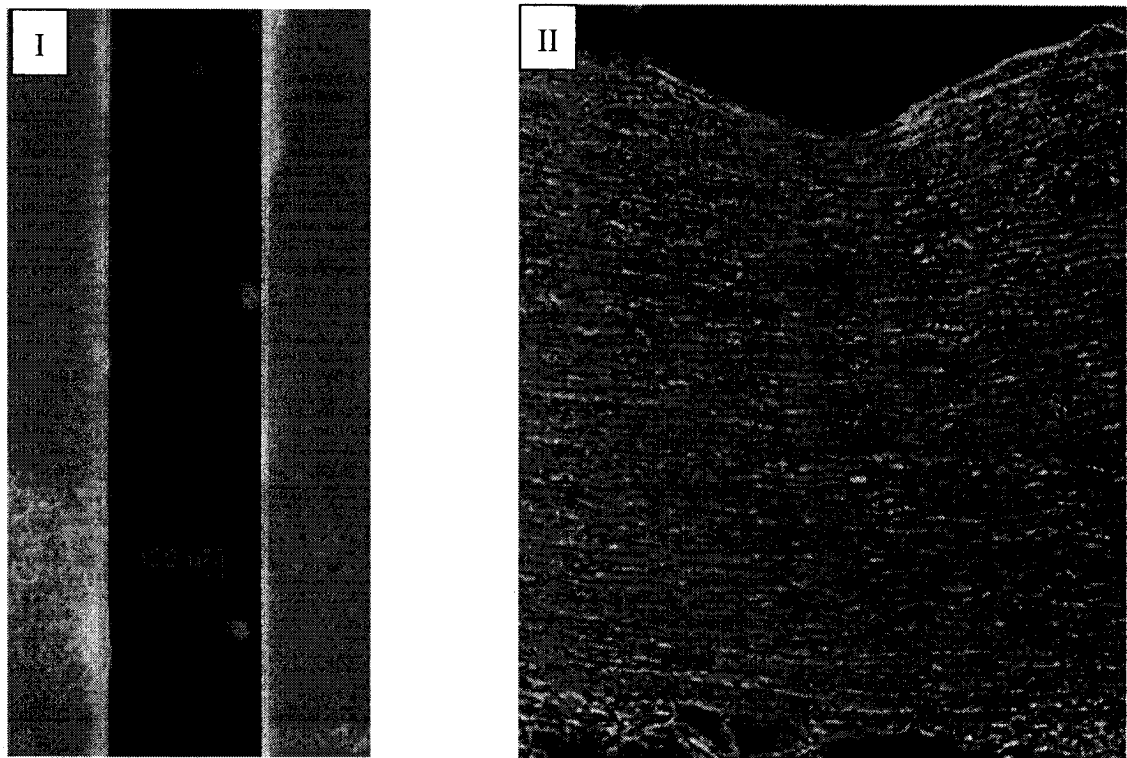


Figure 7.2.9. Confocal microscopy images of: (I) PEI-HA(CH/HA)₄ coated NiTi wires; (II) Cross-section of a damaged artery maintained in contact with the coated wire for 48 h in PBS.

Ex vivo stability of the CH/HA coating in contact with a vascular wall

The HA-FITC derivative was used to monitor the deposition of the multilayer onto the metallic substrate. Fluorescence confocal microscopy observation of HA-FITC-(CH/HA-FITC)₄ coated wires confirmed the uniform presence of HA-FITC on the wire surface, even after the coated wires had been incubated in PBS for several days (Fig. 7.2.9). A porcine aortic sample was incubated for 3 days in PBS while maintained in contact with the coated wire. The treated artery displayed fluorescence attributed to the transfer of FITC-HA from the coated wire-mesh to the artery surface as a result of contact with the stent.

7.2.5. Conclusion

The tremendous potential of the polyelectrolyte multilayer self-assembly methodology to engineer biologically active surfaces lies in its versatility and reproducibility^{6; 40}. Our study demonstrates that the self-assembled deposition of polysaccharide multilayers can be achieved with excellent control of the growth mechanism and the surface coverage, even in the presence of an added drug. The CH/HA system is characterized by a linear growth as demonstrated using the radiolabeled HA-¹¹¹In derivative. From contact angle measurements and ToF-SIMS analysis of deposited multilayers, we established that a minimum of 4 bilayers were needed to mask the metal substrate from its environment. The hydrogel-like surface created by the polysaccharide multilayer enhanced the thromboresistance of the surface, but surprisingly did not reduce PMN adhesion. Platelet adhesion was indeed reduced by 40% in comparison to bare NiTi surfaces which, by themselves, display good haemocompatibility³⁴. The multilayer self-assembly used in this study offers an innovative way to achieve 3-dimensional coatings that fully exploit the biocompatibility of natural polysaccharides such as HA and CH. Importantly,

the L-b-L technique does not require the use of toxic crosslinking agents, such as glutaraldehyde, which could compromise the biocompatibility of the multilayer coating. Interestingly, placing arterial segments *in vitro* in contact with multilayer coated wires for several days resulted in the transfer of the polyelectrolytes, or at least HA, from the wire to the tissue. Given the beneficial biological effects of HA, this translocation of HA to the vascular wall may prove advantageous and lead to further reduction of neointimal hyperplasia.

This study also aimed to investigate the potential use of self-assembled structures for the local delivery of bioactive molecules. The incorporation of SNP within the polysaccharide multilayer resulted in a reduction of platelet adhesion, compared to multilayers devoid of drug. This result confirmed the potential of such biocompatible self-assembled structures as therapeutic drug delivery media. Their suitability as host to a variety of biologically active molecules, such as DNA or proteins, offers numerous opportunities for clinical applications.

ACKNOWLEDGMENT

This work was partly supported by NSERC grants to MT and FMW. We thank Cordis Corporation - Nitinol Devices & Components (Fremont, CA) for their technical and financial support; The authors wish to thank S. Poulin for her precious technical assistance and useful discussions with ToF-SIMS analysis. Thanks also go to J.F. Théoret and N. Jacob from the Montreal Heart Institute for their help in the haemocompatibility assays and P. Cap for manuscript reviewing.

7.2.6. Reference

1. Babapulle, M. N.; Eisenberg, M. J. *Circulation* **2002**, *106*(21), 2734-40.
2. Welt, F. G.; Rogers, C. *Arterioscler Thromb Vasc Biol* **2002**, *22*(11), 1769-76.
3. Babapulle, M. N.; Eisenberg, M. J. *Circulation* **2002**, *106*(22), 2859-66.
4. van der Giessen, W. J.; Lincoff, A. M.; Schwartz, R. S.; van Beusekom, H. M.; Serruys, P. W.; Holmes, D. R. Jr; Ellis, S. G.; Topol, E. J. *Circulation* **1996**, *94*(7), 1690-7.
5. Virmani, R.; Liistro, F.; Stankovic, G.; Di Mario, C.; Montorfano, M.; Farb, A.; Kolodgie, F. D.; Colombo, A. *Circulation* **2002**, *106*(21), 2649-51.
6. Decher, G. *Science* **1997**, *277*, 1232.
7. Chung, A. J.; Rubner, M. F. *Langmuir* **2002**, *18*, 1176-1183.
8. Qiu, X.; Leporatti, S.; Donath, E.; Mohwald, H. *Langmuir* **2001**, *17*, 5375-5380.
9. Pei, R.; Cui, X.; Yang, X.; Wang, E. *Biomacromolecules* **2001**, *2*(2), 463-8.
10. Lvov, Y. u. M.; Sukhorukov, G. B. *Membr Cell Biol* **1997**, *11*(3), 277-303.
11. Chluba, J.; Voegel, J. C.; Decher, G.; Erbacher, P.; Schaaf, P.; Ogier, J. *Biomacromolecules* **2001**, *2*(3), 800-5.
12. Vazquez, E.; Dewitt, D. M.; Hammond, P. T.; Lynn, D. M. *J. Am. Chem. Soc.* **2002**, *124*(47), 13992-12993.
13. Lvov, Y.; Lu, Z.; Schenkman, J. B.; Zu, X.; Rusling, J. F. *J. Am. Chem. Soc.* **1998**, *120*(17), 4073-4080.
14. Thierry, B. J.; Winnik, F. M.; Merhi, Y.; Tabrizian, M. *J. Am. Chem. Soc.* (Published on line) .
15. Abatangelo, G.; Weigel, P. H. Elsevier ed.; Elsevier: Amsterdam, 2000.

16. Heublein, B.; Evagorou, E. G.; Rohde, R.; Ohse, S.; Meliss, R. R.; Barlach, S.; Haverich, A. *Int J Artif Organs* **2002**, 25(12), 1166-73.
17. Finn, A. V.; Gold, H. K.; Tang, A.; Weber, D. K.; Wight, T. N.; Clermont, A.; Virmani, R.; Kolodgie, F. D. *J Vasc Res* **2002**, 39(5), 414-25.
18. Travis, J. A.; Hughes, M. G.; Wong, J. M.; Wagner, W. D.; Geary, R. L. *Circ Res* **2001**, 88(1), 77-83.
19. Geary, R. L.; Nikkari, S. T.; Wagner, W. D.; Williams, J. K.; Adams, M. R.; Dean, R. H. *J Vasc Surg* **1998**, 27(1), 96-106; discussion 106-8.
20. Chajara, A.; Raoudi, M.; Delpech, B.; Leroy, M.; Basuyau, J. P.; Levesque, H. *Arterioscler Thromb Vasc Biol* **2000**, 20(6), 1480-7.
21. Deux, J. F.; Prigent-Richard, S.; d'Angelo, G.; Feldman, L. J.; Puvion, E.; Logeart-Avramoglou, D.; Pelle, A.; Boudghene, F. P.; Michel, J. B.; Letourneur, D. *J Vasc Surg* **2002**, 35(5), 973-81.
22. Chupa, J. M.; Foster, A. M.; Sumner, S. R.; Madihally, S. V.; Matthew, H. W. *Biomaterials* **2000**, 21(22), 2315-22.
23. Morra, M.; Cassineli, C. *J Biomater Sci Polym Ed* **1999**, 10(10), 1107-24.
24. Picart, C.; Mutterer, J.; Richert, L.; Luo, Y.; Prestwich, G. D.; Schaaf, P.; Voegel, J. C.; Lavalle, P. *Proc Natl Acad Sci U S A* **2002**, 99(20), 12531-5.
25. Picart, C.; Lavalle, Ph.; Hubert, P.; Cuisinier, F. J. G.; Decher, D.; Schaaf, P.; Voegel, J.-C. *Langmuir* **2001**, 17, 7414-7424.
26. Serizawa, T.; Yamaguchi, M.; Akashi, M. *Biomacromolecules* **2002**, 3(4), 724-31.
27. Das, S.; Pal, A. J. *Langmuir* **2002**, 18, 458-461.
28. Ariga, K.; Onda, M.; Lvov, Y.; Kunitake, T. *Chemistry Letters* **1997**, 25-26.
29. Wang, P. G.; Xian, M.; Tang, X.; Wu, X.; Wen, Z.; Cai, T.; Janczuk, A. J. *Chem Rev* **2002**, 102(4), 1091-134.
30. Provost, P.; Merhi, Y. *Thromb Res* **1997**, 85(4), 315-26.

31. *Annual Book of ASTM Standards: Medical Devices and Services* American Society for Testing and Materials: 1995; Vol. 13.01, pp 6-8.
32. Gouin, S.; Winnik, F. M. *Bioconjug Chem* **2001**, 12(3), 372-7.
33. In this work, "layer" refers to the increment in thickness after exposure to one of the polyelectrolyte solution.
34. Thierry, B.; Merhi, Y.; Bilodeau, L.; Trépanier, C.; Tabrizian, M. *Biomaterials* **2002**, 23(14), 2997-3005.
35. Merhi, Y.; King, M.; Guidoin, R. *J Biomed Mater Res* **1997**, 34(4), 477-85.
36. Shard, A. G.; Davies, M. C.; Tendler, S. J. B.; Bennedetti, L.; Purbrick, M. D.; Paul, A. J.; Beamson, G. *Langmuir* **1997**, 13, 2808-2814.
37. Delcorte, A.; Bertrand, P.; Arys, X.; Jonas, A.; Wischerhoff, E.; Meyer, B.; Laschewsky, A. *Surface Science* **1996**, 366, 149-165.
38. Morra, M. *J Biomater Sci Polym Ed* **2000**, 11(6), 547-69.
39. DeFife, K. M.; Shive, M. S.; Hagen, K. M.; Clapper, D. L.; Anderson, J. M. *J Biomed Mater Res* **1999**, 44(3), 298-307.
40. Phuvanartnuruks, V.; McCarthy, T. J. *Macromolecules* **1998**, 31(6), 1906-1914.

PART II. MEMBRANE-COVERED STENTS

Membrane covered stents are clinically used or investigated in the treatment of complex diseases of the vasculature such as stenosed vein grafts or aneurysms. The long term success rate of these endovascular procedures remains however suboptimal. Attempts to circumvent issues associated with conventional membrane-covered devices, made with synthetic materials, have investigated the use of biological materials. These materials include exogenous fibrin, collagen, or bovine pericardium. The approach described here further extends this concept as it proposes a chitosan-based biodegradable membrane covered stent. This approach aims at tailoring the properties of the membrane, i.e. mechanical properties, biodegradation, drug delivery ability, to the pathology to be treated.

To engineer such a device, the following steps have been used: (1) identify biological and biocompatible material(s) suitable for the application; (2) optimize the mechanical properties of the biodegradable membrane to allow endovascular implantation of the covered device; (3) to investigate the properties of the membrane in view of specific applications, e.g. burst pressure resistance and water permeation for aneurysm closure, drug delivery ability, etc. A blend of chitosan with polyethylene glycol has been identified as a good candidate for the biodegradable membrane. The excellent biological and mechanical properties of this blend make it a promising starting material for this application. The concept of the biodegradable membrane covered device based on chitosan has been patented and will be the object of further developments. The characterization of the membrane covered devices has also been described in a manuscript to be submitted for publication and included in the present thesis.

8. BIODEGRADABLE MEMBRANE-COVERED STENT

8.1. PAPER 5

Biodegradable Membrane-Covered Stent from Chitosan-Based Polymers: design and characterization

Benjamin Thierry, Yahye Merhi, Maryam Tabrizian

8.1.1. Abstract

Membrane covered devices could help to treat disease of the vasculature such as aneurysm, rupture and fistulas. They are also investigated to reduce embolic complication associated with revascularization of saphenous vein graft. The aim of this study is to design a clinically applicable biodegradable membrane covered stent based on the natural polysaccharide chitosan. The mechanical properties of the membrane is optimized through blending with polyethylene oxide (70:30 % Wt CH:PEO). The membrane was able to sustain the mechanical deformation of the supporting self-expandable metallic stents during its deployment. The membrane was demonstrated to resist physiological transmural pressure (burst pressure resistance >500 mm Hg) and presented a high water permeation resistance ($1 \text{ mL/cm}^2 \text{ min}^{-1}$ at 120 mm Hg). The CH-PEO membrane showed a good haemocompatibility in an *ex vivo* assay. PEO has been shown to reduce the *in vitro* platelet adhesion in comparison to chitosan alone (52.5 % reduction, $P > 0.05$). By complexing heparin with the surface of the membrane caused a

further reduction in platelet adhesion by 50.1% ($p \leq 0.05$). The ability of the membrane covered devices to be used as a drug reservoir was investigated using the precursor of nitric oxide L-Arginine.

Key-word: Membrane covered stent, stent-graft, chitosan, aneurysm, tissue engineering

8.1.2. Introduction

Membrane-covered-stents are used or investigated in the treatment of coronary diseases such as aneurysm, pseudoaneurysm, large dissection of the vascular wall during angioplasty and thrombus containing lesions¹⁻⁴. In particular, they are employed to stabilize the friable plaque in saphenous vein graft diseases. This is expected to reduce the risk of distal embolization following angioplasty of such vessels. Their uses have also been questioned in the treatment of peripheral artery diseases⁵.

The lack of long term biocompatibility of the synthetic polymers currently used as covering materials, either PTFE, Dacron and polyurethane, remains however a major limitation of these devices. To circumvent these limitations, biological polymers-based membrane covered stents with for example exogenous fibrin, collagen, or bovine pericardium for instance have been investigated⁶⁻⁹. While some promising results have been reported with these polymers, a completely engineered biological membrane would present obvious advantages. The rationale for the chitosan-based membrane covered stent proposed here was to develop devices with properties which could be tailored to the specific applications of such endoprosthesis. Chitosan is a biocompatible, non-immunogenic and biodegradable polymer with bioadhesive, wound healing, and antimicrobial properties. Chitosan blended with various polymers have been widely investigated to improve the mechanical properties of chitosan. In particular, chitosan-

polyethylene glycol/oxide (PEO/PEG) interpenetrated networks display excellent mechanical properties with improved ductility in comparison to chitosan alone^{10; 11}. The versatility of the fabrication process describes here allowed us to design membranes with different thickness, structure, and porosity.

Chitosan is also widely used in drug delivery applications and promotes absorption of drugs, peptides and proteins through biological tissues¹²⁻¹⁴. In revascularization procedures, neointimal hyperplasia within the stent struts remains however a consistent cause of failure. Systemic pharmaceutical strategies have been to date mainly unsuccessful. Local drug/gene delivery conjugated with stent implantation yields the hope to eliminate clinical restenosis^{15; 16}. In particular, antiproliferative drug-eluting stents have been shown to significantly reduce restenosis. The long term safety and efficiency as well as the cost/efficiency of these therapeutic strategies remain questionable however. The CH-PEO membrane could be easily loaded with bioactive drugs, proteins, DNA, or radionuclides able to stimulate/inhibit cellular events. L-Arginine (Arg), the precursor of nitric oxide (NO) has been used in this study as a model drug. Arginine has been shown to reduce clinical restenosis when locally delivered through a NO mediated actions^{17; 18}. The cationic drug has been either loaded directly in the membrane or precomplexed with anionic low molecular weight hyaluronic acid. The complexation of the cationic drug with the polyanionic polysaccharide was expected to delay its release and to minimize drug lost during the washing procedures of the membrane. Such precomplexation method with low molecular weight dextran has been successfully used to increase the loading of doxorubicin in chitosan nanoparticles¹⁹.

This paper describes the fabrication and characterization of the CH-PEO based biodegradable membrane-covered stent. This device could be investigated in a wide range of applications such as the treatment of aneurysms, the treatment of vascular graft diseases, malignant obstructive disease and tissue engineering applications. The properties of the membrane were assessed in order to gain insight on its ability to be

used in endovascular applications. Looking forward for vascular tissue engineering applications, an external porous membrane that could be used as a biodegradable scaffold was added. The haemocompatibility of the devices was characterized both in an *ex vivo* porcine model and *in vitro* and optimized through complexation with heparin. Finally, the ability of the membrane to act as a drug reservoir was investigated using the peptide precursor of nitric oxide L-Arginine.

8.1.3. Experimental

8.1.3.1. Chemicals

Chitosan derived from crab shell with a deacetylation degree > 85 % and PEO with an average molecular weight of 1,000,000 daltons were obtained from Sigma Co. Heparin was from Leo (1000 unit/mL). ^3H labeled and unlabeled L-Arginine were purchased from Sigma (L-Arginine hydrochloride; and L-Arginine-2,3- ^3H in aqueous ethanol solution). LMW HA was a gift from Prof. Winnik and was obtained as previously described²⁰. All chemicals were chemical grade.

8.1.3.2. Chitosan-PEO polymers preparation

CH-PEO film was synthesized as films or used for the membrane covered stent. Chitosan was dissolved in 0.1 M aqueous acetic acid (2% w/w) overnight and filtered to get rid of any insoluble material. PEO dissolved in glacial acetic acid was then added to CH/PEO with a ratio of 70/30 by weight. The mixture was then stirred for 4 h and then degassed. A jelly-like solution was then obtained that was either poured in glass

mold for characterization or used to prepare the membrane covered stent as described latter. The gel was allowed to dry at room temperature or freeze-dried for the porous membrane. The dried material was then washed with aqueous 1 N NaOH to remove residual acid and finally thoroughly rinsed with ultrapure water.

8.1.3.3. Membrane-covered stent preparation

Self-expandable stents made from NiTi alloy were mounted on a glass rod as schematized in Fig 8.1. The glass rod could be rotated on the longitudinal axe at controlled rpm. A known amount of CH-PEO gel was then cast onto the stents maintained in rotation. Controlling the rotation speed and as a function of the viscosity of the gel, an uniform layer of CH-PEO covered the stent in a controlled fashion. While maintained in rotation, the gel-covered stent was allowed to dry at room temperature. The dried membrane covered stent was then neutralized as described above before being removed from the glass rod. The device was then allowed to dry and stored for characterization or further modifications.

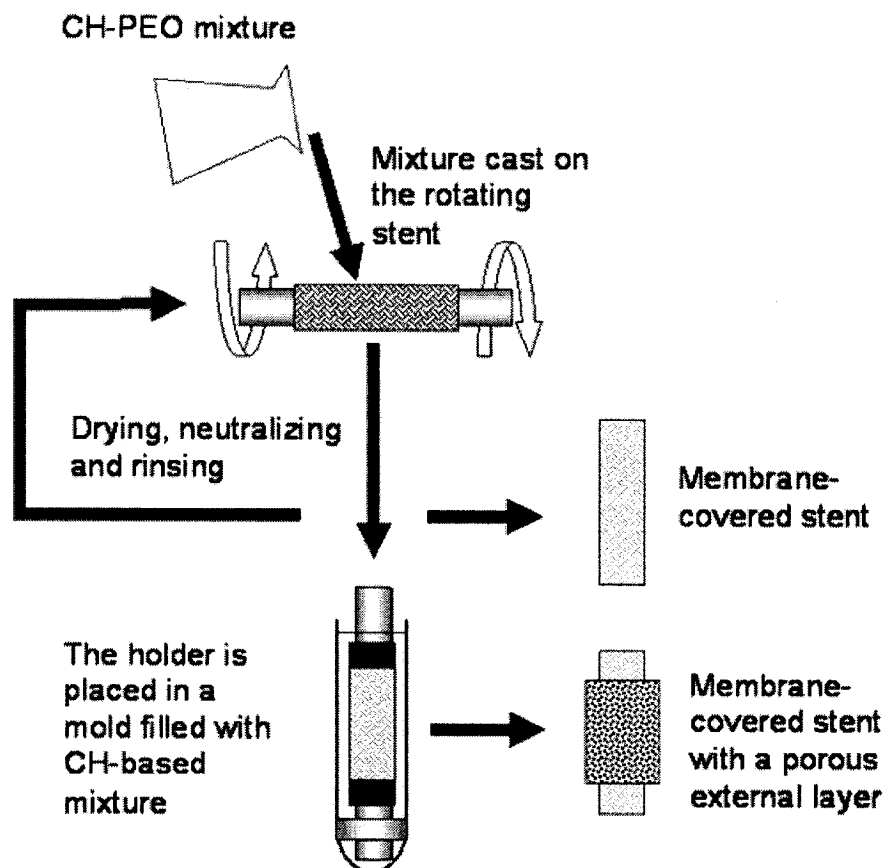


Figure 8.1. Schematic of the preparation of the CH-PEO membrane-covered stent with or without external porous layer

8.1.3.4. Heparin surface complexation

Heparin solution (1 mg/mL in pure water) was used to complex with CH-PEO film. The CH-PEO film was immersed in the heparin solution for two hours at RT to allow the electrostatic interactions to occur and then thoroughly rinsed with water. The dried heparin complexed-CH-PEO- membrane (CH-PEO-Hep) was then used for the haemocompatibility assay.

8.1.3.5. Multilayered membrane covered-stent

Additional layers were deposited to increase the thickness/mechanical properties of the membrane. This was achieved by repeating the same procedure as described in Fig. 8.1. External porous layers were also added onto some membrane-covered-stents. A CH-PEO covered stent was prepared and maintained on the glass holder. The device was placed into a glass mold that was gently filled with CH-PEO mixture. The mold was then frozen at -20°C before being transferred to vacuum vessels and lyophilized. The membrane was then again neutralized with NaOH and rinsed with pure water. This procedure yielded an external macro-porous layer that has been characterized using SEM.

8.1.3.6. Characterization of the membrane

8.1.3.6.1 SEM observation

The devices were allowed to equilibrate in water and then freeze-dried. The membranes were processed prior to metallization with an ultrathin sputter coated gold layer. The samples were imaged using a SEM (Hitachi S-4700 field emission SEM) at an accelerating voltage of 5 kV.

The porosity of the freeze-dried external layer was characterized as described elsewhere²¹. Porous films were prepared in polystyrene well as described above. The porosity of the samples was determined by complex permittivity measurements performed using a vector network analyzer (Model PNA 8358, Agilent Technologies) and a dielectric probe (85070C, Agilent Technologies).

8.1.3.6.2. Swelling behavior

The swelling behavior of chitosan-based membrane was investigated by gravimetric method. Discs of polymers were prepared and allowed to swell in 0.9 M NaCl solution. The swollen polymers were collected at various times, the excess water being removed by blotting against filter paper, and weighted (± 0.1 mg). The swelling ration was calculated knowing the hydrated W_h and dry W_d weight: $(W_h - W_d)/W_h$.

8.1.3.6.3. Water permeation and burst strength

The water permeation and burst strength of the membrane covered stent was determined in PBS as described^{22; 23}. The devices were hydrated for 30 min and completely crushed 5 times to simulate extensive manipulations. They were then cannulated with surgical sutures on semi-rigid silastic tubes at both sides. Water permeability is defined as the amount of saline solution leaked per unit area and time under a physiologic pressure of 120 mm Hg. The burst pressure was characterized by pressurizing the device with an increasing hydrostatic liquid pressure (20 mmHg steps) until membrane failure.

8.1.3.7. Thrombogenicity in an *ex vivo* model

The thromboresistance of the CH-PEO membranes has been investigated by an extracorporeal procedure in *ex vivo* perfusion chambers using radiolabeled ^{51}Cr -platelets and ^{111}In Leukocytes. The radiolabeling, animal surgery, and extracorporeal procedures were achieved as previously described²⁴. 6 pigs were used in the experiments. All procedures followed the American Heart Association guideline for animal research and were approved by the MHI ethic committee. Briefly, the extracorporeal shunt consisted

in a two parallel silicon tubing channel circuit connecting the femoral artery to the perfusion chambers and returning to the femoral vein. Radiolabeled platelets and leukocytes were re-injected into the animals one hour before the beginning of the experiments. CH-PEO mixture was cast on glass slide, dry, rinsed with NaOH and water and finally allowed to dry and stored. Intact endothelium and injured arterial segments were used as respectively thromboresistant and thrombogenic control²⁴. To simulate damaged arteries, intima denuded artery were prepared as followed. Normal porcine aortas were first dissected and then cut into rings, longitudinally opened and cut into segments. The aortic media was then exposed by lifting and peeling off the intima and the adventia together with a thin portion of the subjacent media. The segments were then cut to appropriate size using the cutting device. Such aortic media segments were shown in previous experiments to be very thrombogenic and closely simulate angioplasty damaged arteries.

The samples were hydrated in saline at least 30 min prior to the experiments and then placed in the perfusion chamber. The perfusion procedure was initiated by a 1 min washed with saline. The blood was then allowed to circulate into the extracorporeal circuit for 15 min at a wall shear rate of 424 sec^{-1} . The circuit was then flushed with saline for 30 sec and the samples recovered and fixed in 1.5% glutaraldehyde in gamma-counter vials. The amount of radioactivity was then measured and calculated for background, decay and overlapping of the radionuclides. The total amount of platelets and leukocytes adsorbed on the surface was calculated knowing the activity of blood samples used as reference and using hematology achieved prior to each experiment.

8.1.3.7. Platelet adhesion

Further insights on the haemocompatibility of the chitosan-based membranes were obtained using an *in vitro* platelet adhesion assays. Samples were prepared as 0.6 cm^2

discs using a cutting device. CH, CH-PEO and CH-PEO-Hep were prepared and kept at RT. 1 h before the beginning of the experiments, samples were allowed to rehydrate in saline solution. Damaged arteries used as control were prepared as described above. Fresh blood was drawn from healthy volunteers (120 mL), who were medication free and used for radiolabeling of platelets. The labeled platelets were resuspended in the PPP to 2.5×10^6 platelets/mL. The samples were placed into the bottom of a 96 well polystyrene plate (Corning Inc.). 250 μ L of freshly prepared ^{111}In -platelet solution was then added to each well taking special care that both sides of the samples were in contact with platelet solution. The platelet adhesion was allowed to proceed for 90 min with gentle shaking. After incubation, the samples were recovered and washed 4 times with saline. The samples were then fixed in 1.5 % glutaraldehyde solution and the amount of platelet was determined using the gamma counter.

8.1.3.8. L-Arginine release

CH-PEO mixture was prepared as described above. A stock solution of unlabeled Arg/ ^3H Arg was prepared in water (10^{-3} M with 2 μ L ^3H Arg/mL). In the direct loading experiments, L-Arginine was added to 2 g of the CH-PEO mixture to a final concentration of wt. 0.2 %. In the precomplexation method, LMW HA solubilized in water (1 mg/mL) was mixed with 100 μ L of the Arg solution (COOH/Arg molar ratio: 5:1) and allowed to complex for 1 h. 260 μ L of this mixture was then added to 2 g of the CH-PEO solution. The CH-PEO/Arg mixture with or without LMW HA was left under agitation for 2 h and then poured in polystyrene wells. The membranes were allowed to dry and then neutralized for 2 min with 750 μ L NaOH 1 M and rinsed twice with 1 mL water (2 min each). The rinsing solutions were kept for quantification of Arg released during the washing steps.

The release behaviors of the Arg-loaded membranes were determined in PBS. Membrane cast in the wells were incubated with 1 mL PBS under gentle agitation at RT. At various time, the PBS solution was removed from the wells. The Radioactivity of the solution was determined using liquid scintillation spectrometry (Beckman LS 6500 Liquid Scintillation counter) and correlated after correction for background to the amount of Arg using standard.

8.1.4. Results

8.1.4.1. Device preparation

The method described here to obtain the chitosan membrane-covered stent was reliable and reproducible. Once allowed to dry overnight neutralized with NaOH and rinsed with water, the device could be easily recovered from the holder without any damage. Macroscopic observations showed that a thin membrane uniformly covered the whole stents as shown in Fig. 8.2. Preliminary experiments have shown that the thickness of the membrane could be easily controlled by changing the viscosity of the chitosan mixture and to a lesser extent by controlling the speed of rotation of the glass holder. The thickness of a one-layer CH-PEO membrane was in the range of 100 μm .

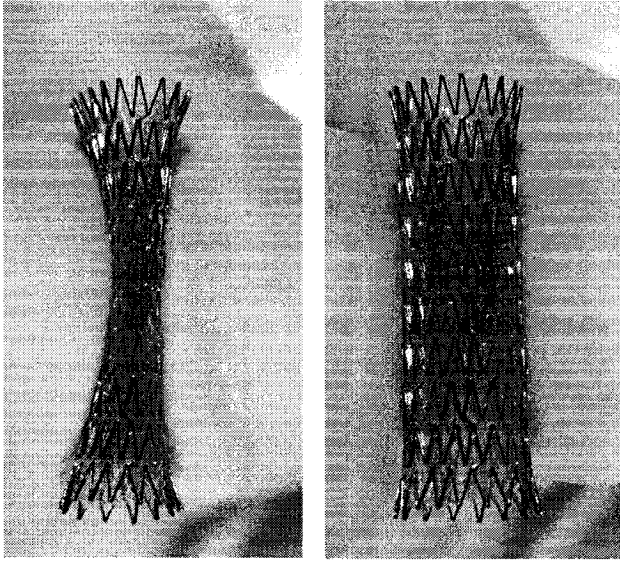


Figure 8.2. Macroscopic observation of the CH-PEO membrane covered stent showing the ability of the membrane to sustain the mechanical deformation of the metallic stent.

One of the challenges in the design of such a device was to optimize the mechanical properties of the membrane so that it could sustain the mechanical deformation associated with stent deployment. As shown in figure 8.2, the hydrated membrane was able to sustain complete crush with no visible damage. This is a good indication that minimally invasive delivery of the device could be achieved easily. Hydrated membrane-covered stents were hand crimped on catheters and maintained cramped with small plastic clamps until dry. Device-loaded catheters were kept at room temperature until further used. The dilatation of the devices was achieved in glass tubing by rehydration and removal of the plastic clamps. The devices completely expanded inside the glass tube. To investigate the effect of the delivery procedure on the membrane, a stent was dilated and then quickly freeze-dried using liquid nitrogen. The lyophilized sample was then gold coated for SEM observations. Using low magnification, we were able to observe that the membrane conserved its integrity and remained firmly attached to the metallic structure (Fig. 8.3). The luminal surface of the membrane was relatively smooth despite “waves”.

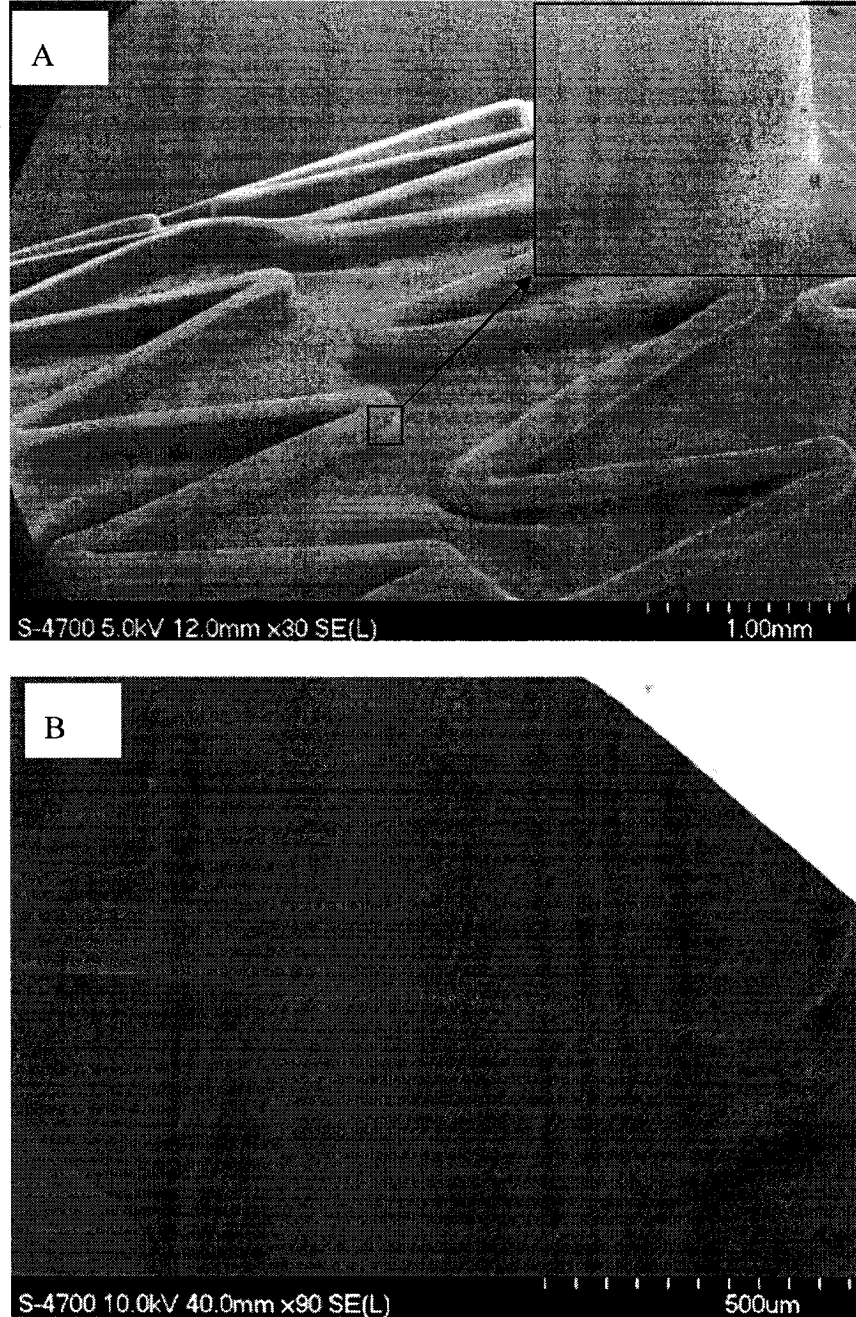


Figure 8.3. Scanning electron microscopic images of the membrane covered stent: (A) External view showing the adhesion of the membrane to the metallic struts (upper right x 450) (B) view of the inside of the membrane showing a stent-struts underlying

8.1.4.2. Membrane characterization

The swelling behavior of CH-PEO membrane in PBS (pH 7.4) is shown in Fig. 8.4 and compared to that of porous CH-PEO membrane obtained by freeze-drying. Rapid swelling of CH-PEO was observed and equilibrium was achieved within 1 min. As expected, porous CH-PEO presented a significantly higher swelling ratio than the CH-PEO membrane. The blend of Chitosan with PEO increased the swelling ratio in comparison to chitosan alone prepared in the same condition than the CH-PEO membrane (1.55 Vs. 1.22 at 10 min).

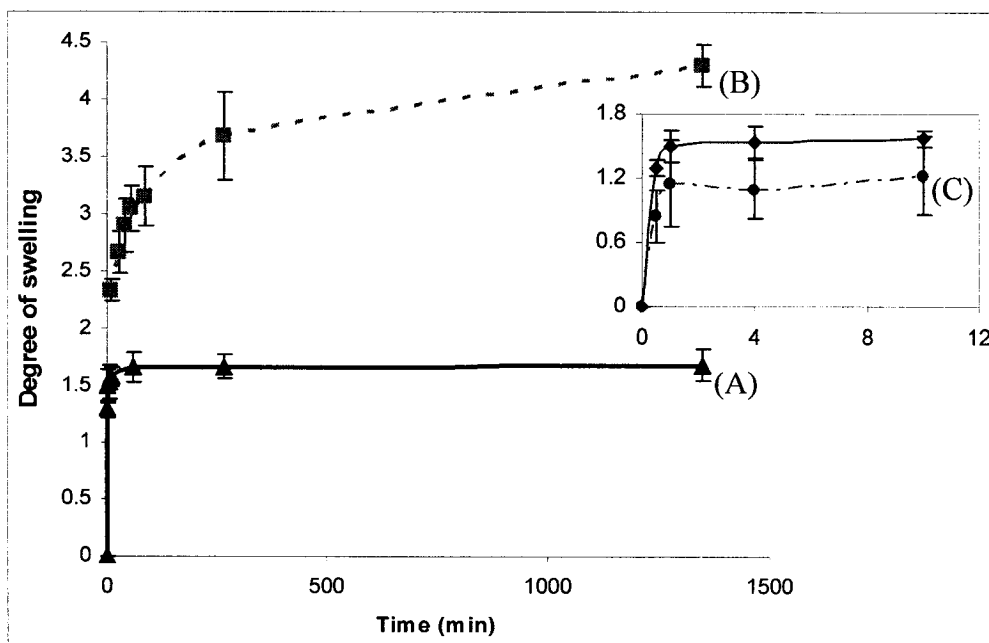


Figure 8.4. Swelling behavior in PBS (pH 7.4) of (A) CH-PEO membrane and (B) CH-PEO porous membrane; The inset shows the swelling behavior of CH-PEO membrane in comparison to (C) CH membrane.

The water permeation at 120 mm Hg was determined to be less than $1 \text{ mL/cm}^2 \text{ min}^{-1}$. No significant linkage of the membrane was observed when the device was pressurized at 120 mm Hg for 30 min. The burst pressure resistance of the 4 tested membrane-covered stents was determined to be higher than 500 mm Hg but the failure point could not be determined since the apparatus used in this work did not allow us to pressurize the membrane higher than 500 mm Hg.

Additional layers could be easily added once the first membrane had formed on the metallic device. Especially, freeze-drying allows one to add a porous outer layer onto the membrane covered device. The porosity of the porous CH-PEO membrane has been investigated and averaged 96 %.

8.1.4.3. Thromboresistance

The thromboresistance of the CH-PEO membrane was investigated in an *ex vivo* porcine assays using radiolabeled platelets and leukocytes (Fig. 8.5 and 8.6). Under the physiological flow conditions used in the study, the Ch-PEO presented low amounts of platelet adhesion in comparison to damaged arteries ($P < 0.05$). Similar results were obtained with leukocytes ($P < 0.005$). Both platelet and leukocyte adhesion onto CH-PEG were in the same range that on arteries with an intact endothelial layer. The sensibility of the assays was however not high enough to quantify precisely the relative thromboresistance of these two surfaces.

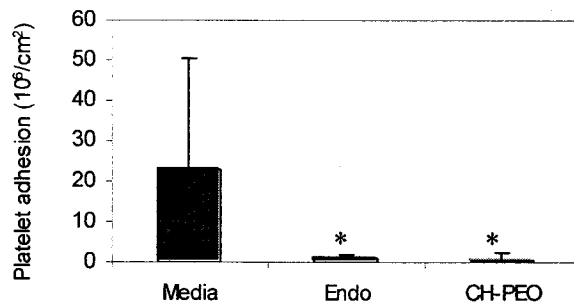


Figure 8.5. Platelet adhesion ($n \geq 5$) in an ex vivo porcine model on CH-PEO, damaged (Media) and intact arteries (Endo); * $p < 0.05$ Vs. Media

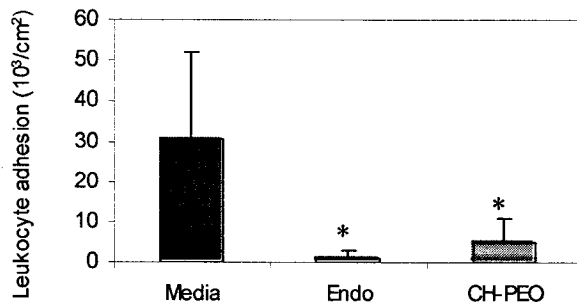


Figure 8.6. Leukocyte adhesion ($n \geq 5$) in an ex vivo porcine model on CH-PEO, damaged (Media) and intact arteries (Endo); * $p < 0.005$ Vs. Media

The effect of PEO and heparin complexation on the haemocompatibility was investigated in the *in vitro* assays. The incorporation of PEO into the chitosan membrane tends to reduce the amount of platelet adhesion as shown in Fig. 8.7 (52.5% reduction, $P > 0.05$, Student-t-test). Complexation of the CH-PEO membrane with heparin improved the resistance to platelet adhesion by 50.1% ($p \leq 0.05$, Student-t-test).

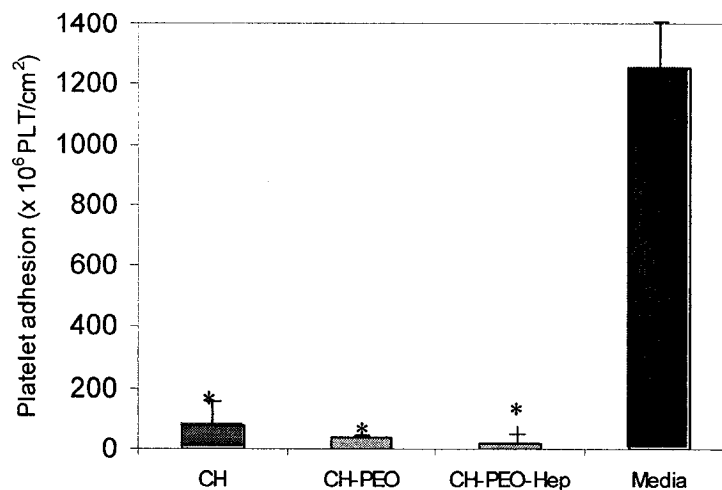


Figure 8.7. Platelet adhesion ($n \geq 4$) after 90 min incubation in PRP on chitosan (CH), CH-PEO and heparin complexed-CH-PEO (CH-PEO-Hep) membranes. Damaged arteries (Media) were used as control; * $p < 0.05$ Vs. Media; + $p < 0.05$ Vs. CH-PEO

3.4. Arginine release

Both direct and indirect loading of the drug in the CH-PEO membrane were characterized by a high loss during the washing steps ($> 80\%$). The precomplexation of the cationic drug with the anionic LMW HA resulted only in a minor increase in the retention of the drug during the washing steps (18 % Vs. 13.6 %). The release behavior of the Arginine loaded membrane in PBS is presented in Fig. 8.8 Both direct and indirect loading resulted in a high burst release in PBS with most of the drug remaining in the membrane being released by the first hour (91% and 86%).

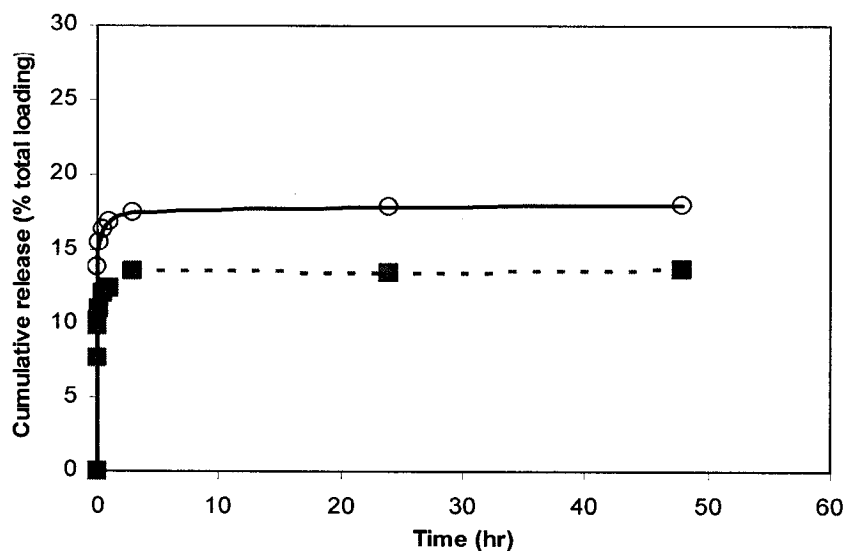


Figure 8.8. Arginine release behavior in PBS of the CH-PEO membrane: - ■- Direct loading and - ○ - precomplexation with anionic LMW HA

8.1.5. Discussion

The present work describes the development of chitosan-based biodegradable membrane covered stents. The main finding was that metallic stent could be covered by a chitosan-based membrane displaying suitable properties for endoluminal implantation. To fulfill any clinical applications, such membrane should (1) be able to sustain the deformation during the endoluminal expansion of the stent; (2) not elicit extensive biological response; (3) be thromboresistant; (4) allowed cellular ingrowths both at the luminal and external surfaces and (5) be able to resist physiological blood pressure. Minimally invasive implantation of stents/membrane-covered stents is widely used in the treatment of obstructive/degenerative pathologies such as coronary and peripheral artery diseases, aneurysm, ruptures and fistulas. They are also investigated in non-vascular malignant diseases in urology or gastroenterology for instance. The most

straightforward applications of membrane-covered stents are currently the endoluminal exclusion of aneurysm and the revascularization of vein graft.

The excellent mechanical properties of the chitosan-PEO blend allowed the hydrated device to be completely crushed on a catheter without noticeable damages to the membrane upon redeployment. In turn, the membrane covered stent could be loaded onto a delivery catheter and expanded through the self-expanding properties of the supporting metallic stents. Preliminary assays have investigated the use of reticulated membranes, using glyoxal or glutaraldehyde, or chitosan alone but these membranes failed to sustain the elastic deformation required during expansion. The blend of chitosan with high molecular weight PEO have been shown to drastically improve the elasticity and strength of chitosan^{10; 11}. The latter has been explained by the intermolecular interactions between chitosan and PEO, especially close to the stoichiometric monomer ratio.

The second key-point in the design of such an endovascular device was the overall biocompatibility and haemocompatibility of the material. Both chitosan and PEO are well-known biocompatible biodegradable materials. In particular, chitosan is widely investigated as wound dressing material, drug delivery vehicle and tissue engineering scaffold²⁵⁻³⁰. Chitosan supports cell attachment and growth and has been successfully investigated in vascular tissue engineering applications³¹. The poor endothelialization of synthetic graft materials has been called as a major cause of failure. In contrast, chitosan supports the attachment and growth of endothelial cells which may in turn enhanced the long-term biocompatibility of the device. Acute blood compatibility of chitosan have however been reported to be an issue with reported ability of the polymer to activate both complement and blood coagulation systems³². A recent exhaustive investigation of the blood compatibility of chitosan has however showed that despite large adsorption of plasma proteins, the polymer was a weak activators of the alternative pathway of the complement and intrinsic pathway of coagulation³³. CH-PEO membranes were tested in an *ex vivo* extracorporeal porcine model using radiolabeled platelets and leukocytes.

Amount of adsorbed platelets and leukocytes were low, and in the same range than those measured on intact aortic segments used a negative control. Both values were significantly lower than the damaged artery model used as positive control. Endothelial denuded arteries have been previously used to simulate angioplasty-damaged blood vessels³⁴. The surprisingly good blood compatibility displayed by the CH-PEO polymer similar to that of intact blood vessels may however be the reflect of lack of sensitivity of the *ex vivo* assay. To get further insight of the haemocompatibility of the CH-PEO membrane, an *in vitro* assay was used to compare the platelet adhesion on CH-PEO membrane with chitosan alone and heparin complexed CH-PEO membrane. The blending of chitosan with PEO tends to reduce the adhesion of platelets. This may be related to the hydrophilicity of PEO that may decrease non-specific adhesion. A further improvement was observed upon surface complexation with heparin. Complexation of chitosan with anionic polysaccharide such as heparin has been widely used to improve its thromboresistance^{32; 35; 36}. Conversely, electrostatic complexation with glycosaminoglycans such as hyaluronic acid has been reported to modulate its biological activity³¹. Complex of chitosan and heparin have also recently been reported to enhance wound healing³⁰.

Along with its mechanical properties and biocompatibility, the choice of chitosan as a base materials relied also on its ability to achieve local delivery of biologically active components¹³. In particular, chitosan has been investigated in therapies directed against cancer or hyperproliferative vascular disease using drugs such as doxorubicin or paclitaxel^{12; 19; 37; 38}. We assessed the loading and delivery of the NO-precursor L-Arginine. Arginine is a low molecular weight cationic drug that has been proved to be effective in the reduction of neointimal hyperplasia^{17; 18}. The release behavior presented in figure 9 shows an initial burst release with small amount of the drug being released after 1 h. Importantly, a significant amount (86.4 %) of the drug was lost during the neutralization and washing procedures. We thus investigated the possibility to control the release behavior by precomplexation of the cationic drug with the polyanionic low molecular weight hyaluronic acid. A similar precomplexation method has been used to improve the release behavior of doxorubicin in chitosan nanoparticles¹⁹. Only a modest

improvement was obtained as the initial loss during the washing procedure remained high (82 %) and most of the drug was released during the initial burst (86 % at 30 min Vs. 91 % for the direct method).

While the membrane-covered device was initially designed for the treatment of occlusive diseases and vein graft stenoses, we investigated its potential use in the setting of endovascular aneurysm closure. The possibility to exclude the aneurysm by the chitosan-based membrane as well as the potential for local delivery of biologically active components such as growth factors are appealing. The CH-PEO membrane could act as a temporary barrier while being used as a template for arterial reconstruction. Organization of the blood thrombi into connective tissue may be expected to solve the issue of endoleak that plague endovascular aneurysm exclusion. Such organisation may be enhanced by the presence of the chitosan based membrane and further accelerated by incorporation of appropriate growth factors. Sealing of the membrane to prevent growth of the aneurysm is however required. The water permeation assays used here showed that the CH-PEO membrane covered stent showed an excellent blockade of saline solution and less than $1 \text{ mL/cm}^2 \text{ min}^{-1}$ was measured. The low volume of solution prevented more precise determination but these values are better or comparable to that reported for commercially available graft such as the cross-linked collagen Dacron impregnated Hemashield[®] ($<10 \text{ mL/cm}^2 \text{ min}^{-1}$). The burst resistance of the membrane should also be high enough to prevent failure upon the aneurismal transmural pressure. Burst pressure resistance of a monolayered CH-PEO membrane was determined to higher than 500 mm Hg. While further investigation is certainly warranted, this value is expected to sustain transmural pressure occurring in aneurysm. Additional CH-PEO layer could be useful to increase the burst resistance. In addition, thrombus formation and tissue ingrowth within the membrane in contact with fluids of the excluded area of the aneurysm could act as additional sealing and reinforcing material. In an attempt to apply the concept of tissue engineering in the field of aneurysm closure, we investigated the possibility to add an external porous layer that could be truly used as a scaffold for vascular cells. Tissue engineering of vascular graft has been the object of much interest due to the unsolved clinical issue of small vascular graft. The advantage of using

biological materials such as collagen as construct is counterbalanced by the inadequate mechanical properties of these polymers. Hybrid graft using dacron sleeves combined with collagen-based construct have been proposed to assure enough burst resistance for *in vivo* implantation^{22; 39-41}. The presence of synthetic sleeves may however be damageable for the long term success of the graft. On the other hand, graft made completely from biodegradable polymers required lengthy *in vitro* tissue formation to display appropriate mechanical properties for implantation. A hybrid device conjugating the mechanical scaffold of the metallic device and the biodegradable chitosan-based porous matrix as proposed here open new opportunities in this field. Metallic stents do not elicit intensive biological reactions such as those commonly observed with polymeric synthetic materials. The metallic component of the hybrid construct can provide the necessary mechanical strength, at least at the acute phase of the tissue organization, while minimizing the amount of non-biodegradable material within the artery in comparison to synthetic polymeric sleeves. In addition, cell ingrowths naturally occurring in chitosan matrix could be easily enhanced by incorporation of growth factors in the chitosan-based membrane^{42; 43}. Much works remain however to do to the optimize such a scaffold for vascular tissue engineering, especially in term of mechanical compliance mismatch with the vascular wall.

8.1.6. Conclusion

This study showed that a biodegradable membrane covered stent could be designed based on the excellent mechanical properties of chitosan-PEO blend. The device could be loaded onto a catheter and expanded without noticeable damage to the membrane, thus authorizing endoluminal delivery. The biological properties of chitosan and its biocompatibility associated with the potential to achieve uniform local delivery of biologically active components to the vascular wall suggest that such device could be used in the treatment of various pathologies such as vascular obstructive diseases,

aneurysms and malignant diseases. While the *in vitro* experiments presented here are promising, further *in vivo* investigations are warranted to prove its clinical potential.

Acknowledgments.

This work was partly supported by NSERC grants. The authors are grateful to Prof. F. Winnik from University of Montreal for advice and critical discussion. We thank Dr. J. Silver from Nitinol Devices & Components (NDC, Fremont, CA) for his advice and technical support; Thanks go to J.F. Théoret and N. Jacob from the Montreal Heart Institute for their help in the haemocompatibility assays and P. Cap for manuscript reviewing.

8.1.7. Reference

1. Campbell PG, Hall JA, Harcombe AA, de Belder MA: The Jomed Covered Stent Graft for coronary artery aneurysms and acute perforation: a successful device which needs careful deployment and may not reduce restenosis. *J Invasive Cardiol* 2000;12:272-6
2. Baldus S, Koster R, Reimers J, Kahler J, Meinertz T, Hamm CW: Membrane-covered stents: a new treatment strategy for saphenous vein graft lesions. *Catheter Cardiovasc Interv* 2001;53:1-4
3. Kribs S: Endovascular stent grafting: a review. *Can Assoc Radiol J* 2001;52:145-52
4. Formichi M, Marois Y, Roby P, Marinov G, Stroman P, King MW, Douville Y, Guidoin R: Endovascular repair of thoracic aortic aneurysm in dogs: evaluation of a nitinol-polyester self-expanding stent-graft. *J Endovasc Ther* 2000;7:47-67

5. Stockx L: Stent-grafts in the superficial femoral artery. *Eur J Radiol* 1998;28:182-8
6. Goodwin SC, Yoon HC, Wong GC, Bonilla SM, Vedantham S, Arora LC: Percutaneous delivery of a heparin-impregnated collagen stent-graft in a porcine model of atherosclerotic disease. *Invest Radiol* 2000;35:420-5
7. Cloft HJ, Kallmes DF, Lin HB, Li ST, Marx WF, Hudson SB, Helm GA, Lopes MB, McGraw JK, Dion JE, Jensen ME: Bovine type I collagen as an endovascular stent-graft material: biocompatibility study in rabbits. *Radiology* 2000;214:557-62
8. Gaspar J, Vonderwalde C, Hong MK, Eid-Lidt G, Almagor Y, Leon MB: [Stent coated with bovine pericardium: in vitro evaluation, in animals, and initial results in humans]. *Arch Cardiol Mex* 2001;71:286-94
9. McKenna CJ, Camrud AR, Sangiorgi G, Kwon HM, Edwards WD, Holmes DR Jr, Schwartz RS: Fibrin-film stenting in a porcine coronary injury model: efficacy and safety compared with uncoated stents. *J Am Coll Cardiol* 1998;31:1434-8
10. Kolhe P, Kannan RM: Improvement in Ductility of Chitosan through Blending and Copolymerization with PEG: FTIR Investigation of Molecular Interactions. *Biomacromolecules* 2003;4:173-80
11. Budtova T, Belnikevich N, Kalyuzhnaya L, Alexeev SB, Vesnebolotskaya S, Zoolshoev Z: Chitosan Modified by Poly(ethylene oxide): Film and Mixture Properties. *J Appl Polym Sci* 2002;84:1114-1122
12. Nsereko S, Amiji M: Localized delivery of paclitaxel in solid tumors from biodegradable chitin microparticle formulations. *Biomaterials* 2002;23:2723-31
13. Singla AK, Chawla M: Chitosan: some pharmaceutical and biological aspects--an update. *J Pharm Pharmacol* 2001;53:1047-67
14. Senel S, Kremer MJ, Kas S, Wertz PW, Hincal AA, Squier CA: Enhancing effect of chitosan on peptide drug delivery across buccal mucosa. *Biomaterials* 2000;21:2067-71

15. Regar E, Sianos G, Serruys PW: Stent development and local drug delivery. *Br Med Bull* 2001;59:227-48
16. Fattori R, Piva T: Drug-eluting stents in vascular intervention. *Lancet* 2003;361:247-9
17. Suzuki T, Hayase M, Hibi K, Hosokawa H, Yokoya K, Fitzgerald PJ, Yock PG, Cooke JP, Suzuki T, Yeung AC: Effect of local delivery of L-arginine on in-stent restenosis in humans. *Am J Cardiol* 2002;89:363-7
18. Kalinowski M, Alfke H, Bergen S, Klose KJ, Barry JJ, Wagner HJ: Comparative trial of local pharmacotherapy with L-arginine, r-hirudin, and molsidomine to reduce restenosis after balloon angioplasty of stenotic rabbit iliac arteries. *Radiology* 2001;219:716-23
19. Mitra S, Gaur U, Ghosh PC, Maitra AN: Tumour targeted delivery of encapsulated dextran-doxorubicin conjugate using chitosan nanoparticles as carrier. *J Control Release* 2001;74:317-23
20. Gouin S, Valencia Grayeb MV, Winnik FM: Gadolinium Diethylenetriamine Pentaacetic Acid/Hyaluronan Conjugates: Preparation, Properties and Applications , in Guiseppi-Elie A, Levon K (eds): *Macromolecule-Metal Complexes, Macromolecular Symposia 186*. Weinheim, Germany, 2002, pp 105-110
21. Bananinchi PO: Complex permittivity. *Bioengi* In press;
22. Berglund JD, Mohseni MM, Nerem RM, Sambanis A: A biological hybrid model for collagen-based tissue engineered vascular constructs. *Biomaterials* 2003;24:1241-54
23. Phaneuf MD, Dempsey DJ, Bide MJ, Quist WC, LoGerfo FW: Coating of Dacron vascular grafts with an ionic polyurethane: a novel sealant with protein binding properties. *Biomaterials* 2001;22:463-9
24. Thierry B, Merhi Y, Bilodeau L, Trépanier C, Tabrizian M: Nitinol versus stainless steel stents: acute thrombogenicity study in an ex vivo porcine model. *Biomaterials* 2002;23:2997-3005

25. Rao SB, Sharma CP: Use of chitosan as a biomaterial: studies on its safety and hemostatic potential. *J Biomed Mater Res* 1997;34:21-8
26. Madihally SV, Matthew HW: Porous chitosan scaffolds for tissue engineering. *Biomaterials* 1999;20:1133-42
27. Richardson SC, Kolbe HV, Duncan R: Potential of low molecular mass chitosan as a DNA delivery system: biocompatibility, body distribution and ability to complex and protect DNA. *Int J Pharm* 1999;178:231-43
28. Zhang M, Li XH, Gong YD, Zhao NM, Zhang XF: Properties and biocompatibility of chitosan films modified by blending with PEG. *Biomaterials* 2002;23:2641-8
29. Ma J, Wang H, He B, Chen J: A preliminary in vitro study on the fabrication and tissue engineering applications of a novel chitosan bilayer material as a scaffold of human neonatal dermal fibroblasts. *Biomaterials* 2001;22:331-6
30. Kweon DK, Song SB, Park YY: Preparation of water-soluble chitosan/heparin complex and its application as wound healing accelerator. *Biomaterials* 2003;24:1595-601
31. Chupa JM, Foster AM, Sumner SR, Madihally SV, Matthew HW: Vascular cell responses to polysaccharide materials: in vitro and in vivo evaluations. *Biomaterials* 2000;21:2315-22
32. Amiji MM: Surface modification of chitosan membranes by complexation- interpenetration of anionic polysaccharides for improved blood compatibility in hemodialysis. *J Biomater Sci Polym Ed* 1996;8:281-98
33. Benesch J, Tengvall P: Blood protein adsorption onto chitosan. *Biomaterials* 2002;23:2561-8
34. Merhi Y, King M, Guidoin R: Acute thrombogenicity of intact and injured natural blood conduits versus synthetic conduits: neutrophil, platelet, and fibrin(ogen) adsorption under various shear-rate conditions. *J Biomed Mater Res* 1997;34:477-85

35. Chandy T, Rao GH: Evaluation of heparin immobilized chitosan-PEG microbeads for charcoal encapsulation and endotoxin removal. *Artif Cells Blood Substit Immobil Biotechnol* 2000;28:65-77
36. Beena MS, Chandy T, Sharma CP: Heparin immobilized chitosan--poly ethylene glycol interpenetrating network: antithrombogenicity. *Artif Cells Blood Substit Immobil Biotechnol* 1995;23:175-92
37. Eroglu M, Irmak S, Acar A, Denkbaz EB: Design and evaluation of a mucoadhesive therapeutic agent delivery system for postoperative chemotherapy in superficial bladder cancer. *Int J Pharm* 2002;235:51-9
38. Suzuki YS, Momose Y, Higashi N, Shigematsu A, Park KB, Kim YM, Kim JR, Ryu JM: Biodistribution and kinetics of holmium-166-chitosan complex (DW-166HC) in rats and mice. *J Nucl Med* 1998;39:2161-6
39. Xue L, Greisler HP: Biomaterials in the development and future of vascular grafts. *J Vasc Surg* 2003;37:472-80
40. Teebken OE, Haverich A: Tissue engineering of small diameter vascular grafts. *Eur J Vasc Endovasc Surg* 2002;23:475-85
41. Tiwari A, Salacinski HJ, Punshon G, Hamilton G, Seifalian AM: Development of a hybrid cardiovascular graft using a tissue engineering approach. *FASEB J* 2002;16:791-6
42. Lee JY, Nam SH, Im SY, Park YJ, Lee YM, Seol YJ, Chung CP, Lee SJ: Enhanced bone formation by controlled growth factor delivery from chitosan-based biomaterials. *J Control Release* 2002;78:187-97
43. Ishihara M, Obara K, Ishizuka T, Fujita M, Sato M, Masuoka K, Saito Y, Yura H, Matsui T, Hattori H, Kikuchi M, Kurita A: Controlled release of fibroblast growth factors and heparin from photocrosslinked chitosan hydrogels and subsequent effect on in vivo vascularization. *J Biomed Mater Res* 2003;64A:551-559

PART III. NANOCOATINGS ON ARTERIES

The development of angioplasty procedures have been a major breakthrough in the field of interventional cardiology. These revascularization procedures combined or not with stent implantation, remain however limited by restenosis, initiated at least partially by the injuries to the vascular wall during the procedure. Conveniently, metallic scaffolds can be modified to present or to deliver bioactive components to the vascular wall. Endovascular stents have been used in the first two parts of this work as templates to engineer new hybrid bioactive devices. While the mechanical scaffold offered by the metallic device has been shown to be highly beneficial in various clinical settings, its presence within the artery may however prevent total healing of the blood vessel. In addition, numerous pathologies would require sustained release of bioactive molecules to the vascular wall without the use of a stent. Local delivery procedures are currently limited by their poor efficiency, most of the drug being washed by the blood flow. Conversely, local delivery of hydrophobic drugs is limited by their poor aqueous solubilities.

Therapies able to protect the damaged vascular wall and to enhance its healing or procedures to target locally pharmaco-active agents would be of major clinical relevance. The emergence of nanotechnologies in the medical field offers fascinating possibilities to develop such new therapeutic strategies. Nanometric self-assembled multilayered structures of natural polysaccharides build up *in situ* onto angioplasty-damaged arteries have been investigated in the last part of the thesis. The hypothesis on which this work relies is that very thin coating could be built up *in situ* and could efficiently protect the damaged blood vessel from blood components. The versatility of the method used, the layer-by-layer technique, was also expected to allow the incorporation of bioactive macromolecules into the multilayers. The proof-of-principle of these self-assembled nanocoatings have been reported in the manuscript 6 of this

thesis published in the *Journal of the American Chemical Society*. The manuscript 7, to be submitted, demonstrates the possibility to incorporate biologically active molecules such as genetic materials into the multilayer.

9. SELF-ASSEMBLED CHITOSAN/HYALURONAN NANOCOATINGS

9.1. PAPER 6

Nanocoatings onto Arteries via Layer-by-Layer Deposition: Towards the In-Vivo Repair of Damaged Blood Vessels

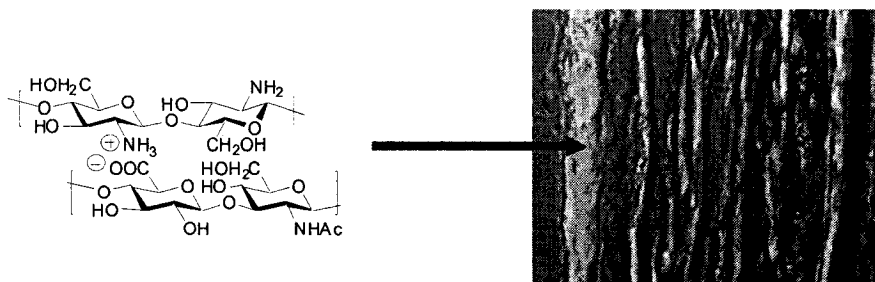
Benjamin Thierry, Françoise M. Winnik, Yahye Merhi, Maryam Tabrizian

Copyright © 2003 ACS. *J. Am. Chem. Soc.*; **2003**; 125(25); 7494-7495.

Reprinted by permission of the American Chemical Society

9.1.1. Abstract

The deposition of polysaccharide-based self-assembled nanocoatings onto damaged arteries is described as a means not only to protect a damaged artery against thrombogenesis, but also to control the healing processes by incorporating biologically active components within the multilayer. As shown by confocal microscopy, the polysaccharide multilayer was retained on the artery in physiological condition and prevented platelet adhesion. Diffusion of the polysaccharides within the artery was also observed and may be used to efficiently target the vascular wall. The NO-precursor L-Arginine was used as drug-model and incorporated within the self-assembled layers.



9.1.2. Communication

The layer-by-layer self-assembly of polyelectrolytes has emerged as a powerful and versatile, yet simple, strategy to engineer surfaces with specific properties.¹ Applications in the biomedical field are scarce, but they hold great promise, as the method permits the construction of thin films containing macromolecules such as proteins, enzymes, or nucleic acids, with targeted properties onto a variety of substrates.² In this communication, we describe the deposition of self-assembled nanocoatings onto arteries, as a means not only to protect an artery damaged during revascularization procedure against blood coagulation, but also to control the healing processes by incorporating bioactive molecules within the multilayer.

Indeed, revascularization procedures are often plagued with complications related to the reobstruction of the treated artery, i.e. restenosis, resulting from injuries induced during the procedure to the vascular wall. These injuries denude the protective endothelial cell lining (endothelium) and initiate excessive vascular cell proliferation within the artery.³ Systemic and local drug delivery via catheters or nanoparticles has been attempted, but such treatments have been largely unsuccessful in alleviating restenosis, due to inefficient targeting of the drug to the site of injury.⁴ Ideal strategies against restenosis should prevent the growth of blood thrombi on damaged arteries, enhance healing, and prevent the proliferation of vascular cells. Interest in local delivery has however been recently diverted by the success of drug eluting stents.⁵ In this communication, we

demonstrate that it is possible to build on damaged arteries a nanoscale self-assembled multilayer obtained by alternating depositions of two polysaccharides, hyaluronan (HA), a polyanion, and chitosan (CH), a polycation. The two polysaccharides (Fig. 9.1.1) have been chosen in view of their biocompatibility, healing capabilities, and anti-inflammatory properties.⁶

First, we characterized in detail the self-assembly of the CH/HA polyelectrolytes on a model surface, namely collagen-coated glass slides, using an ^{111}In -radio labeled HA.⁷ Multilayer growth was a linear function of the number of layers⁸ (slope= $5.1 \mu\text{g } ^{111}\text{In-HA}/\text{cm}^2$ per layer deposited; $r^2= 0.99$, $[\text{NaCl}] = 0.14 \text{ M}$) (Fig. 9.1.2). The electrostatically driven adsorption of the polymers occurred within a few seconds. Increasing the ionic strength of the polymer solutions (from 0.14 M to 1.0 M NaCl) resulted in a decrease of the amount of deposited polymer. Quartz microbalance (QCM) studies indicated a hydrated thickness of about 70 nm for 5 bilayers. Using radio labeled HA instead of HA, resulted in an increase of the multilayer thickness ($\sim 30\%$). The stability of the multilayer was monitored by incubation of a $(\text{CH}/^{111}\text{In-HA})_5$ self-assembly in phosphate buffer saline (PBS) at 40°C . No loss of radioactivity was detected after one week.

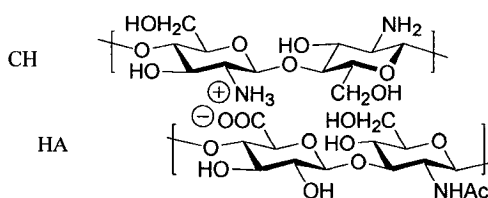


Figure 9.1.1. Chemical structure of chitosan (CH) and hyaluronan (HA)

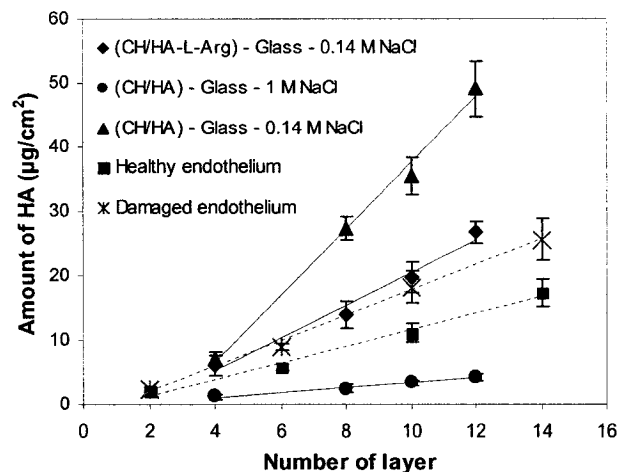


Figure 9.1.2. Amount of ^{111}In -HA Vs. layers; Solid lines: CH/HA (moderate and high ionic strength) and CH/HA-L-Arg on collagen coated glass; Dashed lines: CH/HA on damaged or healthy endothelium. Linear regressions are presented excluding the first bilayer due to substrate effect.

The multilayer was then constructed on damaged and healthy aortic porcine arteries, using a perfusion chamber matching closely conditions achievable *in vivo*. Strong adhesion of the coating on the artery was secured by depositing first a layer of chitosan, a polycation exhibiting excellent bioadhesive properties towards negatively charged surfaces such as those presented by damaged arteries. Linear build up profiles were obtained (Fig. 9.1.2) with lower amounts of polymers being deposited on healthy endothelium, compared to damaged arteries.

The successful deposition of the multilayer and its retention on the arterial wall was monitored by confocal microscopy detection of CH/FITC-HA (fluorescein isothiocyanate) multilayers. A top view of the coated artery indicated that the multilayer uniformly covered the damaged artery. The multilayer-coated artery was subsequently subjected to physiological shear by perfusion in PBS. Imaging of transversal sections

showed that the multilayer was retained on the vascular wall after a 24 h perfusion (Fig. 9.1.3). Remarkably, the multilayer, or at least the fluorescently labeled HA, was detectable within the arterial wall, an indication of the polymer diffusion. Note that an assembly of 5 bilayers allowed the incorporation within the vascular wall of about 20 times more HA ($18.2 \mu\text{g}/\text{cm}^2$ Vs. $0.86 \mu\text{g}/\text{cm}^2$) than passive infusion of a HA solution (1 mg/mL HA in 0.14 M NaCl, 15 min). HA, together with other anionic polysaccharides, such as heparin or fucoidans, is known to inhibit vascular cell proliferation.^{6a,9} Since the biological response of the damaged artery *in vivo* has been correlated to tissue concentration rather than to the administrated dose of active polysaccharides,¹⁰ the CH/HA nanocoatings may act as highly effective inhibitors of restenosis.

Next, CH/HA multilayer-coated arteries were placed in contact with blood in order to assess, via an *in vitro* platelet adhesion assay, the protective effect of the nanocoating against platelet adhesion onto damaged arteries. The growth of thrombus on damaged arterial surfaces was significantly inhibited by the CH/HA multilayers (Fig. 9.1.4; 87% reduction in platelet adhesion, $p < 0.05$). This observation corroborates a previous report that polylysine/alginate self-assembly can act as a barrier material against cell attachment when deposited *in vitro* onto extra-cellular matrix coated surfaces.¹¹ Insulation of the vascular wall from blood components, such as platelets and growing thrombi, results in reduced activation of vascular cells.¹² By cutting off this physiological response, one can expect to block the restenosis pathway early on.

Finally, we set out to evaluate whether CH/HA multilayers can act as localized drug-release systems and promote the artery healing process. Thus, we deposited onto arteries a multilayered assembly containing L-Arginine. This low molecular weight cationic peptide has been reported to reduce restenosis.¹³ It is the precursor of nitric oxide (NO), which is known to affect vascular tone and wall dynamics, to inhibit monocyte and platelet adhesion, and to prevent vascular cell proliferation. Multilayers were constructed by sequential deposition of a CH solution and a solution of a HA/L-Arginine complex (L-Arginine/disaccharide molar ratio: 1/5).¹⁴ Under these conditions,

it was possible to incorporate L-Arginine (213 ng/cm^2 in 5 bilayers) within the multilayer, but the amount of HA per layer was significantly lower than in the case of CH/HA multilayers of identical layer number (Fig. 9.1.2). The small amount of drug loaded within the multilayer was a result of its extraction during the adsorption of the chitosan layers. The release profile of [^3H] L-Arginine from a multilayer placed in PBS featured an initial burst ($\sim 80\%$ release) followed by a slow linear regime.¹⁵

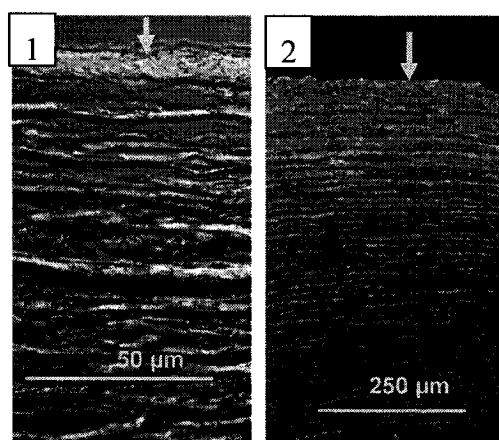


Figure 9.1.3. Confocal microscopy imaging of a section of a (CH/HA-FITC)₅ coated damaged artery showing the transmurular disposition of the fluorescently labeled polymer after 1) 0 h and 2) 24 h perfusion with PBS. The arrow indicates the coated surface exposed to the PBS flow.

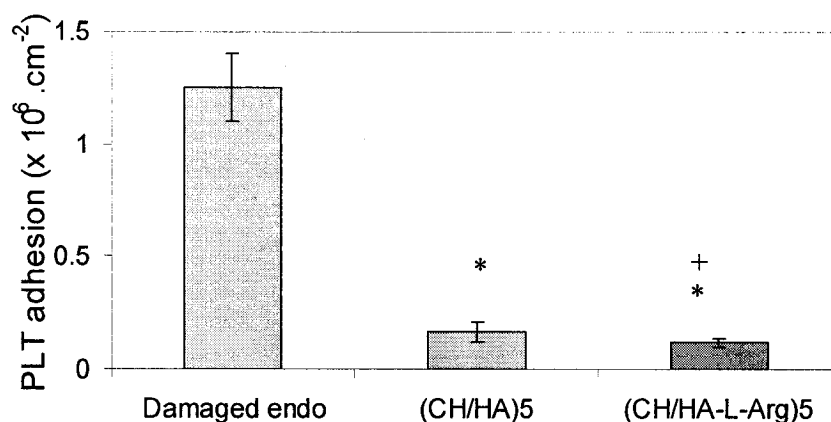


Figure 9.1.4. Platelet adhesion ($n \geq 4$) on damaged endothelium (damaged endo), (CH/HA)5 and (CH/HA-L-Arg)5 coated damaged endothelium ((CH/HA)5 and (CH/HA-L-Arg)5); * $p < 0.05$ Vs. Damaged endo; + $p < 0.05$ Vs. (CH/HA)5 by paired Student-t-test.

Incorporation of L-Arginine in the CH/HA nanocoating further improved its protective effect against platelet adhesion, as demonstrated by a reduction of 30% in the amount of platelet adhesion after 90 min (Fig. 9.1.4, $p < 0.05$), compared to arteries protected by a nanocoating devoid of L-Arginine. Note that, compared to unprotected damaged arteries, L-Arginine loaded CH/HA self-assemblies reduced platelet adhesion by 91% ($p < 0.05$). Conjugation of biologically active components, such as anti-proliferative drugs or hormones to the polymers, is under investigation. This approach is expected to significantly enhance the amount of drug incorporated in a multilayer and to allow its sustained presentation or its gradual release within the arterial wall.

Acknowledgments.

This research is funded by NSERC of Canada. The authors thank JF. Théoret and N. Jacobs for their technical help in the haemocompatibility studies, and L. Villeneuve for the confocal microscopy experiments.

Supporting Information Available.

Experimental details, QCM experiments and L-Arginine release profile. This material is available free of charge via the internet at <http://pubs.acs.org>

9.1.3. References

- (1) Decher, G. *Science* 1997, 277, 1232.
- (2) (a) Vazquez, E.; Dewitt, D.M.; Hammond, P.T.; Lynn, D.M. *J. Am. Chem. Soc.* 2002, 124(47), 13992-13993. (b) Zhou, L.; Estavillo, C.; Schenkman, S.J.B.; Rusling, J.F. *J. Am. Chem. Soc.* 2003, 125(5), 1431-1436,
- (3) Lowe, H.C.; Oesterle, S.N.; Khachigian, L.M. *J. Am. Coll. Cardiol.* 2002, 39, 183.
- (4) Hwang, C.W.; Edelman, E.R. *Circ. Res.* 2002, 90, 826.
- (5) (a) Fox, R. *Circulation* 2001, 104, E9052. (b) Serruys, P.W.; Regar, E.; Carter, A.J. *Heart* 2002, 87, 305.
- (6) (a) Heublein, B.; Evagorou, E.G.; Rohde, R.; Ohse, S.; Meliss, R.R.; Barlach, S. *Int. J. Artif. Organs.* 2002, 25, 1166-73. (b) Singla, A.K.; Chawla, M. *J. Pharm.*

Pharmacol. 2001, 53, 1047-67. (c) Kweon, D.K.; Song, S.B.; Park, Y.Y. *Biomaterials* 2003, 24, 1595-601.

(7) Gouin, S.; Winnik, F.M. *Bioconjug. Chem.* 2001, 12, 372.

(8) In this work, "layer" refers to the increment in thickness after exposure to one of the polyelectrolyte solution.

(9) (a) Matsumoto, Y.; Shimokawa, H.; Morishige, K.; Eto, Y.; Takeshita, A. *J. Cardiovasc. Pharmacol.* 2002, 39, 513. (b) Deux, J.F.; Meddahi-Pelle, A.; Le Blanche, A.F.; Feldman, L.J.; Collic-Jouault, S.; Bree, F.; Boudghene, F.; Michel, J.B.; Letourneur, D. *Arterioscler. Thromb. Vasc. Biol.* 2002, 22, 1604.

(10) (a) Lovich, M.A.; Edelman, E.R. *Proc. Natl. Acad. Sci. U S A* 1999, 96, 11111. (b) Hwang, C.W.; Wu, D.; Edelman, E.R. *Circulation* 2001, 104, 600.

(11) Elbert, D.L.; Herbert, C.B.; Hubbell, J.A. *Langmuir* 1999, 15, 5355.

(12) Hill-West, J.L.; Chowdhury, S.M.; Slepian, M.J.; Hubbell, J.A. *Proc. Natl. Acad. Sci. U S A* 1994, 91, 5967.

(13) Suzuki, T.; Hayase, M.; Hibi, K.; Hosokawa, H.; Yokoya, K.; Fitzgerald, P.J.; Yock, P.G.; Cooke, J.P.; Suzuki, T.; Yeung, A.C. *Am. J. Cardiol.* 2002, 89, 363.

(14) (a) Ariga et al.^{14b} previously reported the used of the pre-complexation method to load proteins in multilayer. (b) Ariga, K; Onda, M; Lvov, Y; Kunatake, Y. *Chem. Lett.* 1997. 27-26

(15) See Supporting Information for L-Arginine release profile

9.1.4. Supporting Informations

Preparation of the multilayer self-assemblies

Sodium Hyaluronate (HA) (MW 500,000, Hyal Pharmaceutical Corp, Mississauga, ON) and chitosan (CH) (HMW, degree of deacetylation: 85 %, from Sigma) were used as received. Solutions of HA (or HA-derivatives) (1 mg/mL in 0.14 M aqueous NaCl) and of CH (1.5 mg/mL in 0.1 M acetic acid (pH 4) containing 0.14 M NaCl) were prepared separately. The build up of the multilayer was accomplished by consecutive adsorption of the oppositely charged polysaccharides onto the substrate. Between each step, the excess polyelectrolyte was removed by rinsing the sample surface with 0.14 M NaCl. The effect of ionic strength was investigated using NaCl solutions ranging in concentration from 0 M to 1 M.

Substrates employed

Surfaces of porcine aortas used to simulate damaged arteries (Damaged endothelium) were prepared by lifting and peeling off the intima together with a thin portion of the adjacent media. Specimens with intact endothelial cell lining were also used as control (Healthy endothelium). Specimens were secured in a polycarbonate perfusion chamber used to deposit the multilayer onto artery walls and for further perfusion with physiological buffered solutions (PBS). The chamber had a window of 0.16 cm² exposing the artery to the solutions (either HA, CH, or 0.14 M NaCl solution during build up and PBS during the perfusion experiments). Collagen coated glass slides and Petri dish used as model surfaces were prepared by treating clean substrates with 10 µL of a 1 mg/mL collagen solution (Type I, CHRONO-LOG) and drying at room temperature.

Characterization using ellipsometry and quartz crystal microbalance (QCM) was achieved, respectively, on silicon wafers and on evaporated gold QCM electrodes. Substrates were cleaned with a piranha solution (concentrated $\text{H}_2\text{SO}_4/\text{H}_2\text{O}_2$ (30 wt % in water) = 3/1 v/v; Piranha solution is extremely energetic and should be handled with extreme caution) and pure water. A polyethyleneimine layer (PEI, MW 70,000, 5 mg/mL) was first adsorbed for 20 min onto these substrates and used as a precursor layer to initiate the layer-by-layer self-assembly.

Characterization of the self-assembled multilayers

CH/HA self-assemblies were characterized on the arteries or on collagen coated glass surfaces using an ^{111}In radio labeled HA (^{111}In -HA). A diethylenetriaminepentaacetic acid/HA conjugate (HA-DTPA) was prepared as described previously (Ref. 7). Radio labeled HA (^{111}In -HA) was prepared by complexation with ^{111}In performed and as follows: 100 μCi $^{111}\text{InCl}_3$ (100 μCi) was added to a solution of HA-DTPA (29 mg) in pure water (20 mL). The solution was maintained at room temperature for 2 hr under stirring, prior to purification by extensive dialysis against water. The solution (29 mL) was kept at 4° C until used. After the build up of the multilayer using ^{111}In labeled HA, the radioactivity of the samples was determined using a gamma counter (1470 Wizard™, Wallac). The amount of ^{111}In -HA in the multilayer was calculated after correction for decay, knowing the activity of a 1 mg/mL ^{111}In -HA solution.

The influence of the radio labeling procedure on the build up processes was assessed using a dissipation enhanced quartz crystal microbalance (QCM-D, Q-Sense, Sweden). A non-radioactive Gd-HA complex was prepared similarly to the ^{111}In -HA and used in the QCM-D experiments. CH/HA multilayers using either non labeled HA or Gd-HA were grown on the gold-coated electrodes and the thickness of the film was determined from the frequency shift, taking into consideration the dissipation due to viscoelasticity. Assuming a constant density of the growing self-assembly, the use of Gd-HA for the

multilayer build up resulted in a modest increase of the thickness when compared with the multilayer prepared using non labeled HA (see Figure 9.1.S1, slope = 13.95 nm/layer ($R^2 = 0.96$) with Gd-HA and slope = 9.07 nm/layer ($R^2 = 0.98$) with non labeled HA). Thus use of the ^{111}In labeled HA to investigate the build up procedures overestimated the amount of HA incorporated in the multilayer by 30% or less.

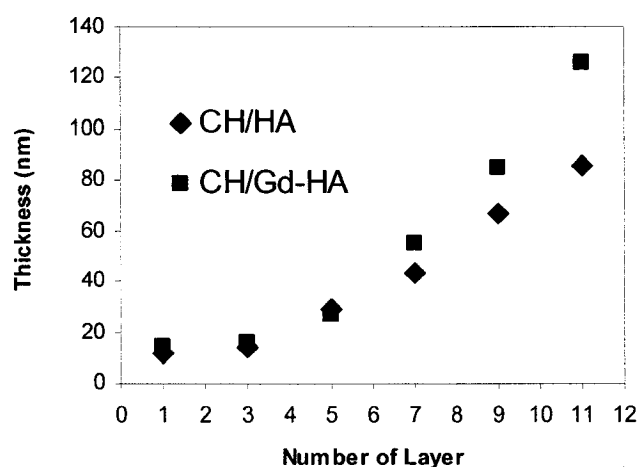


Figure 9.1.S1. Thickness of the CH/HA multilayer self-assemblies prepared using non labeled HA or Gd-labeled HA (Gd-HA) (from QCM-D measurements).

Vascular diffusion of the polymer

The diffusivity of HA in the vascular wall was determined using the parallel plate perfusion chamber described above and a fluorescent derivative of HA (FITC-HA). FITC-HA was prepared by treatment of a solution of HA (80 mg) in aqueous borate buffer (pH 9.4) with fluorescein dichlorotriazine (Sigma) for 3 hr at room temperature, in the dark and under nitrogen (COOH/Fluorescein molar ratio: 25:1). The unreacted dye was removed by dialysis against borate buffer (12 hr) and against water (3 days). FITC-HA was recovered by lyophilization and the purity was assessed by GPC.

CH/FITC-HA self-assemblies (5 bilayers) were deposited directly on damaged porcine aortic samples positioned in the perfusion chamber using silicon tubing and 3 X 10 cc syringes filled with saline, CH (2 cc) and FITC-HA (2 cc). CH and FITC-HA layers were alternatively deposited on the sample for 2 min. Prior to each polyelectrolyte monolayer deposition, the circuit was rinsed with 5 mL of saline solution. The nanocoated samples were then perfused with PBS (137 mM NaCl, 2.7 mM KCl, 4.3 mM Na₂HPO₄, 1.4 mM KH₂PO₄ in pure water at pH 7.4) under physiological wall shear stress (424 sec⁻¹) for 1 min, 2 h and 24 h. The specimens were kept in the dark during all the experiments to prevent photobleaching. To avoid diffusion of the polymers during handling and storage of treated arteries, specimens were snap-frozen in 2-methylbutane using liquid nitrogen and kept at -80°C until used. Tissues were cut into 10 µm thick sections with a cryostat and mounted onto a glass slide prior to fixation with 4% paraformaldehyde. The sections were imaged using an Axiovert inverted microscope equipped with an LSM 510 confocal system (Zeiss). The images were corrected for autofluorescence using non-coated sections of porcine arteries.

L-arginine-loaded multilayers

A mixture of labeled/unlabeled L-Arginine (Arg) from Sigma (L-Arginine hydrochloride, FW: 210.7; and L-Arginine-2,3-³H in aqueous ethanol solution) was added to a solution of HA in 0.14 M NaCl (COOH/Arg molar ratio: 5:1 with 2 µL [³H] Arg/mL). This solution was used to build the multilayer. The effect of the drug on the growth of the layer on collagen-coated glass was studied using ¹¹¹In-HA. To investigate the release of L-Arginine from the multilayers, L-Arginine-loaded multilayers were immersed in PBS and gently stirred. Radioactivity of the solution was determined using liquid scintillation spectrometry (Beckman LS 6500 Liquid Scintillation counter) as a function of immersion time and used to determine the release behavior presented in Figure 9.1.S2.

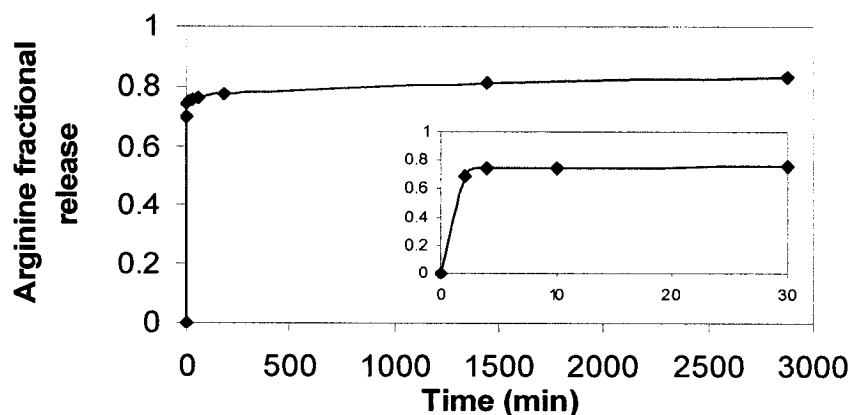


Figure 9.1.S2. Fractional release of L-Arginine loaded multilayer in PBS. The inset shows the initial release.

Thromboresistance of nanocoated arteries

A platelet adhesion assay was used to investigate the protective effect of the self-assembled nanocoatings deposited on damaged arteries. Fresh blood (120 mL) was drawn from healthy volunteers who were medication-free. The blood was collected in syringes preloaded with sodium citrate (3.8% w/v). Platelet-rich plasma (PRP) was prepared by centrifugation of the blood at 1800 rpm for 15 min. The PRP was then centrifuged at 2200 rpm for 10 min and the platelet-poor plasma (PPP) was recovered as the supernatant. Platelets were carefully resuspended in buffer and then incubated with 250 μCi of $^{111}\text{InCl}_3$ for 15 min. The platelets were recovered by centrifugation and resuspended in the PPP to 2.5×10^6 platelets/mL. The multilayer coated arteries were placed into the bottom of a 96 well polystyrene plate (Corning Inc.). 250 μl of freshly prepared ^{111}In -platelet solution was added to each well, taking special care to ensure that both sides of the samples were in contact with the platelet solution. Platelet adhesion was allowed to proceed for 90 min with gentle shaking. After incubation, the samples were recovered, washed 4 times with saline and fixed in a 1.5 % glutaraldehyde

solution. The amount of platelets was determined using a gamma counter (1470 WizardTM, Wallac).

Statistical analysis

Linear regressions are presented excluding the first layers in the nonlinear regime due to the effect of the substrate. The platelet adhesion data were analyzed paired Student-t-test. A P value less than 0.05 was accepted as statistically significant.

9.2. PAPER 7

Self-Assembled Nanocoating of Blood Vessels: Toward Efficient Delivery of DNA to the Vasculature

Benjamin Thierry, Françoise M. Winnik, Yahye Merhi, and Maryam Tabrizian

9.2.1. Introduction

The layer-by-layer (L-b-L) self-assembly of charged polyelectrolytes is a powerful technique enabling excellent control of the surface properties on the nanoscale level¹. It has been widely used to deposit biomacromolecule-containing films onto artificial substrates²⁻⁴. The work described here exploits the versatility of the L-b-L technique to assemble DNA-containing multilayered structures in order to use them to achieve efficient therapeutic gene transfer to the vasculature. Efficient gene transfer to vascular tissue offers new strategies to treat disorders of the vasculature. For example, gene therapy has been shown promising in alleviating restenosis, treating vein graft disease, and has generated hope in the field of angiogenesis and for the regeneration of vascular tissue^{5,7-10}. Thus *in vivo* local delivery of “naked” DNA to tissues, such as the vascular wall, presents great promise, but to date it has been disappointingly inefficient, achieving only low gene transduction ($\sim 1\%$)⁵. More efficient gene transfer methods are required to fulfill the wide therapeutic potential of vascular gene therapy. We reported

recently the L-b-L self-assembly onto damaged blood vessel of two polysaccharides, hyaluronan (HA) and chitosan (CH) (Fig. 9.2.1). Both HA and CH are biocompatible natural polymers which can be internalized by cells. We demonstrated that the multilayer is stable in physiological conditions and, moreover, that it tends to diffuse within the vascular wall. This nanocoating was shown to protect the artery from blood components and to drastically reduce platelet adhesion. The aim of the work described here is to exploit these results in order to deposit, *in situ*, onto a blood vessel, self-assembled nanocoatings loaded with DNA. The hypothesis was that DNA embedded into the self-assembled polysaccharide multilayer might efficiently target vascular cells. The L-b-L technique also allows one to control the nanocoating composition, and in particular the amount of incorporated DNA.

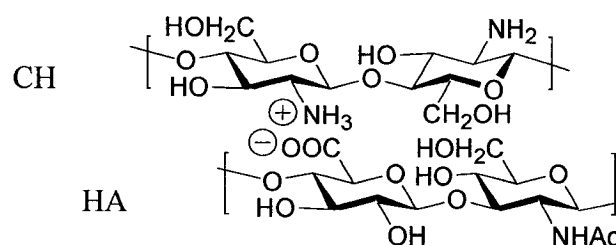


Figure 9.2.1. Polysaccharides used in the self-assembly process

The objectives of this study were to characterize the incorporation of DNA within the CH/HA self-assembly. The buildup of the multilayers was investigated using a dissipation-enhanced quartz microbalance (QCM) able to operate in fluids, thus allowing real-time monitoring of the self-assembly process. The haemocompatibility of the multilayer deposited onto blood vessels was assessed under conditions closer to physiological situation, using a dynamic *in vitro* perfusion assay. The resistance of the self-assembly against fouling by blood proteins was also investigated.

9.2.2. Experimental

Preparation of the Self-Assembled Coatings.

Sodium Hyaluronate (HA) (MW 500,000, Hyal Pharmaceutical Corp, Mississauga, ON), chitosan (CH) (HMW, degree of deacetylation: 85 %, from Sigma) and DNA from calf thymus (Sigma) were used as received. Solutions of HA (1 mg/mL in 0.14 M aqueous NaCl) and of CH (1 mg/mL in 0.1 M acetic acid (pH 4) containing 0.14 M NaCl) and DNA (0.2 mg/mL in 0.14 M aqueous NaCl) were prepared separately. The build up of the multilayer was accomplished by consecutive adsorption of the oppositely charged polyelectrolytes onto the substrate. Between each step, the excess polyelectrolyte was removed by rinsing the sample surface with 0.14 M NaCl.

QCM characterization of the multilayers.

The assembly of the polyelectrolyte systems CH/HA and CH/DNA was characterized using a dissipation enhanced quartz microbalance (QCM-D, Q-Sense, Sweden) on gold-evaporated QCM crystal. The crystals were cleaned with piranha solution (concentrated $\text{H}_2\text{SO}_4/\text{H}_2\text{O}_2$ (30 wt % in water) = 3/1 v/v). A polyethyleneimine layer (PEI, MW 70,000, 5 mg/ mL) was first adsorbed for 20 min onto the crystals and used as a precursor layer to initiate the layer-by-layer self-assembly. The polyelectrolyte solutions were sequentially injected into the measurement cell and the shifts in the Δf were continuously recorded. Once the self-assembly processes was completed, a fibrinogen solution (1 mg/mL) was injected into the QCM cell. The change in the frequency was monitored.

Haemocompatibility in a dynamic assay.

The protective effect of the self-assembled polysaccharide coating onto damaged arteries was investigated using a dynamic *in vitro* model. Fresh blood (120 mL) was drawn from healthy volunteers (n=5) who were medication-free. The blood was collected in syringes preloaded with sodium citrate (3.8% w/v). Platelet-rich plasma (PRP) was prepared by centrifugation of the blood at 1800 rpm for 15 min. The PRP was then centrifuged at 2200 rpm for 10 min and the platelet-poor plasma (PPP) was recovered as the supernatant. Platelets were carefully resuspended in buffer and then incubated with 250 μCi of $^{111}\text{InCl}_3$ for 15 min. The platelets were recovered by centrifugation and resuspended in the PPP to 2.5×10^6 platelets/mL (PRP). Damaged arteries (Media) were prepared by lifting and peeling off the intima together with a thin portion of the adjacent media. The damaged arteries were placed into a polycarbonate perfusion chamber and the buildup of the multilayer $(\text{CH}/\text{HA})_5$ was performed *in situ* as closely as possible to *in vivo* conditions. The coated and un-coated (control exposed to saline solutions) damaged arteries were then perfused with the platelet rich plasma for 30 min at a physiological wall shear stress of 424 sec^{-1} . The samples were rinsed with saline for 1 min and the amount of adhered platelets was quantified using a gamma counter (1470 WizardTM, Wallac).

9.2.3. Results and discussion

Buildup of the multilayers.

Previous experiments with a radiolabeled HA conjugate have shown the linear growth of the CH/HA assembly deposited onto blood vessels⁶. The assembly processes was investigated using the dissipation enhanced-QCM system. The frequency shift and

dissipation corresponding to the fifth overtone are presented in the Fig 9.2.2. As expected, a frequency shift and an increase in the dissipation due to the viscoelastic nature of the film were observed with each injection of the polymer solutions in the cell, indicating a mass increase¹¹. The adsorption of the polymers occurred within few seconds, which is of clinical relevance, since the time required for endovascular procedures should be minimized.

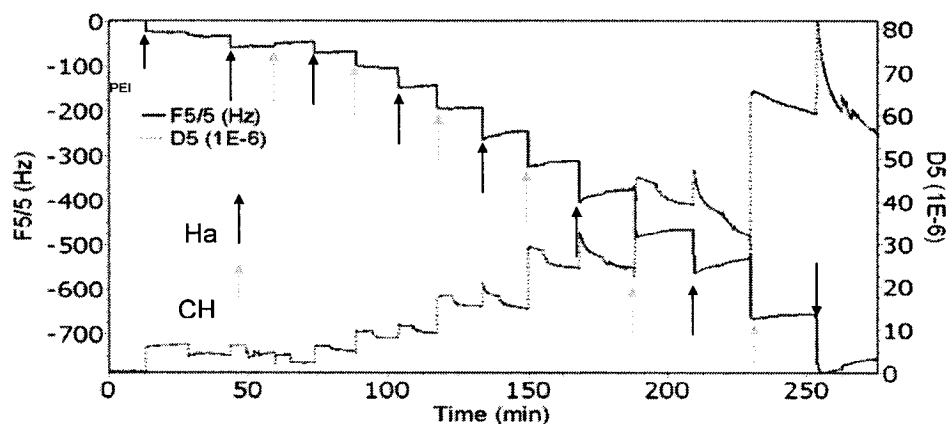


Figure 9.2.2. QCM frequency shift ($\Delta f/v$) during the buildup of the CH/HA multilayer

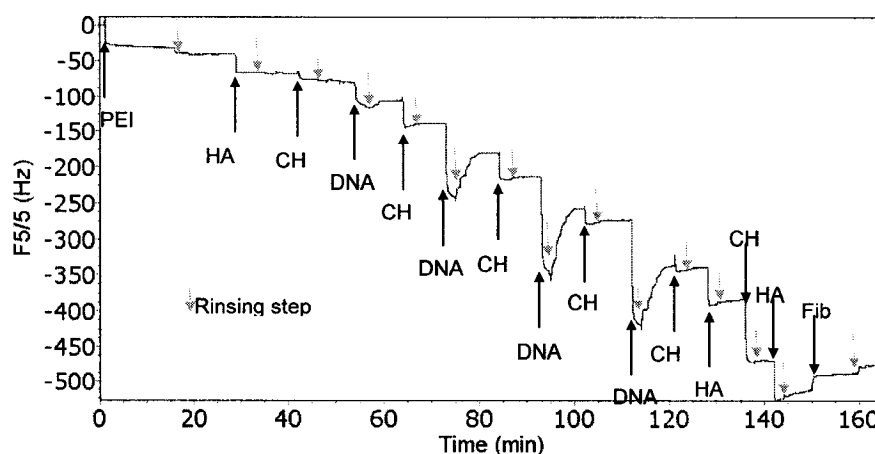


Figure 9.2.3. QCM frequency shift ($\Delta f/v$) during the buildup of the DNA-containing multilayer. The multilayer deposition was initiated with a PEI/HA/CH assembly followed by DNA/CH bilayers as indicated. The completed self-assembly was exposed to a fibrinogen solution (Fib).

Next, the L-b-L assembly of chitosan with DNA was investigated. The multilayer buildup was initiated by a PEI/HA/CH sequence followed by the sequential adsorption of DNA and CH (Fig. 9.2.3). The injection of the DNA solution into the QCM cell resulted in an important shift in the frequency, hence confirming DNA adsorption onto the chitosan layer. Some desorption was observed during the rinsing step. The assembly process did occur on the QCM crystal but an apparent reduction in the adsorbed mass increase during the chitosan adsorption step as the multilayer growth was observed. This may be related to DNA desorption during the adsorption step of chitosan rather than to a decrease in the amount of chitosan absorbed since the charge inversion did occur as shown by the important adsorption of a HA onto the 5th chitosan layer. To optimize the haemocompatibility of the multilayer, the last two bilayers consisted of chitosan and hyaluronan.

The resistance to fouling by blood proteins was then investigated by injecting in the QCM cell a fibrinogen solution. Fibrinogen adsorption on the multilayer would result in a decrease into the frequency. On the contrary, a modest increase of the frequency was observed, as shown in Figure 9.2.3. The latter may indicate a slight desorption of self-assembled polymers poorly incorporated into the multilayer.

Haemocompatibility in a dynamic in vitro assay.

The haemocompatibility of the multilayer-coated arteries have been characterized in a dynamic in vitro model simulating *in vivo* conditions. The nanocoating was deposited *in situ* onto damaged artery using a perfusion chamber exposing a small surface area to the flowing fluids. Once the self-assembly completed, platelet rich plasma prepared from 5 healthy donors was allowed to perfuse the perfusion chamber. Figure 9.2.4 shows the amount of adhered platelets after 30 min perfusion on damaged artery used as control

and damaged artery protected by a (CH/HA)₅ nanocoating. The nanocoating significantly prevented platelet adhesion (70% reduction in mean platelet adhesion, $p=0.01$ by paired student-t-test).

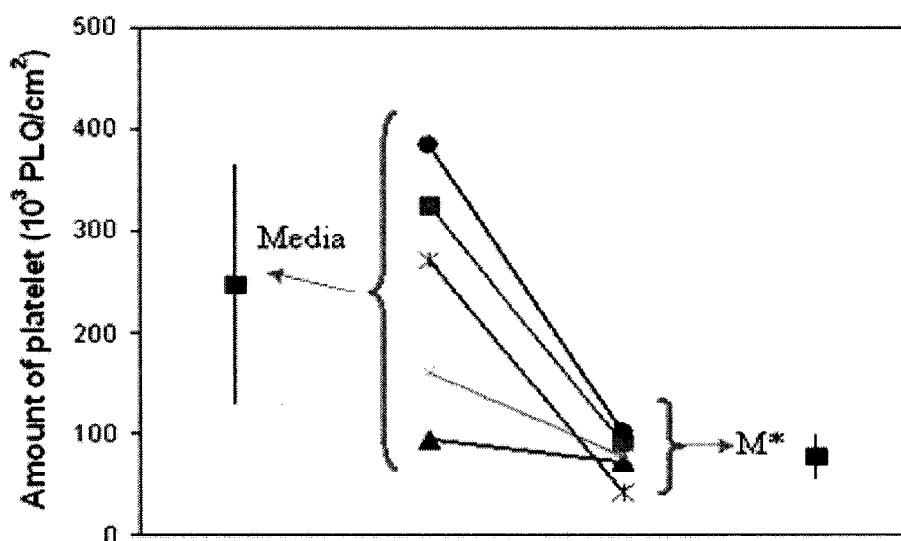


Figure 9.2.4. Platelet adhesion after 30 min perfusion in vitro on damaged arteries (Media), and (CH/HA)₅ coated damaged arteries (M*). Mean \pm SDV are presented ($p=0.001$ by paired Student-t-test)

9.2.4. Conclusion

Gene transfer to the vascular wall appears a promising therapy to treat disorders of the vasculature. Self-assembly of biocompatible polysaccharide containing DNA was investigated in this work as a means to efficiently target DNA to the vascular wall. The self-assemblies were shown to be stable in physiological conditions and the assembly process is rapid enough to be clinically relevant. In addition, the multilayer may protect

damaged blood vessels from blood coagulation, since it inhibits the adsorption of blood proteins, such as fibrinogen. Plasmid DNA was easily incorporated into the CH/HA multilayer. Importantly, the L-b-L technique allows an excellent control of the amount of genetic material loaded into the multilayer, directly related to the number of DNA layer. The therapeutic efficiency of this gene transfer procedure remains however to be determined. The latter will be addressed in future work.

ACKNOWLEDGEMENTS

This research is funded by NSERC of Canada. The authors wish to thank J.F. Théoret and N. Jacobs from the Montreal Heart Institute.

9.2.4. REFERENCES

- 1 Decher, G. *Science* **1997**, 277, 1232.
- 2 Pei, R.; Cui, X.; Yang, X.; Wang, E. *Biomacromolecules* **2001**, 2(2), 463.
- 3 Chluba, J.; Voegel, J. C.; Decher, G.; Erbacher, P.; Schaaf, P.; Ogier, J. *Biomacromolecules* **2001**, 2(3), 800.
- 4 Vazquez, E.; Dewitt, D. M.; Hammond, P. T.; Lynn, D. M. *J. Am. Chem. Soc.* **2002**, 124(47), 13992.
- 5 Taniyama, Y.; Tachibana, K.; Hiraoka, K.; Namba, T.; Yamasaki, K.; Hashiya, N.; Aoki, M.; Ogihara, T.; Yasufumi, K.; Morishita, R. *Circulation* **2002**, 105(10), 1233.
- 6 Thierry, B.; Winnik, F. M.; Merhi, Y.; Tabrizian, M. Submitted .

- 7 Ehsan, A.; Mann, M. J.; Dell'Acqua, G.; Tamura, K.; Braun-Dullaeus, R.; Dzau, V. J. *Circulation* **2002**, *105*(14), 1686.
- 8 Simons, M.; Bonow, R. O.; Chronos, N. A.; Cohen, D. J.; Giordano, F. J.; Hammond, H. K.; Laham, R. J.; Li, W.; Pike, M.; Sellke, F. W.; Stegmann, T. J.; Udelson, J. E.; Rosengart, T. K. *Circulation* **2000**, *102*(11), E73-86.
- 9 Tio, R. A.; Isner, J. M.; Walsh, K. *Semin Interv Cardiol* **1998**, *3*(3-4), 205.
- 10 J. M. *Hosp Pract (Off Ed)* **1999**, *34*(6), 69-74, 76, 79.
- 11 Hook, F.; Kasemo, B.; Nylander, T.; Fant, C.; Sott, K.; Elwing, H. *Anal Chem* **2001**, *73*(24), 5796.

10. CONCLUSIONS AND FUTURE DEVELOPMENTS

This thesis proposes original approaches toward the development of more efficient revascularization procedures. These experimental approaches have been investigated and described in six manuscripts published, to be published, submitted or to be submitted for publication in peer-reviewed scientific journals. They have been the object of eleven presentations in international meetings in the fields of biomaterials and chemistry. A book chapter and a review authored by the candidate are presented in this thesis as an introduction to the experimental work.

10.1. SUMMARY OF RESEARCH

Part I. The work described in the first part of this thesis investigated the development of hybrid coatings of endovascular stents. The first two strategies involved the surface modification of metallic devices by plasma polymerization, followed by covalent immobilization of hyaluronan conjugated or able to be conjugated with a bioactive component (peptides/proteins or radionuclides). The immobilization processes have been extensively investigated and optimized. The method used for the immobilization of hyaluronan is based on a two-step plasma polymerization process that increases the efficiency of the grafted biomolecules¹. This process has been developed at CISRO molecular Science (Australia) by Prof. H.J. Griesser and coworkers for surface modification of polymeric materials.

The conjugation of the biocompatibility of hyaluronan, a component of the extracellular matrix, with the bioactivity of adhesive peptides or growth factors, is expected to create surfaces which mimic biological ones. 3-D hyaluronan scaffolds coupled with RGD peptides have been previously shown to be good candidates as biomimetic scaffolds². The hyaluronan-immobilized metallic surface has shown reduced fouling by platelets. The hyaluronan layer was able to be coupled with avidin used here as a model protein. Such biomimetic surfaces could reduce activation of the blood components and enhance endothelialization of the devices, two features highly beneficial in the setting of stent implantation. This work described in manuscript 2 fulfils the objective 1.a of this thesis.

The clinical experience with radioactive stents has been gained only with P-32 stents³ and further experiments are required to define the clinical potential of these radioactive devices in endovascular procedures. The radioactive stent created through the immobilization of a hyaluronan-DTPA conjugate presents original features that could renew the interest in the field of vascular brachytherapy. First, it allows a wide range of radionuclides to be investigated on the same surface. Radionuclides were homogeneously distributed on the surface and only a low amount of radioactive materials was released in physiological conditions. In addition, while other studies have investigated the use of chelating agent immobilized on the surface of stents to create radioactive devices⁴, the hyaluronan layer onto which the chelating agents were conjugated had excellent biological properties. As a result, the modified surface has shown reduced fouling by blood components, at least by fibrinogen. The description of this work, presented in manuscript 3, fulfils the objective 1.b of this thesis.

The last section of Part I described the development of a bioactive coating based on the Layer-by-Layer self-assembly of polysaccharide multilayers. These polysaccharide-based multilayers have been built up onto metallic devices or onto damaged blood vessels as described later in Part III of this thesis. Despite its tremendous potential, the Layer-by-Layer technique has not been widely investigated up to date in the biomedical

field. Our work aimed at exploiting the versatility and reproducibility of the technique to self-assemble polysaccharide multilayers onto endovascular stents. The self-assembly of hyaluronan with chitosan, two weak polyelectrolytes with interesting biological properties, have been shown for the first time in this thesis. The objective was threefold: (1) improve the haemocompatibility of the device; (2) benefit from the biological activity of HA and CH, especially their wound healing properties (HA and CH) and anti-inflammatory properties (HA) and (3) incorporate a bioactive molecule within the coating. The experimental work described in the manuscript 4 has shown that the CH/HA self-assembly fulfill these objectives. The use of sodium nitroprusside as antiproliferative components need however to be questioned considering the ability of small molecules to rapidly diffuse out of the multilayers. The incorporation of genetic materials into the CH/HA multilayer, which has been shown in the manuscript 7, could be a more promising strategy to inhibit restenosis.

Part II. Chitosan has been used to engineer a biodegradable membrane-covered device for endovascular procedures. The mechanical properties of the membrane have been optimized through blending with a high molecular weight PEG. As a result, the membrane-covered devices have been shown *in vitro* to be able to follow the deformation of the supporting metallic stent during its deployment. In addition, this membrane-covered device was able to sustain physiologic pressure and showed very small water permeability. Haemocompatibility assays have revealed that the thrombogenicity of the membrane could be modulated by surface complexation with heparin. Chitosan has also been widely investigated in the biomedical field for its drug delivery ability⁵. Nitric oxide donors, L-Arginine and sodium nitroprusside, have been used to demonstrate the capability of the membrane to act as a reservoir for therapeutic molecules. A dose respondent inhibition of platelet adhesion for a SNP loaded membrane was observed (see patent in appendix). The chitosan-based membrane-covered device could be found useful in endovascular applications such as aneurysm closure or treatment of vein graft disease as well as for the treatment of various obstructive diseases such as obstructive malignant tumors (e.g. esophageal, biliary, bowel). In view of its potential clinical applications, the biodegradable membrane

covered-stent has been patented (patent enclosed in appendix). The manuscript included in this thesis fulfils the objectives 2.a, 2.b, and 2.c of this work.

Part III. In an attempt to address the limitation of current angioplasty procedures, self-assembled multilayers have been investigated to protect damaged arteries and to control the healing processes by efficiently delivering therapeutic biomolecules to the vascular wall. These nanometric coatings have been deposited onto blood vessels by the Layer-by-Layer technique. The chitosan and hyaluronan self-assembled multilayers have been demonstrated to drastically reduce the thrombogenicity of angioplasty-damaged arteries. In addition, the self-assembled nanocoating has been shown to be stable in physiological conditions and it has been shown to diffuse within the vascular wall. This work has been published in the *Journal of the American Chemical Society*. This manuscript fulfils the objective 3.a and 3.b of this thesis.

The potential of these self-assembled nanocoatings appears very interesting in the setting of disease of the vasculature. First, the protection of the damaged vascular wall from blood components such as platelets and leukocytes is expected to cut early on some of the major pathways leading to restenosis. Second, both hyaluronan and chitosan have very interesting biological properties such as wound healing and anti-inflammatory properties that could enhance the healing of the blood vessel. Finally, the nanocoating could be used to efficiently deliver to the vascular wall drugs or genetic materials. Drug delivery to the vasculature is limited by the poor efficiency of the procedures, most of the drugs being washed by the blood flow. In addition, the lack of solubility of hydrophobic drug prevents exposure of the vessel wall to appropriate amount of drug in these procedures. The Layer-by-Layer technique has been investigated for its ability to incorporate macromolecules within highly controlled nanostructures. To fulfill the objective 3c of this thesis, the possibility to incorporate biomacromolecules such as DNA within the chitosan/hyaluronan multilayers has been demonstrated using calf Thymus DNA. On going experiments will determine the

clinical potential of the self-assembled nanocoating in the treatment of the diseases of the vasculature.

10.2. SUGGESTIONS FOR FUTURE RESEARCH

Most of the works described in this thesis are completed studies that propose new devices or strategies to be used in endovascular procedures. The manuscripts provide the proof-of-principle for these strategies but other studies could be suggested to optimize or further develop this work, especially in view of their clinical relevance. The proposed strategies will be discussed in the next sections from this aspect.

Manuscript 2 demonstrates that biomimetic surfaces could be prepared by the immobilization of hyaluronan and further grafting of bioactive components. Different bioactive surfaces could be used to this extent, such as adhesive peptides (e.g. RGD peptides or adhesive peptides specific to endothelial cells) or growth factors (e.g. VEGF). The method used to immobilize the protein used as a model (avidin) could be readily used to graft such bioactive components on the hyaluronan surface. While previous work has shown that such molecules could retain their activity when immobilized on surface⁶⁻⁹, further assays are required to demonstrate the ability of this strategy to create truly biomimetic surfaces. In the setting of endovascular devices, these surfaces aim at enhancing the endothelialization of the metallic substrate while preventing fouling by blood components.

The plasma polymerized layer should also be investigated for its ability to improve the corrosion properties of metallic implants. Plasma coatings have been indeed previously used to modulate the corrosion behavior of metallic substrates¹⁰. As defined in the introduction of this thesis, the biostability of metallic implants remains a key-factor in

the fate of the implantation and any improvement would be beneficial for their long term biocompatibility.

Manuscript 3 reports that HA-DTPA macromolecules immobilized onto the plasma functionalized surface have been able to chelate various radionuclides. The stability of the surface-complexed radionuclides was good, but better results could be achieved using other chelating agents such as the macrocyclic ligand 1,4,7,10-tetraazacyclododecane tetra-acetic acid (DOTA), with affinities towards radionuclides such as indium or yttrium higher than DTPA¹¹. This could help to prevent adventitious leakage of radioactive elements from the device. The haemocompatibility of the coating should also be characterized in more detail to definitively assess its thromboresistant nature. While it has been shown to reduce fibrinogen adsorption, its ability to resist fouling by platelets or other blood components remains to be demonstrated.

The HA-DTPA radionuclide coating could readily be used to investigate the ability of various radionuclides to prevent restenosis. The major advantage of this coating is that it allows various radionuclides with very different physical properties to be loaded easily on the surface of the stents while improving the overall biocompatibility of the device. This is in contrast with previously used radioactive devices such as P-32 implanted stents used in the clinical trials. While the clinical use of radioactive stents has been hampered by the high rate of restenosis at the edge of the device, the investigation of other radionuclides could prevent this adverse effect. The use of radionuclides with shorter half-life could allow reendothelialization of the vessel. Extension of the irradiated areas by the use of more energetic radionuclides could reduce the “edge-effect”. The versatility of the coating could also be used to load a high dose of radionuclides at the stent’s edges, which has been defined as the “hot-end” approach.

The membrane-covered stent described in manuscript 5 has been shown *in vitro* to fulfill the requirement for such endovascular devices. Optimization of the manufacturing process should be done to reduce the risk of mechanical failure of the

membrane. In general, more extensive mechanical testing should be conducted to assess the mechanical stability of the biodegradable membrane on the metallic scaffold. The feasibility of endovascular delivery should be confirmed by appropriate *in vivo* assays, designed to investigate the safe deployment of the device in the vascular wall. Also, the relation between the mechanical properties of the membrane and its biodegradation, expected to occur within months following implantation should be studied. The biodegradation of the membrane could be modulated by its cross-linking with appropriate agents such as glyoxal or glutaraldehyde but preliminary assays have shown that cross-linking highly reduce the ability of the membrane to sustain deformation during deployment of the device.

The biological activity of the membrane could be modulated either by incorporation of a drug or by complexation with bioactive macromolecules. Chitosan have been widely investigated for its drug delivery ability and numerous drugs, e.g. anti-proliferative or anti-inflammatory, could be loaded in the membrane. Depending on the application, one could modify the membrane to inhibit cellular ingrowths or on the contrary to stimulate it. Modification of the luminal surface with adhesive molecules such as RGD peptide or growth factors could be assessed to enhance the endothelialization of the membrane. This could be especially interesting in the setting of aneurysm closure where the membrane would initially act as a physical barrier preventing blood leaking in the aneurysm while allowing growth of a new neointima on the membrane luminal surface. This strategy could improve the long term success rate of the endovascular closure of aneurysm.

Finally, the addition of a porous outer membrane has been shown to be possible. The membrane-covered devices could thus be readily amenable to tissue engineering strategies. The chitosan scaffold could be seeded with cells prior to implantation in appropriate bioreactors. The advantage of this hybrid device over an entirely biodegradable scaffold is that the mechanical strength of the metallic stent supporting the membrane could reduce the need for extensive *in vitro* culture and increase the success rate of the grafting procedure.

The Layer-by-Layer technique has been used to self-assemble multilayers of chitosan and hyaluronan onto metallic stents and arteries. Most reported work on the Layer-by-Layer technique has been performed with polyelectrolytes such as polystyrenesulfonate (PSS), polyethyleneimine (PEI), and polyallylamine hydrochloride (PAH). Systems with weak polyelectrolytes have not been fully characterized. While much work has been dedicated as described in this thesis to characterize the self-assembly of these two biopolymers, more fundamental studies should be conducted to further investigate the effect of the concentration, pH, molecular weight, etc. These polymers have been chosen due to their biological activities, but other biopolymers of interest could be used such as heparin or DNA.

The capability of these self-assembled multilayers to be used efficiently for drug delivery remains to be demonstrated. This thesis described the use of two small molecules, sodium nitroprusside and L-Arginine as well as a plasmid DNA. Small molecules can diffuse rapidly out of the multilayer and the possibility to control the release kinetics is limited for these compounds. One strategy to be investigated as an on-going work of this project will be to bind the macromolecules to the polyelectrolytes. Depending on the therapeutic activity of the molecules, hydrolysable chemical bonding could be introduced to control the release of the drug upon contact with physiological fluid. This could provide a controllable release kinetic. Combined with the very good reproducibility of the Layer-by-Layer self-assembled multilayers, this would allow the design of very effective drug releasing devices. Other approaches of interest would be to use macromolecules that do not need to be internalized by the cells and can thus exert their activity by membrane-mediated receptors. In the setting of the disease of the vasculature, estradiol could be for instance very efficient to inhibit smooth muscle cells proliferation while enhancing endothelialization of the vessel. As shown in manuscript 6, DNA could be incorporated within the multilayer, which may offer a very promising way to transfect *in vivo* the vascular wall. On going animal studies will investigate the efficiency of the vascular transfection by the nanocoatings.

The multilayers deposited onto metallic devices such as stents should be investigated *in vivo* to determine their clinical potential. The approach mentioned above could be used to optimize the incorporation of the biologically active component. Anti-proliferative

drug such as paclitaxel could be grafted onto hyaluronan, thus allowing a good control of the amount of drug loaded on the stent and of the kinetics of release. The experiment should focus on the synergic effect of the bioactive polymers HA and CH with the anti-proliferative properties of these drugs. Another issue would be to investigate the deposition of thick multilayers. Growth has been limited to 22 layers, and while in theory it is possible to add an infinite number of layers, this remains to be demonstrated with these two biopolymers.

The self-assembled nanocoatings have been successfully deposited *in vitro* and *ex vivo* onto blood vessels. The technical feasibility, i.e. with commercially available drug delivery catheters, of the *in situ* deposition remain to be explored. On going *in vivo* assays will assess this point. The major drawback of the *in situ* deposition is the need for prolonged ischemia of the vessel during the build up of the layers. Clinical application would benefit from the development of a delivery catheter allowing perfusion during the procedures. The development of this type of catheter could be based on existing ones such as the Dispatch catheter. These nanocoatings bare exciting promises but the clinical potential remains to be demonstrated. The first objective was to reduce restenosis after angioplasty by (1) reducing activation of the blood components on the damaged vascular wall, (2) exploiting the biological properties of hyaluronan and chitosan, namely their wound healing (CH and HA) and anti-inflammatory (HA) properties, (3) releasing biologically active molecules into the vascular wall. Experiments should be conducted to assess (1) the effect of the nanocoating itself (points 1 and 2) and (2) the effect of the bioactive component to be release in the vascular wall. Assuming the possibility to efficiently build up the nanocoating *in situ* in a clinical application, several strategies could be investigated such as the delivery of anti-proliferative drugs and delivery of genetic materials to transfect the vascular wall (plasmid or ODN). Many diseases of the vasculature could benefit from this strategy. As an alternative strategy to brachytherapy, delivery of agents such as DTPA-Gd for neutron-activation therapy to inhibit smooth muscle cell proliferation could be investigated. The nanocoating could also be used more generally to deliver molecules to non-angioplasted arteries or to vein grafts prior to or after bypass surgery. Delivery of angiogenic molecules such as vascular endothelial growth

factors could for example be done efficiently using the self-assembled nanocoating. This would offer a promising way to alleviate various diseases of the cardiovascular system. The great potential of these self-assembled nanocoatings has been highlighted in comments which appeared in "Nature – materials update" (see appendix) and "The New Scientist" (21 June 03).

10.2.1. Reference

1. McLean KM, Johnson G, Chatelier RC, Beumer GJ, Steele JG, Griesser HJ: Method of immobilization of carboxymethyl-dextran affects resistance to tissue and cell colonization. *Colloids Surf B Biointerfaces* 2000;18:221-234
2. Glass JR, Dickerson KT, Stecker K, Polarek JW: Characterization of a hyaluronic acid-Arg-Gly-Asp peptide cell attachment matrix. *Biomaterials* 1996;17:1101-8
3. Albiero R, Colombo A: European high-activity (32)P radioactive stent experience. *J Invasive Cardiol* 2000;12:416-21
4. Zamora PO, Osaki S, Som P, Ferretti JA, Choi JS, Hu C, Tsang R, Kuan HM, Singletary S, Stern RA, Oster ZH: Radiolabeling brachytherapy sources with Re-188 through chelating microfilms: stents. *J Biomed Mater Res* 2000;53:244-51
5. Singla AK, Chawla M: Chitosan: some pharmaceutical and biological aspects--an update. *J Pharm Pharmacol* 2001;53:1047-67
6. Tiwari A, Salacinski HJ, Punshon G, Hamilton G, Seifalian AM: Development of a hybrid cardiovascular graft using a tissue engineering approach. *FASEB J* 2002;16:791-6
7. Shakesheff K, Cannizzaro S, Langer R: Creating biomimetic micro-environments with synthetic polymer-peptide hybrid molecules. *J Biomater Sci Polym Ed* 1998;9:507-18

8. Puleo DA, Kissling RA, Sheu MS: A technique to immobilize bioactive proteins, including bone morphogenetic protein-4 (BMP-4), on titanium alloy. *Biomaterials* 2002;23:2079-87
9. Kuhl PR, Griffith-Cima LG: Tethered epidermal growth factor as a paradigm for growth factor- induced stimulation from the solid phase. *Nat Med* 1996;2:1022-7
10. Villiermaux F, Tabrizian M, Yahia L, Czeremuszkin G, Piron DL: Corrosion resistance improvement of NiTi osteosynthesis staples by plasma polymerized tetrafluoroethylene coating. *Biomed Mater Eng* 1996;6:241-54
11. Cremonesi M, Ferrari M, Chinol M, Bartolomei M, Stabin MG, Sacco E, Fiorenza M, Tosi G, Paganelli G: Dosimetry in radionuclide therapies with ⁹⁰Y-conjugates: the IEO experience. *Q J Nucl Med* 2000;44:325-32

11. BIBLIOGRAPHY

ASTM F746, Standard test method for pitting or crevice corrosion of metallic surgical implant materials, in *Annual Book of ASTM standards: Medical devices and services*. Am Soc Test Mater, pp 192-7

ASTM F86, Standard Practice for Surface Preparation and Marking of Metallic Surgical Implants , in *Annual Book of ASTM standards: Medical Devices and Services*. American Society for Testing and Materials, 1995, pp 6-8

ASTM G 5, Standard reference test method for making potentiostatic and potentiodynamic anodic polarization measurements , in *Annual Book of ASTM standards: Metals, test methods and analytical procedures*. Am Soc Test Mater, 1995, pp 48-58

ASTM G102, Standard practice for calculation of corrosion rates and related information from electrochemical measurements, in *Annual Book of ASTM standards: Metals, test methods and analytical procedures*. Am Soc Test Mater, pp 401-407

Anonymous In this work, "layer" refers to the increment in thickness after exposure to one of the polyelectrolyte solutions.

Abatangelo, G. and Weigel, P. H. Redefining Hyaluronan. 2000. Amsterdam, Elsevier.

Albiero R, Adamian M, Kobayashi N, Amato A, Vaghetti M, Di Mario C, Colombo A: Short- and intermediate-term results of (32)P radioactive beta-emitting stent implantation in patients with coronary artery disease: The Milan Dose-Response Study. *Circulation* 2000;101:18-26

Albiero R, Colombo A: European high-activity (32)P radioactive stent experience. *J Invasive Cardiol* 2000;12:416-21

- Amiji MM: Surface modification of chitosan membranes by complexation-interpenetration of anionic polysaccharides for improved blood compatibility in hemodialysis. *J Biomater Sci Polym Ed* 1996;8:281-98
- Ariga K, Onda M, Lvov Y, Kunitake T: Alternate Layer-by-Layer Assembly of Organic Dyes and Proteins is Facilitated by Pre-mixing with Linear Polyions. *Chemistry Letters* 1997;25-26
- Babapulle MN, Eisenberg MJ: Coated stents for the prevention of restenosis: Part I. *Circulation* 2002;106:2734-40
- Babapulle MN, Eisenberg MJ: Coated stents for the prevention of restenosis: Part II. *Circulation* 2002;106:2859-66
- Baldus S, Koster R, Reimers J, Kahler J, Meinertz T, Hamm CW: Membrane-covered stents: a new treatment strategy for saphenous vein graft lesions. *Catheter Cardiovasc Interv* 2001;53:1-4
- Bananinchi PO: Complex permittivity. *Bioengi* In press;
- Barbucci R, Magnani A, Rappuoli R, Lamponi S, Consumi M: Immobilisation of sulphated hyaluronan for improved biocompatibility. *J Inorg Biochem* 2000;79:119-25
- Basmadjian D, Sefton MV, Baldwin SA: Coagulation on biomaterials in flowing blood: some theoretical considerations. *Biomaterials* 1997;18:1511-22
- Beena MS, Chandy T, Sharma CP: Heparin immobilized chitosan--poly ethylene glycol interpenetrating network: antithrombogenicity. *Artif Cells Blood Substit Immobil Biotechnol* 1995;23:175-92
- Belu AM, Davies MC, Newton JM, Patel N: TOF-SIMS characterization and imaging of controlled-release drug delivery systems. *Anal Chem* 2000;72:5625-38
- Benesch J, Tengvall P: Blood protein adsorption onto chitosan. *Biomaterials* 2002;23:2561-8

- Berglund JD, Mohseni MM, Nerem RM, Sambanis A: A biological hybrid model for collagen-based tissue engineered vascular constructs. *Biomaterials* 2003;24:1241-54
- Bhargava B, De Scheerder I, Ping QB, Yanming H, Chan R, Soo Kim H, Kollum M, Cottin Y, Leon MB: A novel platinum-iridium, potentially gamma radioactive stent: evaluation in a porcine model. *Catheter Cardiovasc Interv* 2000;51:364-8
- Bhargava B, Tripuraneni P: Role of intracoronary brachytherapy for in-stent restenosis? *Lancet* 2002;359:543-4
- Brash JL: Exploiting the current paradigm of blood-material interactions for the rational design of blood-compatible materials. *J Biomater Sci Polym Ed* 2000;11:1135-46
- Brenda M, Döring R, Schernau U: Investigation of organic coatings and coating defects with the help of time-of-flight-secondary ion mass spectrometry (TOF-SIMS). *Prog. Org. Coatings* 1999;35:183-189
- Brenner DJ, Miller RC: Long-term efficacy of intracoronary irradiation in inhibiting in-stent restenosis. *Circulation* 2001;103:1330-2
- Budinger L, Hertl M: Immunologic mechanisms in hypersensitivity reactions to metal ions: an overview. *Allergy* 2000;55:108-15
- Budtova T, Belnikevich N, Kalyuzhnaya L, Alexeev SB, Vesnebolotskaya S, Zoolshoev Z: Chitosan Modified by Poly(ethylene oxide): Film and Mixture Properties. *J Appl Polym Sci* 2002;84:1114-1122
- Calderon JG, Harsch A, Gross GW, Timmons RB: Stability of plasma-polymerized allylamine films with sterilization by autoclaving. *J Biomed Mater Res* 1998;42:597-603
- Camera L, Kinuya S, Garmestani K, Wu C, Brechbiel MW, Pai LH, McMurry TJ, Gansow OA, Pastan I, Paik CH, et al: Evaluation of the serum stability and in vivo biodistribution of CHX- DTPA and other ligands for yttrium labeling of monoclonal antibodies. *J Nucl Med* 1994;35:882-9

- Campbell PG, Hall JA, Harcombe AA, de Belder MA: The Jomed Covered Stent Graft for coronary artery aneurysms and acute perforation: a successful device which needs careful deployment and may not reduce restenosis. *J Invasive Cardiol* 2000;12:272-6
- Carter AJ, Scott D, Laird JR, Bailey L, Kovach JA, Hoopes TG, Pierce K, Heath K, Hess K, Farb A, Virmani R: Progressive vascular remodeling and reduced neointimal formation after placement of a thermoelastic self-expanding nitinol stent in an experimental model. *Cathet Cardiovasc Diagn* 1998;44:193-201
- Cassinelli C, Morra M, Pavesio A, Renier D: Evaluation of interfacial properties of hyaluronan coated poly(methylmethacrylate) intraocular lenses. *J Biomater Sci Polym Ed* 2000;11:961-77
- Chajara A, Raoudi M, Delpech B, Leroy M, Basuyau JP, Levesque H: Increased hyaluronan and hyaluronidase production and hyaluronan degradation in injured aorta of insulin-resistant rats. *Arterioscler Thromb Vasc Biol* 2000;20:1480-7
- Chandy T, Rao GH: Evaluation of heparin immobilized chitosan-PEG microbeads for charcoal encapsulation and endotoxin removal. *Artif Cells Blood Substit Immobil Biotechnol* 2000;28:65-77
- Cheneau E, Waksman R, Yazdi H, Chan R, Fourdnadjiev J, Berzingi C, Shah V, Ajani AE, Leborgne L, Tio FO: How to fix the edge effect of catheter-based radiation therapy in stented arteries. *Circulation* 2002;106:2271-7
- Chluba J, Voegel JC, Decher G, Erbacher P, Schaaf P, Ogier J: Peptide hormone covalently bound to polyelectrolytes and embedded into multilayer architectures conserving full biological activity. *Biomacromolecules* 2001;2:800-5
- Chorny M, Fishbein I, Golomb G: Drug delivery systems for the treatment of restenosis. *Crit Rev Ther Drug Carrier Syst* 2000;17:249-84
- Chung AJ, Rubner MF: Methods of Loading and Releasing Low Molecular Weight Cationic Molecules in Weak Polyelectrolytes Multilayer Films. *Langmuir* 2002;18:1176-1183

Chupa JM, Foster AM, Sumner SR, Madhally SV, Matthew HW: Vascular cell responses to polysaccharide materials: in vitro and in vivo evaluations. *Biomaterials* 2000;21:2315-22

Chwirut, D. J., Oktay, H. S., and Ryan, T. Nitinol Interventional Cardiology Devices - FDA's Perspective. Pelton, A., Hodgson, D., Russell, S., and Duerig, T. Shape Memory and Superelastic Technologies. March 1997. Santa Clara, SMST.

Clark GC, Williams DF: The effects of proteins on metallic corrosion. *J Biomed Mater Res* 1982;16:125-34

Clerc CO, Jedwab MR, Mayer DW, Thompson PJ, Stinson JS: Assessment of wrought ASTM F1058 cobalt alloy properties for permanent surgical implants. *J Biomed Mater Res* 1997;38:229-34

Cloft HJ, Kallmes DF, Lin HB, Li ST, Marx WF, Hudson SB, Helm GA, Lopes MB, McGraw JK, Dion JE, Jensen ME: Bovine type I collagen as an endovascular stent-graft material: biocompatibility study in rabbits. *Radiology* 2000;214:557-62

Colombo A, Stankovic G, Moses JW: Selection of coronary stents. *J Am Coll Cardiol* 2002;40:1021-33

Cowman MK, Min L, Balazs EA: Tapping mode atomic force microscopy of hyaluronan: extended and intramolecularly interacting chains. *Biophys. J.* 1998;75:2030-2037

Cremonesi M, Ferrari M, Chinol M, Bartolomei M, Stabin MG, Sacco E, Fiorenza M, Tosi G, Paganelli G: Dosimetry in radionuclide therapies with ⁹⁰Y-conjugates: the IEO experience. *Q J Nucl Med* 2000;44:325-32

Das S, Pal AJ: Layer-by-Layer Self-Assembling of a Low Molecular Weight Organic Material by Different Electrostatic Adsorption Processes. *Langmuir* 2002;18:458-461

Das T, Banerjee S, Samuel G, Sarma HD, Ramamoorthy N, Pillai MR: ¹⁸⁸Re-ethylene dicysteine: a novel agent for possible use in endovascular radiation therapy. *Nucl Med Commun* 2000;21:939-45

De Scheerder I, Verbeken E, Van Humbeeck J: Metallic surface modification. *Semin Interv Cardiol* 1998;3:139-44

Decher G: *Science* 1997;277:1232

DeFife KM, Shive MS, Hagen KM, Clapper DL, Anderson JM: Effects of photochemically immobilized polymer coatings on protein adsorption, cell adhesion, and the foreign body reaction to silicone rubber. *J Biomed Mater Res* 1999;44:298-307

Delcorte A, Bertrand P, Arys X, Jonas A, Wischerhoff E, Meyer B, Laschewsky A: ToF-SIMS study of alternate polyelectrolyte thin films: Chemical surface characterization and molecular secondary ions sampling depth. *Surface science* 1996;366:149-165

Deux JF, Meddahi-Pelle A, Le Blanche AF, Feldman LJ, Collic-Jouault S, Bree F, Boudghene F, Michel JB, Letourneur D: Low molecular weight fucoidan prevents neointimal hyperplasia in rabbit iliac artery in-stent restenosis model. *Arterioscler Thromb Vasc Biol* 2002;22:1604-9

Deux JF, Prigent-Richard S, d'Angelo G, Feldman LJ, Puvion E, Logeart-Avramoglou D, Pelle A, Boudghene FP, Michel JB, Letourneur D: A chemically modified dextran inhibits smooth muscle cell growth in vitro and intimal in stent hyperplasia in vivo. *J Vasc Surg* 2002;35:973-81

Disegi, J. and Zardiackas, L. Retrieval Analysis of Stainless Steel Plate/Screws Implanted for 55 Years. The Proceeding of the 27th Meeting of the Society For Biomaterials. Minneapolis, USA , Society For Biomaterials.

Dolmatch BL, Dong YH, Trerotola SO, Hunter DW, Brennecke LH, LaBounty R: Tissue response to covered Wallstents. *J Vasc Interv Radiol* 1998;9:471-8

Drachman DE, Simon DI: Restenosis: Intracoronary Brachytherapy. *Curr Treat Options Cardiovasc Med.* 2002;4:109-118

Dyet JF, Watts WG, Ettles DF, Nicholson AA: Mechanical properties of metallic stents: how do these properties influence the choice of stent for specific lesions? *Cardiovasc Intervent Radiol* 2000;23:47-54

Edelman ER, Seifert P, Groothuis A, Morss A, Bornstein D, Rogers C: Gold-coated NIR stents in porcine coronary arteries. *Circulation* 2001;103:429-34

Elbert DL, Herbert CB, Hubbell JA: Thin Polymer Layers Formed by Polyelectrolyte Multilayer Techniques on Biological Surfaces. *Langmuir* 1999;15:5355-5362

Emanuelli G, Gatti AM, Cigada A, Brunella MF: Physico-chemical observations on a failed Greenfield vena cava filter. *J Cardiovasc Surg (Torino)* 1995;36:121-5

Eroglu M, Irmak S, Acar A, Denkbaz EB: Design and evaluation of a mucoadhesive therapeutic agent delivery system for postoperative chemotherapy in superficial bladder cancer. *Int J Pharm* 2002;235:51-9

Eto K, Goto S, Shimazaki T, Sakakibara M, Yoshida M, Isshiki T, Handa S: Two distinct mechanisms are involved in stent thrombosis under flow conditions. *Platelets* 2001;12:228-35

Fally, F., Doneux, C., Riga, J., and Verbist, J. J. Quantification of the functional groups present at the surface of plasma polymers deposited from propylamine, allylamine, and propargylamine. *J Appl Polym Sci* v56(n5), p 597. 95.

Fattori R, Piva T: Drug-eluting stents in vascular intervention. *Lancet* 2003;361:247-9

Fili P, Lausmaa J, Musialek J, Mazanec K: Structure and surface of TiNi human implants. *Biomaterials* 2001;22:2131-8

Finn AV, Gold HK, Tang A, Weber DK, Wight TN, Clermont A, Virmani R, Kolodgie FD: A novel rat model of carotid artery stenting for the understanding of restenosis in metabolic diseases. *J Vasc Res* 2002;39:414-25

Fischman DL, Leon MB, Baim DS, Schatz RA, Savage MP, Penn I, Detre K, Veltri L, Ricci D, Nobuyoshi M: A randomized comparison of coronary-stent placement and balloon angioplasty in the treatment of coronary artery disease. Stent Restenosis Study Investigators. *N Engl J Med* 1994;331:496-501

Formichi M, Marois Y, Roby P, Marinov G, Stroman P, King MW, Douville Y, Guidoin R: Endovascular repair of thoracic aortic aneurysm in dogs: evaluation of a nitinol-polyester self-expanding stent-graft. *J Endovasc Ther* 2000;7:47-67

Fox R: American Heart Association 2001 scientific sessions: late-breaking science-drug-eluting stents. *Circulation* 2001;104:E9052

Fox RA, Henson PW: The dosimetry for a coronary artery stent coated with radioactive ¹⁸⁸Re and ³²P. *Phys Med Biol* 2000;45:3643-55

Garasic JM, Edelman ER, Squire JC, Seifert P, Williams MS, Rogers C: Stent and artery geometry determine intimal thickening independent of arterial injury. *Circulation* 2000;101:812-8

Gaspar J, Vonderwalde C, Hong MK, Eid-Lidt G, Almagor Y, Leon MB: [Stent coated with bovine pericardium: in vitro evaluation, in animals, and initial results in humans]. *Arch Cardiol Mex* 2001;71:286-94

Geary RL, Nikkari ST, Wagner WD, Williams JK, Adams MR, Dean RH: Wound healing: a paradigm for lumen narrowing after arterial reconstruction. *J Vasc Surg* 1998;27:96-106; discussion 106-8

Gengenbach, T. R., Vasic, Z. R., Li, S., Chatelier, R. L., and Griesser, H. J. Contributions of restructuring and oxidation to the aging of the surface of plasma polymers containing heteroatoms. *Plasmas Polym v 2*(n 2), p 91-114. 97.

Gershlick AH: Role of stenting in coronary revascularisation. *Heart* 2001;86:104-12

Gimenez-Arnau A, Riambau V, Serra-Baldrich E, Camarasa JG: Metal-induced generalized pruriginous dermatitis and endovascular surgery. *Contact Dermatitis* 2000;43:35-40

Glass JR, Dickerson KT, Stecker K, Polarek JW: Characterization of a hyaluronic acid-Arg-Gly-Asp peptide cell attachment matrix. *Biomaterials* 1996;17:1101-8

Goodwin SC, Yoon HC, Wong GC, Bonilla SM, Vedantham S, Arora LC: Percutaneous delivery of a heparin-impregnated collagen stent-graft in a porcine model of atherosclerotic disease. *Invest Radiol* 2000;35:420-5

Gotman I: Characteristics of metals used in implants. *J Endourol* 1997;11:383-9

Gouin S, Valencia Grayeb MV, Winnik FM: Gadolinium Diethylenetriamine Pentaacetic Acid/Hyaluronan Conjugates: Preparation, Properties and Applications , in Guiseppi-Elie A, Levon K (eds): *Macromolecule-Metal Complexes, Macromolecular Symposia 186*. Weinheim, Germany, 2002, pp 105-110

Gouin S, Winnik FM: Quantitative assays of the amount of diethylenetriaminepentaacetic acid conjugated to water-soluble polymers using isothermal titration calorimetry and colorimetry. *Bioconjug Chem* 2001;12:372-7

Grenadier E, Roguin A, Hertz I, Peled B, Boulos M, Nikolsky E, Amikam S, Kerner A, Cohen S, Beyar R: Stenting very small coronary narrowings (< 2 mm) using the biocompatible phosphorylcholine-coated coronary stent. *Catheter Cardiovasc Interv* 2002;55:303-8

Grewe PH, Deneke T, Machraoui A, Barmeyer J, Muller KM: Acute and chronic tissue response to coronary stent implantation: pathologic findings in human specimen. *J Am Coll Cardiol* 2000;35:157-63

Guidoin R, Marois Y, Douville Y, King MW, Castonguay M, Traore A, Formichi M, Staxrud LE, Norgren L, Bergeron P, Becquemin JP, Egana JM, Harris PL: First-generation aortic endografts: analysis of explanted Stentor devices from the EUROSTAR Registry. *J Endovasc Ther* 2000;7:105-22

Guidoin R, Marois Y, Douville Y, King MW, Castonguay M, Traore A, Formichi M, Staxrud LE, Norgren L, Bergeron P, Becquemin JP, Egana JM, Harris PL: First-

generation aortic endografts: analysis of explanted Stentor devices from the EUROSTAR Registry. *J Endovasc Ther* 2000;7:105-22

Gunn J, Cumberland D: Does stent design influence restenosis? *Eur Heart J* 1999;20:1009-13

Gutensohn K, Beythien C, Bau J, Fenner T, Grewe P, Koester R, Padmanaban K, Kuehnl P: In vitro analyses of diamond-like carbon coated stents. Reduction Of metal ion release, platelet activation, and thrombogenicity. *Thromb Res* 2000;99:577-85

Hallab N, Merritt K, Jacobs JJ: Metal sensitivity in patients with orthopaedic implants. *J Bone Joint Surg Am* 2001;83-A:428-36

Harnek J, Zoucas E, Carlemalm E, Cwikiel W: Differences in endothelial injury after balloon angioplasty, insertion of balloon-expanded stents or release of self-expanding stents: An electron microscopic experimental study. *Cardiovasc Intervent Radiol* 1999;22:56-61

Hartley PG, McArthur SL, McLean KM, Griesser HJ: Physicochemical Properties of Polysaccharide Coatings Based on Grafted Multilayer Assemblies. *Langmuir* 2002;18:2483-2494

Heintz C, Riepe G, Birken L, Kaiser E, Chakfe N, Morlock M, Delling G, Imig H: Corroded nitinol wires in explanted aortic endografts: an important mechanism of failure? *J Endovasc Ther* 2001;8:248-53

Heldman AW, Cheng L, Jenkins GM, Heller PF, Kim DW, Ware M Jr, Nater C, Hruban RH, Rezai B, Abella BS, Bunge KE, Kinsella JL, Sollott SJ, Lakatta EG, Brinker JA, Hunter WL, Froehlich JP: Paclitaxel stent coating inhibits neointimal hyperplasia at 4 weeks in a porcine model of coronary restenosis. *Circulation* 2001;103:2289-95

Heublein B, Evagorou EG, Rohde R, Ohse S, Meliss RR, Barlach S, Haverich A: Polymerized degradable hyaluronan--a platform for stent coating with inherent inhibitory effects on neointimal formation in a porcine coronary model. *Int J Artif Organs* 2002;25:1166-73

- Heublein B, Ozbek C, Pethig K: Silicon carbide-coated stents: clinical experience in coronary lesions with increased thrombotic risk. *J Endovasc Surg* 1998;5:32-6
- Heublein B, Rhode R, Huasdorf G, Hartung W, Haverich R: Biocorrosion, a new principle for temporary cardiovascular implants ? *Eur. Heart J.* 2000;21:286
- Hill-West JL, Chowdhury SM, Slepian MJ, Hubbell JA: Inhibition of thrombosis and intimal thickening by in situ photopolymerization of thin hydrogel barriers. *Proc Natl Acad Sci U S A* 1994;91:5967-71
- Hoffmann R, Jansen C, Konig A, Haager PK, Kerckhoff G, Vom Dahl J, Klauss V, Hanrath P, Mudra H: Stent design related neointimal tissue proliferation in human coronary arteries; an intravascular ultrasound study. *Eur Heart J* 2001;22:2007-14
- Hsieh BT, Hsieh JF, Tsai SC, Lin WY, Huang HT, Ting G, Wang SJ: Rhenium-188-Labeled DTPA: a new radiopharmaceutical for intravascular radiation therapy. *Nucl Med Biol* 1999;26:967-72
- Hutchinson, B. S. and Bumgardner, J. D. Evaluation of the Effect of Cells on the Corrosion Behavior of an Implants Alloys. The Proceeding of the World Biomaterials Congress. 2000. Minneapolis, USA , Society for Biomaterials.
- Hwang CW, Edelman ER: Arterial ultrastructure influences transport of locally delivered drugs. *Circ Res* 2002;90:826-32
- Hwang CW, Wu D, Edelman ER: Physiological transport forces govern drug distribution for stent-based delivery. *Circulation* 2001;104:600-5
- Ishihara M, Obara K, Ishizuka T, Fujita M, Sato M, Masuoka K, Saito Y, Yura H, Matsui T, Hattori H, Kikuchi M, Kurita A: Controlled release of fibroblast growth factors and heparin from photocrosslinked chitosan hydrogels and subsequent effect on in vivo vascularization. *J Biomed Mater Res* 2003;64A:551-559
- Isner JM: Manipulating angiogenesis against vascular disease. *Hosp Pract (Off Ed)* 1999;34:69-74, 76, 79-80 passim

- Jacobs JJ, Skipor AK, Patterson LM, Hallab NJ, Paprosky WG, Black J, Galante JO: Metal release in patients who have had a primary total hip arthroplasty. A prospective, controlled, longitudinal study. *J Bone Joint Surg Am* 1998;80:1447-58
- Janatova J: Activation and control of complement, inflammation, and infection associated with the use of biomedical polymers. *ASAIO J* 2000;46:S53-62
- Kalinowski M, Alfke H, Bergen S, Klose KJ, Barry JJ, Wagner HJ: Comparative trial of local pharmacotherapy with L-arginine, r-hirudin, and molsidomine to reduce restenosis after balloon angioplasty of stenotic rabbit iliac arteries. *Radiology* 2001;219:716-23
- Kandzari DE, Tchong JE, Zidar JP: Coronary artery stents: evaluating new designs for contemporary percutaneous intervention. *Catheter Cardiovasc Interv* 2002;56:562-76
- Kastrati A, Mehilli J, Dirschinger J, Dotzer F, Schuhlen H, Neumann FJ, Fleckenstein M, Pfafferott C, Seyfarth M, Schomig A: Intracoronary stenting and angiographic results: strut thickness effect on restenosis outcome (ISAR-STEREO) trial. *Circulation* 2001;103:2816-21
- Kastrati A, Mehilli J, Dirschinger J, Pache J, Ulm K, Schuhlen H, Seyfarth M, Schmitt C, Blasini R, Neumann FJ, Schomig A: Restenosis after coronary placement of various stent types. *Am J Cardiol* 2001;87:34-9
- Kastrati A, Schomig A, Dirschinger J, Mehilli J, von Welser N, Pache J, Schuhlen H, Schilling T, Schmitt C, Neumann FJ: Increased risk of restenosis after placement of gold-coated stents: results of a randomized trial comparing gold-coated with uncoated steel stents in patients with coronary artery disease. *Circulation* 2000;101:2478-83
- Kessel DO, Wijesinghe LD, Robertson I, Scott DJ, Raat H, Stockx L, Nevelsteen A: Endovascular stent-grafts for superficial femoral artery disease: results of 1-year follow-up. *J Vasc Interv Radiol* 1999;10:289-96
- Khan MA, Williams RL, Williams DF: The corrosion behaviour of Ti-6Al-4V, Ti-6Al-7Nb and Ti-13Nb-13Zr in protein solutions. *Biomaterials* 1999;20:631-7

- Kocsis JF, Llanos G, Holmer E: Heparin-coated stents. *J Long Term Eff Med Implants* 2000;10:19-45
- Kolhe P, Kannan RM: Improvement in Ductility of Chitosan through Blending and Copolymerization with PEG: FTIR Investigation of Molecular Interactions. *Biomacromolecules* 2003;4:173-80
- Koster R, Vieluf D, Kiehn M, Sommerauer M, Kahler J, Baldus S, Meinertz T, Hamm CW: Nickel and molybdenum contact allergies in patients with coronary in- stent restenosis. *Lancet* 2000;356:1895-7
- Kribs S: Endovascular stent grafting: a review. *Can Assoc Radiol J* 2001;52:145-52
- Kuhl PR, Griffith-Cima LG: Tethered epidermal growth factor as a paradigm for growth factor- induced stimulation from the solid phase. *Nat Med* 1996;2:1022-7
- Kweon DK, Song SB, Park YY: Preparation of water-soluble chitosan/heparin complex and its application as wound healing accelerator. *Biomaterials* 2003;24:1595-601
- Lahann J, Klee D, Pluester W, Hoecker H: Bioactive immobilization of r-hirudin on CVD-coated metallic implant devices. *Biomaterials* 2001;22:817-26
- Lee JY, Nam SH, Im SY, Park YJ, Lee YM, Seol YJ, Chung CP, Lee SJ: Enhanced bone formation by controlled growth factor delivery from chitosan-based biomaterials. *J Control Release* 2002;78:187-97
- Lewis AL, Cumming ZL, Goreish HH, Kirkwood LC, Tolhurst LA, Stratford PW: Crosslinkable coatings from phosphorylcholine-based polymers. *Biomaterials* 2001;22:99-111
- Lewis AL, Tolhurst LA, Stratford PW: Analysis of a phosphorylcholine-based polymer coating on a coronary stent pre- and post-implantation. *Biomaterials* 2002;23:1697-706
- Liistro F, Colombo A: Late acute thrombosis after paclitaxel eluting stent implantation. *Heart* 2001;86:262-4

Liistro F, Gimelli G, Di Mario C, Nishida T, Montorfano M, Carlino M, Colombo A: Late acute thrombosis after coronary brachytherapy: when is the risk over? *Catheter Cardiovasc Interv* 2001;54:216-8

Liistro F, Stankovic G, Di Mario C, Takegi T, Chieffo A, Moshiri S, Montorfano M, Carlino M, Briguori C, Pagnotta P, Albiero R, Corvaja N, Colombo A: First Clinical Experience With a Paclitaxel Derivate-Eluting Polymer Stent System Implantation for In-Stent estenosis Immediate and Long-Term Clinical and Angiographic Outcome. *Circulation* 2002;105:1183-1886

Lovich MA, Edelman ER: Tissue concentration of heparin, not administered dose, correlates with the biological response of injured arteries in vivo. *Proc Natl Acad Sci U S A* 1999;96:11111-6

Lowe HC, Oesterle SN, Khachigian LM: Coronary in-stent restenosis: current status and future strategies. *J Am Coll Cardiol* 2002;39:183-93

Lvov Y, Lu Z, Schenkman JB, Zu X, Rusling JF: Direct Electrochemistry of Myoglobin and Cytochrome P450_{cam} in Alternate Layer-by-Layer Films with DNA and Other Polyions. *J. Am. Chem. Soc.* 1998;120:4073-4080

Lvov YuM, Sukhorukov GB: Protein architecture: assembly of ordered films by means of alternated adsorption of oppositely charged macromolecules. *Membr Cell Biol* 1997;11:277-303

Ma J, Wang H, He B, Chen J: A preliminary in vitro study on the fabrication and tissue engineering applications of a novel chitosan bilayer material as a scaffold of human neonatal dermal fibroblasts. *Biomaterials* 2001;22:331-6

Madhally SV, Matthew HW: Porous chitosan scaffolds for tissue engineering. *Biomaterials* 1999;20:1133-42

Maintz D, Fischbach R, Juergens KU, Allkemper T, Wessling J, Heindel W: Multislice CT angiography of the iliac arteries in the presence of various stents: in vitro evaluation of artifacts and lumen visibility. *Invest Radiol* 2001;36:699-704

Manke C, Nitz WR, Lenhart M, Volk M, Geissler A, Feuerbach S, Link J: Magnetic resonance monitoring of stent deployment: in vitro evaluation of different stent designs and stent delivery systems. *Invest Radiol* 2000;35:343-51

Mason M, Vercruysse KP, Kirker KR, Frisch R, Marecak DM, Prestwich GD, Pitt WG: Attachment of hyaluronic acid to polypropylene, polystyrene, and polytetrafluoroethylene. *Biomaterials* 2000;21:31-6

Matsumoto Y, Shimokawa H, Morishige K, Eto Y, Takeshita A: Reduction in neointimal formation with a stent coated with multiple layers of releasable heparin in porcine coronary arteries. *J Cardiovasc Pharmacol* 2002;39:513-22

Matsuno H, Yokoyama A, Watari F, Uo M, Kawasaki T: Biocompatibility and osteogenesis of refractory metal implants, titanium, hafnium, niobium, tantalum and rhenium. *Biomaterials* 2001;22:1253-62

McKelvey AL, Ritchie RO: Fatigue-crack propagation in Nitinol, a shape-memory and superelastic endovascular stent material. *J Biomed Mater Res* 1999;47:301-8

McKenna CJ, Camrud AR, Sangiorgi G, Kwon HM, Edwards WD, Holmes DR Jr, Schwartz RS: Fibrin-film stenting in a porcine coronary injury model: efficacy and safety compared with uncoated stents. *J Am Coll Cardiol* 1998;31:1434-8

McLean DR, Eiger NL: Stent design: implications for restenosis. *Rev Cardiovasc Med* 2002;3 Suppl 5:S16-22

McLean KM, Johnson G, Chatelier RC, Beumer GJ, Steele JG, Griesser HJ: Method of immobilization of carboxymethyl-dextran affects resistance to tissue and cell colonization. *Colloids Surf B Biointerfaces* 2000;18:221-234

McMurry TJ, Pippin CG, Wu C, Deal KA, Brechbiel MW, Mirzadeh S, Gansow OA: Physical parameters and biological stability of yttrium(III) diethylenetriaminepentaacetic acid derivative conjugates. *J Med Chem* 1998;41:3546-9

- Merhi Y, King M, Guidoin R: Acute thrombogenicity of intact and injured natural blood conduits versus synthetic conduits: neutrophil, platelet, and fibrin(ogen) adsorption under various shear-rate conditions. *J Biomed Mater Res* 1997;34:477-85
- Milosev I, Strehblow HH: The behavior of stainless steels in physiological solution containing complexing agent studied by X-ray photoelectron spectroscopy. *J Biomed Mater Res* 2000;52:404-12
- Mitra S, Gaur U, Ghosh PC, Maitra AN: Tumour targeted delivery of encapsulated dextran-doxorubicin conjugate using chitosan nanoparticles as carrier. *J Control Release* 2001;74:317-23
- Morra M: On the molecular basis of fouling resistance. *J Biomater Sci Polym Ed* 2000;11:547-69
- Morra M, Cassineli C: Non-fouling properties of polysaccharide-coated surfaces. *J Biomater Sci Polym Ed* 1999;10:1107-24
- Moussa I, Di Mario C, Di Francesco L, Reimers B, Blengino S, Colombo A: Subacute stent thrombosis and the anticoagulation controversy: changes in drug therapy, operator technique, and the impact of intravascular ultrasound. *Am J Cardiol* 1996;78:13-7
- Mu Y, Kobayashi T, Sumita M, Yamamoto A, Hanawa T: Metal ion release from titanium with active oxygen species generated by rat macrophages in vitro. *J Biomed Mater Res* 2000;49:238-43
- Mukherjee D, Kalahasti V, Roffi M, Bhatt DL, Kapadia SR, Bajzer C, Reginelli J, Ziada KM, Hughes K, Yadav JS: Self-expanding stents for carotid interventions: comparison of nitinol versus stainless-steel stents. *J Invasive Cardiol* 2001;13:732-5
- Nakajima N, Ikada Y: Mechanism of amide formation by carbodiimide for bioconjugation in aqueous media. *Bioconjug Chem* 1995;6:123-30
- Nan H, Ping Y, Xuan C, Yongxang L, Xiaolan Z, Guangjun C, Zihong Z, Feng Z, Yuanru C, Xianghuai L, Tingfei X: Blood compatibility of amorphous titanium oxide films synthesized by ion beam enhanced deposition. *Biomaterials* 1998;19:771-6

- Narins CR, Ellis SG: Prevention of in-stent restenosis. *Semin Interv Cardiol* 1998;3:91-103
- Nelson SR, deSouza NM, Allison DJ: Endovascular stents and stent-grafts: is heparin coating desirable? *Cardiovasc Intervent Radiol* 2000;23:252-5
- New G, Moses JW, Roubin GS, Leon MB, Colombo A, Iyer SS, Tio FO, Mehran R, Kipshidze N: Estrogen-eluting, phosphorylcholine-coated stent implantation is associated with reduced neointimal formation but no delay in vascular repair in a porcine coronary model. *Catheter Cardiovasc Interv* 2002;57:266-71
- Nsereko S, Amiji M: Localized delivery of paclitaxel in solid tumors from biodegradable chitin microparticle formulations. *Biomaterials* 2002;23:2723-31
- Park JY, Gemmell CH, Davies JE: Platelet interactions with titanium: modulation of platelet activity by surface topography. *Biomaterials* 2001;22:2671-82
- Parodi JC, Ferreira M: Historical prologue: why endovascular abdominal aortic aneurysm repair? *Semin Interv Cardiol* 2000;5:3-6
- Pei R, Cui X, Yang X, Wang E: Assembly of Alternating Polycation and DNA Multilayer Films by Electrostatic Layer-by-Layer Adsorption. *Biomacromolecules* 2001;2:463-8
- Pelton AR, DiCello J, Miyazaki S: Optimisation of processing and properties of medical grade Nitinol wire. *Nitinol medical devices and implants* 2000;9:107-118
- Petelenz B, Rajchel B, Bilski P, Misiak R, Bartyzel M, Wilczek K, Alber D: Physical and chemical limitations to preparation of beta radioactive stents by direct neutron activation. *Biomaterials* 2003;24:427-33
- Peuster M, Wohlsein P, Brugmann M, Ehlerding M, Seidler K, Fink C, Brauer H, Fischer A, Hausdorf G: A novel approach to temporary stenting: degradable cardiovascular stents produced from corrodible metal-results 6-18 months after implantation into New Zealand white rabbits. *Heart* 2001;86:563-9

Phaneuf MD, Dempsey DJ, Bide MJ, Quist WC, LoGerfo FW: Coating of Dacron vascular grafts with an ionic polyurethane: a novel sealant with protein binding properties. *Biomaterials* 2001;22:463-9

Phuwanartnuruks V, McCarthy TJ: Stepwise Polymer Surface Modification: Chemistry-Layer-by-Layer Deposition. *Macromolecules* 1998;31:1906-1914

Picart C, Lavalley Ph, Hubert P, Cuisinier FJG, Decher D, Schaaf P, Voegel J-C: Buildup Mechanism for Poly(L-lysine)/Hyaluronic Acid Films onto a Solid Surface. *Langmuir* 2001;17:7414-7424

Picart C, Mutterer J, Richert L, Luo Y, Prestwich GD, Schaaf P, Voegel JC, Lavalley P: Molecular basis for the explanation of the exponential growth of polyelectrolyte multilayers. *Proc Natl Acad Sci U S A* 2002;99:12531-5

Provost P, Merhi Y: Endogenous nitric oxide release modulates mural platelet thrombosis and neutrophil-endothelium interactions under low and high shear conditions. *Thromb Res* 1997;85:315-26

Puleo DA, Kissling RA, Sheu MS: A technique to immobilize bioactive proteins, including bone morphogenetic protein-4 (BMP-4), on titanium alloy. *Biomaterials* 2002;23:2079-87

Qiu X, Leporatti S, Donath E, Mohwald H: Studies on the Drug Release Properties of Polysaccharide Multilayers Encapsulated Ibuprofen Microparticles. *Langmuir* 2001;17:5375-5380

Rao SB, Sharma CP: Use of chitosan as a biomaterial: studies on its safety and hemostatic potential. *J Biomed Mater Res* 1997;34:21-8

Ratner BD: Blood compatibility--a perspective. *J Biomater Sci Polym Ed* 2000;11:1107-19

Reclaru L, Lerf R, Eschler P-Y, Blatter A, Meyer J-M: Pitting, crevice and galvanic corrosion of REX stainless-steel/CoCr orthopedic implant material. *Biomaterials* in Press

Regar E, Sianos G, Serruys PW: Stent development and local drug delivery. *Br Med Bull* 2001;59:227-48

Rensing BJ, Vos J, Smits PC, Foley DP, van den Brand MJ, van der Giessen WJ, de Feijter PJ, Serruys PW: Coronary restenosis elimination with a sirolimus eluting stent: first European human experience with 6-month angiographic and intravascular ultrasonic follow-up. *Eur Heart J* 2001;22:2125-30

Richardson SC, Kolbe HV, Duncan R: Potential of low molecular mass chitosan as a DNA delivery system: biocompatibility, body distribution and ability to complex and protect DNA. *Int J Pharm* 1999;178:231-43

Roguin A, Grenadier E, Linn S, Markiewicz W, Beyar R: Continued expansion of the nitinol self-expanding coronary stent: angiographic analysis and 1-year clinical follow-up. *Am Heart J* 1999;138:326-33

Rondelli G: Corrosion resistance tests on NiTi shape memory alloy. *Biomaterials* 1996;17:2003-8

Rowe AJ: Probing hydration and the stability of protein solutions - a colloid science approach. *Biophys Chem* 2001;93:93-101

Ruiz L, Hilborn JG, Leonard D, Mathieu HJ: Synthesis, structure and surface dynamics of phosphorycholine functional biomimicking polymers. *Biomaterials* 1998;19:987-98

Ryan MP, Williams DE, Chater RJ, Hutton BM, McPhail DS: Why stainless steel corrodes. *Nature* 2002;415:770-4

Ryhanen J, Kallioinen M, Tuukkanen J, Junila J, Niemela E, Sandvik P, Serlo W: In vivo biocompatibility evaluation of nickel-titanium shape memory metal alloy: muscle and perineural tissue responses and capsule membrane thickness. *J Biomed Mater Res* 1998;41:481-8

Ryhanen J, Niemi E, Serlo W, Niemela E, Sandvik P, Pernu H, Salo T: Biocompatibility of nickel-titanium shape memory metal and its corrosion behavior in human cell cultures. *J Biomed Mater Res* 1997;35:451-7

Sapirstein W, Zuckerman B, Dillard J: FDA approval of coronary-artery brachytherapy. *N Engl J Med* 2001;344:297-9

Schmalz G, Schuster U, Schweikl H: Influence of metals on IL-6 release in vitro. *Biomaterials* 1998;19:1689-94

Schulz C, Niederer C, Andres C, Herrmann RA, Lin X, Henkelmann R, Panzer W, Herrmann C, Regulla DF, Wolf I, Ulm K, Alt E: Endovascular irradiation from beta-particle-emitting gold stents results in increased neointima formation in a porcine restenosis model. *Circulation* 2000;101:1970-5

Senel S, Kremer MJ, Kas S, Wertz PW, Hincal AA, Squier CA: Enhancing effect of chitosan on peptide drug delivery across buccal mucosa. *Biomaterials* 2000;21:2067-71

Serizawa T, Yamaguchi M, Akashi M: Alternating bioactivity of polymeric layer-by-layer assemblies: anticoagulation vs procoagulation of human blood. *Biomacromolecules* 2002;3:724-31

Serruys PW, de Jaegere P, Kiemeneij F, Macaya C, Rutsch W, Heyndrickx G, Emanuelsson H, Marco J, Legrand V, Materne P, et al: A comparison of balloon-expandable-stent implantation with balloon angioplasty in patients with coronary artery disease. Benestent Study Group. *N Engl J Med* 1994;331:489-95

Serruys PW, Kay IP: I like the candy, I hate the wrapper: the (32)P radioactive stent. *Circulation* 2000;101:3-7

Serruys PW, Regar E, Carter AJ: Rapamycin eluting stent: the onset of a new era in interventional cardiology. *Heart* 2002;87:305-7

Shakesheff K, Cannizzaro S, Langer R: Creating biomimetic micro-environments with synthetic polymer-peptide hybrid molecules. *J Biomater Sci Polym Ed* 1998;9:507-18

Shard AG, Davies MC, Tendler SJB, Bennedetti L, Purbrick MD, Paul AJ, Beamson G: X-ray Photoelectron Spectroscopy and Time-of-Flight SIMS Investigation of Hyaluronic Acid Derivatives. *Langmuir* 1997;13:2808-2814

Shen M, Pan YV, Wagner MS, Hauch KD, Castner DG, Ratner BD, Horbett TA: Inhibition of monocyte adhesion and fibrinogen adsorption on glow discharge plasma deposited tetraethylene glycol dimethyl ether. *J Biomater Sci Polym Ed* 2001;12:961-78

Sheth S, Litvack F, Dev V, Fishbein MC, Forrester JS, Eigler N: Subacute thrombosis and vascular injury resulting from slotted-tube nitinol and stainless steel stents in a rabbit carotid artery model. *Circulation* 1996;94:1733-40

Shih CC, Lin SJ, Chen YL, Su YY, Lai ST, Wu GJ, Kwok CF, Chung KH: The cytotoxicity of corrosion products of nitinol stent wire on cultured smooth muscle cells. *J Biomed Mater Res* 2000;52:395-403

Shih CC, Lin SJ, Chen YL, Su YY, Lai ST, Wu GJ, Kwok CF, Chung KH: The cytotoxicity of corrosion products of nitinol stent wire on cultured smooth muscle cells. *J Biomed Mater Res* 2000;52:395-403

Shih CC, Shih CM, Chen YL, Su YY, Shih JS, Kwok CF, Lin SJ: Growth inhibition of cultured smooth muscle cells by corrosion products of 316 L stainless steel wire. *J Biomed Mater Res* 2001;57:200-7

Simon C, Palmaz JC, Sprague EA: Protein interactions with endovascular prosthetic surfaces. *J Long Term Eff Med Implants* 2000;10:127-41

Simons M, Bonow RO, Chronos NA, Cohen DJ, Giordano FJ, Hammond HK, Laham RJ, Li W, Pike M, Sellke FW, Stegmann TJ, Udelson JE, Rosengart TK: Clinical trials in coronary angiogenesis: issues, problems, consensus: An expert panel summary. *Circulation* 2000;102:E73-86

Singla AK, Chawla M: Chitosan: some pharmaceutical and biological aspects--an update. *J Pharm Pharmacol* 2001;53:1047-67

Sousa JE, Costa MA, Abizaid AC, Rensing BJ, Abizaid AS, Tanajura LF, Kozuma K, Van Langenhove G, Sousa AG, Falotico R, Jaeger J, Popma JJ, Serruys PW: Sustained

suppression of neointimal proliferation by sirolimus-eluting stents: one-year angiographic and intravascular ultrasound follow-up. *Circulation* 2001;104:2007-11

Sprague EA, Palmaz JC, Simon C, Watson A: Electrostatic forces on the surface of metals as measured by atomic force microscopy. *J Long Term Eff Med Implants* 2000;10:111-25

Stockx L: Stent-grafts in the superficial femoral artery. *Eur J Radiol* 1998;28:182-8

Stoeckel D: Nitinol medical devices and implants. *Min Invas Ther & Allied Technol* 2000;9:81-88

Sturek M, Reddy HK: New tools for prevention of restenosis could decrease the "oculostento" reflex. *Cardiovasc Res* 2002;53:292-3

Suzuki T, Hayase M, Hibi K, Hosokawa H, Yokoya K, Fitzgerald PJ, Yock PG, Cooke JP, Suzuki T, Yeung AC: Effect of local delivery of L-arginine on in-stent restenosis in humans. *Am J Cardiol* 2002;89:363-7

Suzuki YS, Momose Y, Higashi N, Shigematsu A, Park KB, Kim YM, Kim JR, Ryu JM: Biodistribution and kinetics of holmium-166-chitosan complex (DW-166HC) in rats and mice. *J Nucl Med* 1998;39:2161-6

Tamai H, Igaki K, Kyo E, Kosuga K, Kawashima A, Matsui S, Komori H, Tsuji T, Motohara S, Uehata H: Initial and 6-month results of biodegradable poly-l-lactic acid coronary stents in humans. *Circulation* 2000;102:399-404

Taniyama Y, Tachibana K, Hiraoka K, Namba T, Yamasaki K, Hashiya N, Aoki M, Ogihara T, Yasufumi K, Morishita R: Local delivery of plasmid DNA into rat carotid artery using ultrasound. *Circulation* 2002;105:1233-9

Taylor AJ, Gorman PD, Kenwood B, Hudak C, Tashko G, Virmani R: A comparison of four stent designs on arterial injury, cellular proliferation, neointima formation, and arterial dimensions in an experimental porcine model. *Catheter Cardiovasc Interv* 2001;53:420-5

Teebken OE, Haverich A: Tissue engineering of small diameter vascular grafts. *Eur J Vasc Endovasc Surg* 2002;23:475-85

Tepe G, Dinkelborg LM, Brehme U, Muschick P, Noll B, Dietrich T, Greschniok A, Baumbach A, Claussen CD, Duda SH: Prophylaxis of restenosis with (186)re-labeled stents in a rabbit model. *Circulation* 2001;104:480-5

Thierry B, Merhi Y, Bilodeau L, Trépanier C, Tabrizian M: Nitinol versus stainless steel stents: acute thrombogenicity study in an ex vivo porcine model. *Biomaterials* 2002;23:2997-3005

Thierry B, Tabrizian M, Trepanier C, Savadogo O, Yahia L: Effect of surface treatment and sterilization processes on the corrosion behavior of NiTi shape memory alloy. *J Biomed Mater Res* 2000;51:685-93

Thierry B, Winnik FM, Mehri Y, Silver J, Tabrizian M: Radionuclides-hyaluronic acid-conjugate thromboresistant coatings to prevent in-stent restenosis. *Biomaterials (In press)*

Thierry B, Winnik FM, Mehri Y, Silver J, Tabrizian M: Self-Assembled Bioactive Coatings of Endovascular Stents. *Submitted*

Thierry BJ, Winnik FM, Merhi Y, Tabrizian M: Nanocoatings onto Arteries via Layer-by-Layer Deposition: Towards the In-Vivo Repair of Damaged Blood Vessels. *J. Am. Chem. Soc. (In press)*

Thomssen H, Hoffmann B, Schank M, Hohler T, Thabe H, Meyer zum Buschenfelde KH, Marker-Hermann E: Cobalt-specific T lymphocytes in synovial tissue after an allergic reaction to a cobalt alloy joint prosthesis. *J Rheumatol* 2001;28:1121-8

Tio RA, Isner JM, Walsh K: Gene therapy to prevent restenosis, the Boston experience. *Semin Interv Cardiol* 1998;3:205-10

Tiwari A, Salacinski HJ, Punshon G, Hamilton G, Seifalian AM: Development of a hybrid cardiovascular graft using a tissue engineering approach. *FASEB J* 2002;16:791-

Travis JA, Hughes MG, Wong JM, Wagner WD, Geary RL: Hyaluronan enhances contraction of collagen by smooth muscle cells and adventitial fibroblasts : role of CD44 and implications for constrictive remodeling. *Circ Res* 2001;88:77-83

Trepanier C, Leung TK, Tabrizian M, Yahia LH, Bienvenu JG, Tanguay JF, Piron DL, Bilodeau L: Preliminary investigation of the effects of surface treatments on biological response to shape memory NiTi stents. *J Biomed Mater Res* 1999;48:165-71

Trepanier C, Tabrizian M, Yahia LH, Bilodeau L, Piron DL: Effect of modification of oxide layer on NiTi stent corrosion resistance. *J Biomed Mater Res* 1998;43:433-40

Trepanier, C., Venugopalan, R., Messer, R., Zimmerman, J., and Pelton, A. R. Effect of Passivation Treatments on Nickel Release from Nitinol. The Proceeding of the World Biomaterials Congress. Minneapolis, USA , Society for Biomaterials.

Uo M, Watari F, Yokoyama A, Matsuno H, Kawasaki T: Dissolution of nickel and tissue response observed by X-ray scanning analytical microscopy. *Biomaterials* 1999;20:747-55

Vahey JW, Simonian PT, Conrad EU 3rd: Carcinogenicity and metallic implants. *Am J Orthop* 1995;24:319-24

van der Giessen WJ, Lincoff AM, Schwartz RS, van Beusekom HM, Serruys PW, Holmes DR Jr, Ellis SG, Topol EJ: Marked inflammatory sequelae to implantation of biodegradable and nonbiodegradable polymers in porcine coronary arteries. *Circulation* 1996;94:1690-7

van der Giessen WJ, van Beusekom HM, Eijgelshoven MH, Morel MA, Serruys PW: Heparin-coating of coronary stents. *Semin Interv Cardiol* 1998;3:173-6

van Dijk LC, van Holten J, van Dijk BP, Matheijssen NA, Pattynama PM: A precious metal alloy for construction of MR imaging-compatible balloon-expandable vascular stents. *Radiology* 2001;219:284-7

- Vazquez E, Dewitt DM, Hammond PT, Lynn DM: Construction Hydrolytically-Degradable Thin Films via Layer-by-Layer Deposition of Degradable Polyelectrolytes. *J. Am. Chem. Soc.* 2002;124:13992-12993
- Venugopalan R: Corrosion testing of stents: a novel fixture to hold entire device in deployed form and finish. *J Biomed Mater Res* 1999;48:829-32
- Venugopalan R, Trépanier C: Assessing the corrosion behaviour of Nitinol for minimally-invasive device design. *Min Invas Ther & Allied Technol* 2000;9:67-74
- Verheye S, Markou CP, Salame MY, Wan B, King SB 3rd, Robinson KA, Chronos NA, Hanson SR: Reduced thrombus formation by hyaluronic acid coating of endovascular devices. *Arterioscler Thromb Vasc Biol* 2000;20:1168-72
- Verin V, Popowski Y, de Bruyne B, Baumgart D, Sauerwein W, Lins M, Kovacs G, Thomas M, Calman F, Disco C, Serruys PW, Wijns W: Endoluminal beta-radiation therapy for the prevention of coronary restenosis after balloon angioplasty. The Dose-Finding Study Group. *N Engl J Med* 2001;344:243-9
- Villiermaux F, Tabrizian M, Yahia L, Czeremuszkin G, Piron DL: Corrosion resistance improvement of NiTi osteosynthesis staples by plasma polymerized tetrafluoroethylene coating. *Biomed Mater Eng* 1996;6:241-54
- Virmani R, Farb A, Kolodgie FD: Histopathologic alterations after endovascular radiation and antiproliferative stents: similarities and differences. *Herz* 2002;27:1-6
- Virmani R, Kolodgie FD, Dake MD, Silver JH, Jones RM, Jenkins M, Gillespie DL: Histopathologic evaluation of an expanded polytetrafluoroethylene- nitinol stent endoprosthesis in canine iliofemoral arteries. *J Vasc Interv Radiol* 1999;10:445-56
- Virmani R, Liistro F, Stankovic G, Di Mario C, Montorfano M, Farb A, Kolodgie FD, Colombo A: Mechanism of late in-stent restenosis after implantation of a paclitaxel derivate-eluting polymer stent system in humans. *Circulation* 2002;106:2649-51
- Vogler EA: Water and the acute biological response to surfaces. *J Biomater Sci Polym Ed* 1999;10:1015-45

Vrolix MC, Legrand VM, Reiber JH, Grollier G, Schalij MJ, Brunel P, Martinez-Elbal L, Gomez-Recio M, Bar FW, Bertrand ME, Colombo A, Brachman J: Heparin-coated Wiktor stents in human coronary arteries (MENTOR trial). MENTOR Trial Investigators. *Am J Cardiol* 2000;86:385-9

Waksman R, Raizner AE, Yeung AC, Lansky AJ, Vandertie L: Use of localised intracoronary beta radiation in treatment of in-stent restenosis: the INHIBIT randomised controlled trial. *Lancet* 2002;359:551-7

Wang PG, Xian M, Tang X, Wu X, Wen Z, Cai T, Janczuk AJ: Nitric oxide donors: chemical activities and biological applications. *Chem Rev* 2002;102:1091-134

Wang YZ: Corrosion Fatigue, in Uhlig's (ed): *Corrosion Handbook, Second Edition*. 2000, pp 221-232

Wardeh AJ, Kay IP, Sabate M, Coen VL, Gijzel AL, Ligthart JM, den Boer A, Levendag PC, van Der Giessen WJ, Serruys PW: beta-Particle-emitting radioactive stent implantation. A safety and feasibility study. *Circulation* 1999;100:1684-9

Wataha JC, Lockwood PE, Marek M, Ghazi M: Ability of Ni-containing biomedical alloys to activate monocytes and endothelial cells in vitro. *J Biomed Mater Res* 1999;45:251-7

Wataha JC, Nelson SK, Lockwood PE: Elemental release from dental casting alloys into biological media with and without protein. *Dent Mater* 2001;17:409-14

Wataha JC, O'Dell NL, Singh BB, Ghazi M, Whitford GM, Lockwood PE: Relating nickel-induced tissue inflammation to nickel release in vivo. *J Biomed Mater Res* 2001;58:537-44

Wataha JC, Ratanasathien S, Hanks CT, Sun Z: In vitro IL-1 beta and TNF-alpha release from THP-1 monocytes in response to metal ions. *Dent Mater* 1996;12:322-7

Welt FG, Rogers C: Inflammation and restenosis in the stent era. *Arterioscler Thromb Vasc Biol* 2002;22:1769-76

Wever DJ, Veldhuizen AG, de Vries J, Busscher HJ, Uges DR, van Horn JR: Electrochemical and surface characterization of a nickel-titanium alloy. *Biomaterials* 1998;19:761-9

Williams D. F.: Biomaterials and Biocompatibility: An Introduction, in *Fundamental Aspects of Biocompatibility*. Boca Raton, FL, 1981, pp 2-3

Windecker S, Mayer I, De Pasquale G, Maier W, Dirsch O, De Groot P, Wu YP, Noll G, Leskosek B, Meier B, Hess OM: Stent coating with titanium-nitride-oxide for reduction of neointimal hyperplasia. *Circulation* 2001;104:928-33

Wong JYC, Chu DZ, Yamauchi DM, Williams LE, Liu A, Wilczynski S, Wu AM, Shively JE, Doroshov JH, Raubitschek AA: A phase I radioimmunotherapy trial evaluating 90yttrium-labeled anti- carcinoembryonic antigen (CEA) chimeric T84.66 in patients with metastatic CEA-producing malignancies. *Clin Cancer Res* 2000;6:3855-63

Woodman JL, Black J, Jiminez SA: Isolation of serum protein organometallic corrosion products from 316LSS and HS-21 in vitro and in vivo. *J Biomed Mater Res* 1984;18:99-114

Xue L, Greisler HP: Biomaterials in the development and future of vascular grafts. *J Vasc Surg* 2003;37:472-80

Yasuda S, Noguchi T, Gohda M, Arai T, Tsutsui N, Nakayama Y, Matsuda T, Nonogi H: Local delivery of low-dose docetaxel, a novel microtubule polymerizing agent, reduces neointimal hyperplasia in a balloon-injured rabbit iliac artery model. *Cardiovasc Res* 2002;53:481-6

Yoshitomi Y, Kojima S, Yano M, Sugi T, Matsumoto Y, Saotome M, Tanaka K, Endo M, Kuramochi M: Does stent design affect probability of restenosis? A randomized trial comparing Multilink stents with GFX stents. *Am Heart J* 2001;142:445-51

Zamora PO, Osaki S, Som P, Ferretti JA, Choi JS, Hu C, Tsang R, Kuan HM, Singletary S, Stern RA, Oster ZH: Radiolabeling brachytherapy sources with Re-188 through chelating microfilms: stents. *J Biomed Mater Res* 2000;53:244-51

Zhang M, Li XH, Gong YD, Zhao NM, Zhang XF: Properties and biocompatibility of chitosan films modified by blending with PEG. *Biomaterials* 2002;23:2641-8

Zhou L, Estavillo C, Schenkman SJB, Rusling JF: Toxicity Screening by Electrochemical Detection of DNA Damage by Metabolites Generated In Situ in Ultrathin DNA-Enzyme Films. *J. Am. Chem. Soc.* 2003;

APPENDIX

Copy of the U.S. patent “Biodegradable Membrane-Covered Implants”

Reprint of manuscript 5 included in this thesis and published in Biomacromolecules.

Reprint of manuscript 6 included in this thesis and published in the Journal of the American Chemical Society. Reprint of the comment in Nature – Material update is also presented.

BIODEGRADABLE MEMBRANE-COVERED IMPLANT

TECHNICAL FIELD

[0001] The present application relates to the field of medical implants such as stents, which can be coated with a biodegradable membrane containing or not an active ingredient or medicament.

BACKGROUND OF THE INVENTION

[0002] Membrane-covered-stents are used or investigated in the treatments coronary diseases such as aneurysm, pseudoaneurysm, large dissection of the vascular wall during angioplasty and thrombus containing lesions (Baldus S, et al., *Catheter Cardiovasc Interv*; **53**: 1-4, 2001). In particular, covered-stents may be useful to stabilize the friable plaque in saphenous vein graft diseases. This may in turn reduce the risk of distal embolization following angioplasty of such vessels. Their uses have also been questioned in the treatment of peripheral diseases (Stockx L. *Eur J Radiol*; **28**:182-188, 1998). The lack of long term biocompatibility of the synthetic polymers such as PTFE, Dacron and polyurethane currently used as covering material remains however a major limitation of these devices. To circumvent these limitations, biological polymers-based membrane covered stents have been proposed using exogenous fibrin, collagen, or bovine pericardium for instance (Goodwin SC, et al., *Invest Radiol*; **35**:420-425, 2000; Cloft HJ, et al., *Radiology*; **214**:557-562, 2000; Gaspar J, et al., *Arch Cardiol Mex*; **71** :286-294, 2001; and McKenna CJ, et al., *J Am Coll Cardiol*; **31**:1434-1438, 1998). While some promising results have been reported, a completely engineered membrane would present obvious advantages. Chitosan is a biocompatible, non-immunogenic and biodegradable polymer with bioadhesive, wound healing, and antimicrobial properties. Chitosan blend with various polymers have been widely investigated to improve the mechanical properties of chitosan. In particular, chitosan-polyethylene oxide (PEO)/polyethylene glycol (PEG) interpenetrated networks display excellent mechanical properties with improved ductility in comparison to chitosan alone (Kolhe P, and Kannan RM. *Biomacromolecules*; **4**:173-180, 2003; and Budtova T, et al., *J Appl Polym Sci*; **84**: 1114-1122, 2002).

[0003] Chitosan is also widely used in drug delivery application and promotes absorption of drugs, peptides and proteins through biological tissues (Singla AK, and Chawla M. *J Pharm Pharmacol*; **53**:1047-1067, 2001). In revascularization procedures, neointimal hyperplasia within the stent struts remained however a consistent cause of failure. Systemic pharmaceutical strategies have been up to date mainly unsuccessful. Local drug/gene delivery conjugated with stent implantation yields the hope to eliminate clinical restenosis (Fattori R, and Piva T. *Lancet*; **361**:247-249, 2003). In particular, antiproliferative drug-eluting stents have been shown to significantly reduce restenosis. The long term safety and efficiency as well as the cost/efficiency of these therapeutic strategies remain however questioned.

[0004] It would be highly desirable to be provided with a new biodegradable membrane-covered endovascular device and a method for making same.

SUMMARY OF THE INVENTION

[0005] One aim of the present invention is to provide a chitosan-based membrane covered device, such as a stent, with properties that could be tailored to specific applications of such endoprosthesis.

[0006] Another aim of the present invention is to provide a new method for preparing the device on the present invention.

[0007] In accordance with the present invention there is provided a biodegradable membrane covered endovascular device, said device being coated with a solution of chitosan-plasticizer compound dried on the device, forming a flexible polymeric membrane on the device. The plasticizer compound can be for example (without limitation) polyethylene oxide (PEO), cellulose, keratin, collagen, anionic polysaccharide, and poly(α -hydroxy acid).

[0008] The membrane so produced has a further commercial potential as it can be used for treating various diseases when an active ingredient is coupled to the membrane. In such case, the active ingredient can simply be added at the time of forming the membrane, to the solution of chitosan-plasticizer

compound prior to coating the device. Active ingredients that can be useful and that are thus envisioned in the present invention are for example, without limitation, growth factors, anti-proliferative drugs, anti-inflammatory drugs, nitric oxide donor compounds, radionuclides, nucleic acids, peptides, and proteins.

[0009] In a preferred embodiment of the present invention, the device is a stent, having preferably a metallic scaffold made of stainless steel, NiTi alloy, titanium alloys, Conichrome, Phynox, MP35N, cobalt-based alloys, tantalum titanium-zirconium-niobium alloys, titanium-aluminum-vanadium alloy, platinum, tungsten, tantalum, or a combination thereof.

[0010] In a further preferred embodiment, the solution of chitosan-plasticizer compound is a 70:30 weight to weight chitosan:polyethylene oxide solution.

[0011] The term chitosan used herein is meant to include chitosan, chitosan blends or composites complex with a biocompatible synthetic or natural polymer.

[0012] Still in accordance with the present invention, there is provided a method for producing a biodegradable membrane-covered device, said method comprising the steps of:

- a) preparing a solution containing chitosan and a plasticizer compound;
- b) contacting a device to be covered with the solution of step a); and
- c) allowing the solution to dry onto said device.

[0013] In a further embodiment, the method may also comprise after step c) the steps of:

- d) rinsing the device of step c) with an alkaline solution;
- e) rinsing the device of step d) with a physiological buffer;
- f) allowing the device of step e) to dry.

[0014] In one embodiment of the invention, the solution of step a) above is prepared by dissolving in solution chitosan in an acidic medium and the plasticizer compound in an acid and mixing the solutions of chitosan and plasticizer compound together to form the solution used in step a).

[0015] Further in accordance with the present invention, there is also provided a method for treating aneurysm comprising the steps of implanting a device as defined above in a blood vessel of a patient suffering from an aneurysm, such that the device is implanted over the opening of the aneurismal sac in the blood vessel, the chitosan/polyethylene oxide coated device allowing cells to adhere to the device, thereby closing the aneurismal sac.

[0016] In fact, the device of the present invention should not be limited to stent and restenosis, but should also include devices that need to be implanted and that need to release a medicament or an active ingredient at the site of implantation. For example, the device of the present invention can also be used for treating a disease located at the surface of a vessel, such as a blood vessel or the esophagus. The device of the present invention can also be used for treating tumors or cancer, such as esophagus tumors or cancer, for treating vein graft-induced diseases

[0017] The versatility of the fabrication method describes here allows to design membranes with different thickness, structure, and porosity.

[0018] For the purpose of the present invention the following terms are defined below.

[0019] The terms " bioactive drug", "active drug" and "medicament", all used interchangeably, are intended to mean any compound able to stimulate or inhibit cellular events. Examples of such drugs are, without limitation, an anti-proliferative or anti-inflammatory drug, nitric oxide donor compounds, and proteins, DNA, and radionuclides able to stimulate/inhibit cellular events. In a preferred embodiment, an anti-proliferative or anti-inflammatory drug is loaded into the membrane. For example, anti-proliferative drugs can include paclitaxel, sirolimus, tacrolimus, everolimus, dexamethasone, angiopeptin (somatostatin

analogue from a French company: Ibsen), angiotensin converting enzyme inhibitors (Captopril, Cilazapril and Lisinopril), calcium channel blockers (Nifedipine), colchicine, fibroblast growth factor (FGF) antagonists, fish oil, low molecular weight heparin, histamine antagonists, lovastatin, methotrexate, monoclonal antibodies (to PDGF receptors, etc.), nitroprusside, phosphodiesterase inhibitors, prostacyclin analogues, prostaglandin inhibitor (Glaxo), seramin (PDGF antagonist), serotonin blockers, steroids, thioprotease inhibitors, triazolopyrimidine.

BRIEF DESCRIPTION OF THE DRAWINGS

[0020] Fig. 1 is a schematic representation of the CH-PEO membrane covered stent with or without external porous layer, in accordance with one embodiment of the invention;

[0021] Fig. 2 illustrates an *in vitro* assay showing inhibition of platelet adhesion of CH-PEG membrane incubated in the presence of sodium nitroprusside.

[0022] Figs. 3A and 3B illustrate a macroscopic observation of the CH-PEO membrane covered stent showing the ability of the membrane to sustain a mechanical deformation following a compression (Fig. 3A) and the return to the original conformation (Fig. 3B) of a metallic stent;

[0023] Figs. 4A to 4C illustrate scanning electron microscopic images of the membrane covered stent in which Fig. 4A represent an external view of the stent showing the adhesion of the membrane to the metallic struts, Fig. 4B is a view of the inside of the membrane showing the stent-struts underlying and Fig. 4C is a 450X enlarged view the box in Fig. 4A;

[0024] Fig. 5A illustrates the swelling behavior in PBS at pH 7.4 of the CH-PEO membrane (▲), and of the CH-PEO porous membrane (■);

[0025] Fig. 5B illustrates in an inlet of Fig. 5A the swelling behavior in PBS at pH 7.4 of the CH-PEO membrane (◆) in comparison with the CH membrane of the prior art (●);

[0026] Fig. 6 illustrates ^{51}Cr -platelet adhesion ($n \geq 5$) in an *ex vivo* porcine model on CH-PEO, damaged (Media) and intact arteries (Endo), * $p < 0.05$ vs. Media;

[0027] Fig. 7 illustrates ^{111}In -leukocyte adhesion ($n \geq 5$) in an *ex vivo* porcine model on CH-PEO, damaged (Media) and intact arteries (Endo), * $p < 0.05$ vs. Media;

[0028] Fig. 8 illustrates ^{111}In -Platelet adhesion ($n \geq 4$) after a 90 min incubation in PRP on chitosan (CH), CH-PEO and heparin complexed-CH-PEO (CH-PEO-Hep) membranes, where damaged arteries (Media) were used as control, * $p < 0.05$ vs. Media, + $p < 0.05$ vs. CH-PEO; and

[0029] Fig. 9 illustrates the Arginine release behavior in PBS of the CH-PEO membrane of the present invention, either following direct loading (■) or following precomplexation with anionic LMW HA (○).

DETAILED DESCRIPTION OF THE PREFERRED EMBODIMENT

[0030] In accordance with the present invention, there is now provided a method of making chitosan-PEO based biodegradable membrane covered devices, such as stents. The membrane covered devices described here are intended to be used in a wide range of application such as the treatment of aneurysm, the treatment of vascular graft diseases, malignant obstructive disease and tissue engineering applications. The properties of the membrane were investigated in order to gain insight on its ability to be used in endovascular applications. Looking for vascular tissue engineering applications, an external porous membrane that could be used as a biodegradable scaffold was added. The haemocompatibility of the devices was characterized both in an *ex vivo* porcine model and *in vitro* and optimized through complexation with heparin. Finally, the ability of the membrane to act as a drug reservoir was investigated using the peptide precursor of nitric oxide L-Arginine and the NO donor sodium nitroprusside (SNP).

Materials

[0031] Chitosan derived from crab shell with a deacetylation degree > 85 % and PEO with an average molecular weight of 1,000,000 daltons were obtained from Sigma Co. Heparin was from Leo Pharma (Tornhill, CA)(1000 unit/mL). ^3H labeled and unlabeled L-Arginine were purchased from Sigma (L-Arginine hydrochloride; and L-Arginine-2,3- ^3H in aqueous ethanol solution). LMW HA was obtained as previously described. Hyaluronan (HMW 500,000) was from Hyal Pharmaceutical Corp, Mississauga, Ca. All chemicals were chemical grade. SNP was from Sigma Chemicals.

Chitosan-polyethylene oxide (CH-PEO) polymers preparation

[0032] CH-PEO film was synthesized as a film or used for the membrane covered stent. Chitosan was dissolved in 0.1 M aqueous acetic acid (2% w/w) overnight and filtered to get rid of any insoluble material. PEO dissolved in glacial acetic acid was then added to a ratio of CH/PEO: 70/30 by weight. The mixture was then stirred for 4 h and then degassed. A jelly-like solution was then obtained that was either poured in glass mold for characterization or used to prepare the membrane covered stent as described hereinafter. The gel was allowed to dry at room temperature or was freeze dried for the porous membrane. The dry material was then washed with aqueous 1 N NaOH to remove residual acid and finally thoroughly wash with ultrapure water.

Membrane covered stent preparation

[0033] Self-expandable stents made from NiTi alloy were mounted on a glass rod as schematized in Fig 1. The glass rod could be rotated on the longitudinal axis at controlled speed (rpm). A known amount (depending on the experiments, from 0.1g to few grams) of CH-PEO gel was then cast on the stent maintained in rotation. Controlling the rotation speed and as a function of the viscosity of the gel, a uniform layer of CH-PEO covered the stent in a controlled fashion. While maintained in rotation, the gel-covered stent was allowed to dry at room temperature. The dried membrane covering the stent was then neutralized as described above before removing the stent from the glass rod.

The membrane-coated stent was then allowed to dry and was stored for characterization or further modifications.

surface complexation with anionic polymers

[0034] Heparin is being used herein as a model for anionic polymers. Heparin solution was prepared (1 mg/mL in water) and used to complex with CH-PEO film. The CH-PEO film was immersed in the heparin solution for two hours at RT to allow the electrostatic interaction between heparin and CH to occur and then thoroughly rinsed with water. The heparin complexed-CH-PEO-membrane (CH-PEO-Hep) was then dried and further used for the haemocompatibility assay.

Multilayered membrane covered-stent

[0035] Additional layers of CH-PEO were deposited onto a previously prepared layer to form a membrane having increased thickness/mechanical properties. This was achieved by repeating the same procedure as described above in reference to Fig. 1. External porous layers were also added onto membrane-covered-stents. A CH-PEO covered stent was prepared and kept on the glass holder. The device was placed into a glass mold that was gently filled with CH-PEO mixture. The mold was then freeze at -20°C before being transferred to vacuum vessels and being lyophilized until dry. The membrane was then again neutralized with NaOH and rinsed with pure water. This procedure yielded an external macro-porous layer.

Characterization of the membrane

SEM observations

[0036] Membrane covered-stents were observed using SEM. The devices were allowed to equilibrate in water and then freeze-dried. The membranes were processed (i.e. cut) prior to metallization with an ultrathin sputter coated gold layer. The samples were imaged using scanning electronic microscopy (SEM) at an accelerating voltage of 5 kV.

[0037] The porosity of the membrane has been characterized by complex permittivity measurements using a vector network analyzer (Model PNA 8358, Agilent Technologies) and a dielectric probe (85070C, Agilent Technologies).

Swelling behavior

[0038] The swelling behavior of chitosan-based membrane was investigated by gravimetric method. Discs of polymers were prepared and allowed to swell in 0.9 M NaCl solution. The swollen polymers were collected at various times, the excess water being removed by blotting against filter paper, and weighted (± 0.1 mg). The swelling ration was calculated knowing the hydrated W_h and dry W_d weight: $(W_h - W_d)/W_h$.

Water permeation and burst strength

[0039] The water permeation and burst strength of the membrane covered stent was determined in PBS as described (Berglund JD, et al., *Biomaterials*; **24**:1241-1254, 2003). The devices were hydrated for 30 min and completely crushed 5 times to simulate extensive manipulations. They were then cannulated with surgical sutures on semi-rigid silastic tubes at both sides. Water permeability is defined here as the amount of saline solution leaked per unit area and time under a physiologic pressure of 120 mm Hg. The burst pressure was characterized by pressurizing the device with an increasing hydrostatic liquid pressure (20 mmHg steps) until membrane failure.

Thrombogenicity

[0040] The thromboresistance of the CH-PEO membranes have been investigated using an extracorporeal procedure in *ex vivo* perfusion chambers using radiolabeled ^{51}Cr -platelets and ^{111}In Leukocytes. The radiolabeling, animal surgery, and extracorporeal procedures were achieved as previously described (Thierry B, et al., *Biomaterials*; **23**: 2997-3005, 2002). Six (6) pigs were used in the experiments. All procedures followed the American Heart Association guideline for animal research and were approved by the MHI ethic committee. Briefly, the extracorporeal shunt consisted in a two parallel silicon

tubing channel circuit connecting the femoral artery to the perfusion chambers and returning to the femoral vein. Radiolabeled platelets and leukocytes were re-injected into the animals one hour before the beginning of the experiments. CH-PEO mixture was cast on glass slide, dry, rinsed with NaOH and water and finally allowed to dry and stored. Intact endothelium and injured arterial segments were used as respectively thromboresistant and thrombogenic control (Thierry B, et al., *Biomaterials*; **23**: 2997-3005, 2002). To simulate damaged arteries, intima denuded artery were prepared as followed. Normal porcine aortas were first dissected and then cut into rings, longitudinally opened and cut into segments. The aortic media was then exposed by lifting and peeling off the intima and the adventia together with a thin portion of the subjacent media. The segments were then cut to appropriate size using the cutting device. Such aortic media segments were shown in previous experiments to be very thrombogenic and closely simulate angioplasty damaged arteries.

[0041] The samples were hydrated in saline at least 30 min prior to the experiments and then placed in the perfusion chamber. The perfusion procedure was initiated by a 1 min saline wash. The blood was then allowed to circulate into the extracorporeal circuit for 15 min at a wall shear rate of 424 sec^{-1} . The circuit was then flushed with saline for 30 sec and the samples recovered and fixed in 1.5% glutaraldehyde in gamma-counter vials. The amount of radioactivity was then measured and calculated for background, decay and overlapping of the radionuclides. The total amount of platelets and leukocytes adsorbed on the surface was calculated knowing the activity of blood samples used as reference and using hematology achieved prior to each experiment.

Platelet adhesion

[0042] Further insights on the haemocompatibility of the chitosan-based membranes were obtained using an *in vitro* platelet adhesion assays. Samples were prepared as 0.6 cm^2 discs using a cutting device. Chitosan (CH), CH-PEO and CH-PEO-Hep were prepared and kept at room temperature (RT). One (1) hour before the beginning of the experiments, samples were allowed to

rehydrate in saline solution. Damaged arteries used as control were prepared as described above. Fresh blood was drawn from healthy volunteers (120 mL), who were medication free and used for radiolabeling of platelets. The labeled platelets were resuspended in the platelet poor plasma (PPP) to 2.5×10^6 platelets/mL. The samples were placed into the bottom of a 96 well polystyrene plate (Corning Inc.). 250 μ L of freshly prepared ^{111}In -platelet solution was then added to each well taking special care that both sides of the samples were in contact with platelet solution. The platelet adhesion was allowed to proceed for 90 min with gentle shaking. After incubation, the samples were recovered and washed 4 times with saline. The samples were then fixed in 1.5 % glutaraldehyde solution and the amount of platelet was determined using the gamma counter.

SNP loaded CH-PEO membrane.

[0043] Freshly dried CH-Peg films were rehydrated in an aqueous solution of the NO-donor sodium nitroprusside (SNP, Sigma) (83 mg/mL (10%) and 16.6 mg/mL (2%)) for 1 h and then washed with water and let to dry at RT. During all the preparation procedure, the samples were kept in the dark to protect SNP from decomposition.

[0044] Platelet adhesion on SNP loaded membrane was investigated in an *in vitro* assays as described. To assess the effects of potency of SNP towards platelet adhesion, CH-PEG membranes were incubated in platelet rich plasma (PRP) with a physiological dose of SNP (50 μ Mol/L).

L-Arginine release

[0045] L-Arginine (Arg), the precursor of nitric oxide (NO) has been used in the present invention as a model drugs. Arginine has been shown to reduce clinical restenosis when locally delivered through a NO mediated actions (Suzuki T, et al., *Am J Cardiol*; **89**:363-367, 2002). The cationic drug has been either loaded directly in the membrane or precomplexed with anionic low molecular weight hyaluronic acid (LMW HA). The complexation of the cationic drug with the plasticizer polysaccharide was expected to delay its release and to

minimize drug lost during the washing procedures of the membrane. Such precomplexation method with low molecular weight dextran has been successfully used to increase the loading of doxorubicin in chitosan nanoparticles (Mitra S, et al., *J Control Release*; **74**:317-323, 2001).

[0046] CH-PEO mixture was prepared as described above. A stock solution of unlabeled Arg/[³H] Arg was prepared in water (10^{-3} M with 2 μ L [³H] Arg/mL). In the direct loading experiments, L-Arginine was added to 2 g of the CH-PEO mixture to a final concentration of wt. 0.2 %. In the precomplexation method, LMW HA solubilized in water (1 mg/mL) was mixed with 100 μ L of the Arg solution (COOH/Arg molar ratio: 5:1) and allowed to complex for 1 h. 260 μ L of this mixture was then added to 2 g of the CH-PEO solution. The CH-PEO/Arg mixture with or without LMW HA was left under agitation for 2 h and then poured in polystyrene wells. The membranes were allowed to dry and then neutralized for 2 min with 750 μ L NaOH 1 M and rinsed twice with 1 mL water (2 min each). The rinsing solutions were kept for quantification of Arg released during the washing steps.

[0047] The release behaviors of the Arg-loaded membranes were determined in PBS. Membrane cast in the wells were incubated with 1 mL PBS under gentle agitation at RT. At various time, the PBS solution was removed from the well. The Radioactivity of the solution was determined using liquid scintillation spectrometry (Beckman LS 6500 Liquid Scintillation counter) and correlated after correction for background to the amount of Arg using standard.

Device preparation

[0048] The method described here to obtain the chitosan membrane-covered stent was reliable and reproducible. Once allowed to dry overnight and then neutralized with NaOH and rinsed with water, the device could be easily recovered from the holder without any damaged. Macroscopic observations showed that a thin membrane uniformly covered the whole stents as shown in Figs. 3A and 3B. Experiments have shown that the thickness of the membrane could be easily controlled by changing the viscosity of the chitosan mixture and

to a lesser extent by controlling the speed of rotation of the glass holder. The thickness of a one-layer CH-PEO membrane was in the range of 100 μm . One of the challenges in the design of such a device was to optimize the mechanical properties of the membrane so that it could sustained the mechanical deformation associated with stent deployment. As shown in Figs. 3A and 3B, the hydrated membrane was able to sustain complete crush without any visible damages. Minimally invasive delivery of the device could be achieved easily. Hydrated membrane-covered stents were hand crimped on catheters and maintained cramped with small plastic clamps until dry. Device-loaded catheters were kept at room temperature until further used. The dilatation of the devices was achieved in glass tubing by rehydration and removal of the plastic clamps. The devices completely expanded inside the glass tubes. To investigate the effect of the delivery procedure on the membrane, a stent was dilated and then quickly freeze-dried using liquid nitrogen. The lyophilized sample was then gold coated for SEM observations. Using low magnification, it was noted that the membrane conserved its integrity and remained firmly attached to the metallic structure (Figs. 4A to 4C). The luminal surface of the membrane was relatively smooth despite "waves".

Membrane characterization

[0049] The swelling behavior of CH-PEO membrane in PBS (pH 7.4) is shown in Figs. 5A and 5B and compared to that of porous CH-PEO membrane obtained by freeze-drying (Fig. 5A) or to the CH membrane of the prior art (Fig. 5B). Rapid swelling of CH-PEO was observed and equilibrium was achieved within 1 min. As expected, porous CH-PEO presented a significantly higher swelling ratio than the CH-PEO membrane. The blend of Chitosan with PEO increased the swelling ratio in comparison to chitosan alone prepared in the same condition than the CH-PEO membrane (1.55 Vs. 1.22 at 10 min).

[0050] The water permeation at 120 mm Hg was determined to be less than $1 \text{ mL/cm}^2 \text{ min}^{-1}$. No significant linkage of the membrane was observed when the device was pressurized at 120 mm Hg for 30 min. The burst pressure resistance of the 4 tested membrane-covered stents was determined to be higher than 500

mm Hg but the apparatus used in this work did not allow us to pressurize the membrane high enough to its failure. An external membrane could be added to the device as described herein with a mean porosity of about 95%.

Thromboresistance

[0051] The thromboresistance of the CH-PEO membrane was investigated in an *ex vivo* porcine assays using radiolabeled platelets and leukocytes. Under the physiological flow conditions used in the study, the CH-PEO presented low amounts of platelet adhesion in comparison to damaged arteries ($P < 0.05$). Similar results were obtained with leukocytes ($P < 0.005$). Both platelet and leukocyte adhesion onto CH-PEG was in the same range that on arteries with an intact endothelial layer (Figs. 6 and 7).

[0052] The effect of PEO and heparin complexation on the haemocompatibility was investigated in the *in vitro* assays. The incorporation of PEO into the chitosan membrane tends to reduce the amount of platelet adhesion (52.5% reduction, $P > 0.05$, Student-t-test). Complexation of the CH-PEO membrane with heparin improved the resistance to platelet adhesion by 50.1% ($p \leq 0.05$, Student t-test) (Fig. 8).

[0053] Both 10% and 2% loading significantly decrease platelet adhesion in the *in vitro* assays ($8.1 \pm 5.9 \cdot 10^3$ PLQ/cm² for 10% and 13.6 ± 9.1 for 2% 10^3 PLQ/cm² Vs. $37.1 \pm 8.7 \cdot 10^3$ PLQ/cm²). This corresponds to respectively a 78% and 63% inhibition of platelet adhesion ($p < 0.005$). CH-PEG membrane incubated in the presence of SNP also presented a significantly reduced platelet adhesion ($15.8 \pm 8.8 \cdot 10^3$ PLQ/cm²), hence confirming the ability of SNP to inhibit platelet activation (Fig. 2).

Arginine release

[0054] Both direct and indirect loading of the drug in the CH-PEO membrane were characterized by a high loss during the washing steps ($> 80\%$). The precomplexation of the cationic drug with the anionic LMW HA resulted only in a minor increase in the retention of the drug during the washing steps (18 % Vs.

13.6 %). The release behavior of the Arginine loaded membrane in PBS is presented in Fig. 9. Both direct and indirect loading resulted in a high burst release in PBS with most of the drug remaining in the membrane being released by the first hour (91% and 86%).

Discussion

[0055] The present invention describes the development of chitosan-based biodegradable membrane covered endovascular devices such as stents. The main finding was that metallic stent could be covered by a chitosan-based membrane displaying suitable properties for endoluminal implantation. To fulfill any clinical applications, such membrane should (1) be able to sustain the deformation during the endoluminal expansion of the stent; (2) not elicit extensive biological response; (3) be thromboresistant; (4) allowed cellular ingrowths both at the luminal and external surfaces and (5) be able to resist physiological blood pressure. Minimally invasive implantation of stents/membrane-covered stents is widely used in the treatment of obstructive/degenerative pathologies such as coronary and peripheral artery diseases, aneurysm, ruptures and fistulas. They are also investigated in non-vascular malignant diseases in urology or gastroenterology for instance. The most straightforward applications of membrane-covered stents are currently the endoluminal exclusion of aneurysm and the revascularization of vein graft.

[0056] The excellent mechanical properties of the chitosan-PEO blend allowed the hydrated device to be completely crushed on a catheter without noticeable damages to the membrane upon redeployment. In turn, the membrane covered stent could be loaded onto a delivery catheter and expanded through the self-expanding properties of the supporting metallic stents. Assays have investigated the use of reticulated membranes, using glyoxal or glutaraldehyde, or chitosan alone but these membranes failed to sustain the elastic deformation required during expansion. The blend of chitosan with high molecular weight PEO have been shown to drastically improve the elasticity and strength of chitosan (Kolhe P, and Kannan RM. *Biomacromolecules*; 4:173-180, 2003; and Budtova T, et al., *J Appl Polym Sci*;

84: 1114-1122, 2002). The latter has been explained by the intermolecular interactions between chitosan and PEO, especially close to the stoichiometric monomer ratio.

[0057] The second key-point in the design of such an endovascular device was the overall biocompatibility and haemocompatibility of the material. Both chitosan and PEO are well-known biocompatible biodegradable materials. In particular, chitosan is currently widely investigated as wound dressing material, drug delivery vehicle and tissue engineering scaffold (Rao SB, and Sharma CP., *J Biomed Mater Res*; **34**:21-28, 1997; and Madhally SV, and Matthew HW., *Biomaterials*; **20**: 1133-1142, 1999) . Chitosan supports cell attachment and growth and has been successfully investigated in vascular tissue engineering applications (Chupa JM, et al., *Biomaterials*; **21**:2315-2322, 2000). The poor endothelialization of synthetic graft materials has been called as a major cause of failure. In contrast, chitosan supports the attachment and growth of endothelial cells which may in turn enhanced the mid-term biocompatibility of the device. Acute blood compatibility of chitosan have however been reported to be an issue with reported ability of the polymer to activate both complement and blood coagulation systems. A recent exhaustive investigation of the blood compatibility of chitosan has however showed that despite large adsorption of plasma proteins, the polymer was a weak activators of the alternative pathway of the complement and intrinsic pathway of coagulation (Benesch J, and Tengvall P., *Biomaterials*; **23**:2561-2568, 2002). CH-PEO membranes were tested in an *ex vivo* extracorporeal porcine model using radiolabeled platelets and leukocytes. Amount of adsorbed platelets and leukocytes were low and in the same range than those measured on intact aortic segments used a negative control. Both values were significantly lower than the damaged artery model used as positive control. Endothelial denuded arteries have been previously used to simulate angioplasty-damaged blood vessels. To get further insight of the haemocompatibility of the CH-PEO membrane, an *in vitro* assay was used to compare the platelet adhesion on CH-PEO membrane with chitosan alone and heparin complexed CH-PEO membrane. The blending of chitosan with PEO tends to reduce the adhesion of platelets. This may be related to the

hydrophilicity of PEO that may decrease non-specific adhesion. A further improvement was observed upon surface complexation with heparin. Complexation of chitosan with anionic polysaccharide such as heparin has been widely used to improve its thromboresistance. Conversely, electrostatic complexation with glucosaminoglycans (GAGs) such as hyaluronic acid or heparin has been reported to modulate its biological activity (Chupa JM, et al., *Biomaterials*; **21**:2315-2322, 2000). Complex of chitosan and heparin have also recently been reported to enhance wound healing (Kweon DK, et al., *Biomaterials*; **24**:1595-1601, 2003).

[0058] Along with its mechanical properties and biocompatibility, the choice of chitosan as a base materials relied on its ability to achieve local delivery of biologically active components (Singla AK, and Chawla M. *J Pharm Pharmacol*; **53** :1047-1067, 2001). In particular chitosan has been investigated in therapies directed against cancer or hyperproliferative vascular disease using drugs such as doxorubicin or paclitaxel (Mitra S, et al., *J Control Release*; **74**:317-323, 2001; and Nsereko S, and Amiji M., *Biomaterials*; **23**:2723-2731, 2002;). The loading and delivery of the NO-precursor L-Arginine was investigated in the present application. Arginine is a low molecular weight cationic drug that has been proved to be effective in the reduction of neointimal hyperplasia (Suzuki T, et al., *Am J Cardiol*; **89**:363-367, 2002; and Kalinowski M, et al., *Radiology*; **219**:716-723, 2001). The release behavior presented in Fig. 9 shows an initial burst release with small amount of the drug being released after 1 h. Importantly, a significant amount (86.4 %) of the drug was lost during the neutralization and washing procedures. The possibility to control the release behavior by precomplexation of the cationic drug with the plasticizer low molecular weight hyaluronic acid (LMW HA) was thus investigated. Such precomplexation method has been used to improve the release behavior of doxorubicin in chitosan nanoparticles. Only a modest improvement was obtained as the initial loss during the washing procedure remained high (82 %) and most of the drug was released during the initial burst (86 % at 30 min Vs. 91 % for the direct method). Much longer release profile could however be achieved using anionic drug or higher molecular weight molecules. The NO

donor sodium nitroprusside was also loaded into the CH-PEO membrane. A dose-dependant reduction in the amount of adhered platelets was obtained in the in vitro assays. The latter further confirmed the ability of the membrane to act efficiently as a drug delivery system.

[0059] While the membrane-covered device was initially designed for the treatment of occlusive diseases and vein graft stenoses, its potential use in the setting of endovascular aneurysm closure is also considered as a promising application in the present invention. The possibility to exclude the aneurysm by the chitosan-based membrane as well as the potential for local delivery of biologically active components such as growth factors are appealing. The CH-PEO membrane acts as a temporary barrier while being used as a template for arterial reconstruction. Organization of the blood thrombi into connective tissue may be expected to solve the issue of endoleak that plague endovascular aneurysm exclusion. Such organization is enhanced by the presence of the chitosan based membrane and further accelerated by incorporation of appropriate growth factors. Sealing of the membrane to prevent growth of the aneurysm is however required. The water permeation assays used here showed that the CH-PEO membrane covered stent showed an excellent blockade of saline solution and less than $1 \text{ mL/cm}^2 \text{ min}^{-1}$ was measured. The low volume of solution prevented more precise determination but these values are better or comparable to that reported for commercially available graft such as the cross-linked collagen Dacron impregnated Hemashield® ($<10 \text{ mL/cm}^2 \text{ min}^{-1}$). The burst resistance of the membrane should also be high enough to prevent failure upon the aneurismal transmural pressure. Burst pressure resistance of a monolayered CH-PEO membrane was determined to higher than 500 mm Hg. This value is expected to sustain transmural pressure occurring in aneurysm. Additional CH-PEO layer could be useful to increase the burst resistance. In addition, thrombus formation and tissue ingrowths within the membrane in contact with fluids of the excluded area of the aneurysm could act as additional sealing and reinforcing material. In an attempt to apply the concept of tissue engineering in the field of aneurysm closure, the possibility to add an external porous layer that could be truly used as a scaffold for vascular cells

was also investigated. Tissue engineering of vascular graft has been the object of much interest due to the unsolved clinical issue of small vascular graft. The advantage of using biological materials such as collagen as construct is counterbalanced by the inadequate mechanical properties of these polymers. Hybrid graft using dacron sleeves combined with collagen-based construct have been proposed to assure enough burst resistance for *in vivo* implantation (Berglund JD, et al., *Biomaterials*; **24**:1241-1254, 2003; and Xue L, and Greisler HP., *J Vasc Surg*, **37**:472-480, 2003;). The presence of synthetic sleeves may however be damageable for the long term success of the graft. On the other hand, graft made completely from biodegradable polymers required lengthy *in vitro* tissue formation to display appropriate mechanical properties for implantation. A hybrid device conjugating the mechanical scaffold of the metallic device and the biodegradable chitosan-based porous matrix open new opportunities in this field. Metallic stents do not elicit intensive biological reactions such as those commonly observed with polymeric synthetic materials. The metallic component of the hybrid construct can provide the necessary mechanical strength, at least at the acute phase of the tissue organization, while minimizing the amount of non-biodegradable material within the artery in comparison to synthetic polymeric sleeves. In addition, cell ingrowths naturally occurring in chitosan matrix could be easily enhanced by incorporation of growth factors in the chitosan-based membrane (Lee JY, et al., *J Control Release*; **78** :187-197, 2002).

Conclusion

[0060] This study showed that a biodegradable membrane covered stent could be designed based on the excellent mechanical properties of chitosan-PEO blend. The device could be loaded onto a catheter and expanded without noticeable damage to the membrane, thus authorizing endoluminal delivery. The biological properties of chitosan and its biocompatibility associated with the potential to achieve uniform local delivery of biologically active components to the vascular wall suggest that such device could be used in the treatment of various pathologies such as vascular obstructive diseases, aneurysms and malignant diseases. While the *in vitro* experiments presented here are

promising, further *in vivo* investigations are warranted to prove its clinical potential.

[0061] While the invention has been described in connection with specific embodiments thereof, it will be understood that it is capable of further modifications and this application is intended to cover any variations, uses, or adaptations of the invention following, in general, the principles of the invention and including such departures from the present disclosure as come within known or customary practice within the art to which the invention pertains and as may be applied to the essential features hereinbefore set forth, and as follows in the scope of the appended claims.

WHAT IS CLAIMED IS:

1. A biodegradable membrane covered endovascular device, said device being coated with a solution of chitosan-plasticizer compound dried on the device, forming a flexible polymeric membrane on the device.
2. The device of claim 1, wherein the plasticizer compound is selected from the group consisting of polyethylene oxide (PEO), cellulose, keratin, collagen, anionic polysaccharide, and poly(α -hydroxy acid).
3. The device of claim 1, wherein said solution of chitosan-plasticizer compound further comprises an active ingredient.
4. The device of claim 3, wherein said active ingredient is selected from the group consisting of growth factor, anti-proliferative drug, anti-inflammatory drug, nitric oxide donor compound, radionuclide, nucleic acid, peptide, and protein.
5. The device of claim 4, wherein said anti-proliferative drug is selected from the group consisting of paclitaxel, sirolimus, tacrolimus, everolimus, dexamethasone, angiopeptin, angiotensin converting enzyme inhibitor, calcium channel blocker, colchicine, fibroblast growth factor (FGF) antagonists, fish oil, low molecular weight heparin, histamine antagonist, lovastatin, methotrexate, monoclonal antibody specific to PDGF receptor, nitroprusside, phosphodiesterase inhibitor, prostacyclin analogue, prostaglandin inhibitor, seramin, serotonin blockers, steroids, thioprotease inhibitor, triazolopyrimidine.
6. The device of claim 1, wherein said device is a stent.
7. The device of claim 2, wherein said solution of chitosan-plasticizer compound is a 70:30 weight to weight chitosan:polyethylene oxide solution.

8. The device of claim 6, wherein said device has a metallic scaffold made of stainless steel, NiTi alloy, titanium alloys, Conichrome, Phynox, MP35N, cobalt-based alloys, tantalum titanium-zirconium-niobium alloys, titanium-aluminum-vanadium alloy, platinum, tungsten, tantalum, or a combination thereof.
9. The device of claim 1, wherein the polymeric membrane comprises chitosan, or chitosan blends or composites complex with a biocompatible synthetic or natural polymer.
10. A method for producing a biodegradable membrane-covered device, said method comprising the steps of:
 - a) preparing a solution containing chitosan and a plasticizer compound;
 - b) contacting a device to be covered with the solution of step a); and
 - c) allowing the solution to dry onto said device.
11. The method of claim 10, further comprising after step c) the steps of:
 - d) rinsing the device of step c) with an alkaline solution;
 - e) rinsing the device of step d) with a physiological buffer;
 - f) allowing the device of step e) to dry.
12. The method of claim 10, wherein said plasticizer compound is selected from the group consisting of polyethylene oxide (PEO), cellulose, keratin, collagen, anionic polysaccharide, and poly(α -hydroxy acid).
13. The method of claim 10, wherein the solution is prepared by dissolving in solutions chitosan in an acidic medium and the plasticizer compound in an acid and mixing the solutions of chitosan and plasticizer compound together to form the solution used in step a).

14. The method of claim 10, wherein said solution containing chitosan and the plasticizer compound is a 70:30 weight to weight chitosan:polyethylene oxide solution.
15. The method of claim 10, wherein the solution of step a) further comprises an active ingredient.
16. The method of claim 10, wherein said active ingredient is selected from the group consisting of growth factor, anti-proliferative drug, anti-inflammatory drug, nitric oxide donor compound, radionuclide, nucleic acid, peptide, and protein.
17. The method of claim 16, wherein said anti-proliferative drug is selected from the group consisting of paclitaxel, sirolimus, tacrolimus, everolimus, dexamethasone, angiopeptin, angiotensin converting enzyme inhibitor, calcium channel blocker, colchicine, fibroblast growth factor (FGF) antagonists, fish oil, low molecular weight heparin, histamine antagonist, lovastatin, methotrexate, monoclonal antibody specific to PDGF receptor, nitroprusside, phosphodiesterase inhibitor, prostacyclin analogue, prostaglandin inhibitor, seramin, serotonin blockers, steroids, thioprotease inhibitor, triazolopyrimidine.
18. The method of claim 10, wherein said device is a stent.
19. A method for treating aneurysm comprising the steps of implanting a device as defined in claim 6 in a blood vessel of a patient suffering from an aneurysm, such that the device is implanted over the opening of the aneurismal sac in the blood vessel, the chitosan/polyethylene oxide coated device allowing cells to adhere to the device, thereby closing the aneurismal sac.
20. Use of a device as defined in claim 3, for treating a disease located at the surface of a tubular organ.

21. The use of claim 20, wherein the tubular organ is a blood vessel or the esophagus.
22. The use of claim 20, wherein the disease is a tumor.
23. The use of claim 20, wherein the disease is a stenose or another vasculature-related disease.
24. The use of claim 20, wherein the organ is a vein graft used in a by-pass procedure.

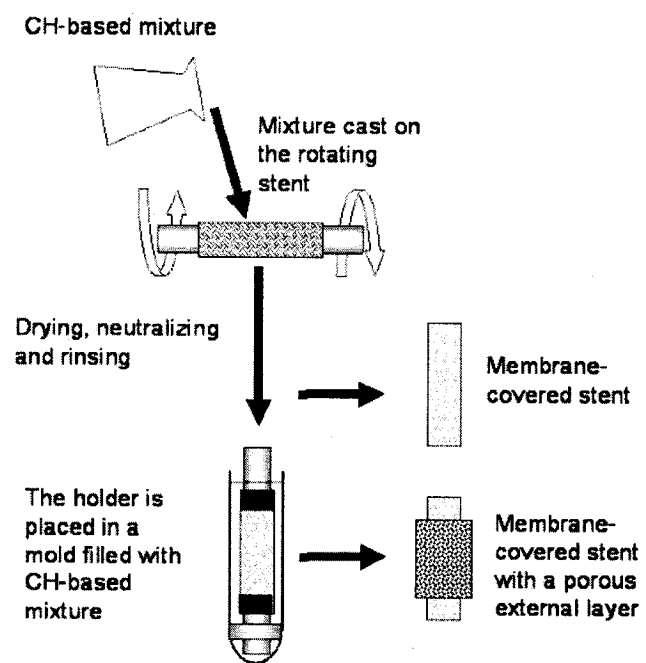


Fig. 1

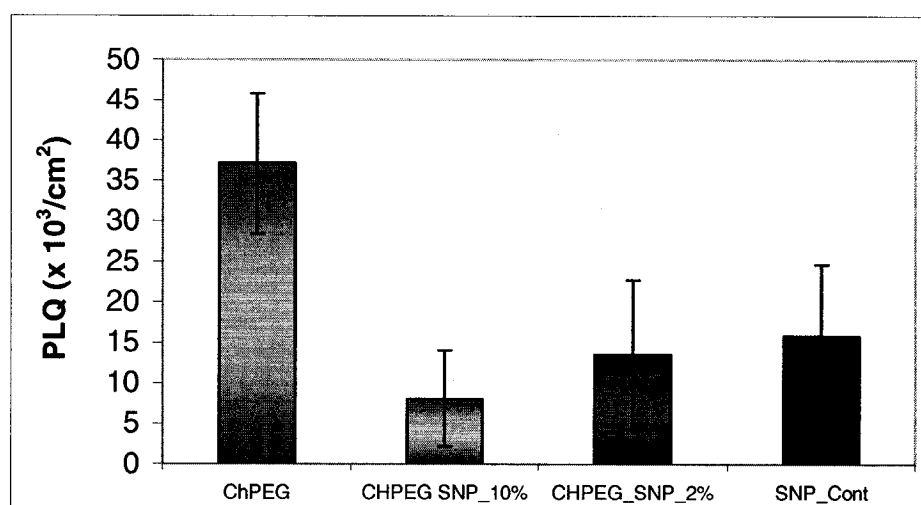


Fig. 2

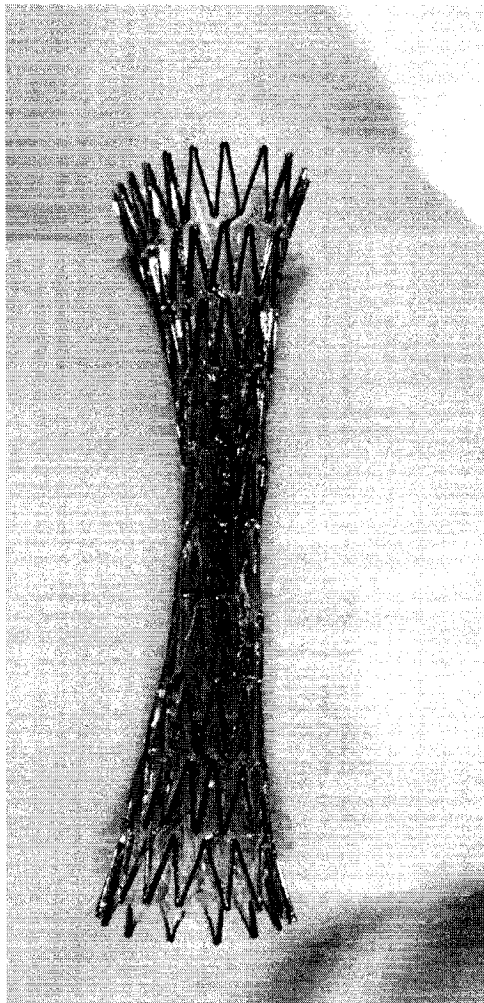


Fig. 3A

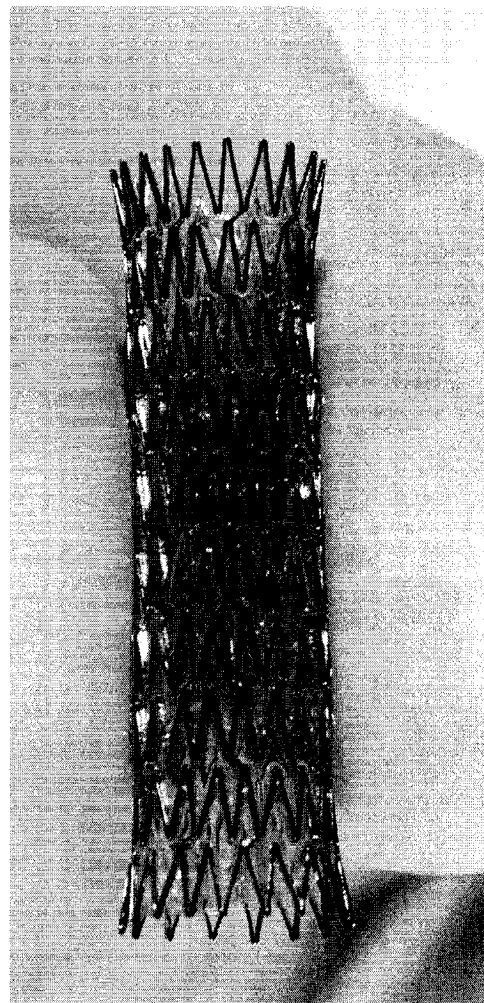


Fig. 3B



Fig. 4A

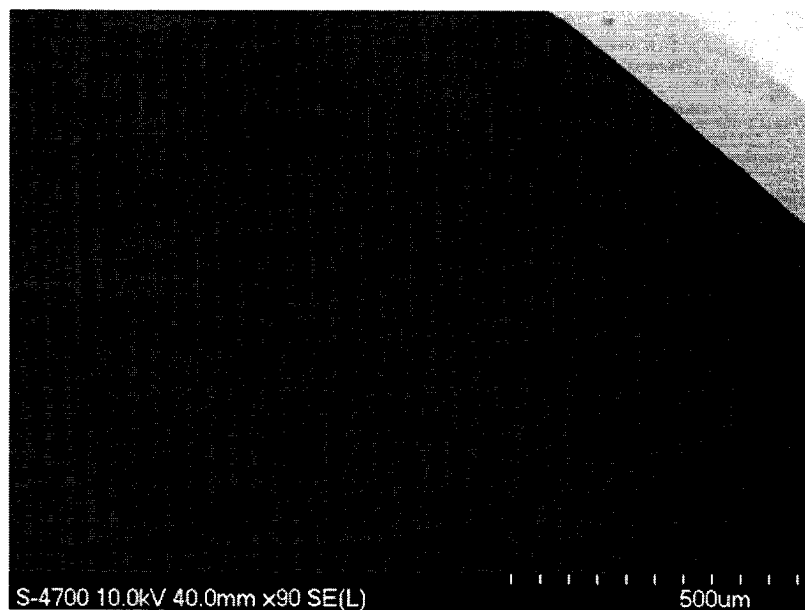


Fig. 4B

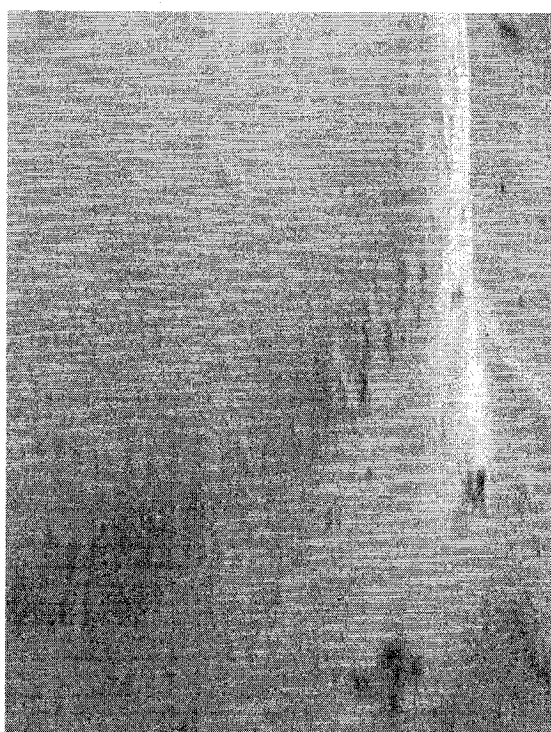


Fig. 4C

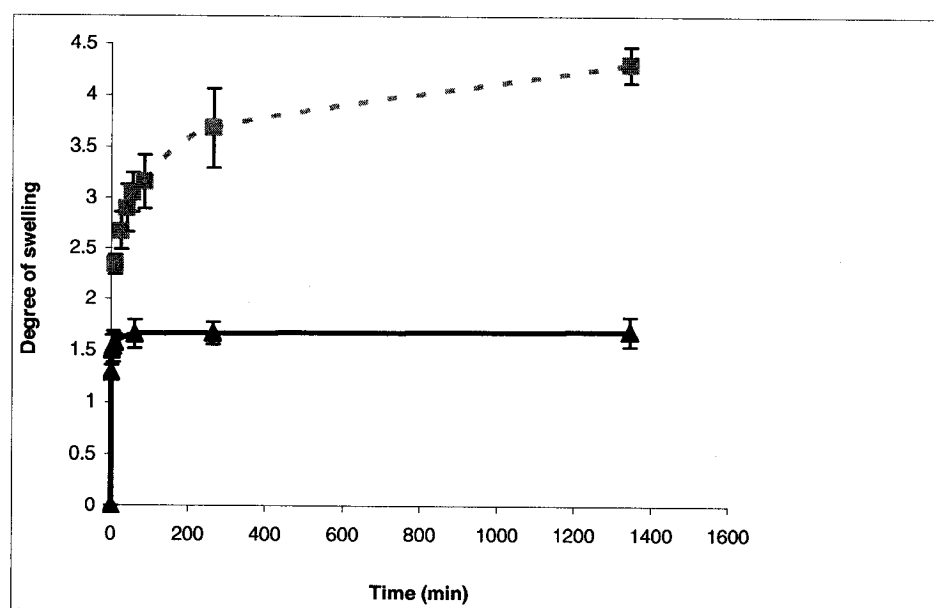


Fig. 5A

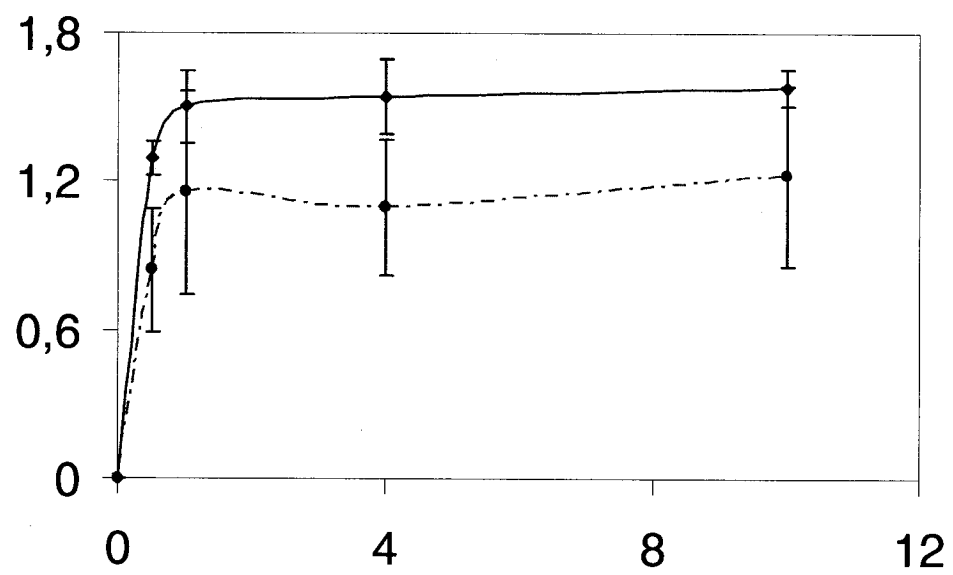


Fig. 5C

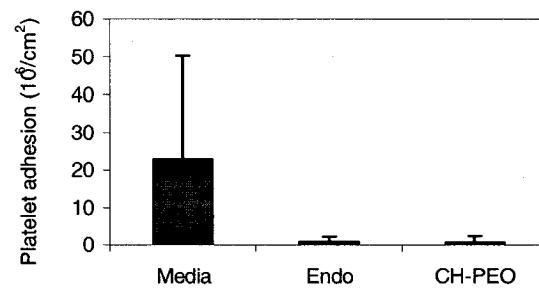


Fig. 6

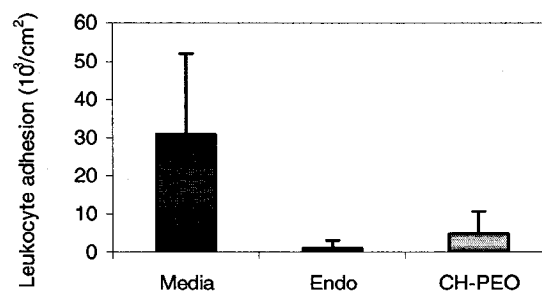


Fig. 7

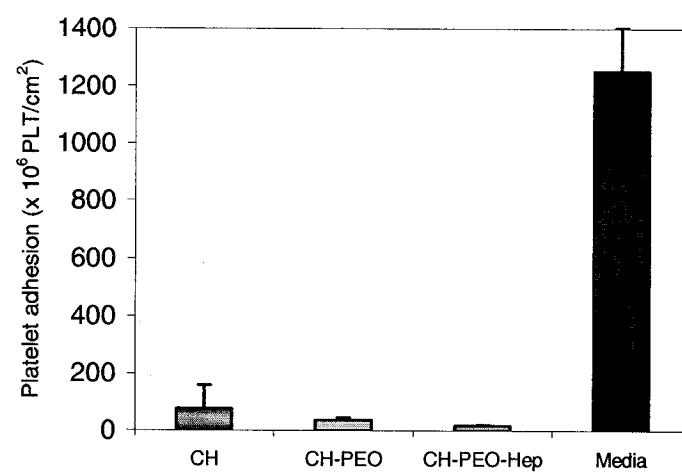


Fig. 8

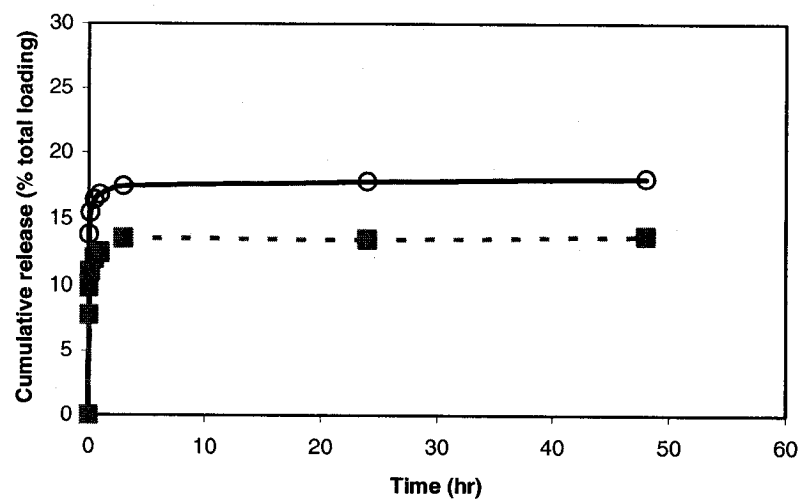


Fig. 9

Bioactive Coatings of Endovascular Stents Based on Polyelectrolyte Multilayers

Benjamin Thierry,[†] Françoise M. Winnik,[‡] Yahye Merhi,[§] Jim Silver,^{||} and Maryam Tabrizian^{*†}

Department of Biomedical Engineering, Mc Gill University, 3775 University Street, Montreal, Qc, H3A 2B4, Canada, Faculté de Pharmacie et département de Chimie, Université de Montréal, C.P. 6128 Succ. Centre ville, Montreal, Qc, H3C 3J7 Canada, Montreal Heart Institute, 5000 rue Belanger Est, Montreal, H1T 1C8, Canada, and Cordis Corporation—Nitinol Devices & Components (NDC), 47533 Westinghouse Drive, Fremont, California 94539

Received June 11, 2003; Revised Manuscript Received August 29, 2003

Layer-by-layer self-assembly of two polysaccharides, hyaluronan (HA) and chitosan (CH), was employed to engineer bioactive coatings for endovascular stents. A polyethyleneimine (PEI) primer layer was adsorbed on the metallic surface to initiate the sequential adsorption of the weak polyelectrolytes. The multilayer growth was monitored using a radiolabeled HA and shown to be linear as a function of the number of layers. The chemical structure, interfacial properties, and morphology of the self-assembled multilayer were investigated by time-of-flight secondary ions mass spectrometry (ToF–SIMS), contact angle measurements, and atomic force microscopy (AFM), respectively. Multilayer-coated NiTi disks presented enhanced antifouling properties, compared to unmodified NiTi disks, as demonstrated by a decrease of platelet adhesion in an in vitro assay (38% reduction; $p = 0.036$). An ex vivo assay on a porcine model indicated that the coating did not prevent fouling by neutrophils. To assess whether the multilayers may be exploited as in situ drug delivery systems, the nitric-oxide-donor sodium nitroprusside (SNP) was incorporated within the multilayer. SNP-doped multilayers were shown to further reduce platelet adhesion, compared to standard multilayers (40% reduction). When NiTi wires coated with a multilayer containing a fluorescently labeled HA were placed in intimate contact with the vascular wall, the polysaccharide translocated on the porcine aortic samples, as shown by confocal microscopy observation of a treated artery. The enhanced thromboresistance of the self-assembled multilayer together with the antiinflammatory and wound healing properties of hyaluronan and chitosan are expected to reduce the neointimal hyperplasia associated with stent implantation.

Introduction

Percutaneous transluminal coronary angioplasty (PTCA) is widely used for the treatment of occlusive blood vessel diseases. Stent implantation, representing as much as 1 000 000 procedures each year, has improved the safety of the procedures and has been shown to reduce restenosis, i.e., the reobstruction of the targeted artery. The reduction of restenosis is attributed to the scaffolding effect of the stent which prevents elastic recoil and constrictive remodeling of the artery.¹ However stent implantation is also associated with an excessive proliferation of vascular smooth muscle cells (SMCs), extracellular matrix synthesis, and a chronic inflammatory reaction which are believed to be initiated by the deep vascular injury and the endothelial cell denudation created during angioplasty and further enhanced by the presence of a foreign metallic device.^{1,2} This complication,

known clinically as in-stent restenosis, occurs in about 15 to 30% of the procedures.

Two new developments in stent technology show promise in alleviating thrombosis and in-stent restenosis. One approach consists attempting to improve the biocompatibility of stents by modifying their surfaces with less thrombogenic and inflammatory materials. These coatings include inorganic materials such as carbon, or silicon carbide, or biomimetic materials such as phosphorylcholine-modified surfaces.^{1,3} Another approach, which has been shown to be particularly effective in lowering SMCs proliferation and significantly delaying in-stent restenosis, is to coat stents with a layer loaded with therapeutic agents, such as Rapamycin or Taxol, which are released gradually at the implantation site.^{1,3} These drugs are usually embedded into a polymeric matrix. However, early work with stents coated with biodegradable polymers, such as polyglycolic acid/poly(lactic acid) copolymers, polycaprolactone poly(hydroxybutyrate valerate), and poly(ethylene oxide)/poly(butylene terephthalate) [PEO/PBTP] as well as nonbiodegradable polymers, such as polyurethane [PUR], silicone [SIL], and poly(ethylene terephthalate) [PETP], were disappointing and indicated that the polymers

* To whom correspondence should be addressed. E-mail: maryam.tabrizian@mcgill.ca.

[†] Mc Gill University.

[‡] Université de Montréal.

[§] Montreal Heart Institute.

^{||} Cordis Corporation—Nitinol Devices & Components.

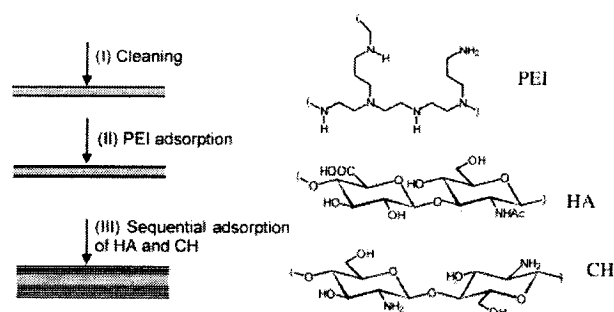


Figure 1. Schematic diagram of the deposition of CH/HA self-assembled multilayer on NiTi substrates; (I) Cleaning of the metallic substrate; (II) Adsorption of a PEI layer; (III) Sequential adsorption of the CH and HA polyelectrolytes. The molecular structures of the polyelectrolytes are presented.

triggered long-term inflammation.⁴ The disappointing clinical results recently obtained with the hexanoyltaxol (QP2)-eluting polymer stents (QuaDS) may also be related to such polymer-induced chronic inflammation at the site of stent implantation.⁵ This set-back underscores the importance of the biocompatibility of the polymer used as drug carrier material. Other methods to create intelligent biocompatible polymeric interfaces need to be investigated as they may provide relief from the many side effects of stent implantation.

We report here novel coatings for stents created by the formation of insoluble interpolymeric complexes generated by depositing oppositely charged polyelectrolytes. The layer-by-layer self-assembly (L-b-L) of polycations and polyanions into multilayers has emerged as an efficient, versatile, yet simple, technique to create biologically active surfaces. The method relies on the sequential charge inversion of a polymeric surface upon successive immersions of this surface in solutions of oppositely charged polyelectrolytes.⁶ The L-b-L technique has been used on various substrates with bioactive molecules, such as drugs, enzymes, DNA, or proteins.^{7–13} Bioactive molecules may be incorporated in the multilayer during the polyelectrolyte deposition process, yielding drug-releasing interfaces on various substrates via a process readily applicable to various substrates. We reported recently the deposition of polyelectrolyte multilayers onto angioplasty damaged arteries, resulting in a drastic reduction of thrombogenicity.¹⁴

We describe the preparation and properties of a new bioactive nanocoating of endovascular devices based on the layer-by-layer self-assembly of two natural polysaccharides, chitosan (CH) and hyaluronan (HA) (Figure 1). Chitosan is a linear polysaccharide containing two β -1,4-linked sugar residues, *N*-acetyl-D-glucosamine and D-glucosamine, distributed randomly along the polymer chain. It is obtained commercially by partial de-*N*-acetylation of chitin. The chitosan used in this study contained approximately 15 mol % *N*-acetyl-D-glucosamine residues. It is only soluble in aqueous solutions of low pH, because its pK_a value is ~ 6.3 . Hyaluronan is a naturally occurring linear high molecular weight anionic polymer ($pK_a = 2.9$) consisting of alternating *N*-acetyl- β -D-glucosamine and β -D-glucuronic acid residues linked (1 \rightarrow 3) and (1 \rightarrow 4), respectively (Figure 1). It plays an important structural and mechanical role in various tissues,

participates in the control of tissue hydration and water transport, and affects numerous biological processes, such as inflammation, tumor metastasis, and development.¹⁵ The exact role of HA in the fibroproliferative response of vascular vessel toward angioplasty, however, remains unclear and contradictory results have been reported.^{16–21} The inhibitive effects of HA with respect to hyperplasia observed after either systemic or local delivery suggest that the antiproliferative effects of HA may be associated with its antiinflammatory properties.¹⁶ Both CH and HA have found a variety of applications in biomedical engineering and in cardiovascular applications.^{22,23} Their use as components of multilayers has been reported in conjunction with oppositely charged polyelectrolytes such as poly(lysine) in the case of HA^{24,25} and dextran sulfate in the case of CH.²⁶

We describe the deposition of CH/HA self-assembled multilayers on metallic substrates and their characterization by time-of-flight-secondary ions mass spectrometry (ToF-SIMS), atomic force microscopy (AFM), confocal microscopy, and dynamic contact angle measurements. Their antifouling properties are evaluated both *in vitro* and *ex vivo* in order to assess whether they may enhance the haemocompatibility of metallic endovascular devices.

To determine if HA/CH multilayers can serve as an *in situ* drug delivery vehicle, we prepared HA/CH multilayers with sodium nitroprusside (Figure 1), following methodologies previously used to introduce various ionic dyes and proteins within polyelectrolyte multilayers.^{27,28} Sodium nitroprusside, a nitrous oxide donor which spontaneously decomposes in biological environments,²⁹ is widely used clinically to reduce blood pressure and has emerged as a promising modality in the treatment of restenosis.³⁰ The success of the NO-based therapies seems to rely on the efficiency of the delivery of therapeutic amounts of NO to the vascular wall. We monitored the effect of SNP incorporation on the physicochemical properties of the multilayers, to ensure that SNP incorporation did not affect the creation of a multilayer, and we assessed the level of platelet adhesion onto CH/HA-coated surfaces in order to gain insight into the possible beneficial clinical effects against in-stent restenosis of a strategy combining the complexation of natural polysaccharides and the *in situ* release of a drug incorporated within the polysaccharide multilayers.

Experimental Section

Substrate Preparation. NiTi disks and wires (Ni: 55.8 wt %) provided by Nitinol Devices & Components (Fremont, CA) were used as substrates. The specimens were polished mechanically to a mirror-like finish using a 0.3- μ m alumina paste (disks) or sand-blasted (wires). They were passivated as recommended by ASTM standard.³¹ They were subsequently thoroughly cleaned using 2-propanol and pure water. Hydrophobic high-density polyethylene, HDPE, (medical grade) was used as substrate for the dynamic contact angle measurements.

Preparation of the Self-Assembled Coatings. Solutions of sodium hyaluronate (HA, molecular weight 600 000 Da, supplied by Hyal, Canada; 1 mg/mL in 0.14 M aqueous

NaCl, pH 6), chitosan (CH, high molecular weight, deacetylation degree >85%, obtained from Sigma Chemicals; 1.5 mg/mL in 0.1 M acetic acid containing 0.14 M NaCl, pH 4), and polyethyleneimine (PEI, branched, molecular weight 70 000 Da, supplied by Aldrich; 5 mg/mL in 0.14 M aqueous NaCl) were prepared separately. Ultrapure water (18.2 M Ω ·cm²) was used in all experiments (Milli Q system, Millipore). The substrate was dipped in the PEI solution and was allowed to adsorb on the surface for 20 min, thus creating a precursor layer to initiate the L-b-L self-assembly. The multilayer build-up was accomplished by sequential dipping of the substrate in the polysaccharide solution (alternating between HA and CH), followed by a 5-min adsorption and a wash with a flow of 0.14 M NaCl (pH 6). (Figure 1).

HA Derivatives Used for Characterization. Diethylenetriaminopentaacetic acid (DTPA), a chelator able to form stable complexes with radionuclides, was linked to HA as previously described to prepare HA-DTPA with a degree of substitution of ~0.15 DTPA/disaccharide unit.³² Radiolabeled ¹¹¹In-HA was prepared as follows: HA-DTPA (29 mg) was dissolved in water (20 mL) for 24 h in a glass vial. Then ¹¹¹InCl₃ (100 μ Ci) was introduced in the vial. The resulting solution was stirred at RT for 2 h to ensure complete complexation. The ¹¹¹In-HA complex was purified by extensive dialysis against water. The final volume was adjusted to obtain a ¹¹¹In-HA concentration of 1 mg/mL (0.8 10⁶ cpm/mg HA).

The fluorescein derivative of HA (HA-FITC) was used to monitor the fate of the polymer deposited on the stent when placed in contact with an artery. It was prepared as follows. A solution of FITC from Sigma (4 mg, COOH/Fluorescein molar ratio: 25:1) was added to a solution of HA (80 mg) in aqueous borate buffer (pH 9.4). The reaction mixture was stirred at RT for 3 h under N₂ in the dark. HA-FITC was purified by dialysis against borate buffer for 12 h and against water for 3 days. It was recovered by lyophilization.

The HA derivatives, ¹¹¹In-HA and HA-fluorescein dichlorotriazine (HA-FITC), were used as described above to characterize the build up of the multilayer.

Sodium Nitroprusside Loading. An aliquot of a stock solution of SNP in water (10 mg/mL) was added to the chitosan coating solution 10 min before beginning the coating procedure to achieve a concentration of 0.2 mol SNP/mol NH₂. The multilayered self-assemblies were built up as described above using the chitosan-SNP solution, instead of a CH solution. All manipulations were done in the dark to prevent decomposition of the SNP.

Characterization. Contact angles were obtained from static contact angle measurements of deionized water droplets. Contact angles of a NiTi surface coated with various numbers of CH/HA layers³³ were measured with a video contact angle system (VCA 2500, AST, Billerica, Ma) applying a 1- μ L droplet of deionized water (18.2 M Ω) on the samples' surfaces. The contact angles were determined semi-manually from the droplet image with a precision of $\pm 2^\circ$.

Time-of-flight secondary ions mass spectrometry analyses were recorded using an ION TOF IV spectrometer (ION-TOF, Germany) equipped with a primary ion Ga⁺ beam

operated at 15 keV. Areas of about 100 and 8 μ m² were analyzed under the so-called "static" condition with ion doses of about 10⁹ ions/cm². The calibration of the mass spectra in the positive mode was based on hydrocarbon peaks such as CH₃⁺, C₂H₂⁺, and C₃H₅⁺ and peaks from the metallic substrates when possible. Relative normalized intensities [$I_{\text{coatings}}/(I_{\text{Ti}} + I_{\text{Ni}})$] were determined by dividing the integral of the coating characteristic peaks by the integral of the titanium and nickel peaks originating from the substrate. Chemical imaging of the masses associated with CH₃CO⁺ (43.017), Ti (47.054), and Ni (57.936) was achieved in the burst alignment mode.

Atomic force microscopy analyses were used to further investigate the growth of the coating on mechanically polished NiTi disks. AFM (Nanoscope III, Digital Instruments, Santa Barbara, CA) was performed in the tapping mode to avoid damaging the surface. Areas of about 5 μ m² were scanned with a scan rate of 0.5 Hz.

Translocation of the Coating from the Metal Surface to the Vascular Wall. The fluorescence of HA-FITC was used to visualize the presence of the polysaccharide coating onto the metallic substrate and to determine its fate when placed in contact with vascular tissues. The specimens were kept in the dark during all of the experiments to prevent photobleaching. HA(CH/HA)₄ multilayers were deposited onto NiTi wires and kept in PBS for various periods of time before being observed with an Axiovert inverted microscope equipped with an LSM 510 confocal system (Zeiss) or kept for translocation studies. Applying a gentle pressure, multilayer coated wires were placed in contact with the luminal surface of fresh aortic porcine arteries placed in a polycarbonate chamber. Wire-contacting arteries were incubated in PBS for 2 days at 4 °C in the dark. Prior to observation by confocal microscopy, the specimens were snap-frozen in 2-methyl-butane using liquid nitrogen and kept at -80 °C, to prevent drug diffusion during handling and storage. Tissues were microtomed into 10 μ m thick sections with a cryostat and mounted onto a glass slide prior to fixation with 4% paraformaldehyde. The sections were imaged. Corrections for the artery autofluorescence were performed using a section of porcine artery not exposed to the fluorescent NiTi wires.

Haemocompatibility. Platelet adhesion was investigated as previously described.^{14,34} Briefly, fresh blood (120 mL) was drawn from healthy, medication-free volunteers. The blood was collected in syringes preloaded with acide citrate dextrose (ACD). Platelet rich plasma (PRP) was prepared by centrifugation of the blood at 1800 rpm for 15 min. The PRP was then centrifuged at 2200 rpm for 10 min, and the platelet poor plasma (PPP) was recovered as the supernatant. Platelets were carefully resuspended in citrate buffer and incubated with 250 μ Ci of ¹¹¹InCl₃ for 15 min. The platelets were recovered by centrifugation, resuspended in PPP to a concentration of 2.5×10^6 platelets/mL. A freshly prepared ¹¹¹In-platelet solution (3 mL) was added to polystyrene dishes (Corning Inc.) containing the test materials. Platelet adhesion was allowed to proceed for 60 min with gentle shaking. After incubation, the samples were recovered, washed 4 times with saline and fixed in a 2% glutaraldehyde solution. The amount

Table 1. Contact Angle with Water as a Function of the Number of Layers

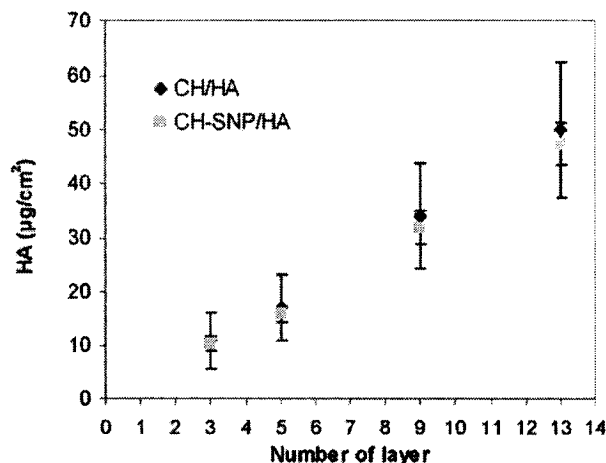
self-assembled coating	contact angle
NiTi	67 ± 4
NiTi/PEI	69 ± 3
NiTi/PEI/HA	42 ± 4
NiTi/PEI/HA/CH	39 ± 3
NiTi/PEI/HA/(CH/HA)	40 ± 2
NiTi/PEI/HA/(CH/HA)CH	36 ± 4
NiTi/PEI/HA/(CH/HA) ₂	33 ± 3
NiTi/PEI/HA/(CH/HA) ₃	31 ± 5
NiTi/PEI/HA/(CH/HA) ₄	29 ± 4

of platelets was determined using a gamma counter (1470 Wizard, Wallac, Finland) after correction for background signal and radioactivity decay.

The adhesion of ¹¹¹In polymorphonuclear neutrophils (PMNs) was investigated using an extracorporeal procedure in ex-vivo perfusion chambers. The radiolabeling, animal surgery, and extracorporeal procedures were performed as previously described.^{34,35} Four pigs weighing 28 ± 3 kg were used in the experiments. All procedures followed the American Heart Association guideline for animal research and were approved by the local ethics committee. The extracorporeal shunt consisted of two parallel silicon tubing channel circuits connecting the femoral artery to the perfusion chambers and returning to the femoral vein. Radiolabeled PMNs were re-injected into the animals 1 h before the beginning of the experiments. A home-built parallel plate flow chamber was used. Injured arterial segments from normal porcine aortas were prepared as described previously and were used as control.³⁵ The perfusion procedure was initiated by a 1-min wash with saline. The blood was allowed to circulate into the extracorporeal circuit for 15 min at a physiological wall shear rate of 424 s⁻¹. The circuit was flushed with saline for 30 s, and the samples were recovered and fixed in 1.5% glutaraldehyde in gamma-counter vials. The total amount of PMNs adsorbed on the surface was calculated knowing the specific activity of blood samples used as reference and using haematology performed prior to each experiment.

Results and Discussion

Preparation and Characterization of the Self-Assembled Coating on Surfaces. The multilayer coating procedure was initiated by the adsorption of a PEI layer onto a substrate, yielding a positively charged surface, subsequently placed in contact, in turn, with a solution of the polyanion HA and a solution of the polycation CH. The multilayer construction was expected to modify greatly the wettability of the substrate. This effect was monitored by measuring the contact angle of a water droplet deposited on the surface (Table 1). Deposition of a layer of PEI and subsequent treatment with a solution of HA resulted in a sharp decrease of the contact angle (42 ± 4 Vs 67 ± 4 for NiTi). The contact angle further decreased with increasing layer number, reaching an angle of about 30° upon deposition of 7 single layers and remaining constant upon further polyelectrolyte layer deposition. In agreement with previously

**Figure 2.** Amount of ¹¹¹In-HA (μg/cm²) as a function of the number of layer for the CH/HA and CH-SNP/HA polyelectrolytes self-assembled onto NiTi substrates; 3 NiTi-PEI-HA(CH/HA)₁, 5 NiTi-PEI-HA(CH/HA)₂ and so on.

reported data, the fact that, after deposition of 4 bilayers, there was no further changes in the contact angle led us to conclude that at least 4 bilayers were necessary to mask the substrate with respect to the properties of the multilayer/water interface.³⁶ As a consequence, HA(CH/HA)₄ self-assembled coatings built on PEI-NiTi were considered as representative of the 3-dimensional polysaccharide multilayer coating and used in the biological assays described below.

The multilayer build-up procedure was monitored next by measuring the radioactivity of multilayers obtained using ¹¹¹In-HA instead of HA. This highly sensitive method allowed us to quantitate the amount of HA deposited in each step and thus to ascertain that the multilayer build-up procedure follows the general L-b-L mechanism. It should be noted that this analytical method gives us information on the construction of ¹¹¹In-HA/CH multilayers and not on HA/CH assemblies. Data presented elsewhere indicate that the use of the labeled HA slightly overestimates the amount of HA incorporated in the multilayer under the conditions employed in this work.¹⁴ The amount of HA in the coating increased linearly with the number of layers (Figure 2, slope: 3.8 μg HA/bilayer, *r*² = 0.99), indicating that the two polyelectrolytes follow a typical linear multilayer construction mechanism.

A more detailed analysis of the nanocoating was obtained by a ToF-SIMS examination of metal surfaces recovered after each coating step. A spectrum of a PEI coated surface presented several nitrogen containing peaks attributed to PEI, e.g., CH₂N⁺ (*m/z* 28.018), C₂H₃N⁺ (*m/z* 41.025), and C₃H₈N⁺ (*m/z* 58.064) (Figure 2) and also several peaks characteristic of NiTi (⁴⁶Ti, *m/z* 45.954), (⁴⁷Ti, *m/z* 46.954), (⁴⁸Ti, *m/z* 47.954), (⁴⁸TiH, *m/z* 48.956), (⁵⁰Ti, *m/z* 45.947), (⁴⁸TiO, *m/z* 63.949), (⁵⁸Ni, *m/z* 57.936), (⁵⁸NiH, *m/z* 58.942), and (⁶⁰Ni, *m/z* 59.931), suggesting that the metal surface has not been fully coated with PEI. Next, we recorded ToF-SIMS spectra of a HA(CH/HA)₄ self-assembled coating (Figure 3). A spectrum of a Si wafer spin-coated with HA was also recorded to allow the attribution of the peaks characteristic of HA. In agreement with a previously reported ToF-SIMS analysis of HA, the spectrum of the HA-coated Si wafer

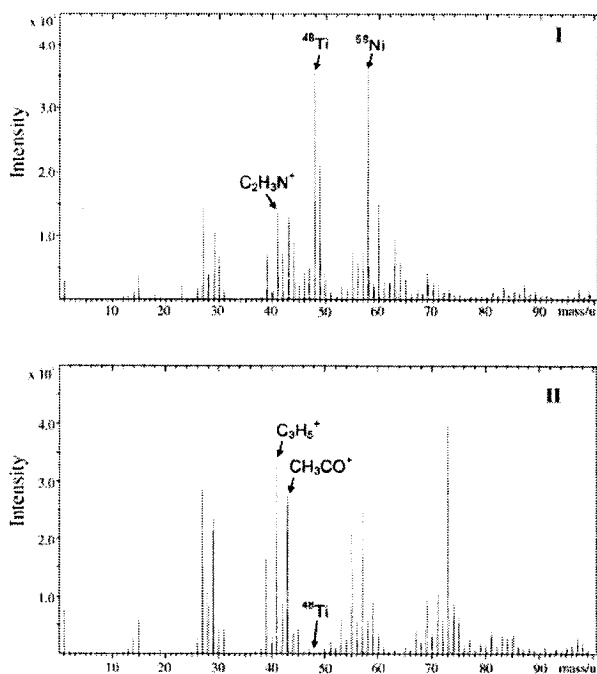


Figure 3. Positive ion ToF SIMS spectra (m/z 0–100) for (I) PEI modified NiTi and (II) PEI-HA(CH/HA)₄ self-assembled coating on NiTi.

Table 2. ToF SIMS Normalized Intensities of the CH₃CO⁺ Peak (M/z 43.0174) as a Function of the Number of Layer

self-assembled coating	CH ₃ CO ⁺ normalized intensity
NiTi/PEI/HA(CH/HA)	32
NiTi/PEI/HA(CH/HA) ₂	60.9
NiTi/PEI/HA(CH/HA) ₄	88.7
NiTi/PEI/HA(CH/HA) ₆	296.8
NiTi/PEI/HA(CH/HA) ₁₀	No metallic signal detected

presented an intense peak at m/z 43.017 attributed to the CH₃CO⁺ ion from the HA *N*-acetyl.³⁷ The normalized intensity of the CH₃CO⁺ peak increases as a function of the number of layers (Table 2). This peak was used to correlate the quantitative information obtained using the ¹¹¹In–HA and the ToF–SIMS analyses. In addition to a peak at m/z 43.0174, the ToF–SIMS spectrum of the HA(CH/HA)₄ coated PEI–NiTi (Figure 3) presents hydrocarbon peaks, such as C₂H₃⁺ (m/z 27.022), C₃H₃⁺ (m/z 39.022), C₃H₅⁺ (m/z 41.0375), and C₄H₇⁺ (m/z 55.053) as well as oxygen and nitrogen containing peaks, such as CH₄N⁺ (m/z 30.033), C₂H₃N⁺ (m/z 41.025), C₂H₂O⁺ (m/z 42.099), C₂H₃O⁺ (m/z 43.017), and C₂H₄NO⁺ (m/z 58.027). Peaks due to the metal substrate were still detectable, but their intensity, compared to that of the carbonaceous species, is much weaker than in the spectrum of the PEI–NiTi sample. No ions originating from the metallic substrate were detected on the spectrum of a HA(CH/HA)₁₀ multilayer coated NiTi sample.

The uniformity of the self-assembled coating on the scale of a cell, a few μm , was assessed by ToF SIMS imaging of HA(CH/HA)₄-coatings. The peak assigned to the CH₃CO⁺ peak was employed. Homogeneous chemical images were obtained over an 8 μm^2 area (Figure 4). Chemical mapping of metallic peaks attributed to the substrate was performed

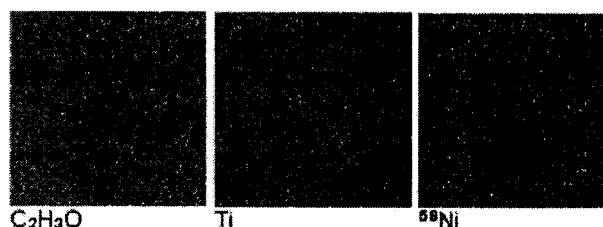


Figure 4. Chemical imaging of a PEI-HA(CH/HA)₄ self-assembled multilayer showing the distribution of CH₃CO⁺ (43.017), Ti (47.054), and Ni (57.936) ions on the surface (7.9 μm^2).

as well, yielding homogeneous images of much lower intensity (Figure 4). This may be attributed to some degree of porosity of the multilayer coating, possibly resulting from exposure of the multilayers to the ultrahigh vacuum imposed by the SIMS analysis. ToF–SIMS investigation of self-assembled multilayer on Si wafers has also shown that atomic or small molecular ions are less surface sensitive than large molecular ions.³⁸

The evolution of surface topography throughout the multilayer construction process was assessed next using atomic force microscopy. Our observations for the sequential deposition onto polished NiTi (I) of PEI–HA(CH/HA)₂ (II), PEI–HA(CH/HA)₅ (III), and PEI–HA(CH/HA)₁₀ (IV) are presented in Figure 5. Note that the naked polished metal surface displays a slightly striated topography, the striations are believed to be caused by the use of a polishing paste consisting of alumina particles $\sim 0.3 \mu\text{m}$ in diameter. These surface features were gradually masked in the coated surfaces and replaced by nanosized clusters. These structures increase in size with the number of layers, reaching a height of a few tens of nanometers and an average diameter of 250 nm. The original pattern featured in the images of the mechanically polished metal is completely masked by a multilayer coating consisting of 13 layers. The appearance and growth of small globular features in the hundred of nanometers range may be the indication of the formation of complex coacervates, as reported previously in the case of the L-b-L self-assembly of poly(L-lysine) and HA.²⁵

One of the objectives of this study was to determine if a L-b-L assembled stent coating can act as a drug reservoir for in situ drug release following stent implantation. To test this hypothesis, an anionic drug, sodium nitroprusside (SNP), was incorporated in the multilayer. It was introduced within the coating during the chitosan deposition step, as the cationic polysaccharide is able to form a complex with SNP by electrostatic interactions. That SNP was incorporated into the coating by this method and that the construction mechanism was not disrupted by the presence of small amounts of SNP was established, by the radiolabeling method described above. No difference was observed in the amount of radiolabeled HA deposited as a function of the number of layers whether the multilayers were constructed with chitosan-SNP or chitosan alone (Figure 2). The ToF SIMS spectrum of an SNP-containing 9-layer assembly exhibited a peak at 55.84 m/z , a value characteristic of Fe which is present in the structure of SNP, but not in any other component of the coating. Taken together the ToF SIMS data and the radiolabeling experiment confirm that premixing

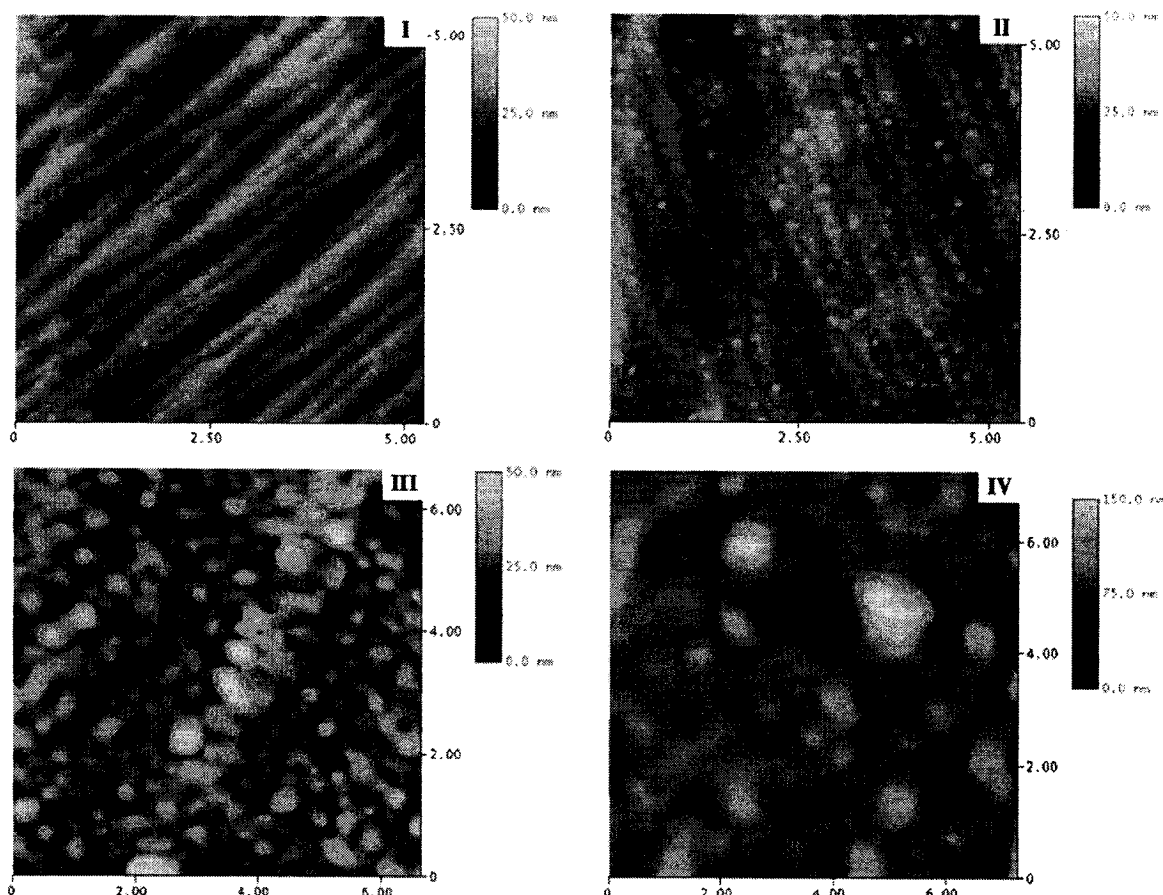


Figure 5. AFM tapping mode height images of (I) the mechanically polished NiTi, (II) PEI-HA(CH/HA)₂ coated NiTi, PEI-HA(CH/HA)₅ coated NiTi and PEI-HA(CH/HA)₁₀ coated NiTi; Z scales are 50 nm for images (I) to (III) and 150 nm for image (IV).

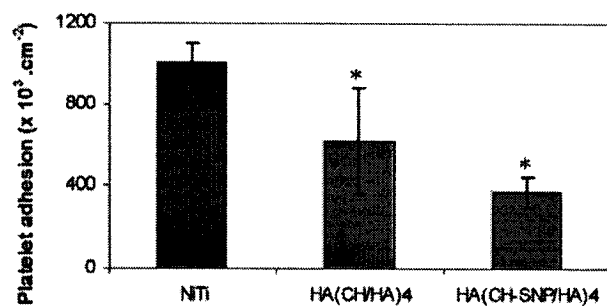


Figure 6. Platelet adhesion on NiTi, NiTi-PEI-HA(CH/HA)₄, and NiTi-PEI-HA(CH-SNP/HA)₄; * $p < 0.05$ Vs NiTi.

chitosan and SNP does not interfere significantly with the L-b-L construction, vouching for the flexibility of the technique in creating functional surfaces.

Haemocompatibility of CH/HA Coated NiTi Surfaces. The thromboresistance of an HA(CH/HA)₄ coated metallic substrate was investigated using a platelet adhesion assay. As depicted in Figure 6, platelet adhesion was significantly reduced by 38% onto NiTi-PEI-HA(CH/HA)₄ after 60 min of exposure to platelet rich plasma (619.7 ± 258.0 10^3 platelets/cm² versus 1005.9 ± 97.7 10^3 platelets/cm² for bare NiTi; $p = 0.036$). The incorporation of sodium nitroprusside within the multilayered coating further decreased platelet adhesion by 40% (371.5 ± 74.5 10^3 platelets/cm² for SNP containing HA(CH/HA)₄ coated NiTi versus 619.7 ± 258.0

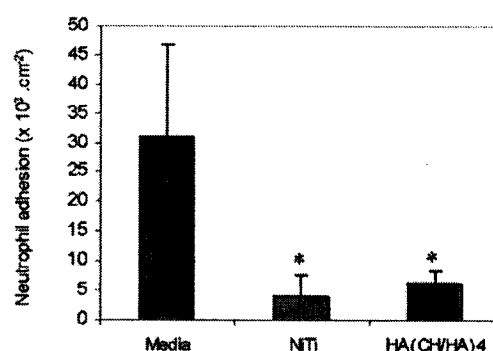


Figure 7. Neutrophil adhesion on damaged artery (Media), NiTi, and NiTi-PEI-HA(CH/HA)₄; Mean \pm SEM; * $P < 0.05$ vs Media (Student-t-test).

10^3 platelets/cm² for HA(CH/HA)₄ NiTi; $P = 0.09$). On the contrary, the CH/HA multilayer did not inhibit polymorphonuclear neutrophils (PMNs) adhesion after a 15-min perfusion in a porcine ex vivo assay (Figure 7). In fact, PMN adhesion *increased* slightly onto the coated surface, compared to bare metal (6.1 ± 2.2 10^3 /cm² vs 3.9 ± 3.8 10^3 /cm²). PMN adhesion on both bare metal and polysaccharide coated metal surfaces was significantly lower than PMN adhesion on the damaged porcine aortic segment used as control (30.9 ± 16.1 10^3 /cm²).

Platelet adhesion is known to be initiated by adsorption of plasma proteins, such as fibrinogen. The antifouling

properties of HA immobilized onto surfaces are well documented. It is believed that they are attributable to the hydration layer surrounding HA molecules on the surface.³⁹ It is expected that reduction of adhesion and activation of platelets could reduce the proliferative vascular response. Interestingly, the multilayer did not prevent neutrophil adhesion in the *ex vivo* assays and even slightly increased their adhesion in comparison to bare metal. This is in agreement with previous reports showing adhesion of monocyte and PMN to antifouling hydrophilic surfaces.⁴⁰ The neutrophil adhesion could result from nonspecific interactions or from specific adhesion through ligand–receptor mediated interactions such as CD 44 that are expressed on leukocytes. The modest neutrophil adhesion onto polysaccharide multilayer remained however far under the level measured onto damaged arteries.

Ex Vivo Stability of the CH/HA Coating in Contact with a Vascular Wall. A fluorescently labeled HA sample, HA-FITC, was used to monitor the deposition of the multilayer onto the metallic substrate. Fluorescence confocal microscopy observation of HA-FITC-(CH/HA-FITC)₄ coated wires confirmed the uniform presence of HA-FITC on the wire surface, even after the coated wires had been incubated in PBS for several days (Figure 8). A porcine aortic sample was incubated for 3 days in PBS while maintained in contact with the coated wire. The treated artery displayed fluorescence attributed to the transfer of FITC-HA from the coated wire-mesh to the artery surface as a result of contact with the stent.

Conclusion

The tremendous potential of the polyelectrolyte multilayer self-assembly methodology to engineer biologically active surfaces lies in its versatility and reproducibility.^{6,41} Our study demonstrates that the self-assembled deposition of polysaccharide multilayers can be achieved with excellent control of the growth mechanism and the surface coverage, even in the presence of an added drug. The CH/HA system is characterized by a linear growth as demonstrated using the radiolabeled HA-¹¹¹In derivative. From contact angle measurements and ToF SIMS analysis of deposited multilayers, we established that a minimum of 4 bilayers were needed to mask the metal substrate from its environment. The hydrogel-like surface created by the polysaccharide multilayer enhanced the thromboresistance of the surface, but surprisingly did not reduce PMN adhesion. Platelet adhesion was indeed reduced by 40% in comparison to bare NiTi surfaces which, by themselves, display good haemocompatibility.³⁴ The multilayer self-assembly used in this study offers an innovative way to achieve 3-dimensional coatings that fully exploit the biocompatibility of natural polysaccharides such as HA and CH. Importantly, the L-b-L technique does not require the use of toxic cross-linking agents, such as glutaraldehyde, which could compromise the biocompatibility of the multilayer coating. Interestingly, placing arterial segments *in vitro* in contact with multilayer coated wires for several days resulted in the transfer of the polyelectrolytes, or at least HA, from the wire to the tissue. Given the

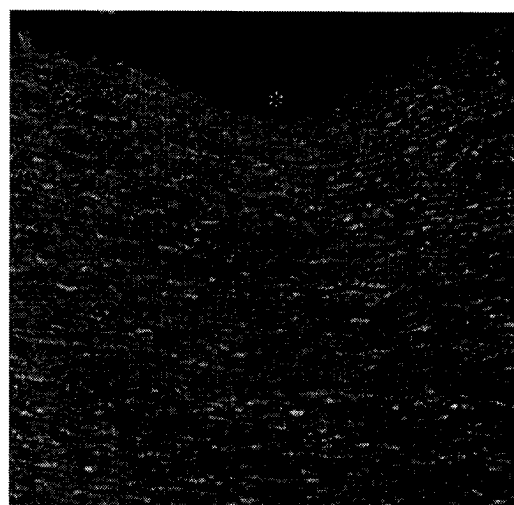


Figure 8. Confocal microscopy images of: (I) PEI/HA-FITC(CH/HA-FITC)₄ coated NiTi wires; (II) Cross-section of a damaged artery maintained in contact with a coated wire for 48 h in PBS showing the presence of HA-FITC translocated from the wire onto the vessel. (*) Groove due to the wire impact on the luminal surface of the artery.

beneficial biological effects of HA, this translocation of HA to the vascular wall may prove advantageous and lead to further reduction of neointimal hyperplasia.

This study also aimed to investigate the potential use of self-assembled structures for the local delivery of bioactive molecules. The incorporation of SNP within the polysaccharide multilayer resulted in a reduction of platelet adhesion, compared to multilayers devoid of drug. This result confirmed the potential of such biocompatible self-assembled structures as therapeutic drug delivery media. Their suitability as host to a variety of biologically active molecules, such as DNA or proteins, offers numerous opportunities for clinical applications.

Acknowledgment. This work was partly supported by NSERC grants and by the Center for Biorecognition system and Biosensors (CBB). We thank Cordis Corporation—Nitinol Devices & Components (Fremont, CA) for their technical and financial support. The authors thank S. Poulin

for her precious technical assistance and useful discussions with ToF SIMS analysis. Thanks also go to J. F. Théoret and N. Jacob from the Montreal Heart Institute for their help in the haemocompatibility assays and P. Cap for manuscript reviewing.

References and Notes

- (1) Babapulle, M. N.; Eisenberg, M. J. *Circulation* **2002**, *106* (21), 2734.
- (2) Welt, F. G.; Rogers, C. *Arterioscler. Thromb. Vasc. Biol.* **2002**, *22* (11), 1769.
- (3) Babapulle, M. N.; Eisenberg, M. J. *Circulation* **2002**, *106* (22), 2859.
- (4) van der Giessen, W. J.; Lincoff, A. M.; Schwartz, R. S.; van Beusekom, H. M.; Serruys, P. W.; Holmes, D. R., Jr; Ellis, S. G.; Topol, E. J. *Circulation* **1996**, *94* (7), 1690.
- (5) Virmani, R.; Liistro, F.; Stankovic, G.; Di Mario, C.; Montorfano, M.; Farb, A.; Kolodgie, F. D.; Colombo, A. *Circulation* **2002**, *106* (21), 2649.
- (6) Decher, G. *Science* **1997**, *277*, 1232.
- (7) Chung, A. J.; Rubner, M. F. *Langmuir* **2002**, *18*, 1176.
- (8) Qiu, X.; Leporatti, S.; Donath, E.; Mohwald, H. *Langmuir* **2001**, *17*, 5375.
- (9) Pei, R.; Cui, X.; Yang, X.; Wang, E. *Biomacromolecules* **2001**, *2* (2), 463.
- (10) Lvov, Y. u. M.; Sukhorukov, G. B. *Membr. Cell Biol.* **1997**, *11* (3), 277.
- (11) Chluba, J.; Voegel, J. C.; Decher, G.; Erbacher, P.; Schaaf, P.; Ogier, J. *Biomacromolecules* **2001**, *2* (3), 800.
- (12) Vazquez, E.; Dewitt, D. M.; Hammond, P. T.; Lynn, D. M. *J. Am. Chem. Soc.* **2002**, *124* (47), 13992.
- (13) Lvov, Y.; Lu, Z.; Schenkman, J. B.; Zu, X.; Rusling, J. F. *J. Am. Chem. Soc.* **1998**, *120* (17), 4073.
- (14) Thierry, B. J.; Winnik, F. M.; Merhi, Y.; Tabrizian, M. *J. Am. Chem. Soc.* **2003**, *125*, 7494.
- (15) Abatangelo, G.; Weigel, P. H., Eds.; Elsevier: Amsterdam, 2000.
- (16) Heublein, B.; Evagorou, E. G.; Rohde, R.; Ohse, S.; Meliss, R. R.; Barlach, S.; Haverich, A. *Int. J. Artif. Organs* **2002**, *25* (12), 1166.
- (17) Finn, A. V.; Gold, H. K.; Tang, A.; Weber, D. K.; Wight, T. N.; Clermont, A.; Virmani, R.; Kolodgie, F. D. *J Vasc Res* **2002**, *39* (5), 414.
- (18) Travis, J. A.; Hughes, M. G.; Wong, J. M.; Wagner, W. D.; Geary, R. L. *Circ. Res.* **2001**, *88* (1), 77.
- (19) Geary, R. L.; Nikkari, S. T.; Wagner, W. D.; Williams, J. K.; Adams, M. R.; Dean, R. H. *J. Vasc. Surg.* **1998**, *27* (1), 96, discussion 106.
- (20) Chajara, A.; Raoudi, M.; Delpech, B.; Leroy, M.; Basuyau, J. P.; Levesque, H. *Arterioscler. Thromb. Vasc. Biol.* **2000**, *20* (6), 1480.
- (21) Deux, J. F.; Prigent-Richard, S.; d'Angelo, G.; Feldman, L. J.; Puvion, E.; Logeart-Avramoglou, D.; Pelle, A.; Boudghene, F. P.; Michel, J. B.; Letourneur, D. *J. Vasc. Surg.* **2002**, *35* (5), 973.
- (22) Chupa, J. M.; Foster, A. M.; Sumner, S. R.; Madhally, S. V.; Matthew, H. W. *Biomaterials* **2000**, *21* (22), 2315.
- (23) Morra, M.; Cassinelli, C. *J. Biomater. Sci. Polym. Ed.* **1999**, *10* (10), 1107.
- (24) Picart, C.; Mutterer, J.; Richert, L.; Luo, Y.; Prestwich, G. D.; Schaaf, P.; Voegel, J. C.; Lavalle, P. *Proc. Natl. Acad. Sci. U.S.A.* **2002**, *99* (20), 12531.
- (25) Picart, C.; Lavalle, Ph.; Hubert, P.; Cuisinier, F. J. G.; Decher, D.; Schaaf, P.; Voegel, J.-C. *Langmuir* **2001**, *17*, 7414.
- (26) Serizawa, T.; Yamaguchi, M.; Akashi, M. *Biomacromolecules* **2002**, *3* (4), 724.
- (27) Das, S.; Pal, A. J. *Langmuir* **2002**, *18*, 458.
- (28) Ariga, K.; Onda, M.; Lvov, Y.; Kunitake, T. *Chem. Lett.* **1997**, 25.
- (29) Wang, P. G.; Xian, M.; Tang, X.; Wu, X.; Wen, Z.; Cai, T.; Janczuk, A. J. *Chem. Rev.* **2002**, *102* (4), 1091.
- (30) Provost, P.; Merhi, Y. *Thromb. Res.* **1997**, *85* (4), 315.
- (31) *Annual Book of ASTM Standards: Medical Devices and Services*; American Society for Testing and Materials: West Conshohocken, PA, 1995; Vol. 13.01, p 6.
- (32) Gouin, S.; Winnik, F. M. *Bioconjugate Chem.* **2001**, *12* (3), 372.
- (33) In this work, "layer" refers to the increment in thickness after exposure to one of the polyelectrolyte solution.
- (34) Thierry, B.; Merhi, Y.; Bilodeau, L.; Trépanier, C.; Tabrizian, M. *Biomaterials* **2002**, *23* (14), 2997.
- (35) Merhi, Y.; King, M.; Guidoin, R. *J. Biomed. Mater. Res.* **1997**, *34* (4), 477.
- (36) Chen, W.; McCarthy, T. J. *Macromolecules* **1997**, *30* (1), 78.
- (37) Shard, A. G.; Davies, M. C.; Tendler, S. J. B.; Bennedetti, L.; Purbrick, M. D.; Paul, A. J.; Beamson, G. *Langmuir* **1997**, *13*, 2808.
- (38) Delcorte, A.; Bertrand, P.; Arys, X.; Jonas, A.; Wischerhoff, E.; Meyer, B.; Laschewsky, A. *Surf. Sci.* **1996**, *366*, 149.
- (39) Morra, M. *J. Biomater. Sci. Polym. Ed.* **2000**, *11* (6), 547.
- (40) DeFife, K. M.; Shive, M. S.; Hagen, K. M.; Clapper, D. L.; Anderson, J. M. *J. Biomed. Mater. Res.* **1999**, *44* (3), 298.
- (41) Phuvanartnuraks, V.; McCarthy, T. J. *Macromolecules* **1998**, *31* (6), 1906.

BM0341834

materials update

search this site:

[advanced search](#)

Monday 09 June 2003

welcome
news
past news
nanozone
research highlights
features
research archive
material of the
month
careers
conference calendar
authors
advertising
about us
contact us

Nature Materials
Subscribe today!

resources

Nature
Nature Materials
Nature
Biotechnology
Nature Science
Update
Nature Physics
Portal
Naturejobs

NPG Subject areas

Access material from all
our publications in your
subject area:

- ☐ Biotechnology
- ☐ Cancer
- ☐ Chemistry
- ☐ Clinical Medicine
- ☐ Dentistry
- ☐ Development

Nanocoatings for arteries

5 June 2003

Maria Bellantone

Layer-by-layer assembly of polyelectrolytes continues to find new and useful applications. As further demonstration of the versatility of this approach for materials engineering, B. Thierry and colleagues report in the *Journal of the American Chemical Society*¹ the creation of biomedical coatings that may repair and possibly heal damaged arteries. They made very thin coatings through sequential deposition of two natural polysaccharides, chitosan and hyaluronan. Conveniently, these coatings adhere better to damaged rather than healthy tissue. When blood flows through the arteries, the presence of the coating reduces platelet adhesion and clot formation on the damaged tissue. This is important because it lowers the chances of restenosis (obstruction of the blood flow) — a major complication following vascular surgery procedures, particularly feared by the frail patients that endure these operations. The authors suggest that, by including biologically active compounds (they add L-arginine, for instance) in the formulation of these coatings, it will be possible to further improve the biomedical performance of these materials.

References

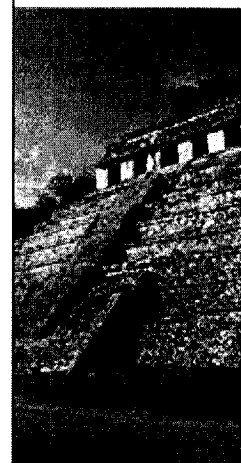
1. Thierry B., Winnik F. M., Merhi Y. & Tabrizian M. Nanocoatings onto arteries via layer-by-layer deposition: toward the *in vivo* repair of damaged blood vessels. *J. Am. Chem. Soc.*, (2003) | [article](#) |

Size Matters

From
photonic
crystals



to building
materials



nature
materials
All that matters

Subscribe today

Nanocoatings onto Arteries via Layer-by-Layer Deposition: Toward the in Vivo Repair of Damaged Blood Vessels

Benjamin Thierry,[†] Françoise M. Winnik,[‡] Yahye Merhi,[§] and Maryam Tabrizian^{*†}

Department of Biomedical Engineering, McGill University, H3A 2B, Faculté de Pharmacie and Département de Chimie, Université de Montréal, H3C 3J7, and Montreal Heart Institute, HIT 1C8, Montreal, Canada

Received January 24, 2003; E-mail: maryam.tabrizian@mcgill.ca

The layer-by-layer self-assembly of polyelectrolytes has emerged as a powerful and versatile, yet simple, strategy to engineer surfaces with specific properties.¹ Applications in the biomedical field are scarce, but they hold great promise, as the method permits the construction of thin films containing macromolecules, such as proteins, enzymes, or nucleic acids, with targeted properties onto a variety of substrates.² In this Communication, we describe the deposition of self-assembled nanocoatings onto arteries, as a means not only to protect an artery damaged during the revascularization procedure against blood coagulation, but also to control the healing processes by incorporating bioactive molecules within the multilayer.

Indeed, revascularization procedures are often plagued with complications related to the reobstruction of the treated artery, that is, restenosis, resulting from injuries induced during the procedure to the vascular wall. These injuries denude the protective endothelial cell lining (endothelium) and initiate excessive vascular cell proliferation within the artery.³ Systemic and local drug delivery via catheters or nanoparticles has been attempted, but such treatments have been largely unsuccessful in alleviating restenosis, due to inefficient targeting of the drug to the site of injury.⁴ Ideal strategies against restenosis should prevent the growth of blood thrombi on damaged arteries, enhance healing, and prevent the proliferation of vascular cells. Interest in local delivery has, however, been recently diverted by the success of drug eluting stents.⁵ In this Communication, we demonstrate that it is possible to build on damaged arteries a nanoscale self-assembled multilayer obtained by alternating depositions of two polysaccharides, hyaluronan (HA), a polyanion, and chitosan (CH), a polycation. The two polysaccharides (Figure 1) have been chosen in view of their biocompatibility, healing capabilities, and antiinflammatory properties.⁶

First, we characterized in detail the self-assembly of the CH/HA polyelectrolytes on a model surface, collagen-coated glass slides, using an ¹¹¹In-radio-labeled HA.⁷ Multilayer growth was a linear function of the number of layers⁸ (slope = 5.1 $\mu\text{g } ^{111}\text{In-HA}/\text{cm}^2$ per layer deposited; $r^2 = 0.99$, $[\text{NaCl}] = 0.14 \text{ M}$) (Figure 2). The electrostatically driven adsorption of the polymers occurred within a few seconds. Increasing the ionic strength of the polymer solutions (from 0.14 to 1.0 M NaCl) resulted in a decrease of the amount of deposited polymer. Quartz microbalance (QCM) studies indicated a hydrated thickness of about 70 nm for 5 bilayers. Using radio-labeled HA instead of HA resulted in an increase of the multilayer thickness (~30%). The stability of the multilayer was monitored by incubation of a (CH/¹¹¹In-HA)₅ self-assembly in phosphate buffer saline (PBS) at 40 °C. No loss of radioactivity was detected after 1 week.

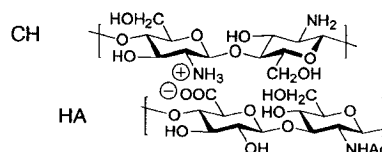


Figure 1. Chemical structure of chitosan (CH) and hyaluronan (HA).

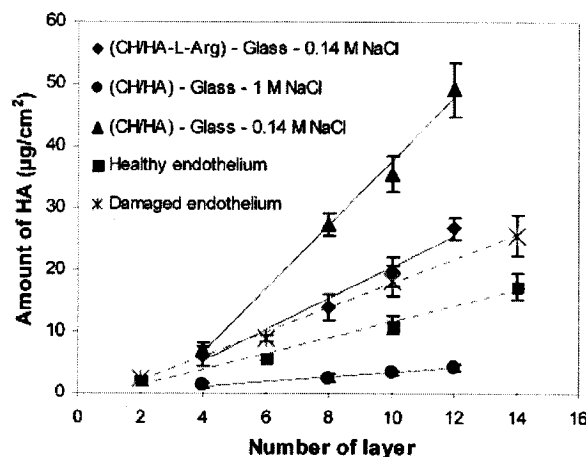


Figure 2. Amount of ¹¹¹In-HA vs layers. Solid lines: CH/HA (moderate and high ionic strength) and CH/HA-L-Arg on collagen-coated glass. Dashed lines: CH/HA on damaged or healthy endothelium. Linear regressions are presented excluding the first bilayer due to the substrate effect.

The multilayer was then constructed on damaged and healthy aortic porcine arteries, using a perfusion chamber matching closely the conditions achievable in vivo. Strong adhesion of the coating on the artery was secured by depositing first a layer of chitosan, a polycation exhibiting excellent bioadhesive properties toward negatively charged surfaces such as those presented by damaged arteries. Linear build up profiles were obtained (Figure 2) with lower amounts of polymers being deposited on healthy endothelium, as compared to damaged arteries.

The successful deposition of the multilayer and its retention on the arterial wall was monitored by confocal microscopy detection of CH/FITC-HA (fluorescein isothiocyanate) multilayers. A top view of the coated artery indicated that the multilayer uniformly covered the damaged artery. The multilayer-coated artery was subsequently subjected to physiological shear by perfusion in PBS. Imaging of transversal sections showed that the multilayer was retained on the vascular wall after a 24 h perfusion (Figure 3). Remarkably, the multilayer, or at least the fluorescently labeled HA, was detectable within the arterial wall, an indication of the polymer diffusion. Note that an assembly of 5 bilayers allowed the incorporation within the vascular wall of about 20 times more HA (18.2 $\mu\text{g}/\text{cm}^2$ vs 0.86 $\mu\text{g}/\text{cm}^2$) than passive infusion of a HA

[†] McGill University.

[‡] Université de Montréal.

[§] Montreal Heart Institute.

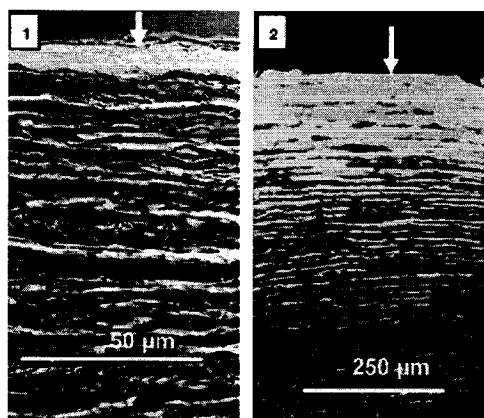


Figure 3. Confocal microscopy imaging of a section of a (CH/HA-FITC)₅-coated damaged artery showing the transmemural disposition of the fluorescently labeled polymer after (1) 0 h and (2) 24 h perfusion with PBS. The arrow indicates the coated surface exposed to the PBS flow.

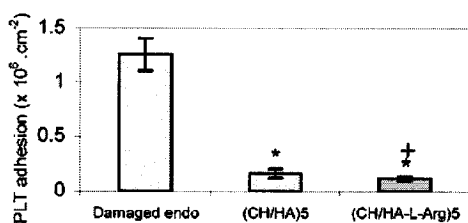


Figure 4. Platelet adhesion ($n \geq 4$) on damaged endothelium (damaged endo), (CH/HA)₅, and (CH/HA-L-Arg)₅-coated damaged endothelium ((CH/HA)₅ and (CH/HA-L-Arg)₅). * represents $p < 0.05$ vs damaged endo; † $p < 0.05$ vs (CH/HA)₅ by the paired student *t*-test.

solution (1 mg/mL HA in 0.14 M NaCl, 15 min). HA, together with other anionic polysaccharides, such as heparin or fucoidans, is known to inhibit vascular cell proliferation.^{6a,9} Because the biological response of the damaged artery in vivo has been correlated to tissue concentration rather than to the administered dose of active polysaccharides,¹⁰ the CH/HA nanocoatings may act as highly effective inhibitors of restenosis.

Next, CH/HA multilayer-coated arteries were placed in contact with blood to assess, via an in vitro platelet adhesion assay, the protective effect of the nanocoating against platelet adhesion onto damaged arteries. The growth of thrombus on damaged arterial surfaces was significantly inhibited by the CH/HA multilayers (Figure 4; 87% reduction in platelet adhesion, $p < 0.05$). This observation corroborates a previous report that polylysine/alginate self-assembly can act as a barrier material against cell attachment when deposited in vitro onto extracellular matrix-coated surfaces.¹¹ Insulation of the vascular wall from blood components, such as platelets and growing thrombi, results in reduced activation of vascular cells.¹² By cutting off this physiological response, one can expect to block the restenosis pathway early on.

Finally, we set out to evaluate whether CH/HA multilayers can act as localized drug-release systems and promote the artery healing process. Thus, we deposited onto arteries a multilayered assembly containing L-arginine. This low molecular weight cationic peptide has been reported to reduce restenosis.¹³ It is the precursor of nitric oxide (NO), which is known to affect vascular tone and wall dynamics, to inhibit monocyte and platelet adhesion, and to prevent

vascular cell proliferation. Multilayers were constructed by sequential deposition of a CH solution and a solution of a HA/L-arginine complex (L-arginine/disaccharide molar ratio: 1/5).¹⁴ Under these conditions, it was possible to incorporate L-arginine (213 ng/cm² in 5 bilayers) within the multilayer, but the amount of HA per layer was significantly lower than that in the case of CH/HA multilayers of identical layer number (Figure 2). The small amount of drug loaded within the multilayer was a result of its extraction during the adsorption of the chitosan layers. The release profile of [³H] L-arginine from a multilayer placed in PBS featured an initial burst (~80% release) followed by a slow linear regime.¹⁵

Incorporation of L-arginine in the CH/HA nanocoating further improved its protective effect against platelet adhesion, as demonstrated by a reduction of 30% in the amount of platelet adhesion after 90 min ($p < 0.05$), as compared to arteries protected by a nanocoating devoid of L-arginine. Note that, as compared to unprotected damaged arteries, L-arginine loaded CH/HA self-assemblies reduced platelet adhesion by 91% ($p < 0.05$). Conjugation of biologically active components, such as antiproliferative drugs or hormones to the polymers, is under investigation. This approach is expected to significantly enhance the amount of drug incorporated in a multilayer and to allow its sustained presentation or its gradual release within the arterial wall.

Acknowledgment. This research is funded by NSERC of Canada. The authors thank J. F. Théoret and N. Jacobs for their technical help in the haemocompatibility studies, and L. Villeneuve for the confocal microscopy experiments.

Supporting Information Available: Experimental details, QCM experiments, and L-arginine release profile (PDF). This material is available free of charge via the Internet at <http://pubs.acs.org>.

References

- (1) Decher, G. *Science* **1997**, *277*, 1232.
- (2) (a) Vazquez, E.; Dewitt, D. M.; Hammond, P. T.; Lynn, D. M. *J. Am. Chem. Soc.* **2002**, *124*, 13992–13993. (b) Zhou, L.; Estavillo, C.; Schenkman, S. J. B.; Rusling, J. F. *J. Am. Chem. Soc.* **2003**, *125*, 1431–1436.
- (3) Lowe, H. C.; Oesterle, S. N.; Khachigian, L. M. *J. Am. Coll. Cardiol.* **2002**, *39*, 183.
- (4) Hwang, C. W.; Edelman, E. R. *Circ. Res.* **2002**, *90*, 826.
- (5) (a) Fox, R. *Circulation* **2001**, *104*, E9052. (b) Serruys, P. W.; Regar, E.; Carter, A. J. *Heart* **2002**, *87*, 305.
- (6) (a) Heublein, B.; Evagorou, E. G.; Rohde, R.; Ohse, S.; Meliss, R. R.; Barlach, S. *Int. J. Artif. Organs* **2002**, *25*, 1166–73. (b) Singla, A. K.; Chawla, M. J. *Pharm. Pharmacol.* **2001**, *53*, 1047–67. (c) Kweon, D. K.; Song, S. B.; Park, Y. Y. *Biomaterials* **2003**, *24*, 1595–601.
- (7) Gouin, S.; Winnik, F. M. *Bioconjugate Chem.* **2001**, *12*, 372.
- (8) In this work, "layer" refers to the increment in thickness after exposure to one of the polyelectrolyte solutions.
- (9) (a) Matsumoto, Y.; Shimokawa, H.; Morishige, K.; Eto, Y.; Takeshita, A. *J. Cardiovasc. Pharmacol.* **2002**, *39*, 513. (b) Deux, J. F.; Meddahi-Pelle, A.; Le Blanche, A. F.; Feldman, L. J.; Collic-Jouault, S.; Bree, F.; Boudghene, F.; Michel, J. B.; Letourneur, D. *Arterioscler., Thromb., Vasc. Biol.* **2002**, *22*, 1604.
- (10) (a) Lovich, M. A.; Edelman, E. R. *Proc. Natl. Acad. Sci. U.S.A.* **1999**, *96*, 11111. (b) Hwang, C. W.; Wu, D.; Edelman, E. R. *Circulation* **2001**, *104*, 600.
- (11) Elbert, D. L.; Herbert, C. B.; Hubbell, J. A. *Langmuir* **1999**, *15*, 5355.
- (12) Hill-West, J. L.; Chowdhury, S. M.; Slepian, M. J.; Hubbell, J. A. *Proc. Natl. Acad. Sci. U.S.A.* **1994**, *91*, 5967.
- (13) Suzuki, T.; Hayase, M.; Hibi, K.; Hosokawa, H.; Yokoya, K.; Fitzgerald, P. J.; Yock, P. G.; Cooke, J. P.; Suzuki, T.; Yeung, A. C. *Am. J. Cardiol.* **2002**, *89*, 363.
- (14) (a) Ariga et al.^{14b} previously reported the use of the precomplexation method to load proteins in the multilayer. (b) Ariga, K.; Onda, M.; Lvov, Y.; Kunatake, Y. *Chem. Lett.* **1997**, 27–26.
- (15) See Supporting Information for the L-arginine release profile.

JA034321X

Nanocoating onto Arteries via Layer-by-Layer Deposition: Towards the In-Vivo Repair of Damaged Blood Vessels

Benjamin J. Thierry,[†] Françoise M. Winnik,[‡] Yahye Merhi,[§] Maryam Tabrizian^{*†}

Department of Biomedical Engineering, McGill university, H3A 2B4, Canada; Faculté de Pharmacie, Université de Montréal, H3C 3J7 Canada; and Montreal Heart Institute, HIT 1C8, Montreal, Canada

Preparation of the multilayer self-assemblies

Sodium Hyaluronate (HA) (MW 500,000, Hyal Pharmaceutical Corp, Mississauga, ON) and chitosan (CH) (HMW, degree of deacetylation: 85 %, from Sigma) were used as received. Solutions of HA (or HA-derivatives) (1 mg/mL in 0.14 M aqueous NaCl) and of CH (1.5 mg/mL in 0.1 M acetic acid (pH 4) containing 0.14 M NaCl) were prepared separately. The build up of the multilayer was accomplished by consecutive adsorption of the oppositely charged polysaccharides onto the substrate. Between each step, the excess polyelectrolyte was removed by rinsing the sample surface with 0.14 M NaCl. The effect of ionic strength was investigated using NaCl solutions ranging in concentration from 0 M to 1 M.

Substrates employed

Surfaces of porcine aortas used to simulate damaged arteries (Damaged endothelium) were prepared by lifting and peeling off the intima together with a thin portion of the adjacent media. Specimens with intact endothelial cell lining were also used as control (Healthy endothelium). Specimens were secured in a polycarbonate perfusion chamber used to deposit the multilayer onto artery walls and for further perfusion with physiological buffered solutions (PBS). The chamber had a window of 0.16 cm² exposing the artery to the solutions (either HA, CH, or 0.14 M NaCl solution during build up and PBS during the perfusion experiments). Collagen coated glass slides and Petri dish used as model surfaces were prepared by treating clean substrates with 10 •L of a 1 mg/mL collagen solution (Type I, CHRONO-LOG) and drying at room temperature.

Characterization using ellipsometry and quartz crystal microbalance (QCM) was achieved, respectively, on silicon wafers and on evaporated gold QCM electrodes. Substrates were cleaned with a piranha solution (concentrated H₂SO₄/H₂O₂ (30 wt % in water) = 3/1 v/v; Piranha solution is extremely energetic and should be handled with extreme caution) and pure water. A polyethyleneimine layer (PEI, MW 70,000, 5 mg/ mL) was first adsorbed for 20 min onto these substrates and used as a precursor layer to initiate the layer-by-layer self-assembly.

Characterization of the self-assembled multilayers

CH/HA self-assemblies were characterized on the arteries or on collagen coated glass surfaces using an ¹¹¹In radio labeled HA (¹¹¹In-HA). A diethylenetriaminepentaacetic acid/HA conjugate (HA-DTPA) was prepared as described previously (Ref. 7). Radio labeled HA (¹¹¹In-HA) was prepared by complexation with ¹¹¹In performed and as follows: 100 µCi ¹¹¹InCl₃ (100 µCi) was added to a solution of HA-DTPA (29 mg) in pure water (20 mL). The solution was maintained at room temperature for 2 hr under stirring, prior to purification by extensive dialysis against water. The solution (29 mL) was kept at 4• C until used. After the build up of the multilayer using ¹¹¹In labeled HA, the radioactivity of the samples was determined using a gamma counter (1470 Wizard™, Wallac). The amount of ¹¹¹In-HA in the multilayer was calculated after correction for decay, knowing the activity of a 1 mg/mL ¹¹¹In-HA solution.

The influence of the radio labeling procedure on the build up processes was assessed using a dissipation enhanced quartz crystal microbalance (QCM-D, Q-Sense, Sweden). A non-

radioactive Gd-HA complex was prepared similarly to the ^{111}In -HA and used in the QCM-D experiments. CH/HA multilayers using either non labeled HA or Gd-HA were grown on the gold-coated electrodes and the thickness of the film was determined from the frequency shift, taking into consideration the dissipation due to viscoelasticity. Assuming a constant density of the growing self-assembly, the use of Gd-HA for the multilayer build up resulted in a modest increase of the thickness when compared with the multilayer prepared using non labeled HA (see Figure S1, slope = 13.95 nm/layer ($R^2 = 0.96$) with Gd-HA and slope = 9.07 nm/layer ($R^2 = 0.98$) with non labeled HA). Thus use of the ^{111}In labeled HA to investigate the build up procedures overestimated the amount of HA incorporated in the multilayer by 30% or less.

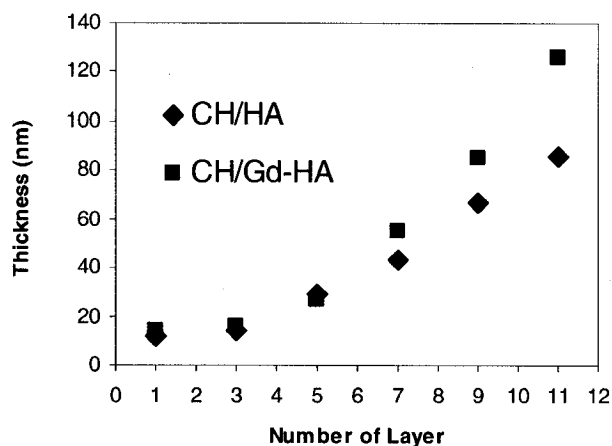


Figure S1. Thickness of the CH/HA multilayer self-assemblies prepared using non labeled HA or Gd-labeled HA (Gd-HA) (from QCM-D measurements).

Vascular diffusion of the polymer

The diffusivity of HA in the vascular wall was determined using the parallel plate perfusion chamber described above and a fluorescent derivative of HA (FITC-HA). FITC-HA was prepared by treatment of a solution of HA (80 mg) in aqueous borate buffer (pH 9.4) with fluorescein dichlorotriazine (Sigma) for 3 hr at room temperature, in the dark and under nitrogen (COOH/Fluorescein molar ratio: 25:1). The unreacted dye was removed by dialysis against borate buffer (12 hr) and against water (3 days). FITC-HA was recovered by lyophilization and the purity was assessed by GPC. CH/FITC-HA self-assemblies (5 bilayers) were deposited directly on damaged porcine aortic samples positioned in the perfusion chamber using silicon tubing and 3 X 10 cc syringes filled with saline, CH (2 cc) and FITC-HA (2 cc). CH and FITC-HA layers were alternatively deposited on the sample for 2 min. Prior to each polyelectrolyte monolayer deposition, the circuit was rinsed with 5 mL of saline solution. The nanocoated samples were then perfused with PBS (137 mM NaCl, 2.7 mM KCl, 4.3 mM Na_2HPO_4 , 1.4 mM KH_2PO_4 in pure water at pH 7.4) under physiological wall shear stress (424 sec^{-1}) for 1 min, 2 h and 24 h. The specimens were kept in the dark during all the experiments to prevent photobleaching. To avoid diffusion of the polymers during handling and storage of treated arteries, specimens were snap-frozen in 2-methylbutane using liquid nitrogen and kept at -80°C until used. Tissues were cut into 10 μm thick sections with a cryostat and mounted onto a glass slide prior to fixation with 4% paraformaldehyde. The sections were imaged using an Axiovert inverted microscope equipped with an LSM 510 confocal system (Zeiss). The images were corrected for autofluorescence using non-coated sections of porcine arteries.

L-arginine-loaded multilayers

A mixture of labeled/unlabeled L-Arginine (Arg) from Sigma (L-Arginine hydrochloride, FW: 210.7; and L-Arginine-2,3- ^3H in aqueous ethanol solution) was added to a solution of HA in 0.14 M NaCl (COOH/Arg molar ratio: 5:1 with 2 $\bullet\text{L}$ [^3H] Arg/mL). This solution was used to build the multilayer. The effect of the drug on the growth of the layer on collagen-coated glass was studied using ^{111}In -HA. To investigate the release of L-Arginine from the multilayers, L-Arginine-loaded multilayers were immersed in PBS and gently stirred. Radioactivity of the solution was determined using liquid scintillation spectrometry (Beckman LS 6500 Liquid Scintillation counter) as a function of immersion time and used to determine the release behavior presented in Figure S2.

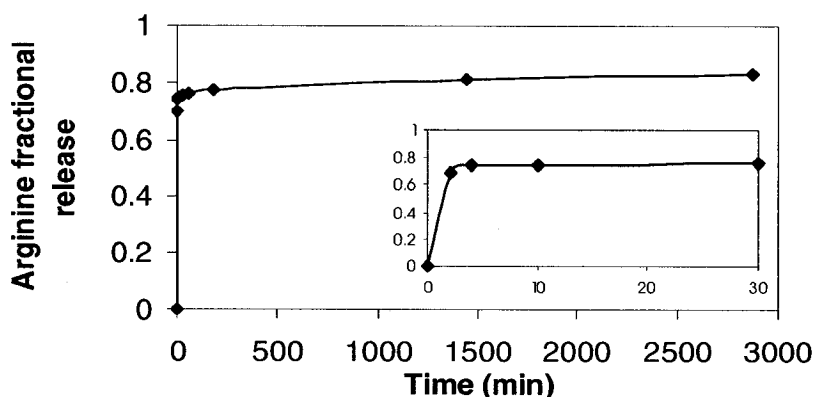


Figure S2. Fractional release of L-Arginine loaded multilayer in PBS. The inset shows the initial release.

Thromboresistance of nanocoated arteries

A platelet adhesion assay was used to investigate the protective effect of the self-assembled nanocoatings deposited on damaged arteries. Fresh blood (120 mL) was drawn from healthy volunteers who were medication-free. The blood was collected in syringes preloaded with sodium citrate (3.8% w/v). Platelet-rich plasma (PRP) was prepared by centrifugation of the blood at 1800 rpm for 15 min. The PRP was then centrifuged at 2200 rpm for 10 min and the platelet-poor plasma (PPP) was recovered as the supernatant. Platelets were carefully resuspended in buffer and then incubated with 250 $\bullet\text{Ci}$ of $^{111}\text{InCl}_3$ for 15 min. The platelets were recovered by centrifugation and resuspended in the PPP to 2.5×10^6 platelets/mL. The multilayer coated arteries were placed into the bottom of a 96 well polystyrene plate (Corning Inc.). 250 $\bullet\text{l}$ of freshly prepared ^{111}In -platelet solution was added to each well, taking special care to ensure that both sides of the samples were in contact with the platelet solution. Platelet adhesion was allowed to proceed for 90 min with gentle shaking. After incubation, the samples were recovered, washed 4 times with saline and fixed in a 1.5 % glutaraldehyde solution. The amount of platelets was determined using a gamma counter (1470 WizardTM, Wallac).

Statistical analysis

Linear regressions are presented excluding the first layers in the nonlinear regime due to the effect of the substrate. The platelet adhesion data were analyzed paired Student-t-test. A P value less than 0.05 was accepted as statistically significant.

Benjamin Thierry

From: KRobbins@wiley.com [KRobbins@wiley.com]
To: Benjamin Thierry
Cc:
Subject: Copyright permission
Attachments:

Sent: Mon 7/21/2003 9:47 AM

Dear Mr. Thierry:

Thank you for your recent request. We grant you the following rights in your Contribution to Journal of Biomedical Materials Research:

1. The right to share with colleagues print or electronic "preprints" of the unpublished Contribution, in form and content as accepted by Wiley for publication in the Journal. Such preprints may be posted as electronic files on your own website for personal or professional use, or on your internal university or corporate networks/intranet, or secure external website at your institution, but not for commercial sale or for any systematic external distribution by a third party (e.g., a listserve or database connected to a public access server). Prior to publication, you must include the following notice on the preprint: "This is a preprint of an article accepted for publication in Journal of Biomedical Materials Research copyright (year) (copyright owner as specified in the Journal)". After publication of the Contribution by Wiley, the preprint notice should be amended to read as follows: "This is a preprint of an article published in [include the complete citation information for the final version of the Contribution as published in the print edition of the Journal]", and should provide an electronic link to the Journal's WWW site, located at the following Wiley URL: <http://www.interscience.Wiley.com/>. You agree not to update the preprint or replace it with the published version of the Contribution.
2. The right, without charge, to photocopy or to transmit online or to download, print out and distribute to a colleague a copy of the published Contribution in whole or in part, for your personal or professional use, for the advancement of scholarly or scientific research or study, or for corporate informational purposes.
3. The right to republish, without charge, in print format, all or part of the material from the published Contribution in a book written or edited by you.
4. The right to use selected figures and tables, and selected text (up to 250 words, exclusive of the abstract) from the Contribution, for your own teaching purposes, or for incorporation within another work by you that is made part of an edited work published (in print or electronic format) by a third party, or for presentation in electronic format on an internal computer network or external website of yours or your employer.
5. The right to include the Contribution in a compilation for classroom use (course packs) to be distributed to students at your institution free of charge or to be stored in electronic format in datarooms for access by students at your institution as part of their course work (sometimes called "electronic reserve rooms") and for in-house training programs at your employer.

Please include the following notice: Journal of Biomedical Materials Research copyright (year) (copyright owner as specified in the

Journal).

Please retain this letter for any future uses you may wish to make of your Contribution that are covered by the above grant of rights and for which no additional correspondence is needed. If you have any questions please call 201-748-8607.

Sincerely,

Kathleen Robbins
John Wiley & Sons, Inc.
Permissions Assistant
111 River Street
Hoboken, NJ 07030
FAX: 201.748.6008
www.wiley.com/go/permissions

----- Forwarded by Gale Krouser/STM/Hoboken/Wiley on 07/18/2003 10:19 AM

"Benjamin Thierry"
<benjamin.thierry@mail.mcgill.ca> To: <gkrouser@wiley.com>
cc:
Subject: Copyright permission
07/17/2003 05:54 PM

To whom may be concerned,

I am about to publish in the Journal of Endovascular therapy a review on the biostability of endovascular devices. I would like to use in this review a figure (Figure 3) previously published by us in the Journal of Biomedical Materials Research :

Thierry B, Tabrizian M, Trépanier C, et al. Effect of surface treatment and sterilization processes on the corrosion behavior of NiTi shape memory alloy. J Biomed Mater Res. 2000;51:685-693.

I would however need a written permission from the Editor of JBMR to use this figure for our review. Could you please provide me with such a permission ?

I am looking forward to receive from you,

Best regards,

Benjamin Thierry,
Department of Biomedical Engineering,
McGill University,
Montreal, Qc, Canada

Tel: (514) 398 1456
Fax: (514) 398 7461
benjamin.thierry@mail.mcgill.ca